ABSTRACT

SHU, XIAOMEI. Pathogenesis and Host Response During Infection of Maize Kernels by *Aspergillus flavus* and *Fusarium verticillioides*. (Under the direction of Dr. Gary A. Payne.)

Developing maize kernels are vulnerable to colonization by microbes. When colonization allows proliferation of the microbe at the expense of the host, disease occurs. The ascomycete fungal pathogens *Aspergillus flavus* and *Fusarium verticillioides* are capable of colonizing maize kernels, causing ear rots and contamination of the kernel with mycotoxins. These diseases lead to significant losses of crop yield and quality, and constitute a threat to food safety and human health. Thus, the significance of these diseases has prompted extensive research efforts to understand these plant-parasite interactions. However, pathogenesis and resistance mechanisms remain poorly characterized, hampering the development of effective control strategies. No commercial maize lines are completely resistant to these fungi. We applied an integrated approach consisting of histology, *in situ* gene expression and transcriptional profiling to better understand the nature of the interactions that occur between maize kernels and these fungi. Maize inbred line B73 was hand pollinated and inoculated with either *A. flavus* or *F. verticillioides* by wounding the kernel with a needle bearing conidia. Histological staining of the kernel sections revealed fungal mycelium in kernels adjacent to the inoculation site by 48 hours post inoculation (hpi), and in all tissues at 96 hpi. Compared with *F. verticillioides*, *A. flavus* more aggressively colonized kernel tissue and formed a unique biofilm-like structure around the scutellum. Transcriptome profiling using RNA-sequencing (RNA-seq) coupled with pathway analysis showed that these fungi were recognized by the kernel tissues prior to visible

colonization. Infection of the kernel by these fungi induced transcriptional changes in defense-related genes, hormone signaling networks, as well as primary and secondary metabolism pathways. To dissect tissue-specific responses of the kernel, RNA *in situ* hybridization and histological staining were carried out in adjacent serial sections. We found that two maize genes, *pathogenesis related protein*, *maize seeds* (*PRms*) and *shrunken-1* (*Sh1*), were expressed in the aleurone and scutellum during infection by these fungi. By staining the adjacent sections, we found that these genes were induced in the tissue before the establishment of fungal colonization. Integration of histology, *in situ* gene expression and transcriptional profiling to study pathogenesis of maize kernels by these two fungi revealed distinctive and common features between the two pathosystems, and provided information that will facilitate the development of resistance genotypes in maize.

Pathogenesis and Host Response During Infection of Maize Kernels by *Aspergillus flavus* and *Fusarium verticillioides*

by
Xiaomei Shu

A dissertation submitted to the Graduate Faculty of
North Carolina State University
in partial fulfillment of the
requirements for the degree of
Doctor of Philosophy

Plant Pathology

Raleigh, North Carolina

2014

APPROVED BY:

Gary A. Payne Committee Chair	Rebecca S. Boston
Robert G. Franks	David P. Livingston

ProQuest LLC.
789 East Eisenhower Parkway
P.O. Box 1346
Ann Arbor, MI 48106 - 1346

BIOGRAPHY

Xiaomei Shu was born in 1983 in Ya'an District, Sichuan Province, China. In 2002, Xiaomei attended Sichuan Agricultural University in Ya'an and graduated in May of 2006 with a bachelor's degree in Biotechnology. Then she accepted the Dual Master's program offered by China Agricultural University and Missouri State University. Xiaomei moved to Beijing, where she started the program in China Agricultural University in August of 2006. In March of 2008, she came to the United States to accomplish the Dual Master's program in Missouri State University in Mountain Grove, Missouri, and graduated in August, 2009 with a master's degree in Plant Science. From there Xiaomei moved to Raleigh, North Carolina, and started her PhD program in the Department of Plant Pathology at North Carolina State University.

ACKNOWLEDGEMENTS

I would like to give my sincere gratitude to my advisor, Dr. Gary Payne, for his instructive guidance on my research. I deeply appreciate his help in the completion of this study and thesis. His profound knowledge, earnest scientific attitude, excellent personality, and constant patience benefited me greatly. I gratefully acknowledge his encouragement, instruction, and friendship. More importantly, his passion in science encourages me to pursue my professional life.

I would like to express my thanks to committee members, Dr. Rebecca Boston, Dr. David Livingston, and Dr. Robert Franks, who have spent time and effort to give me instructions and suggestions for my research and thesis writing. I'd like to give my special appreciation to our lab manager Mr. Gregory OBrian who offered me invaluable technical help and advice for my research. My gratitude also extends to all the people in the Center for Integrated Fungal Research, and all the faculty, staff and students in the Department of Plant Pathology at North Carolina State University, for their friendship and help. Because of them, I have had a wonderful experience to finish my studies at NCSU. I'm also grateful to the United States Department of Agriculture (USDA), National Institute of Food and Agriculture (NIFA) for financial support.

Finally, I'd like to thank my beloved family and friends for their continuous support and encouragement. I would like to express sincere appreciation to my honorable professors, kind friends, and the staff in the university, and all those who helped me to complete my research and thesis.

TABLE OF CONTENTS

LIST OF TABLES

LIST OF FIGURES

Supplemental Material from Chapter Two

LIST OF ABBREVIATIONS

A. flavus: *Aspergillus flavus*

A. fumigatus: *Aspergillus fumigatus*

A. nidulans: Aspergillus nidulans

A. thaliana: *Arabidopsis thaliana*

ABA: abscisic acid

ABC: ATP-binding cassette

AfHis: *histone*, *A. flavus*

Al: aleurone

ALD: aldose reductase

AP2-EREBP: APETALA2/ethylene-responsive element-binding protein

B. elliptica: *Botrytis elliptica*

BAK1: BRASSINOSTEROID INSENSITIVE 1-associated receptor kinase 1

BETL: basal endosperm transfer layer

BRs: brassinosteroids

Bt: *Bacillus thuringiensis*

bZIP: basic leucine zipper

CAST: Council for Agricultural Science and Technology

CEM: corn extract medium

CFRAS-DB: Corn Fungal Resistance Associated Sequences Database

CHS: chalcone synthase

CKs: cytokinins

CORp: cold-regulated protein

CPA: cyclopiazonic acid

Cup: cupin domain containing protein

Cys: cysteine

DON: deoxynivalenol

Em: embryo

En: endosperm

ERFs: ethylene-responsive transcription factors

ET: ethylene

ETI: effector-triggered immunity

F. oxysporum: *Fusarium oxysporum*

F. verticillioides: *Fusarium verticillioides*

FB: fumonisin B

FDA: Food and Drug Administration

FPKM: fragments per kilobase of exon per million fragments mapped

GA: gibberellic acid

GID1: gibberellins recptor1

Gl: glandular layer

GLBs: globulins

GLXs: glyoxalases

gpdA: *glyceraldehyde-3-phosphate dehydrogenase*, *A. nidulans*

GST: glutathione S-transferase

GUS: β-glucuronidase

GWAS: genome-wide association study

h: hour(s)

hpi: hour(s) post inoculation

HR: hypersensitive response

HSPs: heat shock proteins

Inv-CW: cell wall invertase

JA: jasmonic acid

LEAs: late embryogenesis abundant proteins

LOX: lipoxygenase

LRR-RKs: leucine-rich repeat receptor kinase

MAPK: mitogen-activated protein kinase

MATE: multidrug and toxin extrusion

MeJA: methyl jasmonate

MGDP: Maize Gene Discovery Project

min: minute(s)

MLS: minimal medium

MpM1: Mississippi marker 1

N. crassa: *Neurospora crassa*

NBS-LRR: nucleotide binding site and leucine-rich repeats

NLPs: necrosis- and ethylene-inducing protein (Nep)-like proteins

NPP1: necrosis-inducing *Phytophthora* protein 1

NPR1: nonexpresser of PR genes 1

NTD: neural tube defects

OE: overexpression

OPRs: 12-oxo-phytodienoic acid reductases

P. aphanidermatum: *Pythium aphanidermatum*

P. capsici: *Phytophthora capsici*

P. citrophthora: *Phytophthora citrophthora*

P. infestans: *Phytophthora infestans*

P. megakarya: *Phytophthora megakarya*

P. palmivora: *Phytophthora palmivora*

P. sojae: *Phytophthora sojae*

PAMPs: pathogen-associated molecular patterns

PCD: programmed cell death

PDA: potato dextrose agar

PDB: potato dextrose broth

PER1: peroxiredoxin antioxidant 1

PLA: phenylalanine ammonia-lyase

ppb: parts per billion

ppm: parts per million

PR proteins: pathogenesis related proteins

PRms: *pathogenesis related protein*, *maize seeds*

ProFITS: protein families involved in the transduction of signaling

PRRs: pattern recognition receptors

PTI: PAMP-triggered immunity

pyr-4: *pyrimidine-4*

qRT-PCR: quantitative real-time reverse transcription-polymerase chain reaction

QTL: quantitative trait loci

R proteins: resistance proteins

RIP: ribosome-inactivating protein

RLKs: receptor-like kinase

RNA-seq: RNA sequencing

ROS: reactive oxygen species

RPS9: *40S ribosomal protein S9*

SA: salicylic acid

Sc: scutellum

SEM: scanning electron microscopy

Sh1: *shrunken-1*

SS1: sucrose synthase 1

TCA: tricarboxylic acid cycle

TFs: transcription factors

TI: trypsin inhibitor

UDP: uridine diphosphate

UGT: UDP glucosyltransferase

U. maydis: *Ustilago maydis*

V. dahliae: *Verticillium dahliae*

WSI: water stress inducible protein

WT: wild-type

ZmCAT1: *catalase 1*, *Zea mays*

Chapter One

Relationships of the Maize Kernel and Its Fungal Pathogens *Aspergillus flavus* and *Fusarium verticillioides*

Xiaomei Shu[1], Rebecca S. Boston[2], Charles P. Woloshuk[3], and Gary A. Payne[1]

[1] Department of Plant Pathology, North Carolina State University, Raleigh, NC 27695-7567

[2] Department of Plant & Microbial Biology, North Carolina State University, Raleigh, NC 27695

[3] Department of Botany and Plant Pathology, Purdue University, West Lafayette, IN 47907

ABSTRACT

Developing maize kernels interact with a broad range of microbes with different trophic lifestyles and infection strategies. Two pathogens of major importance are *Aspergillus flavus* and *Fusarium verticillioides.* These two are capable of infecting and rotting maize kernels, and producing the toxic compounds aflatoxins and fumonisins, respectively. Achieving disease control has been very difficult. No commercial maize lines resistant to these diseases have been marketed to date. A detailed understanding of these host-parasite interactions could contribute to disease resistance and crop improvement. In this review, we summarize the current knowledge about the pathogenesis and host defense response in these two pathosystems. In particular, we dissect the components of infection, colonization, and host response. Although *A. flavus* and *F. verticillioides* have very different trophic lifestyles and occupy diverse ecological niches, data from several research articles indicate that these two fungi colonize maize kernels in a similar pattern and induce both distinctive and common defense mechanisms of the host. In addition, we discuss recent progress on the development of effective strategies to control *A. flavus* and *F. verticillioides* associated maize ear rot and mycotoxin contamination.

INTRODUCTION

Maize (*Zea mays* L.) is one of the world's three leading grain crops, providing food for humans and animals. It is also an important material for biodiesel production. Over 10 billion bushels of maize were harvested in the United States in 2012. A number of plant pathogens cause diseases in maize resulting in severe yield loss. *Aspergillus flavus* and

Fusarium verticillioides are invasive fungal pathogens capable of infecting maize kernels both in the field and in storage (Payne and Brown, 1998; Wilson et al., 1975). Aflatoxin and fumonisin produced by *A. flavus* and *F. verticillioides*, respectively, are carcinogenic secondary metabolites harmful to humans and animals. Colonization of the kernel by these fungal pathogens often results in mycotoxin contamination, decreased sugar levels, and weight loss (Cardwell et al., 2000; Lillehoj et al., 1979). In the United States, the annual economic costs of crop losses from mycotoxins, including aflatoxins, fumonisins, and deoxynivalenol (DON), were estimated to be $932 million (CAST, 2003).

Development of effective disease control strategies for *A. flavus* and *F. verticillioides* is a high priority; butut traditional control strategies including currently available host resistance to ear rot and mycotoxin contamination are not sufficient to reduce fungal infection when environmental conditions are favorable (Munkvold, 2003; Payne, 1992). Attention has turned recently to gaining a better understanding of these two pathosystems so that we can apply our increased knowledge to develop efficient control strategies to reduce ear rots and minimize mycotoxin contamination of maize.

Over the past few decades, several studies have focused on the pathogenesis of *A. flavus* and *F. verticillioides* in maize kernels (Bush et al., 2004; Duncan and Howard, 2010; Hruska et al., 2013; Koehler, 1942; Marsh and Payne, 1984; Munkvold et al., 1997; Smart et al., 1990). The genetic basis of host resistance has also been studied recently using novel technologies, including quantitative trait loci (QTL) mapping, genome-wide association study (GWAS), and microarray and proteomic approaches (Campos-Bermudez et al., 2013;

Chen et al., 2007; Lanubile et al., 2013; Robertson-Hoyt et al., 2006, 2007a; Zila et al., 2013). Several maize genes and proteins associated with defense response to *A. flavus* and *F. verticillioides* have been identified (Table 1). In some cases common genes have been associated with resistance to both fungi, indicating the possibility of developing comprehensive resistance to both pathogens (Robertson-Hoyt et al., 2007a).

In this review, we describe the current progress in elucidating pathogenesis and host defense in these two pathosystems. We also discuss prospective approaches to breed resistant maize lines using the information generated from molecular, genomic, proteomic and metabolomics studies. Our overall goal is to control maize ear rot and eliminate mycotoxin contamination.

Table 1. Maize genes and/or proteins associated with defense response to *A. flavus* and *F. verticillioides*. Af: associated with defense response to *A. flavus*; Fv: associated with defense response to *F. verticillioides*; G: studied at the gene level; P: studied at the protein level.

Gene and/or proteins	Association	Study level	Reference
PR4	Af and Fv	G	Bravo et al., 2003; Dolezal, 2010; Luo et al., 2011
PR5	Af and Fv	G	Lanubile et al., 2013; Luo et al., 2011
PRms	Af and Fv	G and P	Bravo et al., 2003; Casacuberta et al., 1991, 1992; Cordero et al., 1994; Dolezal, 2010; Murillo et al., 1999
PRm3	Af and Fv	G	Lanubile et al., 2013; Luo et al., 2011
PRm6	Fv	G	Lanubile et al., 2013
PR10	Af	G and P	Chen et al., 2006, 2010b; Dolezal, 2010; Xie et al., 2010
PR10.1	Af	P	Chen et al., 2004; Xie et al., 2010
chitinases	Af and Fv	G and P	Campos-Bermudez et al., 2013; Cordero et al., 1993; Dolezal, 2010; Ji et al., 2000; Lanubile et al., 2010; Luo et al., 2011; Moore et al., 2004; Wu et al., 1994a, 1994b
β-1, 3- glucanase	Af and Fv	G and P	Campos-Bermudez et al., 2013; Chen et al., 2005; Cordero et al., 1993; Ji et al., 2000; Lanubile et al., 2013; Lozovaya et al., 1998; Luo et al., 2011; Wu et al., 1994a, 1994b
β-glucosidase	Af and Fv	G	Campos-Bermudez et al., 2013; Lanubile et al., 2013; Luo et al., 2011
zeamatin	Af and Fv	G and P	Chen et al., 2001; Guo et al., 1997, 1999; Lanubile et al., 2010; Luo et al., 2011
WRKYs	Af and Fv	G	Campos-Bermudez et al., 2013; Lanubile et al., 2010, 2013; Luo et al., 2011
Mybs	Af and Fv	G	Campos-Bermudez et al., 2013; Dolezal, 2010; Lanubile et al., 2010, 2013
LOXs	Af and Fv	G	Dolezal, 2010; Gao et al., 2007, 2009; Lanubile et al., 2013; Wilson et al., 2001
OPRs	Fv	G	Dolezal, 2010; Zhang et al., 2005
GF14-6	Fv	G	Campo et al., 2011
GSTs	Af and Fv	G	Campos-Bermudez et al., 2013; Dolezal, 2010; Lanubile et al., 2010, 2013; Luo et al., 2011
Peroxidases	Af	G and P	Chen et al., 2007; Luo et al., 2011
catalase	Af	P	Magbanua et al., 2007
chitosanase	Af	P	Cuero and Osuji, 1995
amylase inhibitor glycoprotein	Fv	P	Figueira et al., 2003
GLBs	Af and Fv	G and P	Chen et al., 2001, 2002, 2007; Lanubile et al., 2010
LEAs	Af	P	Chen et al., 2002, 2007; Luo et al., 2011
zein	Fv	G	Lanubile et al., 2010, 2013
WSI18	Af	P	Chen et al., 2002

Table 1 Continued

ALD	Af and Fv	G and P	Chen et al., 2002; Lanubile et al., 2010
HSPs	Af and Fv	G and P	Campos-Bermudez et al., 2013; Chen et al., 2002, 2007; Lanubile et al., 2010, 2013; Luo et al., 2011
GLXs	Af and Fv	G and P	Bhatnagar et al., 2008; Chen et al., 2004; Lanubile et al., 2010
Cup	Af	P	Chen et al., 2005
RIP	Af and Fv	P	Chen et al., 2001; Guo et al., 1997, 1999; Nielsen et al., 2001
TIs	Af and Fv	G and P	Baker et al., 2009b; Chen et al., 1998, 1999a, 1999b, 2007; Lanubile et al., 2010; Tubajika and Damann, 2001
lectin-like protein	Af	P	Baker et al., 2009a
CORp	Af	P	Chen et al., 2007
protein kinase	Af and Fv	G and P	Chen et al., 2005; Lanubile et al., 2010, 2013; Luo et al., 2011
protein phosphatases	Fv	G	Lanubile et al., 2010, 2013
translation initiation factors	Af and Fv	G and P	Chen et al., 2005; Lanubile et al., 2010
Sh1	Af and Fv	G	Dolezal, 2010; Lanubile et al., 2013

BIOLOGY OF *A. FLAVUS* AND *F. VERTICILLIOIDES*

Different lifestyles

A. flavus (teleomorph *Petromyces flavus*) is a mycotoxigenic filamentous fungus with diverse ecological niches (St Leger et al., 2000). This fungus is predominately a saprophyte growing on plant and animal debris in the soil or surviving dormant as sclerotia (Cotty, 1998; Horn et al., 2009; Payne and Brown, 1998; Payne and Yu, 2010; Wicklow and Horn, 1984). The ecological significance of this fungus is its important role in nutrient recycling (Payne and Yu, 2010). As an opportunistic fungal pathogen, *A. flavus* is able to infect maize kernels, peanuts, tree nuts, cotton bolls, as well as insects, animals and immunocompromised human patients (Payne and Brown, 1998; Payne, 1992; St Leger et al., 2000). *A. flavus* is considered to be the second leading causal agent of human invasive aspergillosis infecting skin, oral mucosa, and subcutaneous tissue (Hedayati et al., 2007; Rokas et al., 2007).

F. verticillioides (synonym *F. moniliforme*; teleomorph *Gibberella moniliformis*) is another mycotoxin producer occupying different ecological niches. This fungus can be a saprophyte growing in plant residues (Zummo and Scott, 1992). *F. verticillioides* is also considered as a minor pathogen colonizing seeds of pea and rice (Waśkiewicz et al., 2013; Wulff et al., 2010). In maize plants, *F. verticillioides* can be either an endophyte causing symptomless infection, or a pathogen causing visible symptoms, including kernel rot. As an endophyte, *F. verticillioides* is capable of asymptomatically and systemically infecting maize roots, stalks, and kernels at all developmental stages (Munkvold et al., 1997). The endophytic *F. verticillioides* is able to enhance disease resistance to *Ustilago maydis* in maize seedlings

(Lee et al., 2009; Rodriguez Estrada et al., 2012). Under certain conditions, *F. verticillioides* causes maize seedling blight, root rot, stalk rot, and ear rot (Gelderblom et al., 1991; Zummo and Scott, 1992). In addition, *F. verticillioides* is able to infect insects and immunocompromised patients (Pelizza et al., 2011; Sagnelli et al., 2006). *F. verticillioides* associated fusariosis was reported in a stem cell transplantation patient (Tezcan et al., 2009). Another liver transplantation patient was diagnosed as having *F. verticillioides* associated fungemia (Cocchi et al., 2011).

Although *A. flavus* and *F. verticillioides* have very different trophic lifestyles, they can invade immature maize kernels and follow a similar pattern of colonization. Moreover, previous studies suggest that maize kernels have evolved similar resistance mechanisms to defend against these two pathogens (Robertson-Hoyt et al., 2006, 2007a). Comparison of these two pathosystems will help us gain a better understanding of pathogenesis and host resistance in maize kernels.

Aflatoxins and fumonisins

A. flavus is notorious for its ability to produce aflatoxins, a group of potent carcinogenic secondary metabolites. Research led to the structural identification of aflatoxins (Stoloff, 1977). These toxins were isolated from Brazilian peanut meal associated with the outbreak of turkey 'X' disease in England (Cole, 1986). Outbreaks of aflatoxicosis in humans have occurred in both India and Kenya (Krishnamachari et al., 1975; Lewis et al., 2005). Human aflatoxicosis caused by consumption of aflatoxin contaminated food still threatens

public health in developing countries (Williams et al., 2004). Aflatoxin exposure also causes growth impairment in children (Khlangwiset et al., 2011).

Of the aflatoxins produced by *A. flavus*, aflatoxin B1, which is associated with human hepatocellular carcinoma, is the most toxic and potent naturally occurring carcinogen ever characterized (Kew, 2013; CAST, 2003). *A. flavus* also produces lesser amounts of aflatoxin B2 and several other unrelated mycotoxins, including aspertoxin, aflatrem, aspergillic acid, and the indole-tetramic acid mycotoxin cyclopiazonic acid (CPA) (Chang et al., 2009; Horn et al., 2009). CPA, an inhibitor of Ca^{2+} mediated ATPases, targets the liver, kidneys and gastrointestinal tract in animals (CAST, 2003). Because of the high health risks to humans and animals, aflatoxins are strictly regulated by the US Food and Drug Administration (FDA). The levels of total aflatoxins in interstate commerce of food and feed are limited to 20 parts per billion (ppb) (FDA, 2000).

The other group of mycotoxins commonly detected in maize is fumonisins produced by *F. verticillioides* and other *Fusarium* species. *F. verticillioides* is able to synthesize fumonisins at both endophytic and pathogenic stages on maize, making these mycotoxins extremely difficult to eliminate from the food chain (Brown et al., 2008). Fumonisins are toxic to humans and animals by disrupting sphingolipid biosynthesis pathways (Marasas, 2001, 2004; Riley et al., 1994; Voss et al., 2001). Saccardo (1881) first reported that *F. verticillioides* from maize was associated with human pellagra. In the southern African territory of Ttanskei, consumption of *F. verticillioides* and fumonisin contaminated corn was found to be correlated with human esophageal cancer (Miller, 2001; Rheeder et al., 1992).

Fumonisin B1 (FB1), which is the most common mycotoxin produced by *F. verticillioides*, is recognized as the causal agent of equine leukoencephalomalacia as well as pulmonary edema and hydrothorax in swine (Bacon et al., 1992; Harrison et al., 1990; Kellerman et al., 1990; Pienaar et al., 1981; Rheeder et al., 1992). FB1 is also a carcinogenic compound associated with rat liver cancer (Gelderblom et al., 1991, 2004). FB1 associated embryo neural tube defects (NTD) were observed in both humans and rats (Hendricks, 1999; Marasas et al., 2004; Sadler et al., 2002). Due to the potent toxicity of fumonisins to humans and animals, the FDA has established guidelines for their levels in human food products and animal feeds. The total fumonisin levels (FB1, FB2, and FB3) in degermed dry milled corn products are limited to 2 parts per million (ppm) (FDA, 2001).

Virulence

Several putative virulence factors have been identified from *A. flavus*. One example is the endopolygalacturonase, P2c, which plays a critical role in virulence during infection of both maize and cotton bolls (Mellon et al., 2007; Shieh et al., 1997). Another characterized pathogenicity factor is amylase which is involved in starch digestion and pathogenicity during colonization of maize kernels (Mellon et al., 2007). The *A. flavus* phytase encoding gene, *phy1*, is also associated with infection of maize kernels (Reese et al., 2011). Moreover, gene expression and mutant analysis suggest that one of the *A. flavus* necrosis- and ethylene-inducing protein (Nep)-like proteins (NLPs) is a putative pathogenesis factor required for full virulence of this fungus (Dolezal, 2010).

It appears that *F. verticillioides* has evolved tissue-specific virulence factors to attack different tissues of maize plants. The cAMP-dependent protein kinase gene, *fpk1*, is essential for hyphal growth, spore germination, and pathogenicity of this fungus on maize seedlings (Pei-Bao et al., 2010). Fumonisins at high concentrations also have been reported to facilitate infection of maize seedlings by *F. verticillioides* (Arias et al., 2012; Desjardins et al., 1995). Fumonisin-mediated disruption of ceramide biosynthesis in maize roots is associated with seedling blight (Williams et al., 2006, 2007). Although FB1 is able to target the defense-related protein beta-1, 3-glucanase in the germinating embryo, fumonisins are not required for *F. verticillioides* infection of maize kernels (Desjardins and Plattner, 2000; Sanchez-Rangel et al., 2012). Instead, several *F. verticillioides* genes, including the mitogen-activated protein kinase gene, *FvMK1*, the putative hexokinase-encoding gene, *HXK1*, and the putative hexose transporter gene, *fst1*, are pathogenicity factors associated with infection of maize kernels (Kim et al., 2011; Kim and Woloshuk, 2011; Zhang et al., 2011). Furthermore, *F. verticillioides* G-protein regulator genes modulate the maize ET biosynthesis pathway in the kernel (Mukherjee et al., 2011). A *F. verticillioides* fungalysin metalloprotease chitinase-modifying protein is also involved in truncation of maize kernel class IV chitinases, ChitA and ChitB (Naumann et al., 2011).

PATHOGENESIS

Infection and colonization

A. flavus infection in a maize field was first reported in Texas (Taubenhaus, 1920). During the growing season, *A. flavus* conidia produced by conidiophores are dispersed by

insects and wind to maize plants (Jones et al., 1980; Marsh and Payne, 1984; Smart et al., 1990; Widstrom et al., 2003). Airborne *A. flavus* conidia are found to be important sources of environmental inoculum (Mehl and Cotty, 2010). Once on the plant, this fungus is capable of colonizing silks, rachises, spikelets, glumes, kernel surfaces, and all tissues inside the maize kernel (Smart et al., 1990). *A. flavus* enters the undamaged kernel through a few routes, such as the silk, cob, and rachilla (Jones et al., 1980; Marsh and Payne, 1984; Munkvold et al., 1997; Widstrom et al., 2003; Windham and Williams, 1998). Smart et al. (1990) showed that *A. flavus* penetrates the base of undamaged kernels and the pedicel via the vascular tissue. Maize kernels are more resistant to *A. flavus* during the early developmental stages, but are very susceptible during the milk and dent stages (Hesseltine and Bothast, 1977; Ji et al., 2000; Rambo et al., 1974). Scanning electron microscopy (SEM) studies indicate that *A. flavus* can only colonize the yellow-brown silks but not the green unpollinated silks, suggesting that silks are more resistant in the early stages (Marsh and Payne, 1984).

F. verticillioides is the most prevalent fungal species in maize ears (Alborch et al., 2010; Cao et al., 2013; Koehler, 1942). This fungus is capable of infecting maize ears via crown, stalk, and silk (Munkvold et al., 1997). *F. verticillioides* colonization in the pedicel below the black layer was observed by Koehler (1942). SEM studies show that *F. verticillioides* is always located in the pedicel or tip cap end of the asymptomatic maize kernels (Bacon et al., 1992). Moreover, this fungus can be transmitted by seeds (Munkvold et al., 1997). However, inoculation of maize seeds by *F. verticillioides* before planting does not significantly change the yield and vegetative growth, indicating that seed transmission is not

the major route for infection (Yates et al., 2005). Compared with infection pathways via stalk and seed, infection through silk is the most effective pathway leading to kernel colonization by *F. verticillioides* (Munkvold et al., 1997). During kernel development, the dent stage is the most conducive stage for fumonisin production of *F. verticillioides* (Picot et al., 2010, 2011), although it can be produced in younger kernels (Bush et al., 2004).

Both *A. flavus* and *F. verticillioides* are able to penetrate maize kernels through breaks or cracks in the pericarp (Hruska et al., 2013; Scott and Zummo, 1990, 1992). Insect damage and mechanical injury of the external seed pericarp are important routes of infection by these two pathogens (Abbas et al., 2006; Johansson et al., 2006; Smart et al., 1990; Widstrom and Donald, 1996; Widstrom et al., 2003). Infection of developing maize kernels by *A. flavus* typically starts at the tip of the ear where damage is often the most extensive. *A. flavus* infection also can occur at the base of undamaged ears, indicating that this fungus possibly enters these kernels through systemic infection pathways (Jones et al., 1980).

Once in the kernel, both *A. flavus* and *F. verticillioides* are able to colonize all tissue types in the kernel (Brown et al., 1995; Fennel et al., 1973; Jones et al., 1980; Keller et al., 1994; Koehler, 1942; Lillehoj et al., 1976; Smart et al., 1990). *A. flavus* was detected in all tissues of the kernel at 96 hours after wound-inoculation (Dolezal et al., 2013). At this time point, this fungus had formed a biofilm-like structure at the endosperm-scutellum interface, which has not been observed in *F. verticillioides* infected kernels (Dolezal, 2010; Dolezal et al., 2013). *A. flavus* invades the embryo through the scutellum (Smart et al., 1990). A few publications support the idea that *A. flavus* selectively and preferentially targets the germ

when colonizing both nonwounded and wounded kernels (Keller et al., 1994; Koehler, 1942; Mellon et al., 2005; Smart et al., 1990). The highest concentration of aflatoxins was detected in the germ of wound-inoculated kernels (Keller et al., 1994). But extensive colonization was also observed in other kernel regions, such as the aleurone and endosperm (Dolezal et al., 2013).

Although progress has been made elucidating the pathogenesis of kernels by these two pathogens, it has been difficult to characterize in detail the pattern of colonization because environmental conditions greatly affect the outcome of the pathogenesis. Colonization of maize kernels by *F. verticillioides*, in particular, is poorly understood.

Factors affecting fungal infection and colonization

The severity of maize ear rot and mycotoxin accumulation caused by *A. flavus* and *F. verticillioides* varies with the weather conditions, insect activities, and the host genetic background (Parsons and Munkvod, 2010; Payne, 1992). In immature kernels, susceptibility to *A. flavus* and *F. verticillioides* is conditioned by plant stress. Typically, high temperature with drought stress favors increased infection by both fungal pathogens, and favors colonization of the kernel (Cao et al, 2013; Miller, 2001; Sampundo et al., 2005, 2007; Widstrom et al., 2003). Insect and mechanical damage are also associated with increased infection by these two fungi (Abbas et al., 2006; Miller, 2001; Ni et al., 2011; Williams et al., 2002). The southwestern corn borer (*Diatraea grandiosella*) was found to be associated with *A. flavus* infection and aflatoxin accumulation in maize kernels (Windham et al., 1999). Mechanical damage significantly affects the severity of maize ear rot and mycotoxin

contamination caused by *A. flavus* and *F. verticillioides*. Johansson et al. (2006) reported that aflatoxin and fumonisin levels in damaged and broken maize kernels were higher than in whole kernels. Furthermore, needle inoculation methods were less effective in eliciting aflatoxin production than the knife and multiple puncture methods, indicating that more damage of the kernel causes more severe infection (Widstrom et al., 1981). Observations also showed that inoculation of *A. flavus* to embryo-wounded kernels resulted in more fungal growth and aflatoxin B1 accumulation than endosperm-wounded or non-wounded kernels (Brown et al., 1993, 1997). In addition, host genetics undoubtedly plays a central role in *A. flavus* and *F. verticillioides* associated maize ear rot and mycotoxin accumulation (Brown et al., 2013; Campbell et al., 1997; Zila et al., 2013).

Disease control strategies

Cultural practices, such as insect control, prevention of plant stress, crop rotation, changing of planting dates, as well as management of irrigation, fertilization and tillage, are useful to some extent for controlling maize ear rot and subsequent mycotoxin contamination caused by *A. flavus* and *F. verticillioides* (Bruns, 2003; Munkvold, 2003; Park and Price, 2001; Payne et al., 1986, 1989; Sampundo et al., 2007). Efforts have been made to control fungal infection and reduce mycotoxin contamination by early harvest and postharvest management (Bush et al., 2004; Chulze, 2010). But most *A. flavus* resistant maize lines are late maturing (Henry, 2013). Moreover, the sexual stage of *A. flavus* was observed in nature, indicating high evolutionary potential of this pathogen population (Horn et al., 2009;

McDonald and Linde, 2002). It is even more difficult to control *F. verticillioides*-associated ear rot because maize plants may recognize this fungus as a mutualistic endophyte.

Fungicide application does not affect either *A. flavus*-associated maize ear rot incidence or aflatoxin levels (Lillehoj et al., 1984; Mazzoni et al., 2011). But fungicide application significantly reduced maize seedling blight caused by *F. verticillioides* (Munkvold and O'Mara, 2002). In addition, *F. verticillioides*-associated maize ear rot and fumonisin contamination was also significantly reduced by insect control (Blandino et al., 2009; Mazzoni et al., 2011).

Antifungal compounds and biocontrol agents represent alternative strategies to protect maize against infection by toxigenic strains of *A. flavus* and *F. verticillioides*. Bacteria, yeasts, and nontoxigenic *A. flavus* strains were tested as biocontrol agents for reducing *A. flavus* infection and aflatoxin contamination (Etcheverry et al., 2009; Lyn et al., 2009). Great success has been achieved by application of nontoxigenic *A. flavus* and *A. parasiticus* strains in corn fields (Dorner, 2009; Mehl and Cotty, 2011; Yin et al., 2008). One of the biocontrol strains produces CPA, the chronic toxicity of which may be underestimated (King et al., 2011). There are no commercial preparations for biological control of *F. verticillioides* and fumonisin contamination, but potential biocontrol agents have been identified (Bryła et al., 2013). One example is *Bacillus subtilis*, which shows the ability to inhibit *F. verticillioides* growth on maize (Cavaglieri et al., 2004, 2005a, 2005b). *Pseudomonas fluorescens* was also used as a biocontrol agent to reduce *F. verticillioides* infection and promote growth and yield of maize (Nayaka et al., 2009).

Furthermore, some microbes can be used as biocontrol agents to restrict the growth of both *A. flavus* and *F. verticillioides* on maize. *Bacillus amyloliquefaciens* significantly reduces *A. flavus* and *F. verticillioides* count in the soil (Etcheverry et al., 2009), whereas *Kluyveromyces* sp. *L16* limits infection by these pathogens on maize ears (Etcheverry et al., 2009). *Acremonium zeae*, an endophyte of maize, also inhibits growth of both *A. flavus* and *F. verticillioides* (Wicklow et al., 2005). It is likely that these biocontrol agents control diseases by competing against pathogens in the kernel. A number of studies also show the competitive relationship of *A. flavus* and *F. verticillioides* in the same kernel (Marín et al., 1998; Picco et al., 1999; Zummo and Scott, 1992).

However, these control strategies are not sufficient to eliminate maize ear rot and mycotoxin contamination caused by *A. flavus* and *F. verticillioides* (Munkvold, 2003). No strategy is effective when environmental conditions are favorable (Duvick, 2001; Payne, 1992). Developing resistant plant genotypes is one of the most promising strategies to control these diseases. Although progress has been achieved to unravel resistance mechanisms in maize kernels, it is still very difficult to identify resistance and introduce resistance genes into proprietary commercial lines (Brown et al., 2013; Campbell and White, 1995; Duvick, 2001). No commercial maize hybrid is completely resistant to these two fungal species. A better understanding of the resistance mechanisms would facilitate the development of resistant germplasms.

DEFENSE RESPONSE

Physical barriers

The husk and pericarp are the physical barriers that protect the maize kernel from pathogen attack. Good husk coverage and tightness contribute to resistance against *A. flavus* infection and aflatoxin contamination (Wicklow and Horn, 1984; Widstrom et al., 1987, 2003). Aflatoxin levels of loose-husked hybrids are approximately twice as high as those of tight-husked types (Widstrom et al., 1981). Good husk coverage also protects maize kernels from insect damage and *F. verticillioides* infection (Farrar and Davis, 1991; Parsons and Munkvold, 2010; Warfield and Davis, 1996). In addition, a large number of studies show that the wax and cutin layers of maize pericarp provide additional protection of the kernel from infection by both *A. flavus* and *F. verticillioides* (Brown et al., 2006; Guo et al., 1995, 1996, 1997; Hoenisch and Davis, 1994; Sampietro et al., 2009). Duncan and Howard (2010) suggest that the suberized membrane between the pericarp and aleurone also protects the aleurone from colonization by *F. verticillioides*. But once the kernel is damaged, these physical barriers likely will fail to prevent invasion of *A. flavus* and *F. verticillioides* (Johansson et al., 2006; Widstrom et al., 1981).

Pathogen recognition and signal transduction

Plants respond to pathogen attack by perception of the pathogen, signal transduction, transcriptional reprogramming, and accumulation of defense components. Disease resistance (R) proteins function in recognition of pathogen effectors and signal transduction (Martin et al., 2003). Maize *R* genes conferring disease resistance were analyzed using association

mapping and systematic analysis of the maize genome (Olukolu et al., 2013). But no dominant single *R* gene conferring resistance to either *A. flavus* or *F. verticillioides* has been identified, suggesting that resistance to this fungus is quantitative.

Hormone signaling networks play a central role in plant defense against pathogens. Typically, the salicylic acid (SA)-mediated signaling pathway is induced by biotrophic and hemibiotrophic pathogens, whereas resistance to necrotrophs is activated by jasmonic acid (JA) and ethylene (ET) pathways (Derksen et al., 2013; Glazebrook, 2005). Studies of developing maize kernels suggest that the JA pathway is the major player in defense against both *A. flavus* and *F. verticillioides* (Dolezal, 2010; Gao et al., 2009; Goodrich-Tanrikulu et al., 1995; Wilson et al., 2001; Zhang et al., 2005). Disruption of the maize *lipoxygenase 3* (*LOX3*) gene results in increased levels of JA and enhanced resistance to several fungal pathogens, including *F. verticillioides* (Gao et al., 2009), *Colletotrichum graminicola*, *Cochliobolus heterostrophus* (Gao et al., 2007), and *Exserohilum pedicellatum* (Isakeit et al., 2007). However, the maize *lox3* mutant shows increased susceptibility to *A. flavus* and *A. nidulans*, indicating this gene regulates defense responses in a pathogen-specific manner (Gao et al., 2009). Another maize LOX gene, *cssap 92*, is differentially expressed during infection of *A. flavus* and *F. verticillioides* (Wilson et al., 2001). The maize 12-oxo-phytodienoic acid reductases (OPRs) are also involved in biosynthesis of JA. Of the eight *OPRs* identified from the maize genome, *ZmOPR1* and *ZmOPR2* are transiently induced by *F. verticillioides* and other fungal pathogens, including *Cochliobolus carbonum* and *C. heterostrophus* (Zhang et al., 2005). Microarray studies also revealed that both LOX and

OPR genes were up-regulated during *A. flavus* infection (Dolezal, 2010). Methyl jasmonate (MeJA) inhibition of *A. flavus* growth and aflatoxin production was observed in both maize and cotton (Goodrich-Tanrikulu et al., 1995; Burow et al., 1997; Zeringue JR, 2002). The maize JA pathway is also associated with defense response to insects (Schmelz et al., 2003; Shivaji et al., 2010; Yan et al., 2012).

There is evidence showing that the SA pathway is associated with defense against *A. flavus* in maize kernels. Magbanua et al. (2007) showed that lower levels of H_2O_2 and higher levels of SA were detected in *A. flavus*-resistant maize lines as compared with susceptible lines. Although the SA pathway interacts with JA/ET pathways in an antagonistic fashion, a rich body of literature illustrates that all three pathways could be activated simultaneously in plants (Derksen et al., 2013; Mengiste, 2012; Niu et al., 2011). It is likely that both SA and JA pathways are involved in defense against *A. flavus*.

Additionally, *A. flavus* and *F. verticillioides* appear to manipulate the maize gibberellic acid (GA) pathway. GA signaling negatively regulates disease resistance by suppressing the JA pathway in rice and Arabidopsis (Achard et al., 2008; Navarro et al., 2008; Tanaka et al., 2006; Yang et al., 2012). In germinating maize seeds, GA is involved in hydrolysis of endosperm starch and proteins by stimulation of the synthesis of protease and α-amylase (Harvey and Oaks, 1974). The maize *Gibberellin 20 oxidase 2* is also up-regulated upon *A. flavus* infection, indicating changes of GA signaling in this pathosystem (Dolezal, 2010).

In maize kernels, starch degradation and premature germination often occur during infection of *A. flavus* and *F. verticillioides*. Premature germination percentages significantly increased in *A. flavus* inoculated maize kernels compared to the non-inoculated kernels (Guo et al., 1996). Previous observations indicate that *A. flavus* and *F. verticillioides* infection induces changes in carbohydrate metabolism and sugar efflux in maize kernels (Campos-Bermudez et al., 2013; Chen et al., 2010a; Dolezal, 2010; Lanubile et al., 2013). *A. flavus* hydrolases are associated with digestion of the kernel starch during infection (Mellon et al., 2007). Dolezal, 2010 also reported that a maize gene encoding a β-amylase-like enzyme was up-regulated during *A. flavus* pathogenesis. Extensive studies show that the maize trypsin inhibitor (TI) is associated with *A. flavus* resistance by inhibition of the fungal α-amylase (Chen et al., 1998, 1999a, 1999b). Additionally, hormone signaling network associated transcription factors are induced by these two fungal pathogens in the kernel (Campos-Bermudez et al., 2013; Luo et al., 2011). Taken together, these findings suggest that infection by these ear rot fungal pathogens results in modulation of the host hormone signaling network and premature germination in some kernels.

In addition, maize reactive oxygen species (ROS) and programmed cell death (PCD) associated genes, such as the *glutathione S-transferases* (*GSTs*), were highly expressed upon infection by *A. flavus* and *F. verticillioides* (Campos-Bermudez et al., 2013; Dolezal, 2010; Lanubile et al., 2013; Luo et al., 2011; Zila et al., 2013). These two necrotrophic fungal pathogens could take advantage of PCD and acquire nutrients from the dead host tissue (Mengiste, 2012).

Constitutive and inducible defense response

Extensive studies reveal that both constitutive and inducible resistance mechanisms are associated with defense against *A. flavus* in maize kernels. Real-time reverse transcription-polymerase chain reaction (RT-PCR) studies indicate that a set of maize stress-related genes is more highly expressed in *A. flavus*-resistant maize inbred lines compared with susceptible lines (Jiang et al., 2011). When the plants are challenged with *A. flavus*, fewer genes are differentially expressed in resistant lines than in susceptible lines (Luo et al., 2011). Of these genes that are differentially expressed in either resistant or susceptible lines after *A. flavus* infection, several are defense-related genes (Dolezal, 2010; Huang et al., 1997; Ji et al., 2000; Kelley et al., 2012; Luo et al., 2009, 2011). One example is *pathogenesis related 10* (*PR10*), which shows antifungal activity against *A. flavus in vitro*, and is induced upon *A. flavus* infection in the resistance line GT-MAS: gk, but not in the susceptible line Mo17 (Chen et al., 2006). Repression of maize *PR10* using RNAi gene silencing resulted in increased susceptibility to *A. flavus* infection and aflatoxin production (Chen et al., 2010b). Moreover, proteomic studies have shown that resistant maize lines defend against *A. flavus* by accumulating resistance proteins before infection. High levels of antifungal proteins are detected in the kernels, silks and rachises of the resistant lines in advance of infection, while the susceptible lines rely on inducible defenses (Chen et al., 2001; Pechanova et al., 2011; Peethambaran et al., 2010). By comparing embryo-killed and imbibed maize kernels, Chen et al. (2001) also found that both constitutive and inducible proteins were associated with *A. flavus* infection. Many of these genes and proteins identified from *A. flavus*-resistant maize

lines are differentially expressed after *A. flavus* infection, making them ideal candidates for further analysis (Table 1).

Similar to *A. flavus*, *F. verticillioides* induces more drastic gene expression changes in the susceptible maize lines than in the resistant lines (Campos-Bermudez et al., 2013; Lanubile et al., 2010, 2013) The pathogenesis-related genes are also transcribed at higher levels in kernels of the *F. verticillioides*-resistant lines before infection (Campos-Bermudez et al., 2013; Lanubile et al., 2010).

Compelling evidence suggests that distinct and shared mechanisms are involved in resistance to *A. flavus* and *F. verticillioides* in maize kernels. QTL studies show that resistance to *A. flavus* and *F. verticillioides* infection of maize kernels is significantly correlated, indicating existence of common resistance components (Robertson-Hoyt et al., 2006, 2007a). Microarray studies also show that both shared and distinctive defense mechanisms are involved in resistance to *A. flavus* and *F. verticillioides* in maize kernels (Campos-Bermudez et al., 2013; Dolezal, 2010; Lanubile et al., 2010, 2013; Luo et al., 2011). Accumulation of fungal cell wall degrading enzymes, including β-1, 3- glucanases and chitinases, is observed during infection by *A. flavus* and *F. verticillioides* (Cordero et al., 1993; Lozovaya et al., 1998; Moore et al., 2004). Additionally, maize zeamatin and ribosome-inactivating protein (RIP) are associated with defense against both *A. flavus* and *F. verticillioides* (Guo et al., 1997, 1999). However, gene mapping studies indicate that resistance to *A. flavus* ear rot, *F. verticillioides* ear rot, aflatoxin production and fumonisin

production may be at least partially under separate genetic control (Brown et al., 2010; Robertson-Hoyt et al., 2006, 2007a).

Previous studies demonstrate that maize resistance to *A. flavus* is associated with stress tolerance (Chen et al., 2002, 2004, 2007; Jiang et al., 2011). Drought tolerance as well as the abundance of wax deposits on the kernel surface contributes to resistance to aflatoxin production (Tubajika and Damann, 2001). Different levels of defense-related proteins were accumulated in aflatoxin resistant and susceptible maize lines under drought stress (Guo et al., 2008). Proteomic studies showed that *A. flavus* infection also changed the levels of many stress tolerance responsive proteins, including the late embryogenesis abundant proteins (LEAs), heat shock proteins (HSPs), a cold-regulated protein (CORp), the water stress inducible protein 18 (WSI18), and aldose reductase (ALD) (Table 1) (Chen et al., 2002, 2004, 2007).

Tissue-specific defense response

Maize kernels also show tissue-specific resistance to *A. flavus* and *F. verticillioides* (Bravo et al., 2003; Mideros et al., 2012). Mature maize kernels are composed of the pericarp, endosperm and germ (Fig. 1) (Coe, 2001). In addition to the starchy endosperm, the endosperm also contains the aleurone and the basal endosperm transfer layer (BETL). During kernel development, wax and cutin layers form over the aleurone cells on top of the pericarp. The aleurone, which is a single layer of cells beneath the pericarp, is enriched with oils and proteins (Geisler-Lee and Gallie, 2005). Extensive colonization by *A. flavus* and *F. verticillioides* is observed in the aleurone (Dolezal et al., 2013; Duncan and Howard, 2010).

Maize defense-related genes were detected in the aleurone during infection by these two pathogens (Murillo et al., 1999). The placental-chalazal tissue below the BETL forms the black layer during kernel development. The BETL at the basal end of the kernel plays an important role in kernel development and defense response to biotic and abiotic stresses (Miller and Chourey, 1992; Roitsch et al., 2003). Sucrose is broken down into glucose and fructose by a cell wall invertase (Inv-CW), and then imported into the kernel through the BETL (Cheng et al., 1996). The Inv-CWs are also recognized as defense-related compounds in maize and other plant species (Dolezal, 2010; Essmann et al., 2008; Leclere et al., 2008; Roitsch et al., 2003; Sturm and Chrispeels, 1990).

In the maize germ, the embryo is surrounded by the nutrient-rich scutellum. During seed germination, hydrolytic enzymes produced by the scutellum are recruited for starch degradation. The scutellum is also an active region protecting the embryo from pathogen attack. Two maize chitinase genes are expressed exclusively in the aleurone and germ during *A. flavus* infection (Wu et al., 1994a, 1994b). *Pathogenesis related protein*, *maize seeds* (*PRms*), is also induced in the scutellum after *F. verticillioides* infection of germinating maize seeds (Casacuberta et al., 1991, 1992). Bravo et al. (2003) suggest that *PRms* is only expressed in the epithelial cells of the scutellum infected with *F. verticillioides*. Another maize *PR* gene, *PR4*, is induced in the embryo cells that first establish contact with *F. verticillioides*, and is strongly expressed in the epithelial and the outermost parenchyma cells of the scutellum after infection (Bravo et al., 2003). A few other antifungal proteins also show tissue-specific expression patterns in the maize kernel. Maize zeamatin is mainly

localized in the embryo, whereas RIP is mostly localized in the aleurone and epithelium of the scutellum (Guo et al., 1999).

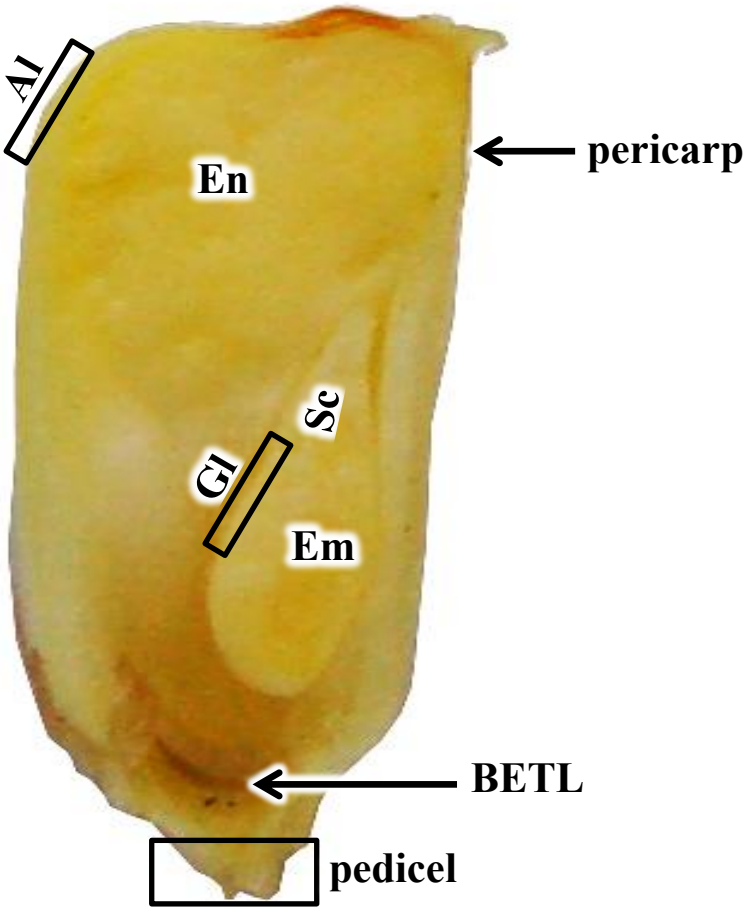

Figure 1. A vertical maize kernel section showing kernel components. Al: aleurone; En: endosperm; Gl: glandular layer; Sc: scutellum; Em: embryo; BETL: basal endosperm transfer layer.

Breeding for resistance

Progress has been made in breeding maize hybrid lines that are resistant to ear rot and mycotoxin contamination caused by *A. flavus* and *F. verticillioides* (Brown et al., 2013; Eller et al., 2010). Since resistance to these diseases is quantitative, there is no evidence of complete resistance in these two pathosystems. Plant breeders have attempted to combine resistance traits of the resistant lines with those of commercialized lines through crossing and selection. A few maize lines are considered to be good genetic breeding sources (Guo et al., 1995; Naidoo et al., 2002; Widstrom et al., 1987; Williams et al., 2008). Six maize lines with aflatoxin-resistance and good agronomic traits have been registered and released by the IITA-Nigeria (International Institute of Tropical Agriculture) and the Southern Regional Research Center of USDA-ARS in New Orleans (SRRC) (Menkir et al., 2008). These maize lines also show resistance to southern corn leaf blight and southern corn rust (Menkir et al., 2008). Aflatoxin resistance associated QTL were also identified from three resistant maize breeding lines, Mp313E, Mp715 and Mp717 (Willcox et al., 2012; Warburton et al., 2009, 2011a). The first gene-based marker, the Mississippi marker 1 (MpM1) which contains a chloroplast precursor gene with multiple polymorphisms, was developed from the aflatoxin resistant maize breeding line Mp313E (Mylroie et al., 2013). Recently, new sources of resistance to *A. flavus* infection and aflatoxin accumulation have been identified from different maize lines using phenotyping and genetic association mapping (Mideros et al., 2014; Warburton et al., 2013). Some aflatoxin-resistant maize germplasms are also resistant

to *F. verticillioides* (Brown et al., 2001), indicating that breeding for resistance to both pathogens is plausible (Campbell et al., 1997; Duvick, 2001; Hamblin and White, 2000). The major QTL associated with resistance to both *A. flavus* and *F. verticillioides* are identified in maize kernels (Robertson-Hoyt et al., 2006; Widstrom et al., 2003). In addition, QTL associated with resistance to *Fusarium* spp. and QTL associated with agronomic performance are not genetically linked, indicating that dissociation of resistance from undesirable agronomic traits is possible (Robertson-Hoyt et al., 2007b). Other tools, such as molecular marker-based breeding and transgenic strategies aimed to reduce fungal growth and mycotoxin production need to be explored.

It is hard to quantify infection and colonization of *A. flavus* and *F. verticillioides* in maize kernels, making assessment of the disease severity extremely difficult. Traditional screening methods can select only for resistance to visible symptoms of *A. flavus* and *F. verticillioides* associated maize ear rot. Invisible infection by these pathogens may not be taken into consideration. To overcome these difficulties, standard protocols have been developed to quantify fungal growth and mycotoxin production in maize kernels using toxin-based and qPCR-based screening methods (Christensen et al., 2012; Duvick, 2001; Mayer et al., 2003). However, it is still very hard to analyze the severity of maize ear rot and mycotoxin levels due to the complexity of the symptoms and the variation between kernels. Novel approaches that can better quantify fungal growth and mycotoxin levels need to be developed.

The 'omics' tools to identify resistance in maize kernels

The information generated from the use of genomic, proteomic and metabolomic tools has revolutionized biological research and provided us with opportunities to achieve resistance in maize kernels. With the rapid development of high throughput 'omics' technologies, a large number of genetic markers associated with *Aspergillus*- and *Fusarium*-ear rot have been identified from various maize populations (Kelley et al., 2010; Robertson-Hoyt et al., 2006, 2007b; Warburton et al., 2011b; Widstrom et al., 2003). These molecular markers could be used in the development of germplasm with enhanced disease resistance and reduced mycotoxin levels. Further studies need to be conducted to evaluate the effectiveness of these markers in breeding for resistance, and integrating resistance genes into maize lines with desirable agronomic traits. Moreover, the genome sequences of maize (Schnable et al., 2009), *A. flavus* (Payne et al., 2006), and *F. verticillioides* (Brown et al., 2008) are available, which greatly facilitate analysis of the data generated using the 'omics' technologies. Transcriptomic studies have been carried out on various maize organs at different developmental stages (Lai et al., 2004; Li et al., 2010; Sekhon et al., 2011). A set of gene and protein databases have been established for maize studies, including the MaizeSequence, MaizeGDB, MapMan, ProFITS, GRASSIUS, CoGePedia, and Maize Protein Atlas databases (Castellana et al., 2013; Doehlemann et al., 2008; Lawrence et al., 2004; Ling et al., 2010; Lyons and Freeling, 2008; Schnable et al., 2009; Usadel et al., 2009; Yilmaz et al., 2009). The Maize Gene Discovery Project (MGDP) sequence analysis software also offers a useful resource for pathway analysis (Lunde et al., 2003). Additionally, the

fungal secretome databases are available to analyze *A. flavus* and *F. verticillioides* secretory proteins (Choi et al., 2010; Lum and Min, 2011). Recently, several new databases have been established to provide information specifically for the maize disease research community. The Corn Fungal Resistance Associated Sequences Database (CFRAS-DB) was created using the integration of gene expression, proteomic, QTL, and sequence databases (Kelley et al., 2010). Another platform was established to identify maize candidate genes specifically for resistance to *A. flavus* infection and aflatoxin contamination (Warburton et al., 2011b). The information contained in these databases could be explored to unravel the mechanisms governing defense response to *A. flavus* and *F. verticillioides*, as well as to develop resistance in maize kernels.

Novel strategies

Transgenic approaches have been used for developing resistance to maize ear rot and mycotoxin contamination caused by *A. flavus* and *F. verticillioides*. Researchers have focused on identifying maize genes and proteins that target ear-feeding insects, ear rot fungi, and subsequent mycotoxin production (Brown et al., 2006; Duvick, 2001; Luo et al., 2009; Picot et al., 2010). Insecticidal protein coding genes from *Bacillus thuringiensis* (*Bt*) have been introduced into commercialized transgenic maize hybrids, which show enhanced resistance to insects and reduced aflatoxin and fumonisin levels (Dowd, 2000; Höfte and Whiteley, 1989; Munkvold et al., 1997). Moreover, overexpression of genes encoding antifungal proteins or genes involved in biosynthesis of antifungal secondary metabolites could confer resistance against these two fungal pathogens in maize kernels (Chen et al.,

1998, 1999a, 1999b). In addition, genetic engineering of maize plants with enhanced defense pathways is promising. Genes that interfere with mycotoxin biosynthesis pathways or are involved in detoxification of these mycotoxins are alternative candidates for transformation. One candidate is the maize gene *glyoxalase I*, which is involved in aflatoxin resistance by removing methylglyoxal (Chen et al., 2004; Bhatnagar et al., 2008). Methylglyoxal is known to facilitate aflatoxin production through up-regulation of aflatoxin biosynthesis genes in *A. flavus*.

In this review, we summarized our current understanding of the host-parasite interactions between maize and its fungal pathogens, *A. flavus* and *F. verticillioides*. These two different fungi are capable of infecting maize kernels and producing mycotoxins. The economic significance of *A. flavus* and *F. verticillioides* associated mycotoxin contamination in maize products has prompted researchers to develop resistance in maize. With the use of novel proteomic and genomic tools, a set of genes and proteins have been associated with defense response to these fungi. There is an increasing possibility of unraveling the mechanism of resistance, and developing integrated resistance to both *A. flavus* and *F. verticillioides* in maize kernels.

LITERATURE CITED

Abbas, H. K., Cartwright, R. D., Xie, W., and Thomas Shier, W. 2006. Aflatoxin and fumonisin contamination of corn (maize, *Zea mays*) hybrids in Arkansas. Crop Protection 25: 1-9.

Achard, P., Gong, F., Cheminant, S., Alioua, M., Hedden, P., and Genschik, P. 2008. The cold-inducible CBF1 factor-dependent signaling pathway modulates the accumulation of the growth-repressing DELLA proteins via its effect on gibberellin metabolism. Plant Cell 20: 2117-2129.

Alborch, L., Bragulat, M. R., and Cabañes, F. J. 2010. Comparison of two selective culture media for the detection of Fusarium infection in conventional and transgenic maize kernels. Letters in Applied Microbiology 50: 270-275.

Arias, S. L., Theumer, M. G., Mary, V. S., and Rubinstein, H. R. 2012. Fumonisins: probable role as effectors in the complex interaction of susceptible and resistant maizehybrids and *Fusarium verticillioides*. Journal of Agricultural and Food Chemistry 60: 5667-5675.

Bacon, C. W., Bennett, R. M., Hinton, D. M., and Voss, K. A. 1992. Scanning electron microscopy of *Fusarium moniliforme* within asymptomatic corn kernels and kernels associated with equine leukoencephalomalacia. Plant Disease 76: 144-148.

Baker, R. L., Brown, R. L., Chen, Z. Y., Cleveland, T. E., and Fakhoury, A. M. 2009a. A Maize Lectin-Like Protein with Antifungal Activity against *Aspergillus flavus*. Journal of Food Protection 72: 120-127.

Baker, R. L., Brown, R. L., Chen, Z. Y., Cleveland, T. E., and Fakhoury, A. M. 2009b. A Maize Trypsin Inhibitor (ZmTIp) with Limited Activity against *Aspergillus flavus*. Journal of Food Protection 72: 185-188.

Bhatnagar, D., Rajasekaran, K., Payne, G., Brown, R., Yu, J., and Cleveland, T. 2008. The 'omics' tools: genomics, proteomics, metabolomics and their potential for solving the aflatoxin contamination problem. World Mycotoxin Journal 1: 3-12.

Blandino, M., Reyneri, A., Vanara, F., Pascale, M., Haidukowski, M., and Campagna, C. 2009. Management of fumonisin contamination in maize kernels through the timing of insecticide application against the European corn borer *Ostrinia nubilalis* Hübner.

Food Additives & Contaminants: Part A, Chemistry, Analysis, Control, Exposure & Risk Assessment 26: 1501-1514.

Bravo, J. M., Campo, S., Murillo, I., Coca, M., and San Segundo, B. 2003. Fungus- and wound-induced accumulation of mRNA containing a class II chitinase of the pathogenesis-related protein 4 (PR-4) family of maize. Plant Molecular Biology 52: 745-759.

Brown, R. L., Cotty, P. J., Cleveland, T. E., and Widstrom, N. W. 1993. Living maize embryo influences accumulation of aflatoxin in maize kernels. Journal of Food Protection 56: 967-971.

Brown, R. L., Cleveland, T. E., Payne, G. A., Woloshuk, C. P., Campbell, K. W., and White, D. G. 1995. Determination of resistance to aflatoxin production in maize kernels and detection of fungal colonization using an *Aspergillus flavus* transformant expressing Escherichia coli β-glucuronidase. Phytopathology 85: 983-989.

Brown, R. L., Cleveland, T. E., Payne, G. A., Woloshuk, C. P., and White, D. G. 1997. Growth of an *Aspergillus flavus* transformant expressing *Escherichia coli* beta-glucuronidase in maize kernels resistant to aflatoxin production. Journal of Food Protection 60: 84-87.

Brown, R. L., Chen, Z. Y., Menkir, A., Cleveland, T. E., Cardwell, K., Kling, J., and White, D. G. 2001. Resistance to Aflatoxin Accumulation in Kernels of Maize Inbreds Selected for Ear Rot Resistance in West and Central Africa. Journal of Food Protection 64: 396-400.

Brown, R. L., Chen, Z. Y., Menkir, A., and Cleveland, T. E. 2006. Proteomics to identify resistance factors in corn - a review. Mycotoxin Research 22: 22-26.

Brown, D. W., Butchko, R. A., and Proctor, R. H. 2008. Genomic analysis of *Fusarium verticillioides*. Food Additives & Contaminants: Part A, Chemistry, Analysis, Control, Exposure & Risk Assessment 25: 1158-1165.

Brown, R. L., Chen, Z. Y., Warburton, M., Luo, M., Menkir, A., Fakhoury, A., and Bhatnagar, D. 2010. Discovery and characterization of proteins associated with aflatoxin-resistance: evaluating their potential as breeding markers. Toxins (Basel) 2: 919-933.

Brown, R. L., Menkir, A., Chen, Z. Y., Bhatnagar, D., Yu, J., Yao, H., and Cleveland, T. E. 2013. Breeding aflatoxin-resistant maize lines using recent advances in technologies - a review. Food Additives & Contaminants: Part A 30: 1382-1391.

Bruns, H. A. 2003. Controlling Aflatoxin and Fumonisin in Maize by Crop Management. Toxin Reviews 22: 153-173.

Bryła, M., Roszko, M., Szymczyk, K., Jędrzejczak, R., Obiedziński, M. W., and Sękul, J. 2013. Fumonisins in plant-origin food and fodder - a review. Food Additives & Contaminants: Part A, Chemistry, Analysis, Control, Exposure & Risk Assessment 30: 1626-1640.

Burow, G. B., Nesbitt, T. C., Dunlap, J., and Keller, N. P. 1997. Seed Lipoxygenase Products Modulate *Aspergillus* Mycotoxin Biosynthesis. Molecular Plant-Microbe Interactions 10: 380-387.

Bush, B. J., Carson, M. L., Cubeta, M. A., Hagler, W. M., and Payne, G. A. 2004. Infection and Fumonisin Production by *Fusarium verticillioides* in Developing Maize Kernels. Phytopathology 94: 88-93.

Campbell, K. W., and White, D. G. 1995. Evaluation of corn genotypes for resistance to *Aspergillus* ear rot, kernel infection, and aflatoxin production. Plant Disease 79: 1039-1045.

Campbell, K. W., Hamblin, A. M., and White, D. G. 1997. Inheritance of Resistance to Aflatoxin Production in the Cross Between Corn Inbreds B73 and LB31. Phytopathology 87: 1144-1147.

Campos-Bermudez, V. A., Fauguel, C. M., Tronconi, M. A., Casati, P., Presello, D. A., and Andreo, C. S. 2013. Transcriptional and metabolic changes associated to the infection by *Fusarium verticillioides* in maize inbreds with contrasting ear rot resistance. PLoS One 8: e61580.

Campo, S., Peris-Peris, C., Montesinos, L., Penas, G., Messeguer, J., and San Segundo, B. 2011. Expression of the maize ZmGF14-6 gene in rice confers tolerance to drought stress while enhancing susceptibility to pathogen infection. Journal of Experimental Botany 63: 983-999.

Cao, A., Santiago, R., Ramos, A. J., Marín, S., Reid, L. M., and Butrón, A. 2013.

Environmental factors related to fungal infection and fumonisin accumulation during the development and drying of white maize kernels. International Journal of Food Microbiology 164: 15-22.

Cardwell, K. F., Kling, J. G., Maziya-Dixon, B., and Bosque-Pérez, N. A. 2000. Interactions Between *Fusarium verticillioides*, *Aspergillus flavus*, and Insect Infestation in Four Maize Genotypes in Lowland Africa. Phytopathology 90: 276-284.

Casacuberta, J. M., Puigdomenech, P., and San Segundo, B. 1991. A gene coding for a basic pathogenesis-related (PR-like) protein from *Zea mays*. Molecular cloning and induction by a fungus (*Fusarium moniliforme*) in germinating maize seeds. Plant Molecular Biology 16: 527-536.

Casacuberta, J. M., Raventos, D., Puigdomenech, P., and San Segundo, B. 1992. Expression of the gene encoding the PR-like protein PRms in germinating maize embryos. Molecular Genetics and Genomics 234: 97-104.

CAST. 2003. Mycotoxins: Risks in plant, animal, and human systems. In: Potential Economic Costs of Mycotoxins in the United States Cast Task Force Report No. 139. January: p.136-142.

Castellana, N. E., Shen, Z., He, Y., Walley, J. W., Cassidy, C. J., Briggs, S. P., and Bafna, V. 2013. An Automated Proteogenomic Method Utilizes Mass Spectrometry to Reveal Novel Genes in *Zea mays*. Molecular & Cellular Proteomics 13: 157-167.

Cavaglieri, L., Passone, A., and Etcheverry, M. 2004. Screening procedures for selecting rhizobacteria with biocontrol effects upon *Fusarium verticillioides* growth and fumonisin B1 production. Research in Microbiology 155: 747-754.

Cavaglieri, L., Orlando, J., Rodríguez, M. I., Chulze, S., and Etcheverry, M. 2005a. Biocontrol of *Bacillus subtilis* against *Fusarium verticillioides in vitro* and at the maize root level. Research in Microbiology 156: 748-754.

Cavaglieri, L. R., Andrés, L., Ibáñez, M., and Etcheverry, M. G. 2005b. Rhizobacteria and their potential to control *Fusarium verticillioides*: effect of maize bacterisation and inoculum density. Antonie Van Leeuwenhoek 87: 179-187.

Chang, P. K., Horn, B. W., and Dorner, J. W. 2009. Clustered genes involved in cyclopiazonic acid production are next to the aflatoxin biosynthesis gene cluster in *Aspergillus flavus*. Fungal Genetics and Biology 46: 176-182.

Chen, Z. Y., Brown, R. L., Lax, A. R., Guo, B. Z., Cleveland, T. E., and Russin, J. S. 1998. Resistance to *Aspergillus flavus* in Corn Kernels Is Associated with a 14-kDa Protein. Phytopathology 88: 276-281.

Chen, Z. Y., Brown, R. L., Lax, A. R., Cleveland, T. E., and Russin, J. S. 1999a. Inhibition of plant-pathogenic fungi by a corn trypsin inhibitor overexpressed in *Escherichia coli*. Applied and Environmental Microbiology 65: 1320-1324.

Chen, Z. Y., Brown, R. L., Russin, J. S., Lax, A. R., and Cleveland, T. E. 1999b. A Corn Trypsin Inhibitor with Antifungal Activity Inhibits *Aspergillus flavus* alpha-Amylase. Phytopathology 89: 902-907.

Chen, Z. Y., Brown, R. L., Cleveland, T. E., Damann, K. E., and Russin, J. S. 2001. Comparison of Constitutive and Inducible Maize Kernel Proteins of Genotypes Resistant or Susceptible to Aflatoxin Production. Journal of Food Protection 64: 1785-1792.

Chen, Z. Y., Brown, R. L., Damann, K. E., and Cleveland, T. E. 2002. Identification of Unique or Elevated Levels of Kernel Proteins in Aflatoxin-Resistant Maize Genotypes Through Proteome Analysis. Phytopathology 92: 1084-1094.

Chen, Z. Y., Brown, R. L., Damann, K. E., and Cleveland, T. E. 2004. Identification of a Maize Kernel Stress-Related Protein and Its Effect on Aflatoxin Accumulation. Phytopathology 94: 938-945.

Chen, Z. Y., Brown, R. L., Menkir, A., Damann, K., and Cleveland, T. E. 2005. Proteome analysis of near isogenic maize lines differing in the level of resistance against *Aspergillus flavus* infection/aflatoxin production. Phytopathology 95: S19.

Chen, Z. Y., Brown, R. L., Rajasekaran, K., Damann, K. E., and Cleveland, T. E. 2006. Identification of a Maize Kernel Pathogenesis-Related Protein and Evidence for Its Involvement in Resistance to *Aspergillus flavus* Infection and Aflatoxin Production. Phytopathology 96: 87-95.

Chen, Z. Y., Brown, R. L., Damann, K. E., and Cleveland, T. E. 2007. Identification of Maize Kernel Endosperm Proteins Associated with Resistance to Aflatoxin Contamination by *Aspergillus flavus*. Phytopathology 97: 1094-1103.

Chen, L. Q., Hou, B. H., Lalonde, S., Takanaga, H., Hartung, M. L., Qu, X. Q., Guo, W. J., Kim, J. G., Underwood, W., Chaudhuri, B., Chermak, D., Antony, G., White, F. F.,

Somerville, S. C., Mudgett, M. B., and Frommer, W. B. 2010a. Sugar transporters for intercellular exchange and nutrition of pathogens. Nature 468: 527-532.

Chen, Z. Y., Brown, R. L., Damann, K. E., and Cleveland, T. E. 2010b. PR10 expression in maize and its effect on host resistance against *Aspergillus flavus* infection and aflatoxin production. Molecular Plant Pathology 11: 69-81.

Cheng, W. H., Taliercio, E. W., and Chourey, P. S. 1996. The Miniature1 Seed Locus of Maize Encodes a Cell Wall Invertase Required for Normal Development of Endosperm and Maternal Cells in the Pedicel. Plant Cell 8: 971-983.

Choi, J., Park, J., Kim, D., Jung, K., Kang, S., and Lee, Y. H. 2010. Fungal secretome database: integrated platform for annotation of fungal secretomes. BMC Genomics 11: 105.

Christensen, S., Borrego, E., Shim, W. B., Isakeit, T., and Kolomiets, M. 2012. Quantification of fungal colonization, sporogenesis, and production of mycotoxins using kernel bioassays. Journal of Visualized Experiments 23: e3727.

Chulze, S. N. 2010. Strategies to reduce mycotoxin levels in maize during storage: a review. Food Additives & Contaminants: Part A, Chemistry, Analysis, Control, Exposure & Risk Assessment 27: 651-657.

Cocchi, S., Codeluppi, M., Venturelli, C., Bedini, A., Grottola, A., Gennari, W., Cavrini, F., Di Benedetto, F., De Ruvo, N., Rumpianesi, F., Gerunda, G. E., and Guaraldi, G. 2011. *Fusarium verticillioides* fungemia in a liver transplantation patient: successful treatment with voriconazole. Diagnostic Microbiology and Infectious Disease 71: 438-441.

Coe, E. H., Jr. 2001. The origins of maize genetics. Nature Reviews Genetics 2: 898-905.

Cole, R. J. 1986. Etiology of Turkey 'X' disease in retrospect: a case for the involvement of cyclopiazonic acid. Mycotoxin Research 2: 3-7.

Cordero, M. J., Raventos, D., and San Segundo, B. 1993. Differential Expression and Induction of Chitinases and β-1,3-Glucanases in Response to Fungal Infection During Germination of Maize Seeds. Molecular Plant-Microbe Interactions 7: 23-31.

Cordero, M. J., Raventos, D., and San Segundo, B. 1994. Expression of a maize proteinase inhibitor gene is induced in response to wounding and fungal infection: systemic wound-response of a monocot gene. The Plant Journal 6: 141-150.

Cotty, P. 1998. Aflatoxin and sclerotial production by *Aspergillus flavus*: Influence of pH. Phytopathology 78: 1250-1253.

Cuero, R. G., and Osuji, G. O. 1995. *Aspergillus flavus*-induced chitosanase in germinating corn and peanut seeds: *A. flavus* mechanism for growth dominance over associated fungi and concomitant aflatoxin production. Food Additives & Contaminants 12: 479-483.

Derksen, H., Rampitsch, C., and Daayf, F. 2013. Signaling cross-talk in plant disease resistance. Plant Science 207: 79-87.

Desjardins, A. E., Plattner, R. D., Nelsen, T. C., and Leslie, J. F. 1995. Genetic analysis of fumonisin production and virulence of *Gibberella fujikuroi* mating population A (*Fusarium moniliforme*) on maize (*Zea mays*) seedlings. Applied and Environmental Microbiology 61: 79-86.

Desjardins, A. E., and Plattner, R. D. 2000. Fumonisin B(1)-nonproducing strains of *Fusarium verticillioides* cause maize (*Zea mays*) ear infection and ear rot. Journal of Agricultural and Food Chemistry 48: 5773-5780.

Doehlemann, G., Wahl, R., Horst, R. J., Voll, L. M., Usadel, B., Poree, F., Stitt, M., Pons-Kuhnemann, J., Sonnewald, U., Kahmann, R., and Kamper, J. 2008. Reprogramming a maize plant: transcriptional and metabolic changes induced by the fungal biotroph *Ustilago maydis*. The Plant Journal 56: 181-195.

Dolezal, A. L. 2010. Interactions Between *Aspergillus flavus* and the Developing Maize Kernel. Doctoral dissertation Retrieved from ProQuest Dissertations and Theses: OCLC Number: 704568905.

Dolezal, A. L., Obrian, G. R., Nielsen, D. M., Woloshuk, C. P., Boston, R. S., and Payne, G. A. 2013. Localization, morphology and transcriptional profile of *Aspergillus flavus* during seed colonization. Molecular Plant Pathology 14: 898-909.

Dorner, J. W. 2009. Biological Control of Aflatoxin Contamination in Corn Using a Nontoxigenic Strain of *Aspergillus flavus*. Journal of Food Protection 72: 801-804.

Dowd, P. F. 2000. Indirect reduction of ear molds and associated mycotoxins in *Bacillus thuringiensis* corn under controlled and open field conditions: utility and limitations. Journal of Economic Entomology 93: 1669-1679.

Duncan, K. E., and Howard, R. J. 2010. Biology of maize kernel infection by *Fusarium verticillioides*. Molecular Plant-Microbe Interactions 23: 6-16.

Duvick, J. 2001. Prospects for reducing fumonisin contamination of maize through genetic modification. Environmental Health Perspectives 109 Suppl 2: 337-342.

Eller, M. S., Payne, G. A., and Holland, J. B. 2010. Selection for Reduced *Fusarium* Ear Rot and Fumonisin Content in Advanced Backcross Maize Lines and Their Topcross Hybrids. Crop Science 50: 2249-2260.

Essmann, J., Schmitz-Thom, I., Schon, H., Sonnewald, S., Weis, E., and Scharte, J. 2008. RNA interference-mediated repression of cell wall invertase impairs defense in source leaves of tobacco. Plant Physiology 147: 1288-1299.

Etcheverry, M. G., Scandolara, A., Nesci, A., Vilas Boas Ribeiro, M. S., Pereira, P., and Battilani, P. 2009. Biological interactions to select biocontrol agents against toxigenic strains of *Aspergillus flavus* and *Fusarium verticillioides* from maize. Mycopathologia 167: 287-295.

Farrar, J., and Davis, R. 1991. Relationships among ear morphology, western flower thrips, and *Fusarium* ear rot of corn. Phytopathology 81: 661-666.

FDA. 2000. Guidance for Industry: Guidance for Industry: Action Levels for Poisonous or Deleterious Substances in Human Food and Animal Feed. U.S. Department of Health and Human Services, Food and Drug Administration: August 2000.

FDA. 2001. Guidance for Industry: Fumonisin Levels in Human Foods and Animal Feeds; Final Guidance. U.S. Department of Health and Human Services, Food and Drug Administration: Revised November 9, 2001.

Fennell, D., Bothast, R., Lillehoj, E., and Peterson, R. 1973. Bright Greenish-Yellow Fluorescence and Associated Fungi in White Corn Naturally Contaminated with Aflatoxin. Cereal Chemistry 50: 404-413.

Figueira, E. L. Z., Hirooka, E. Y., Mendiola-Olaya, E., and Blanco-Labra, A. 2003. Characterization of a Hydrophobic Amylase Inhibitor from Corn (*Zea mays*) Seeds

with Activity Against Amylase from *Fusarium verticillioides*. Phytopathology 93: 917-922.

Gao, X., Shim, W.B., Gobel, C., Kunze, S., Feussner, I., Meeley, R., Balint-Kurti, P., and Kolomiets, M. 2007. Disruption of a maize 9-lipoxygenase results in increased resistance to fungal pathogens and reduced levels of contamination with mycotoxin fumonisin. Molecular Plant-Microbe Interactions 20: 922-933.

Gao, X., Brodhagen, M., Isakeit, T., Brown, S. H., Gobel, C., Betran, J., Feussner, I., Keller, N. P., and Kolomiets, M. V. 2009. Inactivation of the lipoxygenase ZmLOX3 increases susceptibility of maize to *Aspergillus* spp. Molecular Plant-Microbe Interactions 22: 222-231.

Geisler-Lee, J., and Gallie, D. R. 2005. Aleurone Cell Identity Is Suppressed Following Connation in Maize Kernels. Plant Physiology 139: 204-212.

Gelderblom, W. C. A., Kriek, N. P. J., Marasas, W. F. O., and Thiel, P. G. 1991. Toxicity and carcinogenicity of the *Fusanum monilzforine* metabolite, fumonisin B1, in rats. Carcinogenesis 12: 1247-1251.

Gelderblom, W. C., Rheeder, J. P., Leggott, N., Stockenstrom, S., Humphreys, J., Shephard, G. S., and Marasas, W. F. 2004. Fumonisin contamination of a corn sample associated with the induction of hepatocarcinogenesis in rats-role of dietary deficiencies. Food and Chemical Toxicology 42: 471-479.

Glazebrook, J. 2005. Contrasting Mechanisms of Defense Against Biotrophic and Necrotrophic Pathogens. Annual Review of Phytopathology 43: 205-227.

Goodrich-Tanrikulu, M., Mahoney, N. E., and Rodriguez, S. B. 1995. The plant growth regulator methyl jasmonate inhibits aflatoxin production by *Aspergillus flavus*. Microbiology 141: 2831-2837.

Guo, B. Z., Russin, J. S., Cleveland, T. E., Brown, R. L., and Widstrom, N. W. 1995. Wax and Cutin Layers in Maize Kernels Associated with Resistance to Aflatoxin Production by *Aspergillus favus*. Journal of Food Protection 58: 296-300.

Guo, B. Z., Russin, J. S., Brown, R. L., Cleveland, T. E., and Widstrom, N. W. 1996. Resistance to Aflatoxin Contamination in Corn as Influenced by Relative Humidity and Kernel Germination. Journal of Food Protection 59: 276-281.

Guo, B. Z., Chen, Z. Y., Brown, R. L., Lax, A. R., Cleveland, T. E., Russin, J. S., Mehta, A. D., Selitrennikoff, C. P., and Widstrom, N. W. 1997. Germination induces accumulation of specific proteins and antifungal activities in corn kernels. Phytopathology 87: 1174-1178.

Guo, B. Z., Cleveland, T. E., Brown, R. L., Widstrom, N. W., Lynch, R. E., and Russin, J. S. 1999. Distribution of antifungal proteins in maize kernel tissues using immunochemistry. Journal of Food Protection 62: 295-299.

Guo, B., Chen, Z. Y., Lee, R. D., and Scully, B. T. 2008. Drought stress and preharvest aflatoxin contamination in agricultural commodity: genetics, genomics and proteomics. Journal of Integrative Plant Biology 50: 1281-1291.

Hamblin, A. M., and White, D. G. 2000. Inheritance of resistance to *Aspergillus* ear rot and aflatoxin production of corn from tex6. Phytopathology 90: 292-296.

Harrison, L. R., Colvin, B. M., Greene, J. T., Newman, L. E., and Cole, J. R. 1990. Pulmonary Edema and Hydrothorax in Swine Produced by Fumonisin B1, a Toxic Metabolite of *Fusarium Moniliforme*. Journal of Veterinary Diagnostic Investigation 2: 217-221.

Harvey, B. M. R., and Oaks, A. 1974. The Role of Gibberellic Acid in the Hydrolysis of Endosperm Reserves in *Zea mays*. Planta (Berl.) 121: 67-74.

Hedayati, M. T., Pasqualotto, A. C., Warn, P. A., Bowyer, P., and Denning, D. W. 2007. *Aspergillus flavus*: human pathogen, allergen and mycotoxin producer. Microbiology 153: 1677-1692.

Hendricks, K. 1999. Fumonisins and neural tube defects in South Texas. Epidemiology 10: 198-200.

Henry, W. B. 2013. Maize aflatoxin accumulation segregates with early maturing selections from an S2 breeding cross population. Toxins (Basel) 5: 162-172.

Hesseltine, C., and Bothast, R. 1977. Mold development in ears of corn from tasseling to harvest. Mycologia 9: 328-340.

Hoenisch, R., and Davis, R. 1994. Relationship between kernel pericarp thickness and susceptibility to *Fusarium* ear rot in field corn. Plant Disease 78: 517-519.

Höfte, H., and Whiteley, H. R. 1989. Insecticidal crystal proteins of *Bacillus thuringiensis*. Microbiological Reviews 53: 242-255.

Horn, B. W., Moore, G. G., and Carbone, I. 2009. Sexual reproduction in *Aspergillus flavus*. Mycologia 101: 423-429.

Hruska, Z., Yao, H., Kincaid, R., Darlington, D., Brown, R. L., Bhatnagar, D., and Cleveland, T. E. 2013. Fluorescence Imaging Spectroscopy (FIS) for Comparing Spectra from Corn Ears Naturally and Artificially Infected with Aflatoxin Producing Fungus. Journal of Food Science 78: T1313-T1320.

Huang, Z., White, D. G., and Payne, G. A. 1997. Corn Seed Proteins Inhibitory to *Aspergillus flavus* and Aflatoxin Biosynthesis. Phytopathology 87: 622-627.

Isakeit, T., Gao, X., and Kolomiets, M. 2007. Increased Resistance of a Maize Mutant Lacking the 9-Lipoxygenase Gene, ZmLOX3, to Root Rot Caused by *Exserohilum pedicellatum*. Phytopathology 155: 758-760.

Ji, C., Norton, R. A., Wicklow, D. T., and Dowd, P. F. 2000. Isoform patterns of chitinase and beta-1,3-glucanase in maturing corn kernels (*Zea mays* L.) associated with *Aspergillus flavus* milk stage infection. Journal of Agricultural and Food Chemistry 48: 507-511.

Jiang, T., Zhou, B., Luo, M., Abbas, H. K., Kemerait, R., Lee, R. D., Scully, B. T., and Guo, B. 2011. Expression Analysis of Stress-Related Genes in Kernels of Different Maize (*Zea mays* L.) Inbred Lines with Different Resistance to Aflatoxin Contamination. Toxins (Basel) 3: 538-550.

Johansson, A. S., Whitaker, T. B., Hagler, W. M., Jr., Bowman, D. T., Slate, A. B., and Payne, G. 2006. Predicting aflatoxin and fumonisin in shelled corn lots using poor-quality grade components. Journal of AOAC International 89: 433-440.

Jones, R. K., Duncan, H. E., Payne, G. A., and Leonard, K. J. 1980. Factors influencing infection by *Aspergillus flavus* in silk-inoculated corn. Plant Diseases 64: 859-863.

Keller, N. P., Butchko, R., Sarr, B., and Phillips, T. D. 1994. A Visual Pattern of Mycotoxin Production in Maize Kernels by *Aspergillus* spp. Phytopathology 84: 483-488.

Kellerman, T. S., Marasas, W. F. O., Thiel, P. G., Gelderblom, W. C. A., Cawood, M., and Coetzer, J. A. W. 1990. Leucoencephalomalacia in two horses induced by oral dosing of fumonisin B1. Onderstepoort Journal of Veterinary Research 57: 269-275.

Kelley, R. Y., Gresham, C., Harper, J., Bridges, S. M., Warburton, M. L., Hawkins, L. K., Pechanova, O., Peethambaran, B., Pechan, T., Luthe, D. S., Mylroie, J. E., Ankala, A., Ozkan, S., Henry, W. B., and Williams, W. P. 2010. Integrated database for identifying candidate genes for *Aspergillus flavus* resistance in maize. BMC Bioinformatics 11 Suppl 6: S25.

Kelley, R. Y., Williams, W. P., Mylroie, J. E., Boykin, D. L., Harper, J. W., Windham, G. L., Ankala, A., and Shan, X. 2012. Identification of maize genes associated with host plant resistance or susceptibility to *Aspergillus flavus* infection and aflatoxin accumulation. PLoS One 7: e36892.

Kew, M. C. 2013. Aflatoxins as a cause of hepatocellular carcinoma. Journal of Gastrointestinal and Liver Diseases 22: 305-310.

Khlangwiset, P., Shephard, G. S., and Wu, F. 2011. Aflatoxins and growth impairment: A review. Critical Reviews in Toxicology 41: 740-755.

Kim, H., Smith, J. E., Ridenour, J. B., Woloshuk, C. P., and Bluhm, B. H. 2011. HXK1 regulates carbon catabolism, sporulation, fumonisin B production and pathogenesis in *Fusarium verticillioides*. Microbiology 157: 2658-2669.

Kim, H., and Woloshuk, C. P. 2011. Functional characterization of fst1 in *Fusarium verticillioides* during colonization of maize kernels. Molecular Plant-Microbe Interactions 24: 18-24.

King, E. D., Bobby Bassi, A. B., Jr., Ross, D. C., and Druebbisch, B. 2011. An industry perspective on the use of "atoxigenic" strains of *Aspergillus flavus* as biological control agents and the significance of cyclopiazonic acid. Toxin Reviews 30: 33-41.

Koehler, B. 1942. Natural mode of entrance of fungi into Corn ears and some symptoms that indicate infection. Journal of Agricultural Research 64: 421-442.

Krishnamachari, K. A., Bhat, R. V., Nagarajan, V., and Tilak, T. B. 1975. Hepatitis due to aflatoxicosis. An outbreak in Western India. The Lancet 1: 1061-1063.

Lai, J., Dey, N., Kim, C. S., Bharti, A. K., Rudd, S., Mayer, K. F., Larkins, B. A., Becraft, P., and Messing, J. 2004. Characterization of the maize endosperm transcriptome and its comparison to the rice genome. Genome Research 14: 1932-1937.

Lanubile, A., Pasini, L., and Marocco, A. 2010. Differential gene expression in kernels and silks of maize lines with contrasting levels of ear rot resistance after *Fusarium verticillioides* infection. Journal of Plant Physiology 167: 1398-1406.

Lanubile, A., Logrieco, A., Battilani, P., Proctor, R. H., and Marocco, A. 2013. Transcriptional changes in developing maize kernels in response to fumonisin-producing and nonproducing strains of *Fusarium verticillioides*. Plant Science 210: 183-192.

Lawrence, C. J., Dong, Q., Polacco, M. L., Seigfried, T. E., and Brendel, V. 2004. MaizeGDB, the community database for maize genetics and genomics. Nucleic Acids Research 32: D393-D397.

Leclere, S., Schmelz, E., and Chourey, P. 2008. Cell wall invertase-deficient miniature1 kernels have altered phytohormone levels. Phytochemistry 69: 692-699.

Lee, K., Pan, J. J., and May, G. 2009. Endophytic *Fusarium verticillioides* reduces disease severity caused by *Ustilago maydis* on maize. FEMS Microbiology Letters 299: 31-37.

Lewis, L., Onsongo, M., Njapau, H., Schurz-Rogers, H., Luber, G., Kieszak, S., Nyamongo, J., Backer, L., Dahiye, A.M., Misore, A., DeCock, K., and Rubin, C. 2005. Aflatoxin contamination of commercial maize products during an outbreak of acute aflatoxicosis in eastern and central Kenya. Environmental Health Perspectives 113: 1763-1767.

Li, P., Ponnala, L., Gandotra, N., Wang, L., Si, Y., Tausta, S. L., Kebrom, T. H., Provart, N., Patel, R., Myers, C. R., Reidel, E. J., Turgeon, R., Liu, P., Sun, Q., Nelson, T., and Brutnell, T. P. 2010. The developmental dynamics of the maize leaf transcriptome. Nature Genetics 42: 1060-1067.

Lillehoj, E. B., Kwolek, W. F., Peterson, R. E., Shotwell, O. L., and Hesseltine, C. W. 1976. Aflatoxin Contamination, Fluorescence, and Insect Damage in Corn Infected with *Aspergillus flavus* before Harvest. Cereal Chemistry 53: 505-512.

Lillehoj, E. B., Calvert, O. H., Kwolek, W. F., and Zuber, M. S. 1979. Aflatoxin variation among corn samples with varying ratios of *Aspergillus flavus*-inoculated/noninoculated kernels. Journal - Association of Official Analytical Chemists 62: 1083-1086.

Lillehoj, E. B., McMillian, W. W., Widstrom, N. W., Guthrie, W. D., Jarvis, J. L., Barry, D., and Kwolek, W. F. 1984. Aflatoxin contamination of maize kernels before harvest. Interaction of *Aspergillus flavus* spores, corn earworm larvae and fungicide applications. Mycopathologia 86: 77-81.

Ling, Y., Du, Z., Zhang, Z., and Su, Z. 2010. ProFITS of maize: a database of protein families involved in the transduction of signalling in the maize genome. BMC Genomics 11: 580.

Lozovaya, V. V., Waranyuwat, A., and Widholm, J. M. 1998. Beta-1,3-Glucanase and resistance to *Aspergillus flavus* infection in maize. Crop Science 38: 1255-1260.

Lum, G., and Min, X. J. 2011. FunSecKB: the Fungal Secretome KnowledgeBase. Database (Oxford): bar001.

Lunde, C. F., Morrow, D. J., Roy, L. M., and Walbot, V. 2003. Progress in maize gene discovery: a project update. Functional & Integrative Genomics 3: 25-32.

Luo, M., Brown, R. L., Chen, Z. Y., and Cleveland, T. E. 2009. Host genes involved in the interaction between *Aspergillus flavus* and maize. Toxin Reviews 28: 118-128.

Luo, M., Brown, R. L., Chen, Z. Y., Menkir, A., Yu, J., and Bhatnagar, D. 2011. Transcriptional Profiles Uncover *Aspergillus flavus*-Induced Resistance in Maize Kernels. Toxins (Basel) 3: 766-786.

Lyn, M. E., Abbas, H. K., Zablotowicz, R. M., and Johnson, B. J. 2009. Delivery systems for biological control agents to manage aflatoxin contamination of pre-harvest maize. Food Additives & Contaminants: Part A, Chemistry, Analysis, Control, Exposure & Risk Assessment 26: 381-387.

Lyons, E., and Freeling, M. 2008. How to usefully compare homologous plant genes and chromosomes as DNA sequences. The Plant Journal 53: 661-673.

Magbanua, Z. V., De Moraes, C. M., Brooks, T. D., Williams, W. P., and Luthe, D. S. 2007. Is catalase activity one of the factors associated with maize resistance to *Aspergillus flavus*? Molecular Plant-Microbe Interactions 20: 697-706.

Marasas, W. F. 2001. Discovery and occurrence of the fumonisins: a historical perspective. Environmental Health Perspectives 109 Suppl 2: 239-243.

Marasas, W. F., Riley, R. T., Hendricks, K. A., Stevens, V. L., Sadler, T. W., Gelineau-van Waes, J., Missmer, S. A., Cabrera, J., Torres, O., Gelderblom, W. C., Allegood, J., Martinez, C., Maddox, J., Miller, J. D., Starr, L., Sullards, M. C., Roman, A. V., Voss, K. A., Wang, E., and Merrill, A. H., Jr. 2004. Fumonisins disrupt sphingolipid metabolism, folate transport, and neural tube development in embryo culture and in vivo: a potential risk factor for human neural tube defects among populations consuming fumonisin-contaminated maize. Journal of Nutrition 134: 711-716.

Marín, S., Sanchis, V., Arnau, F., Ramos, A. J., and Magan, N. 1998. Colonisation and competitiveness of *Aspergillus* and *Penicillium* species on maize grain in the presence of *Fusarium moniliforme* and *Fusarium proliferatum*. International Journal of Food Microbiology 45: 107-117.

Marsh, S. F., and Payne, G. A. 1984. Scanning EM Studies on the Colonization of Dent Corn By *Aspergillus flavus*. Phytopathology 74: 557-561.

Martin, G. B., Bogdanove, A. J., and Sessa, G. 2003. Understanding the functions of plant disease resistance proteins. Annual Review of Plant Biology 54: 23-61.

Mayer, Z., Bagnara, A., Färber, P., and Geisen, R. 2003. Quantification of the copy number of nor-1, a gene of the aflatoxin biosynthetic pathway by real-time PCR, and its correlation to the cfu of *Aspergillus flavus* in foods. International Journal of Food Microbiology 82: 143-151.

Mazzoni, E., Scandolara, A., Giorni, P., Pietri, A., and Battilani, P. 2011. Field control of *Fusarium* ear rot, *Ostrinia nubilalis* (Hübner), and fumonisins in maize kernels. Pest Management Science 67: 458-465.

McDonald, B. A., and Linde, C. 2002. Pathogen population genetics, evolutionary potential, and durable resistance. Annual Review of Phytopathology 40: 349-379.

Mehl, H. L., and Cotty, P. J. 2010. Variation in Competitive Ability Among Isolates of *Aspergillus flavus* from Different Vegetative Compatibility Groups During Maize Infection. Phytopathology 100: 150-159.

Mehl, H. L., and Cotty, P. J. 2011. Influence of the Host Contact Sequence on the Outcome of Competition among *Aspergillus flavus* Isolates during Host Tissue Invasion. Applied and Environmental Microbiology 77: 1691-1697.

Mellon, J. E., Dowd, M. K., and Cotty, P. J. 2005. Substrate utilization by *Aspergillus flavus* in inoculated whole corn kernels and isolated tissues. Journal of Agricultural and Food Chemistry 53: 2351-2357.

Mellon, J., Cotty, P. J., and Dowd, M. 2007. *Aspergillus flavus* hydrolases: Their roles in pathogenesis and substrate utilization. Applied Microbiology and Biotechnology 77: 497-504.

Mengiste, T. 2012. Plant Immunity to Necrotrophs. Annual Review of Phytopathology 50: 267-294.

Menkir, A., Brown, R. L., Bandyopadhyay, R., and Cleveland, T. E. 2008. Registration of six tropical maize germplasm lines with resistance to aflatoxin contamination. Journal of Plant Registrations 2: 246-250.

Mideros, S. X., Windham, G. L., Williams, W. P., and Nelson, R. J. 2012. Tissue-Specific Components of Resistance to *Aspergillus* Ear Rot of Maize. Phytopathology 102: 787-793.

Mideros, S. X., Warburton, M. L., Jamann, T. M., Windham, G. L., Williams, W. P., and Nelson, R. J. 2014. Quantitative Trait Loci Influencing Mycotoxin Contamination of Maize: Analysis by Linkage Mapping, Characterization of Near-Isogenic Lines, and Meta-Analysis. Crop Science 54: 127-142.

Miller, M. E., and Chourey, P. S. 1992. The Maize Invertase-Deficient miniature-1 Seed Mutation Is Associated with Aberrant Pedicel and Endosperm Development. Plant Cell 4: 297-305.

Miller, J. D. 2001. Factors that affect the occurrence of fumonisin. Environmental Health Perspectives 2: 321-324.

Moore, K. G., Price, M. S., Boston, R. S., Weissinger, A. K., and Payne, G. A. 2004. A Chitinase from Tex6 Maize Kernels Inhibits Growth of *Aspergillus flavus*. Phytopathology 94: 82-87.

Mukherjee, M., Kim, J. E., Park, Y. S., Kolomiets, M. V., and Shim, W. B. 2011. Regulators of G-protein signalling in *Fusarium verticillioides* mediate differential host-pathogen responses on nonviable versus viable maize kernels. Molecular Plant Pathology 12: 479-491.

Munkvold, G. P., McGee, D. C., and Carlton, W. M. 1997. Importance of Different Pathways for Maize Kernel Infection by *Fusarium moniliforme*. Phytopathology 87: 209-217.

Munkvold, G. P., and O'Mara, J. K. 2002. Laboratory and Growth Chamber Evaluation of Fungicidal Seed Treatments for Maize Seedling Blight Caused by *Fusarium* Species. Plant Disease 86: 143-150.

Munkvold, G. P. 2003. Cultural and genetic approaches managing mycotoxins in maize. Annual Review of Phytopathology 41: 99-116.

Murillo, I., Cavallarin, L., and Segundo, B. S. 1999. Cytology of Infection of Maize Seedlings by *Fusarium moniliforme* and Immunolocalization of the Pathogenesis-Related PRms Protein. Phytopathology 89: 737-747.

Mylroie, J. E., Warburton, M. L., and Wilkinson, J. R. 2013. Development of a gene-based marker correlated to reduced aflatoxin accumulation in maize. Euphytica 194: 431-441.

Naidoo, G., Forbes, A. M., Paul, C., White, D. G., and Rocheford, T. R. 2002. Resistance to *Aspergillus* Ear Rot and Aflatoxin Accumulation in Maize F1 Hybrids. Crop Science 42: 360-364.

Naumann, T. A., Wicklow, D. T., and Price, N. P. 2011. Identification of a chitinase-modifying protein from *Fusarium verticillioides*: truncation of a host resistance protein by a fungalysin metalloprotease. Journal of Biological Chemistry 286: 35358-35366.

Navarro, L., Bari, R., Achard, P., Lisón, P., Nemri, A., Harberd, N. P., and Jones, J. D. 2008. DELLAs Control Plant Immune Responses by Modulating the Balance of Jasmonic Acid and Salicylic Acid Signaling. Current Biology 18: 650-655.

Nayaka, S. C., Shankar, A. C., Reddy, M. S., Niranjana, S. R., Prakash, H. S., Shetty, H. S., and Mortensen, C. N. 2009. Control of *Fusarium verticillioides*, cause of ear rot of maize, by *Pseudomonas fluorescens*. Pest Management Science 65: 769-775.

Ni, X., Wilson, J. P., Buntin, G. D., Guo, B., Krakowsky, M. D., Lee, R. D., Cottrell, T. E., Scully, B. T., Huffaker, A., and Schmelz, E. A. 2011. Spatial Patterns of Aflatoxin Levels in Relation to Ear-Feeding Insect Damage in Pre-Harvest Corn. Toxins 3: 920-931.

Nielsen, K., Payne, G. A., and Boston, R. S. 2001. Maize ribosome-inactivating protein inhibits normal development of *Aspergillus nidulans* and *Aspergillus flavus*. Molecular Plant-Microbe Interactions 14: 164-172.

Niu, D. D., Liu, H. X., Jiang, C. H., Wang, Y. P., Wang, Q. Y., Jin, H. L., and Guo, J. H. 2011. The Plant Growth-Promoting Rhizobacterium *Bacillus cereus* AR156 Induces Systemic Resistance in *Arabidopsis thaliana* by Simultaneously Activating Salicylate- and Jasmonate/Ethylene-Dependent Signaling Pathways. Molecular Plant-Microbe Interactions 24: 533-542.

Olukolu, B. A., Negeri, A., Dhawan, R., Venkata, B. P., Sharma, P., Garg, A., Gachomo, E., Marla, S., Chu, K., Hasan, A., Ji, J., Chintamanani, S., Green, J., Shyu, C. R., Wisser, R., Holland, J., Johal, G., and Balint-Kurti, P. 2013. A connected set of genes associated with programmed cell death implicated in controlling the hypersensitive response in maize. Genetics 193: 609-620.

Park, D. L., and Price, W. D. 2001. Reduction of aflatoxin hazards using ammoniation. Reviews Of Environmental Contamination And Toxicology 171: 139-175.

Parsons, M. W., and Munkvold, G. P. 2010. Associations of planting date, drought stress, and insects with *Fusarium* ear rot and fumonisin B1 contamination in California maize. Food Additives & Contaminants: Part A, Chemistry, Analysis, Control, Exposure & Risk Assessment 27: 591-607.

Payne, G. A., Cassel, D. K., and Adkins, C. R. 1986. Reduction of aflatoxin contamination in corn by irrigation and tillage. Phytopathology 76: 679-684.

Payne, G. A., Kamprath, E. J., and Adkins, C. R. 1989. Increased Aflatoxin Contamination in Nitrogen-Stressed Corn. Plant Disease 73: 556-559.

Payne, G. A. 1992. Aflatoxin in maize. Critical Reviews in Plant Sciences 10: 423-440.

Payne, G. A., and Brown, M. P. 1998. Genetics and physiology of aflatoxin biosynthesis. Annual Review of Phytopathology 36: 329-362.

Payne, G. A., Nierman, W. C., Wortman, J. R., Pritchard, B. L., Brown, D., Dean, R. A., Bhatnagar, D., Cleveland, T. E., Machida, M., and Yu, J. 2006. Whole genome comparison of *Aspergillus flavus* and *A. oryzae.* Medical Mycology 44: 9-11.

Payne, A. G., and Yu, J. 2010. Ecology, Development and Gene Regulation in *Aspergillus flavus*. *Aspergillus*: Molecular Biology and Genomics. Edited by Masayuki Machida and Katsuya Gomi Caister Academic Press: 159.

Pechanova, O., Pechan, T., Williams, W. P., and Luthe, D. S. 2011. Proteomic analysis of the maize rachis: potential roles of constitutive and induced proteins in resistance to *Aspergillus flavus* infection and aflatoxin accumulation. Proteomics 11: 114-127.

Peethambaran, B., Hawkins, L., Windham, G. L., Williams, W. P., and Luthe, D. S. 2010. Anti-fungal activity of maize silk proteins and role of chitinases in *Aspergillus flavus* resistance. Toxin Reviews 29: 27-39.

Pei-Bao, Z., Ren, A. Z., Xu, H. J., and Li, D. C. 2010. The gene fpk1, encoding a cAMP-dependent protein kinase catalytic subunit homolog, is required for hyphal growth, spore germination, and plant infection in *Fusarium verticillioides*. Journal of Microbiology and Biotechnology 20: 208-216.

Pelizza, S. A., Stenglein, S. A., Cabello, M. N., Dinolfo, M. I., and Lange, C. E. 2011. First record of *Fusarium verticillioides* as an entomopathogenic fungus of grasshoppers. Journal of Insect Science 11: 70.

Picco, M., Nesci, A., Barros, G., Cavaglieri, L., and Etcheverry, M. 1999. Aflatoxin B1 and fumosin B1 in mixed cultures of *Aspergillus flavus* and *Fusarium proliferatum* on maize. Natural Toxins 7: 331-336.

Picot, A., Barreau, C., Pinson-Gadais, L., Caron, D., Lannou, C., and Richard-Forget, F. 2010. Factors of the *Fusarium verticillioides*-maize environment modulating fumonisin production. Critical Reviews in Microbiology 36: 221-231.

Picot, A., Barreau, C., Pinson-Gadais, L., Piraux, F., Caron, D., Lannou, C., and Richard-Forget, F. 2011. The dent stage of maize kernels is the most conducive for fumonisin biosynthesis under field conditions. Applied and Environmental Microbiology 77: 8382-8390.

Pienaar, J. G., Kellerman, T. S., and Marasas, W. F. 1981. Field outbreaks of leukoencephalomalacia in horses consuming maize infected by *Fusarium verticillioides* (= *F. moniliforme*) in South Africa. Journal of the South African Veterinary Association 52: 21-24.

Rambo, G., Tuite, J., and Crane, P. 1974. Preharvest inoculation and infection of dent corn ears with *Aspergillus flavus* and *A. parasiticus*. Phytopathology 64: 797-800.

Reese, B. N., Payne, G. A., Nielsen, D. M., and Woloshuk, C. P. 2011. Gene expression profile and response to maize kernels by *Aspergillus flavus*. Phytopathology 101: 797-804.

Rheeder, J. P., Marasas, W. F. O., Thiel, P. G., Sydenham, E. W., Shephard, G. S., and Schalkwyk, D. J. 1992. *Fusarium moniliforme* and Fumonisins in Corn in Relation to Human Esophageal Cancer in Transkei. Phytopathology 82: 353-357.

Riley, R. T., Voss, K. A., Yoo, H. S., Gelderblom, W. C. A., and Merrill, A. H. 1994. Mechanism of Fumonisin Toxicity and Carcinogenesis. Journal of Food Protection 57: 638-645.

Robertson-Hoyt, L. A., Jines, M. P., Balint-Kurti, P. J., Kleinschmidt, C. E., White, D. G., Payne, G. A., Maragos, C. M., Molnar, T. L., and Holland, J. B. 2006. QTL Mapping for *Fusarium* Ear Rot and Fumonisin Contamination Resistance in Two Maize Populations. Crop Science 46: 1734-1743.

Robertson-Hoyt, L. A., Kleinschmidt, C. E., White, D. G., Payne, G. A., Maragos, C. M., and Holland, J. B. 2007a. Relationships of Resistance to *Fusarium* Ear Rot and Fumonisin Contamination with Agronomic Performance of Maize. Crop Science 47: 1770-1778.

Robertson-Hoyt, L. A., Betran, J., Payne, G. A., White, D. G., Isakeit, T., Maragos, C. M., Molnar, T. L., and Holland, J. B. 2007b. Relationships Among Resistances to *Fusarium* and *Aspergillus* Ear Rots and Contamination by Fumonisin and Aflatoxin in Maize. Phytopathology 97: 311-317.

Rodriguez Estrada, A. E., Jonkers, W., Kistler, H. C., and May, G. 2012. Interactions between *Fusarium verticillioides*, *Ustilago maydis*, and *Zea mays*: an endophyte, a pathogen, and their shared plant host. Fungal Genetics and Biology 49: 578-587.

Roitsch, T., Balibrea, M. E., Hofmann, M., Proels, R., and Sinha, A. K. 2003. Extracellular invertase: key metabolic enzyme and PR protein. Journal of Experimental Botany 54: 513-524.

Rokas, A., Payne, G., Fedorova, N. D., Baker, S. E., Machida, M., Yu, J., Georgianna, D. R., Dean, R. A., Bhatnagar, D., Cleveland, T. E., Wortman, J. R., Maiti, R., Joardar, V., Amedeo, P., Denning, D. W., and Nierman, W. C. 2007. What can comparative genomics tell us about species concepts in the genus *Aspergillus*? Studies in Mycology 59: 11-17.

Saccardo, P. A. 1881. Fungi italici autographice delineati. Patavii 879.

Sadler, T. W., Merrill, A. H., Stevens, V. L., Sullards, M. C., Wang, E., and Wang, P. 2002. Prevention of fumonisin B1-induced neural tube defects by folic acid. Teratology 66: 169-176.

Sagnelli, C., Fumagalli, L., Prigitano, A., Baccari, P., Magnani, P., and Lazzarin, A. 2006. Successful voriconazole therapy of disseminated *Fusarium verticillioides* infection in an immunocompromised patient receiving chemotherapy. Journal of Antimicrobial Chemotherapy 57: 796-798.

Samapundo, S., Devliehgere, F., De Meulenaer, B., and Debevere, J. 2005. Effect of water activity and temperature on growth and the relationship between fumonisin production and the radial growth of *Fusarium verticillioides* and *Fusarium proliferatum* on corn. Journal of Food Protection 68: 1054-1059.

Samapundo, S., Devlieghere, F., De Meulenaer, B., Lamboni, Y., Osei-Nimoh, D., and Debevere, J. M. 2007. Interaction of water activity and bicarbonate salts in the inhibition of growth and mycotoxin production by *Fusarium* and *Aspergillus* species of importance to corn. International Journal of Food Microbiology 116: 266-274.

Sampietro, D. A., Vattuone, M. A., Presello, D. A., Fauguel, C. M., and Catalán, C. A. N. 2009. The pericarp and its surface wax layer in maize kernels as resistance factors to fumonisin accumulation by *Fusarium verticillioides*. Crop Protection 28: 196-200.

Sanchez-Rangel, D., Sanchez-Nieto, S., and Plasencia, J. 2012. Fumonisin B1, a toxin produced by *Fusarium verticillioides*, modulates maize beta-1,3-glucanase activities involved in defense response. Planta 235: 965-978.

Schmelz, E. A., Alborn, H. T., Banchio, E., and Tumlinson, J. H. 2003. Quantitative relationships between induced jasmonic acid levels and volatile emission in *Zea mays* during Spodoptera exigua herbivory. Planta 216: 665-673.

Schnable, P. S., Ware, D., Fulton, R. S., Stein, J. C., Wei, F., Pasternak, S., Liang, C., Zhang, J., Fulton, L., Graves, T. A., Minx, P., Reily, A. D., Courtney, L., Kruchowski, S. S., Tomlinson, C., Strong, C., Delehaunty, K., Fronick, C., Courtney, B., Rock, S. M., Belter, E., Du, F., Kim, K., Abbott, R. M., Cotton, M., Levy, A., Marchetto, P., Ochoa, K., Jackson, S. M., Gillam, B., Chen, W., Yan, L., Higginbotham, J., Cardenas, M., Waligorski, J., Applebaum, E., Phelps, L., Falcone, J., Kanchi, K., Thane, T., Scimone, A., Thane, N., Henke, J., Wang, T., Ruppert, J., Shah, N., Rotter, K., Hodges, J., Ingenthron, E., Cordes, M., Kohlberg, S., Sgro, J., Delgado, B., Mead, K., Chinwalla, A., Leonard, S., Crouse, K., Collura, K., Kudrna, D., Currie, J., He, R., Angelova, A., Rajasekar, S., Mueller, T., Lomeli, R., Scara, G., Ko, A., Delaney, K., Wissotski, M., Lopez, G., Campos, D., Braidotti, M., Ashley, E., Golser, W., Kim, H., Lee, S., Lin, J., Dujmic, Z., Kim, W., Talag, J., Zuccolo, A., Fan, C., Sebastian, A., Kramer, M., Spiegel, L., Nascimento, L., Zutavern, T., Miller, B., Ambroise, C., Muller, S., Spooner, W., Narechania, A., Ren, L., Wei, S., Kumari, S., Faga, B., Levy, M. J., McMahan, L., Van Buren, P., Vaughn, M. W., Ying, K., Yeh, C. T., Emrich, S. J., Jia, Y., Kalyanaraman, A., Hsia, A. P., Barbazuk, W. B., Baucom, R. S., Brutnell, T. P., Carpita, N. C., Chaparro, C., Chia, J. M., Deragon, J. M., Estill, J. C., Fu, Y., Jeddeloh, J. A., Han, Y., Lee, H., Li, P., Lisch, D. R., Liu, S., Liu, Z., Nagel, D. H., McCann, M. C., SanMiguel, P., Myers, A. M., Nettleton, D., Nguyen, J., Penning, B. W., Ponnala, L., Schneider, K. L., Schwartz, D. C., Sharma, A., Soderlund, C., Springer, N. M., Sun, Q., Wang, H., Waterman, M., Westerman, R., Wolfgruber, T. K., Yang, L. Y., Y., Zhang, L., Zhou, S., Zhu, Q., Bennetzen, J. L., Dawe, R. K., Jiang, J., Jiang, N., Presting, G. G., Wessler, S. R., Aluru, S., Martienssen, R. A., Clifton, S. W., McCombie, W. R., Wing, R. A., and Wilson, R. K. 2009. The B73 Maize Genome: Complexity, Diversity, and Dynamics. Science 326: 1112-1115.

Scott, G. E., and Zummo, N. 1990. Registration of Mp313E Parental Line of Maize. Crop Science 30: 1378-1378.

Scott, G. E., and Zummo, N. 1992. Registration of Mp420 germplasm line of maize. Crop Science 32: 1296.

Sekhon, R. S., Lin, H., Childs, K. L., Hansey, C. N., Buell, C. R., de Leon, N., and Kaeppler, S. M. 2011. Genome-wide atlas of transcription during maize development. The Plant Journal 66: 553-563.

Shieh, M. T., Brown, R. L., Whitehead, M. P., Cary, J. W., Cotty, P. J., Cleveland, T. E., and Dean, R. A. 1997. Molecular genetic evidence for the involvement of a specific polygalacturonase, P2c, in the invasion and spread of *Aspergillus flavus* in cotton bolls. Applied and Environmental Microbiology 63: 3548-3552.

Shivaji, R., Camas, A., Ankala, A., Engelberth, J., Tumlinson, J. H., Williams, W. P., Wilkinson, J. R., and Luthe, D. S. 2010. Plants on constant alert: elevated levels of jasmonic acid and jasmonate-induced transcripts in caterpillar-resistant maize. Journal of Chemical Ecology 36: 179-191.

Skibbe, D. S., Doehlemann, G., Fernandes, J., and Walbot, V. 2010. Maize tumors caused by *Ustilago maydis* require organ-specific genes in host and pathogen. Science 328: 89-92.

Smart, M. G., Wicklow, D. T., and Caldwell, R. W. 1990. Pathogenesis in *Aspergillus* Ear Rot of Maize: Light Microscopy of Fungal Spread from Wounds. Phytopathology 80: 1287-1294.

St Leger, R. J., Screen, S. E., and Shams-Pirzadeh, B. 2000. Lack of host specialization in *Aspergillus flavus*. Applied and Environmental Microbiology 66: 320-324.

Stoloff, L. 1977. Aflatoxins-An overview. In J. V. Rodricks, C. W. Hesseltine, and M. A. Mehlman (eds.), Mycotoxins in Human and Animal Health. Pathotox Publishers. ILL:p.7-28.

Sturm, A., and Chrispeels, M. 1990. cDNA cloning of carrot extracellular β-fructosidase and its expression in response to wounding and bacterial infection. Plant Cell 2: 1107-1119.

Tanaka, N., Matsuoka, M., Kitano, H., Asano, T., Kaku, H., and Komatsu, S. 2006. gid1, a gibberellin-insensitive dwarf mutant, shows altered regulation of probenazole-inducible protein (PBZ1) in response to cold stress and pathogen attack. Plant, Cell and Environment 29: 619-631.

Taubenhaus, J. J. 1920. A study of the black and yellow molds of ear corn. Texa Agricultural Experiment Station Bull 290: 3.

Tezcan, G., Ozhak-Baysan, B., Alastruey-Izquierdo, A., Ogunc, D., Ongut, G., Yildiran, S. T., Hazar, V., Cuenca-Estrella, M., and Rodriguez-Tudela, J. L. 2009. Disseminated fusariosis caused by *Fusarium verticillioides* in an acute lymphoblastic leukemia patient after allogeneic hematopoietic stem cell transplantation. Journal of Clinical Microbiology 47: 278-281.

Tubajika, K. M., and Damann, K. E. 2001. Sources of resistance to aflatoxin production in maize. Journal of Agricultural and Food Chemistry 49: 2652-2656.

Usadel, B., Poree, F., Nagel, A., Lohse, M., Czedik-Eysenberg, A., and Stitt, M. 2009. A guide to using MapMan to visualize and compare Omics data in plants: a case study in the crop species, Maize. Plant, Cell and Environment 32: 1211-1229.

Voss, K. A., Riley, R. T., Norred, W. P., Bacon, C. W., Meredith, F. I., Howard, P. C., Plattner, R. D., Collins, T. F., Hansen, D. K., and Porter, J. K. 2001. An overview of rodent toxicities: liver and kidney effects of fumonisins and *Fusarium moniliforme*. Environmental Health Perspectives 109 Suppl 2: 259-266.

Warburton, M. L., Brooks, T. D., Krakowsky, M. D., Shan, X., Windham, G. L., and Williams, W. P. 2009. Identification and Mapping of New Sources of Resistance to Aflatoxin Accumulation in Maize. Crop Science 49: 1403-1408.

Warburton, M. L., Williams, W. P., Hawkins, L., Bridges, S. M., Gresham, C., Harper, J., Ozkan, S., Mylroie, J. E., and Shan, X. 2011a. A Public Platform for the Verification of the Phenotypic Effect of Candidate Genes for Resistance to Aflatoxin Accumulation and *Aspergillus flavus* Infection in Maize. Toxins 3: 754-765.

Warburton, M., Brooks, T. D., Windham, G. L., and Paul Williams, W. 2011b. Identification of novel QTL contributing resistance to aflatoxin accumulation in maize. Molecular Breeding 27: 491-499.

Warburton, M. L., Williams, W. P., Windham, G. L., Murray, S. C., Xu, W., Hawkins, L. K., and Duran, J. F. 2013. Phenotypic and Genetic Characterization of a Maize Association Mapping Panel Developed for the Identification of New Sources of Resistance to *Aspergillus flavus* and Aflatoxin Accumulation. Crop Science 53: 2374-2383.

Warfield, C. Y., and Davis, R. M. 1996. Importance of the husk covering on the susceptibility of corn hybrids to *Fusarium* ear rot. Plant Disease 80: 208-210.

Waśkiewicz, A., Stępień, L., Wilman, K., and Kachlicki, P. 2013. Diversity of pea-associated *F. proliferatum* and *F. verticillioides* populations revealed by FUM1 sequence analysis and fumonisin biosynthesis. Toxins (Basel) 5: 488-503.

Wicklow, D. T., and Horn, B. W. 1984. *Aspergillus flavus* Sclerotia Form in Wound-Inoculated Preharvest Corn. Mycologia 76: 503-505.

Wicklow, D. T., Roth, S., Deyrup, S. T., and Gloer, J. B. 2005. A protective endophyte of maize: *Acremonium zeae* antibiotics inhibitory to *Aspergillus flavus* and *Fusarium verticillioides*. Mycological Research 109: 610-618.

Widstrom, N. W., Wilson, D. M., and McMillian, W. W. 1981. Aflatoxin contamination of preharvest corn as influenced by timing and method of inoculation. Applied and Environmental Microbiology 42: 249-251.

Widstrom, N., McMillian, W., and Wilson, D. 1987. Segregation for resistance to aflatoxin contamination among seeds on an ear of hybrid maize. Crop Science 27: 961-963.

Widstrom, N. W., and Donald, L. S. 1996. The Aflatoxin Problem with Corn Grain. Pages 219-280 in: Advances in Agronomy, Academic Press.

Widstrom, N. W., Guo, B. Z., and Wilson, D. M. 2003. Integration of crop management and genetics for control of preharvest aflatoxin contamination of corn. Toxin Reviews 22: 199-227.

Willcox, M. C., Davis, G. L., Warburton, M. L., Windham, G. L., Abbas, H. K., Betrán, J., Holland, J. B., and Williams, W. P. 2012. Confirming quantitative trait loci for aflatoxin resistance from Mp313E in different genetic backgrounds. Molecular Breeding 32: 15-26.

Williams, W. P., Buckley, P. M., and Windham, G. L. 2002. Southwestern corn borer (Lepidoptera: Crambidae) damage and aflatoxin accumulation in maize. Journal of Economic Entomology 95: 1049-1053.

Williams, J. H., Phillips, T. D., Jolly, P. E., Stiles, J. K., Jolly, C. M., and Aggarwal, D. 2004. Human aflatoxicosis in developing countries: a review of toxicology, exposure, potential health consequences, and interventions. The American Journal of Clinical Nutrition 80: 1106-1122.

Williams, L. D., Glenn, A. E., Bacon, C. W., Smith, M. A., and Riley, R. T. 2006. Fumonisin production and bioavailability to maize seedlings grown from seeds inoculated with *Fusarium verticillioides* and grown in natural soils. Journal of Agricultural and Food Chemistry 54: 5694-5700.

Williams, L. D., Glenn, A. E., Zimeri, A. M., Bacon, C. W., Smith, M. A., and Riley, R. T. 2007. Fumonisin disruption of ceramide biosynthesis in maize roots and the effects on plant development and *Fusarium verticillioides*-induced seedling disease. Journal of Agricultural and Food Chemistry 55: 2937-2946.

Williams, W. P., Windham, G. L., and Buckley, P. M. 2008. Diallel analysis of aflatoxin accumulation in maize. Crop Science 48: 134-138.

Wilson, D. M., Huang, L. H., and Jay, E. 1975. Survival of *Aspergillus flavus* and *Fusarium moniliforme* in high-moisture corn stored under modified atmospheres. Journal of Applied Microbiology 30: 592-595.

Wilson, R. A., Gardner, H. W., and Keller, N. P. 2001. Cultivar-dependent expression of a maize lipoxygenase responsive to seed infesting fungi. Molecular Plant-Microbe Interactions 14: 980-987.

Windham, G., and Williams, W. 1998. *Aspergillus flavus* Infection and Aflatoxin Accumulation in Resistant and Susceptible Maize Hybrids. Plant Disease 82: 281-284.

Windham, G. L., Williams, W. P., and Davis, F. M. 1999. Effects of the Southwestern Corn Borer on *Aspergillus flavus* Kernel Infection and Aflatoxin Accumulation in Maize Hybrids. Plant Disease 83: 535-540.

Wu, S., Kriz, A. L., and Widholm, J. M. 1994a. Nucleotide sequence of a maize cDNA for a class II, acidic beta-1,3-glucanase. Plant Physiology 106: 1709-1710.

Wu, S., Kriz, A. L., and Widholm, J. M. 1994b. Molecular analysis of two cDNA clones encoding acidic class I chitinase in maize. Plant Physiology 105: 1097-1105.

Wulff, E. G., Sørensen, J. L., Lübeck, M., Nielsen, K. F., Thrane, U., and Torp, J. 2010. *Fusarium* spp. associated with rice Bakanae: ecology, genetic diversity, pathogenicity and toxigenicity. Environmental Microbiology 12: 649-657.

Xie, Y. R., Chen, Z. Y., Brown, R. L., and Bhatnagar, D. 2010. Expression and functional characterization of two pathogenesis-related protein 10 genes *from Zea mays*. Journal of Plant Physiology 167: 121-130.

Yan, Y., Christensen, S., Isakeit, T., Engelberth, J., Meeley, R., Hayward, A., Emery, R. J., and Kolomiets, M. V. 2012. Disruption of *OPR7* and *OPR8* reveals the versatile functions of jasmonic acid in maize development and defense. Plant Cell 24: 1420-1436.

Yang, D. L., Yao, J., Mei, C. S., Tong, X. H., Zeng, L. J., Li, Q., Xiao, L. T., Sun, T. P., Li, J., Deng, X. W., Lee, C. M., Thomashow, M. F., Yang, Y., He, Z., and He, S. Y. 2012. Plant hormone jasmonate prioritizes defense over growth by interfering with gibberellin signaling cascade. Proceedings of the National Academy of Sciences 109: E1192-1200.

Yates, I. E., Widstrom, N. W., Bacon, C. W., Glenn, A., Hinton, D. M., Sparks, D., and Jaworski, A. J. 2005. Field performance of maize grown from *Fusarium verticillioides*-inoculated seed. Mycopathologia 159: 65-73.

Yilmaz, A., Nishiyama, M. Y., Jr., Fuentes, B. G., Souza, G. M., Janies, D., Gray, J., and Grotewold, E. 2009. GRASSIUS: a platform for comparative regulatory genomics across the grasses. Plant Physiology 149: 171-180.

Yin, Y. N., Yan, L. Y., Jiang, J. H., and Ma, Z. H. 2008. Biological control of aflatoxin contamination of crops. Journal of Zhejiang University Science. B 9: 787-792.

Zeringue JR, H. J. 2002. Effects of methyl jasmonate on phytoalexin production and aflatoxin control in the developing cotton boll. Biochemical Systematics and Ecology 30: 497-503.

Zhang, J., Simmons, C., Yalpani, N., Crane, V., Wilkinson, H., and Kolomiets, M. 2005. Genomic analysis of the 12-oxo-phytodienoic acid reductase gene family of *Zea mays*. Plant Molecular Biology 59: 323-343.

Zhang, Y., Choi, Y. E., Zou, X., and Xu, J. R. 2011. The FvMK1 mitogen-activated protein kinase gene regulates conidiation, pathogenesis, and fumonisin production in *Fusarium verticillioides*. Fungal Genetics and Biology 48: 71-79.

Zila, C. T., Samayoa, L. F., Santiago, R., Butrón, A., and Holland, J. B. 2013. A Genome-Wide Association Study Reveals Genes Associated with *Fusarium* Ear Rot Resistance in a Maize Core Diversity Panel. G3 (Bethesda) 3: 2095-2104.

Zummo, N., and Scott, G. E. 1992. Interaction of *Fusarium moniliforme* and *Aspergillus flavus* on kernel infection and aflatoxin contamination in maize ears. Plant Disease 76: 771-772.

Chapter Two

Comparative Transcriptomics of Developing Maize Kernels Reveals Different Patterns of Response to *Aspergillus flavus* and *Fusarium verticillioides* Infection

Xiaomei Shu[1], Gregory R. OBrian[1], David P. Livingston[2], Rebecca S. Boston[3], Charles P. Woloshuk[4], and Gary A. Payne[1]

[1] Department of Plant Pathology, North Carolina State University, Raleigh, NC 27695-7567

[2] Department of Crop Science, North Carolina State University, Raleigh, NC 27695

[3] Department of Plant & Microbial Biology, North Carolina State University, Raleigh, NC 27695

[4] Department of Botany and Plant Pathology, Purdue University, West Lafayette, IN 47907

ABSTRACT

Aspergillus flavus and *Fusarium verticillioides* are capable of infecting maize kernels and producing mycotoxins. Pathogenesis and host response in these host-parasite interactions remain poorly understood. In this study, we monitored colonization by these two fungi in the kernel. Visible colonization of the kernel was evident at 48 hours post inoculation (hpi) and both fungi reached the germ by 72 hpi, but colonization patterns by the two fungi differed. We also analyzed transcriptome changes of kernels during infection by these two fungi at 24, 48, and 72 hpi using RNA sequencing (RNA-seq). The results show that a set of defense-related genes was associated with both pathosystems, indicating a conserved response to fungal infection. Pathway analysis revealed that the signaling network regulated by plant hormones played an important role in shaping maize responses to these two pathogens. Of the known plant defense pathways, genes in the jasmonic acid (JA) and ethylene (ET) pathways appeared to be the most highly expressed during infection by both fungi. Infection by these two fungi also induced other changes in primary and secondary metabolism pathways of the maize kernel. These data indicate that both distinctive and shared mechanisms are involved in host response to pathogens of maize. The maize genes that are associated with defense response to both *A. flavus* and *F. verticillioides* are novel candidates to develop comprehensive resistance to both pathogens.

INTRODUCTION

Aspergillus flavus is an opportunistic fungal pathogen that can either live as a saprophyte in the soil or as a pathogen of many plant species. Hosts of *A. flavus* include

maize kernels, peanuts, cotton seeds and tree nuts (Payne, 1992; St Leger et al., 2000). Unlike *A. flavus*, *Fusarium verticillioides* grows primarily as an endophyte on maize. *F. verticillioides* can cause maize seedling blight, ear rot, and stalk rot under certain conditions (Bacon et al., 1992; Pei-Bao et al., 2010). However, both *A. flavus* and *F. verticillioides* can infect maize kernels and produce mycotoxins that are toxic to humans and livestock. Effective resistance to these two fungi in commercial maize lines has been difficult to achieve (Payne et al., 1986). A lack of understanding of the mechanisms of resistance has hampered the development of effective control strategies.

Plants have developed elaborate mechanisms to respond to various environmental cues, including attack by plant pathogens. Two strategies have evolved to detect pathogens. The first strategy involves recognition of conserved pathogen elicitors called pathogen-associated molecular patterns (PAMPs), which lead to PAMP-triggered immunity (PTI) (Jones and Dangl, 2006). PAMPs are detected by extracellular plant receptor proteins called pattern recognition receptors (PRRs). The second strategy is associated with recognition of pathogen effectors by intracellular plant receptors and initiation of effector-triggered immunity (ETI). Plant receptors, called resistance (R) proteins, are activated directly or indirectly by the pathogen. ETI is typically activated by adapted pathogens, whereas PTI is often associated with non-host resistance (Mengiste, 2012). Both ETI and PTI could be activated at the same time depending on the presence of effectors and PAMPs (Dodds and Rathjen, 2010). Previous studies support the idea that effectors from *A. flavus* and *F. verticillioides* are involved in infection of maize kernels (Bluhm et al., 2008; Dolezal et al.,

2013); but the mechanisms governing interactions between maize and these fungal pathogens remain unclear.

Infection by pathogens often induces both transcriptional and metabolic changes of the host. ETI is often associated with a hypersensitive response (HR) and programmed cell death (PCD). In *Arabidopsis thaliana*, recognition of biotrophic and hemibiotrophic pathogens is predominantly governed by ETI (Glazebrook, 2005). The salicylic acid (SA) signaling pathway plays a major role in the defense response to biotrophic and hemibiotrophic pathogens in plants. However, necrotrophs take advantage of host cell death and acquire nutrients from the dead tissue (Mengiste, 2012). Resistance to necrotrophs is mainly activated by jasmonic acid (JA) and ethylene (ET) signaling pathways. There is cross talk among the SA-, JA-, and ET-mediated pathways leading to both synergistic and antagonistic interactions (Derksen et al., 2013). Other phytohormone signaling pathways, such as the abscisic acid (ABA), auxin, cytokinin (CKs), brassinosteroids (BRs), and gibberellic acid (GA) pathways, also interact with SA, JA and ET signaling pathways and form a regulatory network in plants (Denancé et al., 2013; Derksen et al., 2013; Iglesia et al., 2011; Pieterse et al., 2009; Yang et al., 2013).

The plant regulatory genes encoding protein kinases/phosphatases and transcription factors (TFs) are the key players in activation of the innate immune responses (Brodensen et al., 2006; Zhang et al., 2012). Many TFs are targets of mitogen-activated protein kinase (MAPK) phosphorylation which modulates nuclear activity and regulates gene expression. The WRKY, MYB, and basic leucine zipper (bZIP) TFs are the master regulators in plant

immunity (Bhattarai et al., 2010; Eulgem and Somssich, 2007; Singh et al., 2002). In the protein families involved in the transduction of signaling (ProFITS) database, 1025 kinase genes, 2543 TF genes, and 1046 ubiquitin-proteasome related genes were predicted in the maize genome (Ling et al., 2010). The ProFITS database provides annotation tools to analyze large-scale data sets generated by using the 'omics' tools, including microarray, RNA-seq, and proteomics technologies.

Progress has been made in understanding host-parasite interactions between maize and its fungal pathogens. Both *A. flavus* and *F. verticillioides* can invade undamaged maize kernels through the silk channel (Duncan and Howard, 2010; Marsh and Payne, 1984; Smart et al., 1990). These pathogens also enter the kernel through injury caused by insects and mechanical damage (Lillehoj et al., 1975; Koehler, 1942; Sobek and Munkvold, 1999). Once in the kernel, these fungi are capable of colonizing all kernel tissue types, and contaminating the kernel with mycotoxins (Dolezal et al., 2013; Duncan and Howard, 2010; Koehler, 1942). Microarray and proteomic studies have been conducted to dissect maize transcriptional changes during infection by *A. flavus*, *F. verticillioides* and *Ustilago maydis* (Brown et al., 2013; Chen et al., 2002; Dolezal, 2010; Kelley et al., 2012; Lanubile et al., 2010; Luo et al., 2011; Pechanova et al., 2011; Skibbe et al., 2010). Pathogenic development and internal colonization by *A. flavus* in maize kernels were paired with transcriptional changes in the pathogen (Dolezal et al., 2013) and host (Dolezal, 2010). In this study, we expanded their investigation of pathogenesis by *A. flavus* and conducted a parallel analysis of infection and gene transcription by *F. verticillioides*. Whereas Dolezal (2010) examined the expression of

approximately 9,000 maize genes by Affymetrix DNA microarrays, we employed RNA-seq to examine the expression of all of the maize genes in response to infection by these two fungi.

RNA-seq is a recent technology that enables the study of the whole transcriptome using an ultra-high-throughput ('next-generation') sequencing technology. This technology allows unbiased quantification of transcripts with a higher sensitivity and broader genome coverage than microarrays (Marioni et al., 2008). Fu et al. (2009) demonstrated that the accuracy of RNA-seq is higher than microarrays. RNA-seq has been proven to be a powerful tool to characterize the transcriptome of different plant species and to identify plant genes that are differentially expressed during pathogen invasion (Chen et al., 2010a; Kawahara et al., 2012; Kim et al., 2011; Li et al., 2010; Lu et al., 2010; Xu et al., 2011; Zenoni et al., 2010; Zhang et al., 2010; Zhu et al., 2013). In this study, we monitored colonization of immature maize kernels by *A. flavus* and *F. verticillioides,* and analyzed dynamic transcriptional changes of the kernel during colonization using RNA-seq. We identified a set of maize genes associated with these two plant-parasite interactions. These genes are potential candidates for marker-assisted breeding and genetic engineering.

MATERIALS AND METHODS

Plant material, fungal inoculation, and sampling

Fungal strains (*A. flavus* NRRL *3357*, *F. verticillioides n16*) were grown on potato dextrose agar (PDA) plates at 28^{o}C for 5 days. Conidial suspensions were harvested by adding sterile distilled water containing 0.5% (v/v) Triton X-100 (Fisher) and scraping the

plates using a glass spreader. The concentration of conidia was quantified using a hemocytometer (Hausser Scientific) and diluted to 1×10^6 conidia/ml for inoculation. Maize inbred line B73 was grown at the Central Crops Research Station near Clayton, NC. Maize ears were hand-pollinated and covered with paper bags until inoculation at 21-22 days after pollination. Inoculation was conducted by wounding the kernel with a 3 mm needle bearing approximately 13 conidia. Kernels for the mock treatment were inoculated with sterile distilled water containing 0.5% (v/v) Triton X-100. Kernels from three biological replications (3 separate ears) were collected at 4, 12, 24, 48, 72, and 96 hpi for histology or transcriptome analysis. Kernels for histological analysis were placed in tissue imbedding capsules (Fisher) and fixed in modified FAA fixative (Table 1). Kernels for RNA analysis were frozen in liquid nitrogen immediately and stored at -80^{o}C until RNA extraction and sequencing by Illumina HiSeq.

Tissue fixation, embedding, and microscopy

Kernels were fixed and dehydrated using the protocol modified from Livingston et al. (2009, 2013). Kernels were put in a microwave oven (Pelco) with vacuum at 35^{o}C for 2 h (Table 1). The kernels were then dehydrated in the microwave oven with vacuum at 32^{o}C through a flex (Fisher) and xylene (Fisher) series (Table 1). Dehydrated kernels were embedding in paraffin (SPI) (Table 1). The paraffin blocks were sectioned with a RM2255 microtome (Leica) and mounted on slides (Gold Seal). Slides were dried on a hot plate overnight and stored at room temperature. Paraffin was removed by dipping the slides in 100% xylene (Table 2). Sections were then rehydrated with an ethanol series (Table 2).

Safranin and fast green staining were applied to differentiate tissue structure of maize kernels and the fungus grown in the kernel. The rehydrated sections were stained with safranin, dehydrated with an ethanol series, and counter stained with fast green (Fisher) (Table 2). Stained sections were mounted in permount mounting medium (Fisher) and covered with coverslips. Images of stained tissues were collected on an Eclipse E600 light microscope (Nikon). Images were captured on an Infinity1-3C digital camera, and analyzed with the software Infinity Analyze (Lumenera).

Table 1. Microwave fixation, dehydration, and embedding steps to process maize kernels. Table is adapted from Livingston et al. (2009).

Step	Chemical medium	Time	Temperature (^{o}C)	Wattage (watts)	Vacuum (Hg)
Fixation					
	modified FAA*	2 h	35	650	20
Dehydration					
	70% flex	30 min	32	650	20
	80% flex	30 min	32	650	20
	95% flex	30 min	32	650	20
	100% flex	30 min	32	650	20
	100% flex	30 min	32	650	20
	1:1 (v/v) flex: xylene	30 min	32	650	20
	1:1 (v/v) flex: xylene	30 min	32	650	20
	100% xylene	30 min	32	650	20
	100% xylene	30 min	32	650	20
	1:1 (v/v) xylene: paraffin	30 min	65	650	20
	1:1 (v/v) xylene: paraffin	30 min	65	650	20
Embedding					
	100% paraffin	1 h	65	650	20
	100% paraffin	1 h	65	650	20

* modified FAA fixative is 40% (v/v) distilled H_2O, 45% (v/v) methanol, 10% (v/v) formaldehyde, and 5% (v/v) glacial acetic acid.

Table 2. Safranin and fast green staining protocol for sections of maize kernel at room temperature.

Step	Chemical medium	Time
Paraffin removing		
	100% xylene	20 min
Rehydration		
	100% ethanol	10 s
	95% (v/v) ethanol	10 s
	70% (v/v) ethanol	10 s
	50% (v/v) ethanol	10 s
Staining		
	safranin	2 h
Dehydration		10 s
	50% (v/v) ethanol	10 s
	70% (v/v) ethanol	10 s
	95% (v/v) ethanol	10 s
	100% ethanol	10 s
Counterstaining		
	fast green	1 min
Post staining		
	100% xylene	until covered with coverslips

RNA-isolation, Illumina library preparation, and sequencing

Eight frozen kernels from individual ears were pooled and ground in liquid nitrogen with a mortar and pestle. About one hundred milligrams of ground tissue was added to 0.75 ml of saturated phenol, pH 6.6 (Fisher), and homogenized for 2 min. Samples were then dissolved in Tris EDTA buffer, pH 8.0 (ACROS Organics), extracted with 5:1 acid phenol: chloroform, pH 4.5 (Fisher), and precipitated with ice-cold 100% ethanol (ACROS Organics) overnight. Total RNA was further purified with an RNeasy Mini Kit (Qiagen) according to the manufacturer's instructions. The quality and concentration of RNA was analyzed using an RNA Pico chip on an Agilent Bioanalyzer. The cDNA library construction and sequencing runs were carried out using reversible terminator dye chemistry on the Illumina HiSeq by the Genomic Sciences Laboratory, North Carolina State University. Multiple samples with different barcodes were loaded in three lanes and sequenced to obtain 100 bp single-end reads.

RNA-seq data analysis

Illumina reads were sorted by barcodes, and adapter sequences were trimmed. The raw sequencing reads were then analyzed using the iPlant Collaborative Discovery Environment (Matasci and McKay, 2013). Reads of the same individual from multiple lanes were then concatenated using the software named 'Concatenate Multiple Files'. The quality of the reads was checked using FastQC 0.10.1 and then aligned to the maize genome (Ensembl 14) by using TopHat2-SE (Trapnell et al., 2012). Maize transcripts were assembled using Cufflinks2, and the gene expression levels were analyzed using Cuffdiff2 (Trapnell et

al., 2012). The MaizeCyc database and the bioinformatics software Biocyc were used for pathway analysis (Caspi et al., 2012).

Validation of RNA-seq data by qRT-PCR

Three μg of total RNA was treated with DNase (Promega) for cDNA synthesis using a First Strand cDNA Synthesis Kit (Fermentas), and then qRT-PCR was performed using a SYBR® Green kit (Applied Biosystems) according to the manufacturer's instructions. The expression levels of the 18S rRNA gene were used for normalization. Data were analyzed by the comparative CT method with the amount of target given by the calibrator $2^{-\Delta\Delta CT}$.

RESULTS

Colonization by *A. flavus* and *F. verticillioides* in maize kernels

Maize kernels developing in the field were inoculated with either *A. flavus* or *F. verticillioides* and the colonization of maize kernels by each fungus was followed by histological examination. Colonization by each fungus was first observed in aleurone and endosperm tissue near the site of inoculation at 48 hpi. No fungal colonization was observed in kernels inoculated with either *A. flavus* or *F. verticillioides* and harvested at 4, 12 and 24 hpi. *A. flavus* extensively colonized the single layer of cells within the aleurone and cell death and disruption was associated with fungal mycelium (Fig. 1A). In contrast, many aleurone cells appeared intact during *F. verticillioides* colonization at 48 hpi (Fig. 1B). By 72 hpi, the aleurone and endosperm were colonized by both fungi (Fig. 1D-E). We observed *A. flavus* mycelium, but not *F. verticillioides* mycelium in the germ at 72 hpi (Fig. 1D- E). At 96 hpi, both fungi were observed in the aleurone, endosperm, and germ. The morphology of

A. flavus changed as it reached the embryo forming a fungal mat structure (Fig. 1D as reported by Dolezal et al., 2013). This specialized structure resembles the biofilm formed by *Aspergillus fumigatus* in human lung (Ramage et al., 2009). Compared with *F. verticillioides*, we observed that *A. flavus* more extensively colonized the kernel at 24, 48 and 72 hpi. The results are supported by RNA-seq data which show that the percent of *A. flavus* reads were consistently higher than the percent of *F. verticillioides* reads in the infected kernels at 24, 48 and 72 hpi, respectively (Fig. 1F; Table S1).

Figure 1. Colonization of maize kernels by *A. flavus* and *F. verticillioides*. A, A vertical kernel section. B, The percent of fungal reads in the total reads of *A. flavus* or *F. verticillioides* infected kernels. C-H, Light microscope images taken from sections stained with safranin and fast green. Arrows denote fungal colonization. C, Aleurone of a mock inoculated kernel. D, *A. flavus* colonization in the destroyed aleurone layer. E, *F. verticillioides* colonization in the partially intact aleurone layer. F, The endosperm-scutellum interface of a mock inoculated kernel. G, *A. flavus* colonization at the endosperm-scutellum interface with the formation of a biofilm-like structure. H, The endosperm-scutellum interface inoculated with *F. verticillioides*. *Af*: *A. flavus*; *Fv*: *F. verticillioides*. hpi: hours post inoculation. Al: aleurone; En: endosperm; Sc: scutellum. Scale bars: 30 μm.

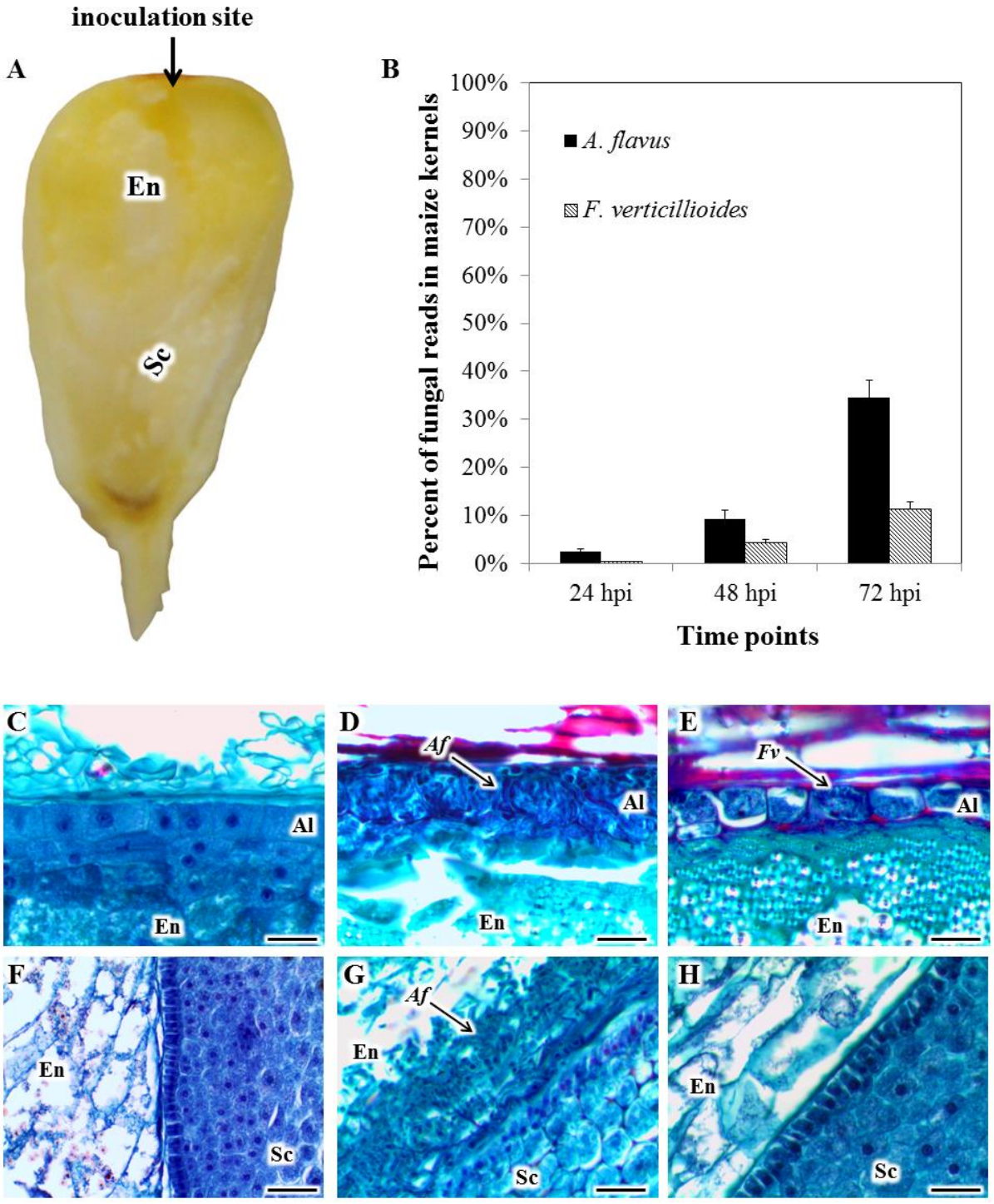
A
inoculation site
En
Sc
B
Percent of fungal reads in maize kernels
100%
90%
80%
70%
60%
50%
40%
30%
20%
10%
0%
A. flavus
F. verticillioides
24 hpi
48 hpi
72 hpi
Time points
C
Al
En
D
Af
Al
En
E
Fv
Al
En
F
En
Sc
G
Af
En
Sc
H
En
Sc

Dynamic changes of the maize transcriptome during *A. flavus* and *F. verticillioides* infection

Illumina RNA-seq was performed to explore transcriptome changes of kernels in response to *A. flavus* and *F. verticillioides*. Approximately 6.17 to 42.31 million raw reads were generated in each sample. Over 99.9% of these reads were of high quality and used for data analysis (Table S1). Of these high quality reads, 36-88% was aligned to the maize genome and used to analyze gene expression levels (Table S1). The 24 hpi time point was chosen to capture the early defense response before visible fungal colonization was observed. The 48 and 72 hpi time points were selected to analyze the later defense response.

To explore the effect of wound inoculation on maize gene expression, non-wounded kernels also were sequenced. We compared gene expression levels of fungal infected kernels with non-wounded and mock inoculated kernels. Very similar results were obtained using the non-wounded and mock inoculated controls (data not shown). The results suggest that wound inoculation did not dramatically change host gene expression in our studies. Thus we used mock inoculated kernels collected at 24, 48 and 72 hpi as respective controls for these time points.

The CummeRbund volcano plots in Figure S1 show an overview of host gene expression changes between the pairs of mock inoculated and *A. flavus*/*F. verticillioides* infected kernels. Figure 2 shows the total numbers of up- and down-regulated maize genes over time in these two systems. Following *A. flavus* infection, 349, 254 and 1193 genes were up-regulated at 24, 48, and 72 hpi, respectively, while 51, 42 and 157 genes were down-

regulated at the same time points. The results indicate that many genes were differentially up-regulated early in the infection process. In contrast, 11, 260 and 868 genes were up-regulated, and 0, 2 and 15 genes were down-regulated during infection by *F. verticillioides* at 24, 48, and 72 hpi, respectively. A few of the same genes were up-regulated at all three time points (Fig. 2B). A dramatic change in the number of up-regulated genes infected with *F. verticillioides* occurred at 48 hpi. Compared with *F. verticillioides*, more dramatic gene expression changes occurred in the kernel upon *A. flavus* infection. However, many genes were regulated in similar patterns by these two fungi (Table S2). Additionally, there were more differentially expressed genes in later time points than in earlier time points in both systems, revealing broader physiological and metabolic changes at later time points.

We verified the expression levels of selected genes by quantitative real-time RT-PCR (qRT-PCR) (data not shown). Although Walley et al. (2013) found that protein abundance and mRNA levels were poorly correlated in maize kernels; we also compared our RNA-seq data with maize kernel proteomic data (Castellana et al., 2013; Walley et al., 2013). Over five hundred of the total 1655 differentially expressed genes that we observed in this study were also detected at the protein level under normal conditions (Walley et al., 2013). Proteins encoded by the defense-related genes shown in Table S2 have been found in different tissues under normal growth conditions (Castellana et al., 2013; Walley et al., 2013).

To predict putative resistance mechanisms induced in kernels during infection, we assigned the differentially expressed maize genes into functional categories using MaizeSequence, MaizeGDB, MapMan, ProFITS, GRASSIUS, CoGePedia and Maize

Protein Atlas databases (Table S2) (Castellana et al., 2013; Lawrence et al., 2004; Ling et al., 2010; Lyons and Freeling, 2008; Schnable et al., 2009; Usadel et al., 2009; Yilmaz et al., 2009). To gain additional insights into the putative function of maize genes identified in this study, differentially expressed maize genes were placed into biosynthetic and regulatory pathways using the bioinformatics software Biocyc (Caspi et al., 2012). Figure S2 shows the overview of host metabolic pathway changes during *A. flavus* and *F. verticillioides* infection at 72 hpi. The results show broad transcriptional and presumably metabolic changes of the kernel during fungal infection. Genes associated with biotic and abiotic stresses, signaling transduction, transcription regulation, primary metabolism, and secondary metabolism were enriched during infection by these two fungi (Fig. 3; Table S2).

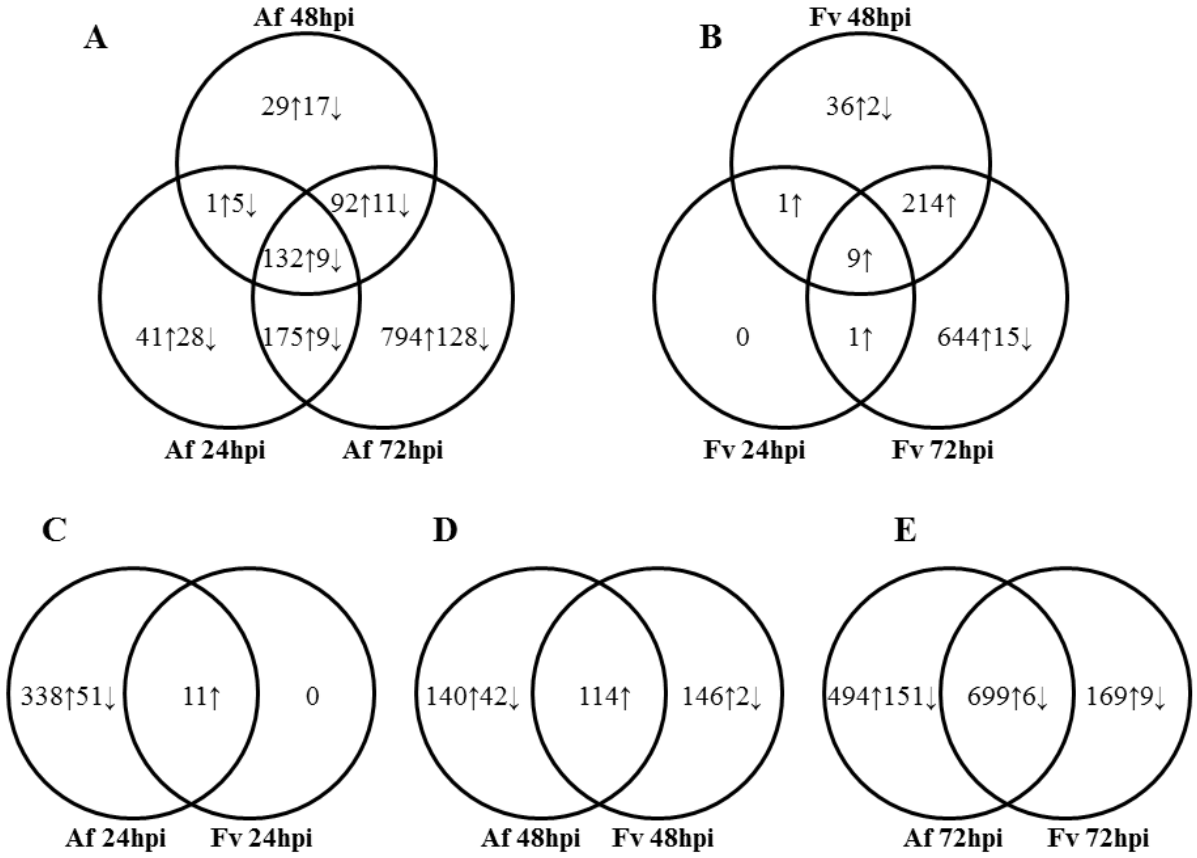

Figure 2. Dynamic changes of kernel transcriptome during *A. flavus* and *F. verticillioides* infection. Total numbers of up-regulated genes denoted by "↑", and down-regulated genes denoted by "↓" of treatment-specific and shared between/among treatments are displayed in Venn diagrams. A and B, number of maize genes differentially expressed in response to *A. flavus* (A) and *F. verticillioides* (B) infection at 24, 48 and 72 hpi; C, D and E, number of maize genes differentially expressed in response to *A. flavus* and *F. verticillioides* infection at 24 hpi (C), 48 hpi (D) and 72 hpi (E). hpi: hours post inoculation. Af: *A. flavus* inoculated kernels; Fv: *F. verticillioides* inoculated kernels.

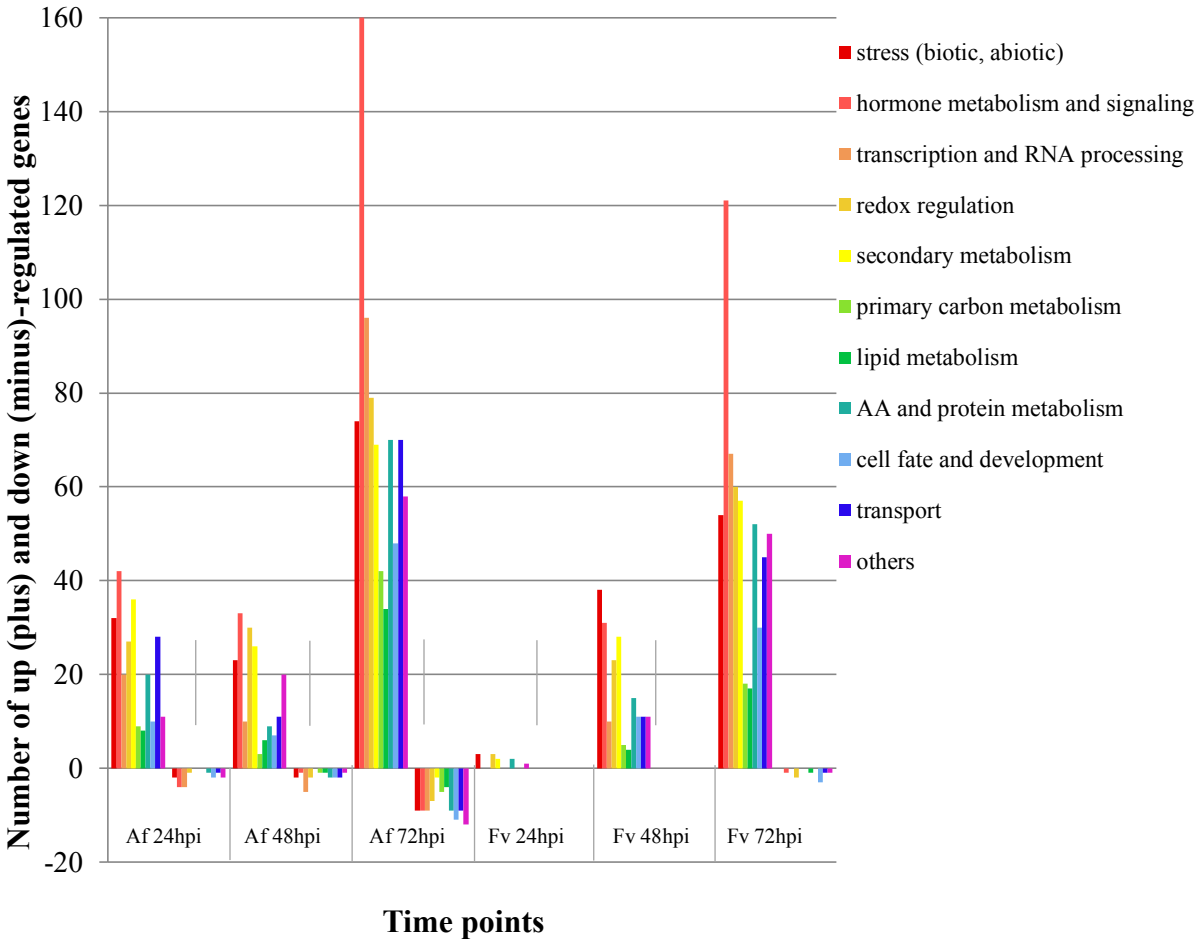

Figure 3. Functional categories of maize genes differentially regulated upon infection by *A. flavus* and *F. verticillioides*. Colored bars represent the number of regulated genes with annotated function. Positive bars denote numbers of up-regulated genes. Negative bars denote numbers of down-regulated genes. hpi: hours post inoculation. Af: *A. flavus* inoculated kernels; Fv: *F. verticillioides* inoculated kernels.

Expression changes of known and putative defense genes

As expected, genes associated with response to biotic and abiotic stresses, redox regulation, hormone metabolism and transcriptional regulation were differentially expressed in response to these two fungi (Fig. 3). By 24 hpi, a large number of maize genes were differentially expressed in *A. flavus* infected kernels, indicating that defense reactions were elicited by *A. flavus* before visible colonization was observed. Compared with *A. flavus* infected kernels, less genes were differentially expressed at 24 hpi during *F. verticillioides* infection (Fig. 3).

Of the defense-related genes transcriptionally induced during infection, an *R* gene (GRMZM2G032602) was up-regulated by both *A. flavus* and *F. verticillioides* (Table S2). Several leucine-rich repeat receptor kinase (LRR-RKs) and receptor-like kinase (RLKs) genes, which are putative *R* genes, were up-regulated upon infection by these two fungi (Table S2). Moreover, a number of *pathogenesis related* (*PR*) genes and *PR*-like genes were up-regulated by infection by these two fungi, including *PR-4*, *PR-5*, *PR-10*, *chitinases*, and *endoglucanases* (Table S2). However, *chitinase chem5* (GRMZM2G453805) and *endoglucanase 1* (GRMZM2G151257) were up-regulated only in kernels infected by *A. flavus*, and a *PR*-like gene (GRMZM2G178199) was down-regulated by *A. flavus* at 72 hpi. The expression level of this gene also was decreased slightly in *A. flavus* infected kernels at 24 and 48 hpi as well as in *F. verticillioides* infected kernels. Of the *PR*-like genes, two thaumatin-like protein genes were up-regulated by *A. flavus*. One of them was up-regulated

also by *F. verticillioides* infection at 72 hpi. Notably, none of these *PR*-like genes was differentially expressed during *F. verticillioides* infection at 24 hpi.

Expression changes of hormone signaling genes

Our RNA-seq data suggest that the host hormone signaling network plays an important role in the defense response to these fungal pathogens. Plants can synthesize SA from chorismate and shikimate (Wildermuth et al., 2001). A few genes associated with SA biosynthesis were up-regulated during *A. flavus* infection at 72 hpi, including the *benzoate carboxyl methyltransferase* (GRMZM2G126772), *shikimate dehydrogenase* (GRMZM2G107402), *3-phosphoshikimate 1-carboxyvinyltransferase* (GRMZM5G877500), and *Shikimate O hydroxycinnamoyltransferase* (GRMZM2G158083) (Table S2). The expression level of *benzoate carboxyl methyltransferase* was 32.94 fold higher in *A. flavus* infected kernels than mock inoculated kernels at 72 hpi. These data suggest that the SA biosynthesis pathway was up-regulated by *A. flavus* infection at 72 hpi. No SA biosynthesis genes were differentially expressed in *F. verticillioides* infected kernels. Additionally, a few JA biosynthesis genes, including a few *12-oxo-phytodienoic acid reductases* (*OPRs*) and *lipoxygenases* (*LOXs*), were up-regulated in response to both fungi (Table S2). Expression levels of the *OPRs* in *A. flavus* infected kernels were much higher than in *F. verticillioides* infected kernels, indicating that *A. flavus* induced higher levels of JA accumulation. Genes associated with ET biosynthesis and signaling, including the *1-aminocyclopropane-1-carboxylate oxidase* and *ethylene-responsive transcription factors* (*ERFs*), were also up-regulated by these two fungi (Table S2).

We also observed gene expression changes in other hormone signaling pathways, including ABA, auxin, GA and BR pathways (Fig. 4; Table S2). A few ABA metabolism genes were up-regulated by both fungi, indicating the induction of ABA pathway in these two pathosystems. Of these ABA biosynthesis genes, *aldehyde oxidase* (GRMZM2G141535) and xanthine dehydrogenase (GRMZM2G019799) were up-regulated by *A. flavus* infection. Additionally, a set of auxin metabolism and signaling genes was up-regulated by these two fungi. However, the auxin biosynthesis gene *indole-3-acetate beta-glucosyltransferase* (GRMZM2G024131) and the auxin signaling gene, *SAUR11 - auxin-responsive SAUR family member* (GRMZM2G432060), were down-regulated during *A. flavus* infection. Furthermore, the GA biosynthesis genes, including the *gibberellin 20 oxidase 2* (GRMZM2G099467), were up-regulated following infection by both fungi. However, three GA signaling genes were down-regulated during *A. flavus* infection at 72 hpi, including the gibberellins receptor gene *GID1L2* (*GID1*) (GRMZM2G049675) and *chitin-inducible gibberellin-responsive protein 2* (GRMZM2G028438). However, another *GID1* (GRMZM2G104938) was up-regulated upon *A. flavus* infection at the same time point. None of these GA signaling genes were differentially expressed during *F. verticillioides* infection. The GA degradation associated genes, *Gibberellin 2-beta-dioxygenases* (GRMZM2G031724 and GRMZM2G022679), were also up-regulated by *F. verticillioides* infection at 72 hpi. Additionally, we observed several BR biosynthesis genes and two *BRASSINOSTEROID INSENSITIVE 1-associated receptor kinase 1* (*BAK1*) genes (GRMZM2G349665 and GRMZM2G145440) that were up-regulated in these two systems. *BAK1* is an *RLK* known for its role in PTI and BR signaling in *A. thaliana* (Chinchilla et al., 2007). A set of CK

biosynthesis genes was also up-regulated in response to these two fungi except for a *cytokinin-O-glucosyltransferase 3* (GRMZM5G854655), which was slightly down-regulated by *A. flavus* infection at 72 hpi. However, the zeatin biosynthesis gene *isopentenyl transferase IPT2* (GRMZM2G084462) was down-regulated by *A. flavus* at all three time points.

Expression of signal transduction genes associated with host defense

In this study, we observed that a large number of kinase genes, TF genes, and ubiquitin-proteasome related genes were differentially expressed upon infection by these two fungi, including MAPK genes (Table S2). As expected, we observed TF genes that are associated with resistance to these fungi, including members of the WRKY, MYB, NAC, bZIP, zinc finger, and APETALA2/ethylene-responsive element-binding protein (AP2-EREBP) (Table S2). Members of these TFs are the key regulators in plant disease resistance and stress tolerance (Alves et al., 2013; Johnson et al., 2007; Li et al., 2011; Shim and Choi, 2013; Voitsik et al., 2013). One of the up-regulated MYB genes, *MYB 42* (GRMZM2G419239), is a negative regulator of the maize lignin biosynthesis gene, *caffeic acid O-methyl-transferase* (Fornalé et al., 2006). Additionally, two R2R3MYB TF genes were up-regulated by both fungi. R2R3MYB TFs were reported to restrict necrosis induced by biotic and abiotic stresses in *A. thaliana* (Mengiste et al., 2003). We also observed a set of *AP2-EREBPs* up-regulated by *A. flavus* and *F. verticillioides*. AP2-EREBP TFs are known to integrate ET and JA signaling pathways and regulate defense-related gene expression (Fig. 4)

(Pré et al., 2008). However, a few TF genes were down-regulated upon *A. flavus* infection but not *F. verticillioides*.

Expression changes of genes involved in programmed cells death

In this study, we found that protein degradation and cell death associated genes were differentially expressed during *A. flavus* and *F. verticillioides* infection in maize kernels. As we described above, many ubiquitin-proteasome related genes were up-regulated (Table S2). Two of them were specifically down-regulated by *A. flavus*. The proteolysis-related hydrolase and protease inhibitor genes were also up-regulated by these two fungi (Table S2). In tomato, resistance to *Botrytis cinerea* is mediated by JA signaling and the JA-dependent genes, *protease inhibitor I* and *II* (El Oirdi et al., 2011). Cordero et al. (1994) identified a maize proteinase inhibitor gene that was associated with fungal infection, wounding, ABA and methyl jasmonate treatment. However, we found a few protease inhibitor genes that were down-regulated during *A. flavus* infection, including a cystatin gene (GRMZM2G401374). Cystatins are cell death suppressors in plants (Belenghi et al., 2003; Solomon et al., 1999). A few other cell death associated genes were also up-regulated in response to *A. flavus* and *F. verticillioides* infection. One example is the cell death suppressor gene, *lethal leaf-spot 1* (GRMZM2G339563) (Gray et al., 1997), which was up-regulated by *A. flavus* infection at 72 hpi. Maize *Lethal leaf-spot 1* mutants show enhanced resistance to fungal pathogens *Cochliobolus heterostrophus* and *Puccinia sorghi* (Simmons et al., 1998).

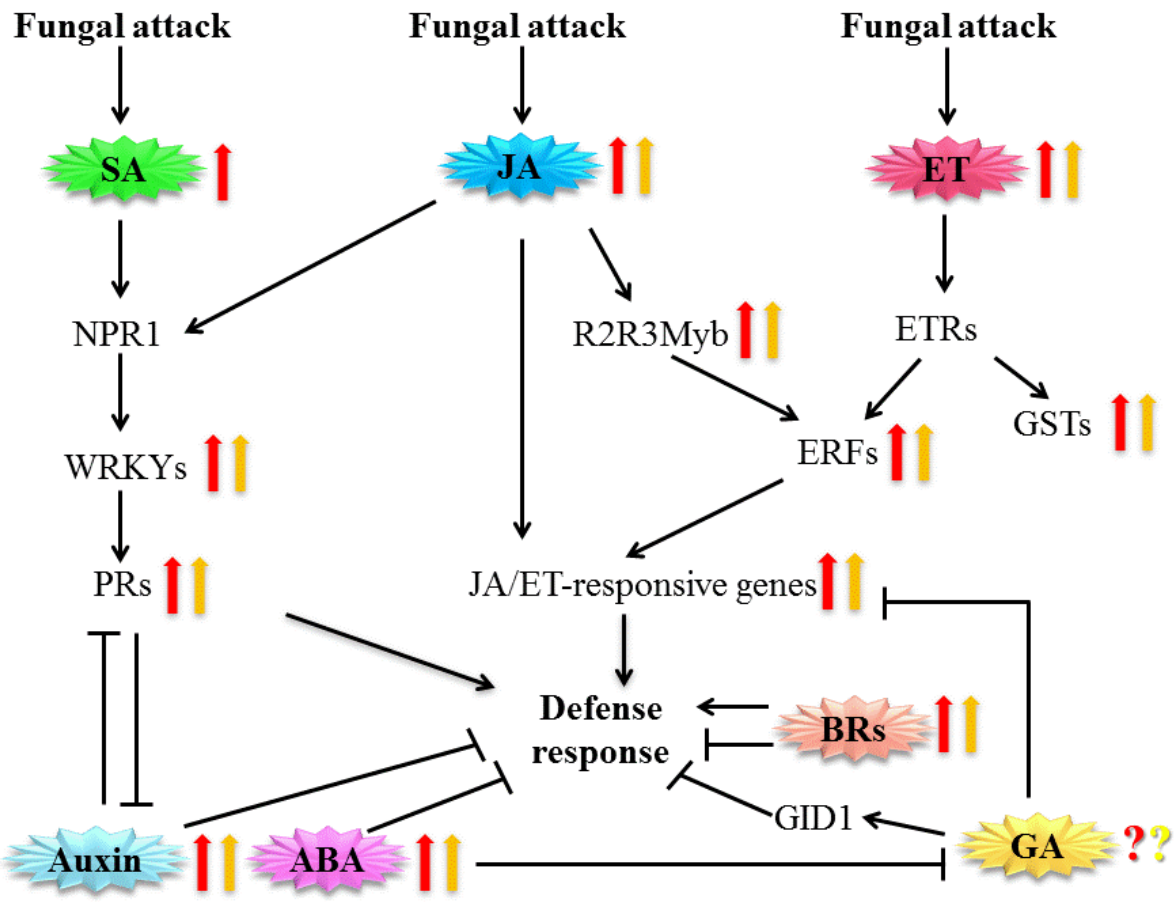

Figure 4. Hypothetical networking by phytohormones in maize defense responses during *A. flavus* and *F. verticillioides* infection. Black arrows denote positive effect. Inhibition lines denote negative effect. Red arrows denote genes or pathways up-regulated during *A. flavus* infection. Yellow arrows denote genes or pathways up-regulated during *F. verticillioides* infection. Question marks denote pathways up- or –down-regulated. ET, ethylene; JA, jasmonic acid; SA, salicylic acid; GA, gibberellic acid; ABA, abscisic acid; BRs, brassinosteroids. Figure is adapted from Pieterse et al. (2009).

Expression changes of secondary metabolism genes

Expression levels of secondary metabolism genes were greatly enhanced during infection by these two fungi, including the *glutathione S-transferases* (*GSTs*) (Table S2). One example is *GST 15* (GRMZM2G150474), which was also up-regulated by *U. maydis* at 12 hpi (Doehlemann et al., 2008). We observed that GST regulated genes were also up-regulated by these fungi, including a few *phenylalanine ammonia-lyases* (*PLAs*) and a *chalcone synthase* (*CHS*) (GRMZM2G422750) (Gomez et al., 2004; Loyall et al., 2000). Transcript levels of two phenylalanine biosynthesis genes were also significantly increased during infection by these two fungi. The major phenylpropanoids downstream of PAL are substrates of lignin and flavonoids, which are the source of anthocyanins and phytoalexins. Two anthocyanin biosynthesis genes were up-regulated in these two pathosystems, including a *leucoanthocyanidin dioxygenase* (GRMZM2G162158), which is a key enzyme in anthocyanin biosynthesis. Lignin and wax metabolism genes were also differentially expressed during infection by *A. flavus* and *F. verticillioides*. Most of these genes were up-regulated by these two fungi.

Expression changes of primary metabolism genes

Infection by these two fungi also changed primary metabolism of the kernel. We observed that genes involved in carbohydrate metabolism pathways were differentially expressed during infection by *A. flavus* and *F. verticillioides* (Table S2). A number of *amylase*, *invertase*, and sugar transporter genes were up-regulated by these two fungi, indicating changes of the starch and sugar biosynthesis pathways. However, the *miniature*

seed1 (GRMZM2G119689), which encodes an invertase, as well as two sugar transporter genes (GRMZM2G418343 and GRMZM2G087901) was down-regulated during *A. flavus* infection. In addition, a glycosyl transferase gene (GRMZM2G026889), a sucrose biosynthesis gene, *Sucrose-phosphatase 2* (GRMZM2G097641), and two UDP-glucose biosynthesis genes, *inorganic diphosphatases* (GRMZM2G032619 and GRMZM2G120079) were also up-regulated in these two interactions. Notably, changes of minor carbohydrate metabolism genes only occurred during *A. flavus* infection. Furthermore, we observed transcriptional induction of the tricarboxylic acid cycle (TCA) and calvin cycle during infection by these fungi.

We also observed gene expression changes in amino acid/protein metabolism and lipid metabolism pathways. Expression levels of numerous lipid metabolism genes were significantly increased during infection by these fungi, including two *LOX* genes as described above. Dramatic expression changes of genes associated with cell wall metabolism and modification occurred during infection by these two fungi, suggesting the induction of plant basal defense response by these fungi. Moreover, genes encoding transporters of amino acid/proteins, metal and various substrates were differentially expressed in these two systems, including the ATP-binding cassette (ABC) transporter genes. ABC transporter family members are known to be associated with disease resistance, detoxification and transport of diverse substrates (Cho and Cho, 2012).

DISCUSSION

We compared transcriptome changes in maize seeds in response to spatial and temporal colonization by two maize pathogens, *A. flavus* and *F. verticillioides*. *A. flavus* is a saprophyte that can be an opportunistic pathogen of developing maize kernels, whereas *F. verticillioides* can establish both and endophytic and pathogenic relationship with maize kernels. We predicted that maize kernels might respond differently to these two organisms having different trophic lifestyles.

Infection by *A. flavus* resulted in the greatest transcriptome changes in the host (Fig. 2; Table S2). This could have been due to more extensive colonization by *A. flavus* than by *F. verticillioides*. When inoculated at the same position on the kernel, *A. flavus* was observed in the germ 24 h earlier than *F. verticillioides*. There was a common set of genes whose transcription was induced by both fungi (Fig. 2). For example, we observed a NBS-LRR resistance gene (Collins et al., 1998) reported to be more highly expressed during infection by *Bipolaris maydis* infection and to respond to SA treatment (Cheng et al., 2012). We also observed elevated expression levels of *PR*-like genes during infection by *A. flavus* and *F. verticillioides*, including *PR4*, *PR5*, *PR10*, *Seed chitinase A*, *chitinase chem5*, *glucan beta-1, 3-glucanase* and *thaumatin-like proteins*. Some of these maize *PR*-like genes are important components in response to various stimuli. Accumulation of *PR-4* transcripts was observed in maize plants upon infection by *F. verticillioides* and *U. maydis* (Bravo et al., 2003; Doehlemann et al., 2008). Maize *PR-1* and *PR-5* are associated with chemical induction of SAR and resistance to downy mildew (Morris et al., 1998). But *PR-1* expression was not

significantly changed in this study. Another maize *PR* gene, *PR-10*, which shows RNase activities *in vitro*, has been found to be associated with *A. flavus* infection and various biotic and abiotic stresses (Chen et al., 2006, 2010b; Xie et al., 2010).

Some plant chitinases and endoglucanases, which may have cell wall-degrading activities (Bravo et al., 2003; Huynh et al., 1992; Wu et al., 1994a, 1994b), are also PR proteins functioning downstream of SA and JA/ET signaling pathways (Vidal et al., 1998). In maize plants, *chitinases* and *β-1, 3- glucanases* were reported to be involved in resistance to *A. flavus* and *F. verticillioides* (Cordero et al., 1993; Ji et al., 2000; Lozovaya et al., 1998; Moore et al., 2004). Sánchez-Rangel et al. (2012) found that Fumonisin B1 targeted beta-1, 3-glucanase of the germinating maize embryo. Holmes et al. (2008) also identified the maize seed chitinase A and thaumatin-like proteins as inhibitors of *A. flavus* fungal growth and aflatoxin biosynthesis. Members of the thaumatin-like proteins were characterized to be PR proteins in *A. thaliana*, barley, wheat and apple (Hejgaard et al., 1991; Hu and Reddy, 1997; Krebitz et al., 2003; Wang et al., 2010). These *PR*-like genes that we identified in this study are putative *PR* genes that might play important roles in maize resistance to a broad spectrum of pathogens.

In this study, we also identified several genes in maize encoding pathway enzymes for plant hormones that were differentially expressed in response to these fungi (Fig. 4 and 5; Table S2). Based on transcriptional profiling results, the defense response to *A. flavus* and *F. verticillioides* in maize kernels appeared to be predominantly governed by the JA/ET signaling pathways, which antagonize the SA signaling pathway (Glazebrook, 2005).

Members of MYB and ERF TFs, which are downstream of the JA/ET signaling pathways, were up-regulated in response to these fungi (Table S2). But the key gene in the crosstalk between SA and JA pathways, *nonexpresser of PR genes 1* (*NPR1*) (Mengiste, 2012), was not differentially expressed in this study. However, a few SA biosynthesis genes were specifically up-regulated during *A. flavus* infection. Additionally, the up-regulation of *PR-5* as well as several WRKY TF genes suggests that the SA signaling pathway may play a role in these interactions. WRKY TFs are the key regulators of SAR and *PR* gene expression in *A. thaliana* (Pape et al., 2010; van Verk et al., 2011). The role of SA in disease resistance is complex in plants. In *A. thaliana* and tomato plants, elevated SA levels enhance resistance to hemibotrophic pathogens, but promote susceptibility to necrotrophs (El Oirdi et al., 2011; Rahman et al., 2012; Veronese et al., 2006). Endogenous SA levels are higher in the monocot rice plants compared with the dicot plants tobacco and *A. thaliana* (Yang et al., 2004). The role of SA signaling in maize response to *A. flavus* and *F. verticillioides* needs to be further explored. In *A. thaliana*, WRKY, MYB and bZIP TFs are known to regulate the SA- and JA/ET-dependent systemic resistance (Dong, 2004; Durrant and Dong, 2004; Nimchuk et al., 2003; Wang et al., 2006). Expression of these TF genes appeared to be associated with induction of SA, JA and ET signaling pathways in maize kernels.

We also observed gene expression changes in the ABA, auxin, and GA pathways that affect the three innate defense pathways (Fig. 4), suggesting a complex regulatory network triggered by this fungus. ABA, auxin and GA mainly regulate plant growth and development. ABA and auxin signaling pathways suppress SA signaling in plants (Pieterse et al., 2009;

Wang et al., 2007). SA-mediated down-regulation of auxin signaling was also observed in response to biotic and abiotic stresses in *A. thaliana* (Iglesia et al., 2011). Elevated auxin levels and transcriptional induction of auxin-responsive genes were also observed in maize during *U. maydis* infection (Doehlemann et al., 2008; Turian and Hanilton, 1960). In *A. thaliana*, GA produced by *Gibberella fujikyroi* inhibits JA-dependent necrotroph resistance via GA-mediated degradation of DELLA proteins (Navarro et al., 2008). Hormones synthesized by pathogens may also alter the hormone homeostasis and interfere with the endogenous plant hormones (Navarro et al., 2008). Whether *A. flavus* and *F. verticillioides* themselves produce hormones and contribute to pathogenicity needs to be explored.

GA signaling is suppressed by ABA signaling in plants (Fig. 5). In maize kernels, GA stimulates the synthesis of protease and α-amylase to promote hydrolysis of endosperm starch and proteins, whereas ABA inhibits this process (Harvey and Oaks, 1974). Both SA and ABA antagonize GA-promoted seed germination in barley kernels (An and Lin, 2011; Xie et al., 2007). Our results indicate that up-regulation of ABA/auxin signaling pathways may contribute to the inhibition of SA signaling. The inhibition of SA signaling would attenuate host resistance and promote fungal colonization. Our data indicate that regulation of GA pathway is complicated during infection by *A. flavus* and *F. verticillioides*. It is likely that both GA signaling and GA degradation pathways were changed during infection. Down-regulation of the GA signaling pathway may release the inhibition of JA/ET signaling in the kernel. Additionally, our data indicate that various BRs and CKs are involved in defense against these two fungi. BRs are important components in disease resistance in *A. thaliana*,

tobacco and rice plants (Belkhadir et al., 2012; Nakashita et al., 2003). BR-mediated defense response with H_2O_2 accumulation was reported in maize leaves (Zhang et al., 2010). Previous studies indicate that CKs were involved in disease resistance in plants (Angra-Sharma and Sharma, 1999; Siemens et al., 2006; Walters and McRoberts, 2006). Changes of CK metabolism was observed during colonization by *Colletotrichum graminicola* on maize leaves (Behr et al., 2012). Taken together, we hypothesize that the hormone homeostasis plays a critical role in defense response to *A. flavus* and *F. verticillioides* in developing maize kernels (Fig. 4 and 5).

Our data revealed that transcription levels of *GSTs*, *PLAs* and *CHS* were significantly increased during infection by *A. flavus* and *F. verticillioides*. Plant glutathione is thought to be the most sensitive soluble antioxidant responsive to biotic and abiotic stress (Ogawa, 2005). GSTs serve as antioxidants participating in reactive oxygen species (ROS) scavenging and reducing damage caused by pathogens or chemical-associated oxidative stress (Mauch and Dudler, 1993; Sytykiewicz, 2011). GST accumulation after *Alternaria brassicicola* infection was described in *A. thaliana* (Mukherjee et al., 2010). *GST* was reported to be associated with *Erysiphe graminis* infection in wheat (Dudler et al., 1991). During infection by *A. flavus* and *F. verticillioides*, we observed up-regulation of genes involved in biosynthesis of secondary metabolites, including phenylalanine, anthocyanin, alkaloid, flavonoid, isoprenoids, phenols and phenylpropanoid. Members of these secondary metabolites are known antifungal protectants against *U. maydis* in maize (Basse, 2005; Doehlemann et al., 2008). Doehlemann et al. (2008) reported that anthocyanin accumulation

and induction of *leucoanthocyanidin dioxygenase* gene expression were associated with *U. maydis* infection. *A. thaliana*, anthocyanin accumulation was regulated by JA, which is a defense signal molecule (Shan et al., 2009).

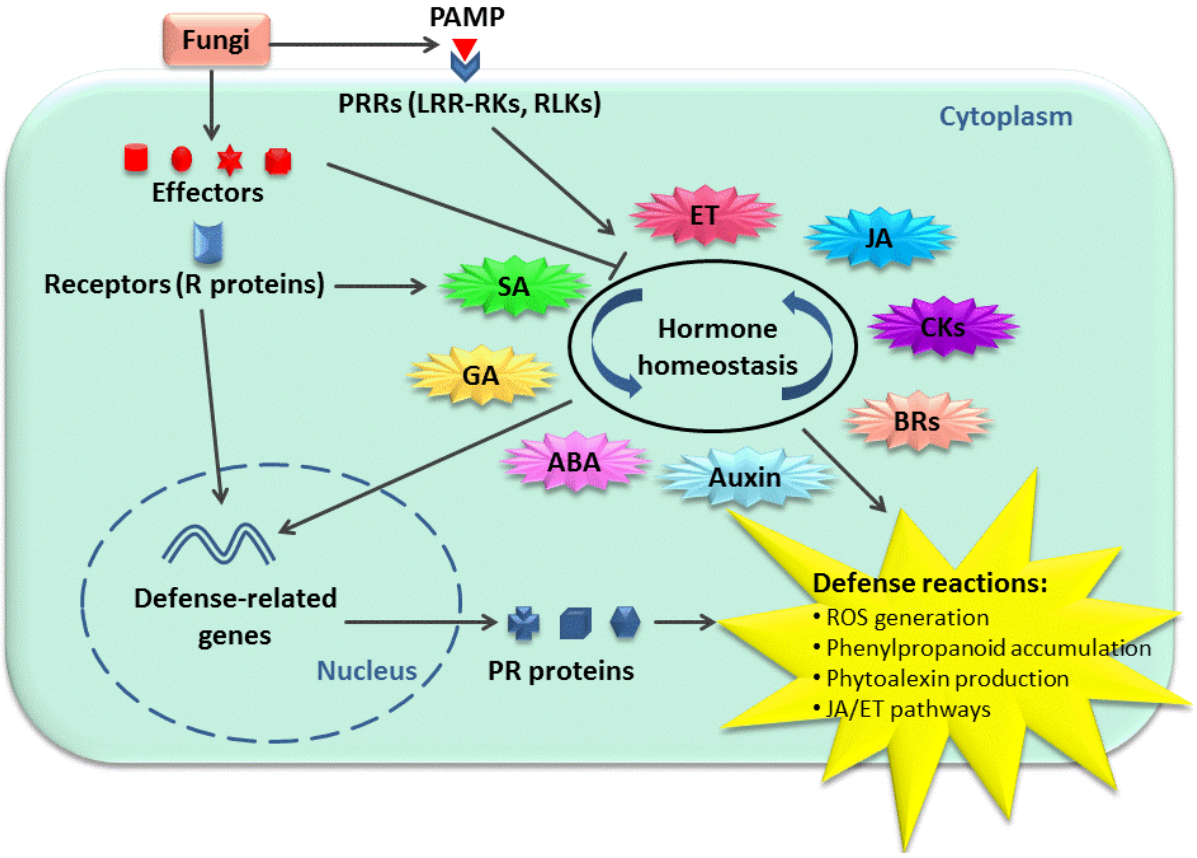

Figure 5. Hypothetical interactions between maize kernel and its fungal pathogens *A. flavus* and *F. verticillioides*. Arrows denote positive effect; inhibition lines denote negative effect. ET, ethylene; JA, jasmonic acid; SA, salicylic acid; GA, gibberellic acid; ABA, abscisic acid; CK, cytokinin; BRs, brassinosteroids. Figure is adapted from Denancé et al. (2013).

In addition, colonization by *A. flavus* and *F. verticillioides* appeared to remodel primary metabolism of maize kernels. Perhaps metabolic changes of the kernel provide essentially substrates for defense pathways. Carbohydrate metabolism pathways were impaired during infection of the kernel by these two fungi. In *A. thaliana*, amino acid homeostasis plays a critical role in the SA-dependent defense response (Liu et al., 2010). Our results also reflect the dramatic changes of cell wall modification, energy metabolism and transport of various substrates. The plant cell wall plays an essential role in pathogen recognition, signal transduction and activation of defense responses (Lloyd et al., 2011). Reinforcement of the plant cell wall is part of the basal defense response against pathogens (Egea et al., 2001; Underwood, 2012). Disruption of the plant cell wall by pathogen-derived cell wall-degrading enzymes often occurred during fungal invasion. Plants developed various strategies to attenuate pathogen attack, such as up-regulation of cell wall biosynthesis pathways to maintain the cell integrity (Mengiste, 2012).

In summary, we identified a set of maize genes that were differentially expressed during infection by *A. flavus* and *F. verticillioides* (Table S2). Several of these maize genes that we observed in our study have been reported to be responsive to either *A. flavus* or *F. verticillioides*, or both (Table 3).We deciphered similar patterns of defense response associated with *A. flavus* and *F. verticillioides* infection in immature maize kernels. Both ETI and PTI are likely to be involved in these two interactions (Fig. 5). Our results indicate that colonization by these fungi leads to accumulation of ROS, PCD, accumulation of secondary metabolites, and changes of the host regulatory network (Fig. 5). Hormone homeostasis and their regulatory network appear to be vital in disease resistance in maize. With this

information, we can start to understand and genetically engineer networks involved in host defense. Metabolic profiling and functional analysis of putative host defense-related genes could be conducted to characterize networks controlling disease resistance to these maize ear rot fungi.

Table 3. Comparison of maize genes and/or proteins that have been observed in this study and in previous studies. Af: associated with defense response to *A. flavus*; Fv: associated with defense response to *F. verticillioides*.

Gene and/or proteins	Association in previous studies	Association in this study	Reference
PR4	Af and Fv	Af and Fv	Bravo et al., 2003; Dolezal, 2010; Luo et al., 2011
PR5	Af and Fv	Af and Fv	Lanubile et al., 2013; Luo et al., 2011
PR10	Af	Af and Fv	Chen et al., 2006, 2010b; Dolezal, 2010; Xie et al., 2010
chitinases	Af and Fv	Af and Fv	Campos-Bermudez et al., 2013; Cordero et al., 1993; Dolezal, 2010; Ji et al., 2000; Lanubile et al., 2010; Luo et al., 2011; Moore et al., 2004; Wu et al., 1994a, 1994b
β-1, 3- glucanase	Af and Fv	Af and Fv	Campos-Bermudez et al., 2013; Chen et al., 2005; Cordero et al., 1993; Ji et al., 2000; Lanubile et al., 2013; Lozovaya et al., 1998; Luo et al., 2011; Wu et al., 1994a, 1994b
β-glucosidase	Af and Fv	Af and Fv	Campos-Bermudez et al., 2013; Lanubile et al., 2013; Luo et al., 2011
WRKYs	Af and Fv	Af and Fv	Campos-Bermudez et al., 2013; Lanubile et al., 2010, 2013; Luo et al., 2011
Mybs	Af and Fv	Af and Fv	Campos-Bermudez et al., 2013; Dolezal, 2010; Lanubile et al., 2010, 2013
LOXs	Af and Fv	Af and Fv	Dolezal, 2010; Gao et al., 2007, 2009; Lanubile et al., 2013; Wilson et al., 2001
OPRs	Fv	Af and Fv	Dolezal, 2010; Zhang et al., 2005
GSTs	Af and Fv	Af and Fv	Campos-Bermudez et al., 2013; Dolezal, 2010; Lanubile et al., 2010, 2013; Luo et al., 2011
Peroxidases	Af	Af and Fv	Chen et al., 2007; Luo et al., 2011
GLBs	Af and Fv	Af and Fv	Chen et al., 2001, 2002, 2007; Lanubile et al., 2010
LEAs	Af	Af and Fv	Chen et al., 2002, 2007; Luo et al., 2011
zein	Fv	Af	Lanubile et al., 2010, 2013
HSPs	Af and Fv	Af and Fv	Campos-Bermudez et al., 2013; Chen et al., 2002, 2007; Lanubile et al., 2010, 2013; Luo et al., 2011
TIs	Af and Fv	Af	Baker et al., 2009b; Chen et al., 1998, 1999a, 1999b, 2007; Lanubile et al., 2010; Tubajika and Damann, 2001
lectin-like protein	Af	Af and Fv	Baker et al., 2009a
protein kinase	Af and Fv	Af and Fv	Chen et al., 2005; Lanubile et al., 2010, 2013; Luo et al., 2011
protein phosphatases	Fv	Af and Fv	Lanubile et al., 2010, 2013

LITERATURE CITED

Alves, M. S., Dadalto, S. P., Gonçalves, A. B., De Souza, G. B., Barros, V. A., and Fietto, L. G. 2013. Plant bZIP Transcription Factors Responsive to Pathogens: A Review. International Journal of Molecular Sciences 14: 7815-7828.

An, Y. Q., and Lin, L. 2011. Transcriptional regulatory programs underlying barley germination and regulatory functions of Gibberellin and abscisic acid. BMC Plant Biology 11: 105.

Angra-Sharma, R., and Sharma, D. K. 1999. Cytokinins in pathogenesis and disease resistance of *Pyrenophora teres*-barley and *Dreschslera maydis*-maize interactions during early stages of infection. Mycopathologia 148: 87-95.

Bacon, C. W., Bennett, R. M., Hinton, D. M., and Voss, K. A. 1992. Scanning electron microscopy of *Fusarium moniliforme* within asymptomatic corn kernels and kernels associated with equine leukoencephalomalacia. Plant Disease 76: 144-148.

Baker, R. L., Brown, R. L., Chen, Z. Y., Cleveland, T. E., and Fakhoury, A. M. 2009a. A Maize Lectin-Like Protein with Antifungal Activity against *Aspergillus flavus*. Journal of Food Protection 72: 120-127.

Baker, R. L., Brown, R. L., Chen, Z. Y., Cleveland, T. E., and Fakhoury, A. M. 2009b. A Maize Trypsin Inhibitor (ZmTIp) with Limited Activity against *Aspergillus flavus*. Journal of Food Protection 72: 185-188.

Basse, C. W. 2005. Dissecting defense-related and developmental transcriptional responses of maize during *Ustilago maydis* infection and subsequent tumor formation. Plant physiology 138: 1774-1784.

Behr, M., Motyka, V., Weihmann, F., Malbeck, J., Deising, H. B., and Wirsel, S. G. 2012. Remodeling of Cytokinin Metabolism at Infection Sites of *Colletotrichum graminicola* on Maize Leaves. Molecular Plant-Microbe Interactions 25: 1073-1082.

Belenghi, B., Acconcia, F., Trovato, M., Perazzolli, M., Bocedi, A., Polticelli, F., Ascenzi, P., and Delledonne, M. 2003. AtCYS1, a cystatin from *Arabidopsis thaliana*, suppresses hypersensitive cell death. European Journal of Biochemistry 270: 2593-2604.

Belkhadir, Y., Jaillais, Y., Epple, P., Balsemão-Pires, E., Dangl, J. L., Chory, J. 2012. Brassinosteroids modulate the efficiency of plant immune responses to microbe-associated molecular patterns. Proceedings of the National Academy of Sciences of the United States of America 109: 297-302.

Bhattarai, K. K., Atamian, H. S., Kaloshian, I., and Eulgem, T. 2010. WRKY72-type transcription factors contribute to basal immunity in tomato and Arabidopsis as well as gene-for-gene resistance mediated by the tomato R gene Mi-1. The Plant Journal 63: 229-240.

Bluhm, B. H., Kim, H., Butchko, R. A. E., and Woloshuk, C. P. 2008. Involvement of ZFR1 of *Fusarium verticillioides* in kernel colonization and the regulation of FST1, a putative sugar transporter gene required for fumonisin biosynthesis on maize kernels. Molecular Plant Pathology 9: 203-211.

Bravo, J. M., Campo, S., Murillo, I., Coca, M., and San Segundo, B. 2003. Fungus- and wound-induced accumulation of mRNA containing a class II chitinase of the pathogenesis-related protein 4 (PR-4) family of maize. Plant Molecular Biology 52: 745-759.

Brodersen, P., Petersen, M., Bjorn Nielsen, H., Zhu, S., Newman, M. A., Shokat, K. M., Rietz, S., Parker, J., and Mundy, J. 2006. Arabidopsis MAP kinase 4 regulates salicylic acid- and jasmonic acid/ethylene-dependent responses via EDS1 and PAD4. The Plant Journal 47: 532-546.

Brown, R. L., Menkir, A., Chen, Z. Y., Bhatnagar, D., Yu, J., Yao, H., and Cleveland, T. E. 2013. Breeding aflatoxin-resistant maize lines using recent advances in technologies - a review. Food Additives & Contaminants: Part A: Chemistry, Analysis, Control, Exposure & Risk Assessment 30: 1382-1391.

Campos-Bermudez, V. A., Fauguel, C. M., Tronconi, M. A., Casati, P., Presello, D. A., and Andreo, C. S. 2013. Transcriptional and metabolic changes associated to the infection by *Fusarium verticillioides* in maize inbreds with contrasting ear rot resistance. PLoS One 8: e61580.

Caspi, R., Altman, T., Dreher, K., Fulcher, C. A., Subhraveti, P., Keseler, I. M., Kothari, A., Krummenacker, M., Latendresse, M., Mueller, L. A., Ong, Q., Paley, S., Pujar, A., Shearer, A. G., Travers, M., Weerasinghe, D., Zhang, P., and Karp, P. D. 2012. The

MetaCyc database of metabolic pathways and enzymes and the BioCyc collection of pathway/genome databases. Nucleic Acids Research 40: D742-D753.

Castellana, N. E., Shen, Z., He, Y., Walley, J. W., Cassidy, C. J., Briggs, S. P., and Bafna, V. 2013. An Automated Proteogenomic Method Utilizes Mass Spectrometry to Reveal Novel Genes in *Zea mays*. Molecular & Cellular Proteomics 13: 157-167.

Chen, Z. Y., Brown, R. L., Lax, A. R., Guo, B. Z., Cleveland, T. E., and Russin, J. S. 1998. Resistance to *Aspergillus flavus* in Corn Kernels Is Associated with a 14-kDa Protein. Phytopathology 88: 276-281.

Chen, Z. Y., Brown, R. L., Lax, A. R., Cleveland, T. E., and Russin, J. S. 1999a. Inhibition of plant-pathogenic fungi by a corn trypsin inhibitor overexpressed in *Escherichia coli*. Applied and Environmental Microbiology 65: 1320-1324.

Chen, Z. Y., Brown, R. L., Russin, J. S., Lax, A. R., and Cleveland, T. E. 1999b. A Corn Trypsin Inhibitor with Antifungal Activity Inhibits *Aspergillus flavus* alpha-Amylase. Phytopathology 89: 902-907.

Chen, Z. Y., Brown, R. L., Cleveland, T. E., Damann, K. E., and Russin, J. S. 2001. Comparison of Constitutive and Inducible Maize Kernel Proteins of Genotypes Resistant or Susceptible to Aflatoxin Production. Journal of Food Protection 64: 1785-1792.

Chen, Z. Y., Brown, R. L., Damann, K. E., and Cleveland, T. E. 2002. Identification of Unique or Elevated Levels of Kernel Proteins in Aflatoxin-Resistant Maize Genotypes Through Proteome Analysis. Phytopathology 92: 1084-1094.

Chen, Z. Y., Brown, R. L., Menkir, A., Damann, K., and Cleveland, T. E. 2005. Proteome analysis of near isogenic maize lines differing in the level of resistance against *Aspergillus flavus* infection/aflatoxin production. Phytopathology 95: S19.

Chen, Z. Y., Brown, R. L., Rajasekaran, K., Damann, K. E., and Cleveland, T. E. 2006. Identification of a Maize Kernel Pathogenesis-Related Protein and Evidence for Its Involvement in Resistance to *Aspergillus flavus* Infection and Aflatoxin Production. Phytopathology 96: 87-95.

Chen, Z. Y., Brown, R. L., Damann, K. E., and Cleveland, T. E. 2007. Identification of Maize Kernel Endosperm Proteins Associated with Resistance to Aflatoxin Contamination by *Aspergillus flavus*. Phytopathology 97: 1094-1103.

Chen, C., Farmer, A. D., Langley, R. J., Mudge, J., Crow, J. A., May, G. D., Huntley, J., Smith, A. G., and Retzel, E. F. 2010a. Meiosis-specific gene discovery in plants: RNA-Seq applied to isolated *Arabidopsis* male meiocytes. BMC Plant Biology 10: 280.

Chen, Z. Y., Brown, R. L., Damann, K. E., and Cleveland, T. E. 2010b. PR10 expression in maize and its effect on host resistance against *Aspergillus flavus* infection and aflatoxin production. Molecular Plant Pathology 11: 69-81.

Cheng, Y., Li, X., Jiang, H., Ma, W., Miao, W., Yamada, T., and Zhang, M. 2012. Systematic analysis and comparison of nucleotide-binding site disease resistance genes in maize. FEBS Journal 279: 2431-2443.

Chinchilla, D., Zipfel, C., Robatzek, S., Kemmerling, B., Nürnberger, T., Jones, J. D., Felix, G., and Boller, T. 2007. A flagellin-induced complex of the receptor FLS2 and BAK1 initiates plant defence. Nature 448: 497-500.

Cho, M. J., and Cho, H. T. 2012. The function of ABCB transporters in auxin transport. Plant Signaling & Behavior 8: e22990.

Collins, N. C., Webb, C. A., Seah, S., Ellis, J. G., Hulbert, S. H., and Pryor, A. 1998. The Isolation and Mapping of Disease Resistance Gene Analogs in Maize. Molecular Plant-Microbe Interactions 11: 968-978.

Cordero, M. J., Raventos, D., and San Segundo, B. 1993. Differential Expression and Induction of Chitinases and β-1,3-Glucanases in Response to Fungal Infection During Germination of Maize Seeds. Molecular Plant-Microbe Interactions 7: 23-31.

Cordero, M. J., Raventos, D., and San Segundo, B. 1994. Expression of a maize proteinase inhibitor gene is induced in response to wounding and fungal infection: systemic wound-response of a monocot gene. The Plant Journal 6: 141-150.

Denancé, N., Sánchez-Vallet, A., Goffner, D., and Molina, A. 2013. Disease resistance or growth: the role of plant hormones in balancing immune responses and fitness costs. Frontiers in Plant Science 4: 155.

Derksen, H., Rampitsch, C., and Daayf, F. 2013. Signaling cross-talk in plant disease resistance. Plant Science 207: 79-87.

Dodds, P. N., and Rathjen, J. P. 2010. Plant immunity: towards an integrated view of plant-pathogen interactions. Nature Reviews Genetics 11: 539-548.

Doehlemann, G., Wahl, R., Horst, R. J., Voll, L. M., Usadel, B., Poree, F., Stitt, M., Pons-Kuhnemann, J., Sonnewald, U., Kahmann, R., and Kamper, J. 2008. Reprogramming a maize plant: transcriptional and metabolic changes induced by the fungal biotroph *Ustilago maydis*. The Plant Journal 56: 181-195.

Dolezal, A. L. 2010. Interactions Between *Aspergillus flavus* and the Developing Maize Kernel. Doctoral dissertation Retrieved from ProQuest Dissertations and Theses: OCLC Number: 704568905.

Dolezal, A. L., Obrian, G. R., Nielsen, D. M., Woloshuk, C. P., Boston, R. S., and Payne, G. A. 2013. Localization, morphology and transcriptional profile of *Aspergillus flavus* during seed colonization. Molecular Plant Pathology 14: 898-909.

Dong, X. 2004. NPR1, all things considered. Current Opinion in Plant Biology 7: 547-552.

Dudler, R., Hertig, C., Rebmann, G., Bull, J., and Mauch, F. 1991. A pathogen-induced wheat gene encodes a protein homologous to glutathione-S-transferases. Molecular Plant-Microbe Interactions 4: 14-18.

Duncan, K. E., and Howard, R. J. 2010. Biology of maize kernel infection by *Fusarium verticillioides*. Molecular Plant-Microbe Interactions 23: 6-16.

Egea, C., Ahmed, A. S., Candela, M., and Candela, M. E. 2001. Elicitation of peroxidase activity and lignin biosynthesis in pepper suspension cells by *Phytophthora capsici*. Journal of Plant Physiology 158: 151-158.

El Oirdi, M., El Rahman, T. A., Rigano, L., El Hadrami, A., Rodriguez, M. C., Daayf, F., Vojnov, A., and Bouarab, K. 2011. *Botrytis cinerea* manipulates the antagonistic effects between immune pathways to promote disease development in tomato. Plant Cell 23: 2405-2421.

Eulgem, T., and Somssich, I. E. 2007. Networks of WRKY transcription factors in defense signaling. Current Opinion in Plant Biology 10: 366-371.

Fornalé, S., Sonbol, F. M., Maes, T., Capellades, M., Puigdomènech, P., Rigau, J., and Caparrós-Ruiz, D. 2006. Down-regulation of the maize and *Arabidopsis thaliana*

caffeic acid O-methyl-transferase genes by two new maize R2R3-MYB transcription factors. Plant Molecular Biology 62: 809-823.

Fu, X., Fu, N., Guo, S., Yan, Z., Xu, Y., Hu, H., Menzel, C., Chen, W., Li, Y., Zeng, R., and Khaitovich, P. 2009. Estimating accuracy of RNA-Seq and microarrays with proteomics. BMC Genomics 10: 161.

Gao, X., Shim, W. B., Gobel, C., Kunze, S., Feussner, I., Meeley, R., Balint-Kurti, P., and Kolomiets, M. 2007. Disruption of a maize 9-lipoxygenase results in increased resistance to fungal pathogens and reduced levels of contamination with mycotoxin fumonisin. Molecular Plant-Microbe Interactions 20: 922-933.

Gao, X., Brodhagen, M., Isakeit, T., Brown, S. H., Gobel, C., Betran, J., Feussner, I., Keller, N. P., and Kolomiets, M. V. 2009. Inactivation of the lipoxygenase ZmLOX3 increases susceptibility of maize to *Aspergillus* spp. Molecular Plant-Microbe Interactions 22: 222-231.

Glazebrook, J. 2005. Contrasting Mechanisms of Defense Against Biotrophic and Necrotrophic Pathogens. Annual Review of Phytopathology 43: 205-227.

Gomez, L. D., Noctor, G., Knight, M. R., and Foyer, C. H. 2004. Regulation of calcium signalling and gene expression by glutathione. Journal of Experimental Botany 55: 1851-1859.

Gray, J., Close, P. S., Briggs, S. P., and Johal, G. S. 1997. A novel suppressor of cell death in plants encoded by the *Lls1* gene of maize. Cell Host & Microbe 89: 25-31.

Harvey, B. M. R., and Oaks, A. 1974. The Role of Gibberellic Acid in the Hydrolysis of Endosperm Reserves in *Zea mays*. Planta (Berl.) 121: 67-74.

Hejgaard, J., Jacobsen, S., and Svendsen, I. 1991. Two antifungal thaumatin-like proteins from barley grain. FEBS Letters 291: 127-131.

Holmes, R. A., Boston, R. S., and Payne, G. A. 2008. Diverse inhibitors of aflatoxin biosynthesis. Applied Microbiology and Biotechnology 78: 559-572.

Hu, X., and Reddy, A. S. 1997. Cloning and expression of a PR5-like protein from *Arabidopsis*: inhibition of fungal growth by bacterially expressed protein. Plant Molecular Biology 34: 949-959.

Huynh, Q. K., Hironaka, C. M., Levine, E. B., Smith, C. E., Borgmeyer, J. R., and Shah, D. M. 1992. Antifungal proteins from plants. Purification, molecular cloning, and antifungal properties of chitinases from maize seed. The Journal of Biological Chemistry 267: 6635-6640.

Iglesias, M. J., Terrile, M. C., and Casalongue, C. A. 2011. Auxin and salicylic acid signalings counteract the regulation of adaptive responses to stress. Plant Signaling & Behavior 6: 452-454.

Ji, C., Norton, R. A., Wicklow, D. T., and Dowd, P. F. 2000. Isoform patterns of chitinase and beta-1,3-glucanase in maturing corn kernels (*Zea mays* L.) associated with *Aspergillus flavus* milk stage infection. Journal of Agricultural and Food Chemistry 48: 507-511.

Johnson, E. T., Berhow, M. A., and Dowd, P. F. 2007. Expression of a Maize Myb Transcription Factor Driven by a Putative Silk-Specific Promoter Significantly Enhances Resistance to *Helicoverpa zea* in Transgenic Maize. Journal of Agricultural and Food Chemistry 55: 2998-3003.

Jones, J. D. G., and Dangl, J. L. 2006. The plant immune system. Nature 444: 323-329.

Kawahara, Y., Oono, Y., Kanamori, H., Matsumoto, T., Itoh, T., and Minami, E. 2012. Simultaneous RNA-Seq Analysis of a Mixed Transcriptome of Rice and Blast Fungus Interaction. PLoS One 7: e49423.

Kelley, R. Y., Williams, W. P., Mylroie, J. E., Boykin, D. L., Harper, J. W., Windham, G. L., Ankala, A., and Shan, X. 2012. Identification of maize genes associated with host plant resistance or susceptibility to *Aspergillus flavus* infection and aflatoxin accumulation. PLoS One 7: e36892.

Kim, K. H., Kang, Y. J., Kim, D. H., Yoon, M. Y., Moon, J. K., Kim, M. Y., Van, K., and Lee, S. H. 2011. RNA-Seq analysis of a soybean near-isogenic line carrying bacterial leaf pustule-resistant and -susceptible alleles. DNA Research 18: 483-497.

Koehler, B. 1942. Natural mode of entrance of fungi into Corn ears and some symptoms that indicate infection. Journal of Agricultural Research 64: 421-442.

Krebitz, M., Wagner, B., Ferreira, F., Peterbauer, C., Campillo, N., Witty, M., Kolarich, D., Steinkellner, H., Scheiner, O., and Breiteneder, H. 2003. Plant-based Heterologous Expression of Mal d 2, a Thaumatin-like Protein and Allergen of Apple (*Malus*

domestica), and its Characterization as an Antifungal Protein. Journal of Molecular Biology 329: 721-730.

Lanubile, A., Pasini, L., and Marocco, A. 2010. Differential gene expression in kernels and silks of maize lines with contrasting levels of ear rot resistance after *Fusarium verticillioides* infection. Journal of Plant Physiology 167: 1398-1406.

Lanubile, A., Logrieco, A., Battilani, P., Proctor, R. H., and Marocco, A. 2013. Transcriptional changes in developing maize kernels in response to fumonisin-producing and nonproducing strains of *Fusarium verticillioides*. Plant Science 210: 183-192.

Lawrence, C. J., Dong, Q., Polacco, M. L., Seigfried, T. E., and Brendel, V. 2004. MaizeGDB, the community database for maize genetics and genomics. Nucleic Acids Research 32: D393-D397.

Li, P., Ponnala, L., Gandotra, N., Wang, L., Si, Y., Tausta, S. L., Kebrom, T. H., Provart, N., Patel, R., Myers, C. R., Reidel, E. J., Turgeon, R., Liu, P., Sun, Q., Nelson, T., and Brutnell, T. P. 2010. The developmental dynamics of the maize leaf transcriptome. Nature Genetics 42: 1060-1067.

Li, C. W., Su, R. C., Cheng, C. P., Sanjaya, You, S. J., Hsieh, T. H., Chao, T. C., and Chan, M. T. 2011. Tomato RAV transcription factor is a pivotal modulator involved in the AP2/EREBP-mediated defense pathway. Plant Physiology 156: 213-227.

Lillehoj, E. B., Kwolek, W. F., Fennell, D. I., and Milburn, M. S. 1975. Aflatoxin Incidence and Association with Bright Greenish-Yellow Fluorescence and Insect Damage in a Limited Survey of Freshly Harvested High-Moisture Corn. Cereal Chemistry 52: 403-411.

Ling, Y., Du, Z., Zhang, Z., and Su, Z. 2010. ProFITS of maize: a database of protein families involved in the transduction of signalling in the maize genome. BMC Genomics 11: 580.

Liu, G., Ji, Y., Bhuiyan, N. H., Pilot, G., Selvaraj, G., Zou, J., and Wei, Y. 2010. Amino acid homeostasis modulates salicylic acid-associated redox status and defense responses in *Arabidopsis*. Plant Cell 22: 3845-3863.

Livingston, D. P., Tuong, T. D., Haigler, C. H., Avci, U., Tallury, S. P. 2009. Rapid Microwave Processing of Winter Cereals for Histology Allows Identification of Separate Zones of Freezing Injury in the Crown. Crop Science 49: 1837-1842.

Livingston, D. P., Henson, C. A., Tuong, T. D., Wise, M. L., Tallury, S. P., and Duke, S. H. 2013. Histological Analysis and 3D Reconstruction of Winter Cereal Crowns Recovering from Freezing: A Unique Response in Oat (*Avena sativa* L.). PLoS One 8: e53468.

Lloyd, A. J., William Allwood, J., Winder, C. L., Dunn, W. B., Heald, J. K., Cristescu, S. M., Sivakumaran, A., Harren, F. J., Mulema, J., Denby, K., Goodacre, R., Smith, A. R., and Mur, L. A. 2011. Metabolomic approaches reveal that cell wall modifications play a major role in ethylene-mediated resistance against *Botrytis cinerea*. The Plant Journal 67: 852-868.

Loyall, L., Uchida, K., Braun, S., Furuya, M., and Frohnmeyer, H. 2000. Glutathione and a UV light-induced glutathione S-transferase are involved in signaling to chalcone synthase in cell cultures. Plant Cell 12: 1939-1950.

Lozovaya, V. V., Waranyuwat, A., and Widholm, J. M. 1998. Beta-1,3-Glucanase and resistance to *Aspergillus flavus* infection in maize. Crop Science 38: 1255-1260.

Lu, T., Lu, G., Fan, D., Zhu, C., Li, W., Zhao, Q., Feng, Q., Zhao, Y., Guo, Y., Li, W., Huang, X., and Han, B. 2010. Function annotation of the rice transcriptome at single-nucleotide resolution by RNA-seq. Genome Research 20: 1238-1249.

Luo, M., Brown, R. L., Chen, Z. Y., Menkir, A., Yu, J., and Bhatnagar, D. 2011. Transcriptional Profiles Uncover *Aspergillus flavus*-Induced Resistance in Maize Kernels. Toxins (Basel) 3: 766-786.

Lyons, E., and Freeling, M. 2008. How to usefully compare homologous plant genes and chromosomes as DNA sequences. The Plant Journal 53: 661-673.

Marioni, J. C., Mason, C. E., Mane, S. M., Stephens, M., and Gilad, Y. 2008. RNA-seq: an assessment of technical reproducibility and comparison with gene expression arrays. Genome Research 18: 1509-1517.

Marsh, S., and Payne, G. 1984. Preharvest Infection of Corn Silks and Kernels by *Aspergillus flavus*. Phytopathology 74: 1284-1289.

Matasci, N., and McKay, S. 2013. Phylogenetic Analysis with the iPlant Discovery Environment. Page Unit6 in: Current Protocols in Bioinformatics, John Wiley & Sons, Inc.

Mauch, F., and Dudler, R. 1993. Differential induction of distinct glutathione-S-transferases of wheat by xenobiotics and by pathogen attack. Plant Physiology 102: 1193-1201.

Mengiste, T., Chen, X., Salmeron, J., and Dietrich, R. 2003. The BOTRYTIS SUSCEPTIBLE1 gene encodes an R2R3MYB transcription factor protein that is required for biotic and abiotic stress responses in Arabidopsis. Plant Cell 15: 2551-2565.

Mengiste, T. 2012. Plant Immunity to Necrotrophs. Annual Review of Phytopathology 50: 267-294.

Moore, K. G., Price, M. S., Boston, R. S., Weissinger, A. K., and Payne, G. A. 2004. A Chitinase from Tex6 Maize Kernels Inhibits Growth of *Aspergillus flavus*. Phytopathology 94: 82-87.

Morris, S. W., Vernooij, B., Titatarn, S., Starrett, M., Thomas, S., Wiltse, C. C., Frederiksen, R. A., Bhandhufalck, A., Hulbert, S., and Uknes, S. 1998. Induced resistance responses in maize. Molecular Plant-Microbe Interactions 11: 643-658.

Mukherjee, A. K., Carpm, M. J., Zuchman, R., Ziv, T., Horwitz, B. A., and Gepstein, S. 2010. Proteomics of the response of *Arabidopsis thaliana* to infection with *Alternaria brassicicola*. Journal of Proteomics 73: 709-720.

Nakashita, H., Yasuda, M., Nitta, T., Asami, T., Fujioka, S., Arai, Y., Sekimata, K., Takatsuto, S., Yamaguchi, I., and Yoshida, S. 2003. Brassinosteroid functions in a broad range of disease resistance in tobacco and rice. The Plant Journal 33: 887-898.

Navarro, L., Bari, R., Achard, P., Lisón, P., Nemri, A., Harberd, N. P., and Jones, J. D. 2008. DELLAs Control Plant Immune Responses by Modulating the Balance of Jasmonic Acid and Salicylic Acid Signaling. Current Biology 18: 650-655.

Nimchuk, Z., Eulgem, T., Holt, B. F., and Dangl, J. L. 2003. RECOGNITION AND RESPONSE IN THE PLANT IMMUNE SYSTEM. Annual Review of Genetics 37: 579-609.

Ogawa, K. 2005. Glutathione-associated regulation of plant growth and stress responses. Antioxidants & Redox Signaling 7: 973-981.

Pape, S., Thurow, C., and Gatz, C. 2010. The Arabidopsis PR-1 promoter contains multiple integration sites for the coactivator NPR1 and the repressor SNI1. Plant Physiology 154: 1805-1818.

Payne, G. A., Cassel, D. K., and Adkins, C. R. 1986. Reduction of aflatoxin contamination in corn by irrigation and tillage. Phytopathology 76: 679-684.

Payne, G. A. 1992. Aflatoxin in maize. Critical Reviews in Plant Sciences 10: 423-440.

Pechanova, O., Pechan, T., Williams, W. P., and Luthe, D. S. 2011. Proteomic analysis of the maize rachis: potential roles of constitutive and induced proteins in resistance to *Aspergillus flavus* infection and aflatoxin accumulation. Proteomics 11: 114-127.

Pei-Bao, Z., Ren, A. Z., Xu, H. J., and Li, D. C. 2010. The gene *fpk1*, encoding a cAMP-dependent protein kinase catalytic subunit homolog, is required for hyphal growth, spore germination, and plant infection in *Fusarium verticillioides*. Journal of Microbiology and Biotechnology 20: 208-216.

Pieterse, C. M., Leon-Reyes, A., Van der Ent, S., and Van Wees, S. C. 2009. Networking by small-molecule hormones in plant immunity. Nature Chemical Biology 5: 308-316.

Pré, M., Atallah, M., Champion, A., De Vos, M., Pieterse, C. M., and Memelink, J. 2008. The AP2/ERF domain transcription factor ORA59 integrates jasmonic acid and ethylene signals in plant defense. Plant Physiology 147: 1347-1357.

Rahman, T. A., Oirdi, M. E., Gonzalez-Lamothe, R., and Bouarab, K. 2012. Necrotrophic Pathogens Use the Salicylic Acid Signaling Pathway to Promote Disease Development in Tomato. Molecular Plant-Microbe Interactions 25: 1584-1593.

Ramage, G., Mowat, E., Jones, B., Williams, C., and Lopez-Ribot, J. 2009. Our Current Understanding of fungal Biofilms. Critical Reviews in Microbiology 35: 340-355.

Sánchez-Rangel, D., Sánchez-Nieto, S., and Plasencia, J. 2012. Fumonisin B1, a toxin produced by *Fusarium verticillioides*, modulates maize beta-1,3-glucanase activities involved in defense response. Planta 235: 965-978.

Schnable, P. S., Ware, D., Fulton, R. S., Stein, J. C., Wei, F., Pasternak, S., Liang, C., Zhang, J., Fulton, L., Graves, T. A., Minx, P., Reily, A. D., Courtney, L., Kruchowski, S. S., Tomlinson, C., Strong, C., Delehaunty, K., Fronick, C., Courtney, B., Rock, S. M., Belter, E., Du, F., Kim, K., Abbott, R. M., Cotton, M., Levy, A., Marchetto, P., Ochoa, K., Jackson, S. M., Gillam, B., Chen, W., Yan, L., Higginbotham, J., Cardenas, M., Waligorski, J., Applebaum, E., Phelps, L., Falcone, J., Kanchi, K., Thane, T., Scimone, A., Thane, N., Henke, J., Wang, T., Ruppert, J., Shah, N., Rotter, K., Hodges, J., Ingenthron, E., Cordes, M., Kohlberg, S., Sgro, J., Delgado, B., Mead, K., Chinwalla, A., Leonard, S., Crouse, K., Collura, K., Kudrna, D., Currie, J., He, R., Angelova, A., Rajasekar, S., Mueller, T., Lomeli, R., Scara, G., Ko, A., Delaney, K., Wissotski, M., Lopez, G., Campos, D., Braidotti, M., Ashley, E., Golser, W., Kim, H., Lee, S., Lin, J., Dujmic, Z., Kim, W., Talag, J., Zuccolo, A., Fan, C., Sebastian, A., Kramer, M., Spiegel, L., Nascimento, L., Zutavern, T., Miller, B., Ambroise, C., Muller, S., Spooner, W., Narechania, A., Ren, L., Wei, S., Kumari, S., Faga, B., Levy, M. J., McMahan, L., Van Buren, P., Vaughn, M. W., Ying, K., Yeh, C. T., Emrich, S. J., Jia, Y., Kalyanaraman, A., Hsia, A. P., Barbazuk, W. B., Baucom, R. S., Brutnell, T. P., Carpita, N. C., Chaparro, C., Chia, J. M., Deragon, J. M., Estill, J. C., Fu, Y., Jeddeloh, J. A., Han, Y., Lee, H., Li, P., Lisch, D. R., Liu, S., Liu, Z., Nagel, D. H., McCann, M. C., SanMiguel, P., Myers, A. M., Nettleton, D., Nguyen, J., Penning, B. W., Ponnala, L., Schneider, K. L., Schwartz, D. C., Sharma, A., Soderlund, C., Springer, N. M., Sun, Q., Wang, H., Waterman, M., Westerman, R., Wolfgruber, T. K., Yang, L. Y., Y., Zhang, L., Zhou, S., Zhu, Q., Bennetzen, J. L., Dawe, R. K., Jiang, J., Jiang, N., Presting, G. G., Wessler, S. R., Aluru, S., Martienssen, R. A., Clifton, S. W., McCombie, W. R., Wing, R. A., and Wilson, R. K. 2009. The B73 Maize Genome: Complexity, Diversity, and Dynamics. Science 326: 1112-1115.

Shan, X., Zhang, Y., Peng, W., Wang, Z., and Xie, D. 2009. Molecular mechanism for jasmonate-induction of anthocyanin accumulation in Arabidopsis. Journal of Experimental Botany 60: 3849-3860.

Shim, J. S., and Choi, Y. D. 2013. Direct regulation of WRKY70 by AtMYB44 in plant defense responses. Plant Signaling & Behavior 8: e20783.

Siemens, J., Keller, I., Sarx, J., Kunz, S., Schuller, A., Nagel, W., Schmülling, T., Parniske, M., and Ludwig-Müller, J. 2006. Transcriptome Analysis of Arabidopsis Clubroots Indicate a Key Role for Cytokinins in Disease Development. Molecular Plant-Microbe Interactions 19: 480-494.

Simmons, C., Hantke, S., Grant, S., Johal, G. S., and Briggs, S. P. 1998. The Maize Lethal Leaf Spot 1 Mutant Has Elevated Resistance to Fungal Infection at the Leaf Epidermis. Molecular Plant-Microbe Interactions 11: 1110-1118

Singh, K. B., Foley, R. C., and Oñate-Sánchez, L. 2002. Transcription factors in plant defense and stress responses. Current Opinion in Plant Biology 5: 430-436.

Skibbe, D. S., Doehlemann, G., Fernandes, J., and Walbot, V. 2010. Maize tumors caused by *Ustilago maydis* require organ-specific genes in host and pathogen. Science 328: 89-92.

Smart, M. G., Wicklow, D. T., and Caldwell, R. W. 1990. Pathogenesis in *Aspergillus* Ear Rot of Maize: Light Microscopy of Fungal Spread from Wounds. Phytopathology 80: 1287-1294.

Sobek, E. A., and Munkvold, G. P. 1999. European corn borer (Lepidoptera: Pyralidae) larvae as vectors of *Fusarium moniliforme*, causing kernel rot and symptomless infection of maize kernels. Journal of Economic Entomology 92: 503-509.

Solomon, M., Belenghi, B., Delledonne, M., Menachem, E., and Levine, A. 1999. The involvement of cysteine proteases and protease inhibitor genes in the regulation of programmed cell death in plants. Plant Cell 11: 431-444.

St Leger, R. J., Screen, S. E., and Shams-Pirzadeh, B. 2000. Lack of host specialization in *Aspergillus flavus*. Applied and Environmental Microbiology 66: 320-324.

Sytykiewicz, H. 2011. Expression Patterns of Glutathione Transferase Gene (*GstI*) in Maize Seedlings Under Juglone-Induced Oxidative Stress. International Journal of Molecular Sciences 12: 7982-7995.

Trapnell, C., Roberts, A., Goff, L., Pertea, G., Kim, D., Kelley, D. R., Pimentel, H., Salzberg, S. L., Rinn, J. L., and Pachter, L. 2012. Differential gene and transcript expression analysis of RNA-seq experiments with TopHat and Cufflinks. Nature Protocols 7: 562-578.

Tubajika, K. M., and Damann, K. E. 2001. Sources of resistance to aflatoxin production in maize. Journal of Agricultural and Food Chemistry 49: 2652-2656.

Turian, G., and Hamilton, R. H. 1960. Chemical detection of 3-indolylacetic acid in *Ustilago zeae* tumors. Biochimica et Biophysica Acta 41: 148-150.

Underwood, W. 2012. The plant cell wall: a dynamic barrier against pathogen invasion. Frontiers in Plant Science 3: 85.

Usadel, B., Poree, F., Nagel, A., Lohse, M., Czedik-Eysenberg, A., and Stitt, M. 2009. A guide to using MapMan to visualize and compare Omics data in plants: a case study in the crop species, Maize. Plant, Cell & Environment 32: 1211-1229.

van Verk, M. C., Bol, J. F., and Linthorst, H. J. 2011. WRKY transcription factors involved in activation of SA biosynthesis genes. BMC Plant Biology 11: 89.

Veronese, P., Nakagami, H., Bluhm, B., Abuqamar, S., Chen, X., Salmeron, J., Dietrich, R. A., Hirtm, H., and Mengiste, T. 2006. The membrane-anchored BOTRYTIS-INDUCED KINASE1 plays distinct roles in Arabidopsis resistance to necrotrophic and biotrophic pathogens. Plant Cell 18: 257-273.

Vidal, S., Eriksson, A. R. B., Montesano, M., Denecke, J., and Palva, E. T. 1998. Cell Wall-Degrading Enzymes from *Erwinia carotovora* Cooperate in the Salicylic Acid-Independent Induction of a Plant Defense Response. Molecular Plant-Microbe Interactions 11: 23-32.

Voitsik, A. M., Muench, S., Deising, H. B., and Voll, L. M. 2013. Two recently duplicated maize NAC transcription factor paralogs are induced in response to *Colletotrichum graminicola* infection. BMC Plant Biology 13: 85.

Walley, J. W., Shen, Z., Sartor, R., Wu, K. J., Osborn, J., Smith, L. G., and Briggs, S. P. 2013. Reconstruction of protein networks from an atlas of maize seed proteotypes. Proceedings of the National Academy of Sciences 110: E4808-E4817.

Walters, D. R., and McRoberts, N. 2006. Plants and biotrophs: a pivotal role for cytokinins? Trends in Plant Science 11: 581-586.

Wang, D., Amornsiripanitch, N., and Dong, X. 2006. A Genomic Approach to Identify Regulatory Nodes in the Transcriptional Network of Systemic Acquired Resistance in Plants. PLoS Pathogens 2: e123.

Wang, D., Pajerowska-Mukhtar, K., Culler, A. H., and Dong, X. 2007. Salicylic Acid Inhibits Pathogen Growth in Plants through Repression of the Auxin Signaling Pathway. Current Biology 17: 1784-1790.

Wang, X., Tang, C., Deng, L., Cai, G., Liu, X., Liu, B., Han, Q., Buchenauer, H., Wei, G., Han, D., Huang, L., and Kang, Z. 2010. Characterization of a pathogenesis-related thaumatin-like protein gene *TaPR5* from wheat induced by stripe rust fungus. Plant Physiology 139: 27-38.

Wildermuth, M. C., Dewdney, J., Wu, G., and Ausubel, F. M. 2001. Isochorismate synthase is required to synthesize salicylic acid for plant defence. Nature 414: 562-565.

Wilson, R. A., Gardner, H. W., and Keller, N. P. 2001. Cultivar-dependent expression of a maize lipoxygenase responsive to seed infesting fungi. Molecular Plant-Microbe Interactions 14: 980-987.

Wu, S., Kriz, A. L., and Widholm, J. M. 1994a. Nucleotide sequence of a maize cDNA for a class II, acidic beta-1,3-glucanase. Plant Physiology 106:1709-1710.

Wu, S., Kriz, A.L., and Widholm, J.M. 1994b. Molecular analysis of two cDNA clones encoding acidic class I chitinase in maize. Plant Physiology 105: 1097-1105.

Xie, Z., Zhang, Z. L., Hanzlik, S., Cook, E., and Shen, Q. J. 2007. Salicylic acid inhibits gibberellin-induced alpha-amylase expression and seed germination via a pathway involving an abscisic-acid-inducible WRKY gene. Plant Molecular Biology 64: 293-303.

Xie, Y. R., Chen, Z. Y., Brown, R. L., and Bhatnagar, D. 2010. Expression and functional characterization of two pathogenesis-related protein 10 genes from *Zea mays*. Journal of Plant Physiology 167: 121-130.

Xu, L., Zhu, L., Tu, L., Liu, L., Yuan, D., Jin, L., Long, L., and Zhang, X. 2011. Lignin metabolism has a central role in the resistance of cotton to the wilt fungus *Verticillium dahliae* as revealed by RNA-Seq-dependent transcriptional analysis and histochemistry. Journal of Experimental Botany 62: 5607-5621.

Yang, Y., Qi, M., and Mei, C. 2004. Endogenous salicylic acid protects rice plants from oxidative damage caused by aging as well as biotic and abiotic stress. The Plant Journal 40: 909-919.

Yang, D. L., Yang, Y., and He, Z. 2013. Roles of Plant Hormones and Their Interplay in Rice Immunity. Molecular Plant 6: 675-685.

Yilmaz, A., Nishiyama, M. Y., Jr., Fuentes, B. G., Souza, G. M., Janies, D., Gray, J., and Grotewold, E. 2009. GRASSIUS: a platform for comparative regulatory genomics across the grasses. Plant Physiology 149: 171-180.

Zenoni, S., Ferrarini, A., Giacomelli, E., Xumerle, L., Fasoli, M., Malerba, G., Bellin, D., Pezzotti, M., and Delledonne, M. 2010. Characterization of transcriptional complexity during berry development in *Vitis vinifera* using RNA-Seq. Plant Physiology 152: 1787-1795.

Zhang, J., Simmons, C., Yalpani, N., Crane, V., Wilkinson, H., and Kolomiets, M. 2005. Genomic analysis of the 12-oxo-phytodienoic acid reductase gene family of *Zea mays*. Plant Molecular Biology 59: 323-343.

Zhang, G., Guo, G., Hu, X., Zhang, Y., Li, Q., Li, R., Zhuang, R., Lu, Z., He, Z., Fang, X., Chen, L., Tian, W., Tao, Y., Kristiansen, K., Zhang, X., Li, S., Yang, H., Wang, J., and Wang, J. 2010. Deep RNA sequencing at single base-pair resolution reveals high complexity of the rice transcriptome. Genome Research 20: 646-654.

Zhang, A., Zhang, J., Ye, N., Cao, J., Tan, M., Zhang, J., and Jiang, M. 2010. ZmMPK5 is required for the NADPH oxidase-mediated self-propagation of apoplastic H2O2 in brassinosteroid-induced antioxidant defence in leaves of maize. Journal of Experimental Botany 61: 4399-4411.

Zhang, H., Li, D., Wang, M., Liu, J., Teng, W., Cheng, B., Huang, Q., Wang, M., Song, W., Dong, S., Zheng, X., and Zhang, Z. 2012. The *Nicotiana benthamiana* Mitogen-Activated Protein Kinase Cascade and WRKY Transcription Factor Participate in Nep1Mo-Triggered Plant Responses. Molecular Plant-Microbe Interactions 25:1639-1653.

Zhu, Q. H., Stephen, S., Kazan, K., Jin, G., Fan, L., Taylor, J., Dennis, E. S., Helliwell, C. A., and Wang, M. B. 2013. Characterization of the defense transcriptome responsive to *Fusarium oxysporum*-infection in Arabidopsis using RNA-seq. Gene 512: 259-266.

Chapter Three

Aspergillus flavus and *Fusarium verticillioides* Induce Tissue-Specific Gene Expression of *PRms* and *Sh1* in Developing Maize Kernels

Xiaomei Shu[1], David P. Livingston[2], Robert G. Franks[3], Rebecca S. Boston[3], Charles P. Woloshuk[4], and Gary A. Payne[1*]

[1] Department of Plant Pathology, North Carolina State University, Raleigh, NC 27695-7567

[2] Department of Crop Science, North Carolina State University, Raleigh, NC 27695

[3] Department of Plant & Microbial Biology, North Carolina State University, Raleigh, NC 27695

[4] Department of Botany and Plant Pathology, Purdue University, West Lafayette, IN 47907

ABSTRACT

Aspergillus flavus and *Fusarium verticillioides* are fungal pathogens capable of colonizing maize kernels and contaminating them with mycotoxins. Development of effective control strategies is extremely difficult because pathogenesis and host responses remain poorly understood. In this study, we monitored colonization and host tissue-specific gene expression during infection by these two fungi. Immature maize kernels were inoculated with either *A. flavus* or *F. verticillioides* 21-22 days after pollination. Kernels were harvested at 4, 12, 24, 48, 72, 96 and 120 hours post inoculation (hpi). Histological studies showed that the two fungi had a similar pattern of colonization. RNA *in situ* hybridization and qRT-PCR analysis showed that maize *pathogenesis related protein*, *maize seeds* (*PRms*) was expressed in the aleurone and scutellum during infection by these two fungi. However, *shrunken-1* (*Sh1*) was expressed in the embryo before fungal infection, and it was induced in the aleurone and scutellum by both fungi. By comparing histological and RNA *in situ* hybridization results from adjacent serial sections, we found that these two genes were expressed before visible colonization. These studies provide a better understanding of these two host-parasite interactions, giving additional information about the mechanisms conferring resistance to these diseases in maize.

INTRODUCTION

Maize (*Zea mays* L.), one of the most economically important and widely grown crops, is used for human food, livestock feed and alcohol production. Over 97 million acres were planted in the United States in 2013 (Data from National Agricultural Statistics

Service). Maize ear rots and mycotoxin contamination caused by *Aspergillus flavus* and *Fusarium verticillioides* are chronic problems in the United States and all over the world (Bush et al., 2004; Payne, 1992). Aflatoxins and fumonisins produced by *A. flavus* and *F. verticillioides*, respectively, are carcinogenic secondary metabolites (Munkvold, 2003; CAST, 2003). Current management and breeding strategies are not sufficient to control maize diseases caused by these fungi. Breeding strategies have slowed due to the sporatic occurrence of the disease, the lack of reliable phenotyping, and limited knowledge on interaction of these fungi with their hosts.

A. flavus is an opportunistic fungal pathogen capable of infecting immature maize kernels under favorable conditions, including high temperature and water stress (Horn et al., 2009; Jones et al., 1980; Payne et al., 1998; Payne, 1992). Aflatoxin accumulation was detected in undamaged kernels, indicating direct infection of the kernel by this fungus can occur without obvious kernel injury (Anderson et al., 1975; Hesseltine et al., 1976; Lee et al., 1980). This fungus can invade ears through the silk channel or other openings in the husks. Once inside the ear the fungus colonizes kernel surfaces and enters undamaged kernels either through the pedicel region (Marsh and Payne, 1984; Smart et al., 1990) or through wounds created by insect or mechanical injury of the pericarp (Lillehoj et al., 1975; Smart et al., 1990; Widstrom et al., 2003). *A. flavus* colonization appears to occur in the later stages of kernel development (Payne, 1983), and once inside the kernel, the fungus can colonize all tissue types with the most extensive colonization occurring in the germ (Dolezal et al., 2013; Fennel et al., 1973; Keller et al., 1994; Smart et al., 1990). Other maize ear rot associated

fungi, including *F. verticillioides*, also infect the kernel at later developmental stages, and the route of infection has been associated with the pedicel (Bush et al., 2004; Johann, 1935; Koehler, 1942; Manns and Adams, 1923).

Unlike *A. flavus*, *F. verticillioides* is predominantly an endophyte in maize plants, but can cause disease in immature kernels under certain conditions (Cao et al., 2013; Munkvold et al., 1997). Koehler (1942) argued that *F. verticillioides* is the most prevalent microbe in maize kernels. Previous studies showed that this fungus enters the kernel through the silk channel of the ear, infects kernels and causes ear rots (Duncan and Howard, 2010). Insect feeding and mechanical damage of the kernel also facilitate invasion of *F. verticillioides* (Koehler, 1942; Maiorano et al., 2009; Munkvold, 2003; Sobek and Munkvold, 1999; Warfield and Davis, 1996).

Maize plants have evolved some common mechanisms to defend against ear rot fungi (Mideros et al., 2014). Physical and chemical barriers are extremely important in innate immunity of immature maize kernels (Johansson et al., 2006). A set of maize genes are associated with defense response to both *A. flavus* and *F. verticillioides* (Dolezal, 2010). The accumulation of antifungal compounds often confers resistance to fungal invasion in the kernel (Kelley et al., 2012; Murillo et al., 1999). Pathogenesis related (PR) proteins, lipoxygenases, α-amylase inhibitors, ribosome-inactivating protein (RIP), and zeamatin are known antifungal compounds in maize kernels (Casacuberta et al., 1992; Fakhoury and Woloshuk, 2001; Guo et al., 1997; Moore et al., 2004; Nielsen et al., 2001; Wilson et al., 2001). A set of maize genes encoding these antifungal compounds was reported to be

associated with defense response to fungal infection. One example is maize *PRms* (AC205274.3_FG001) which was associated with *F. verticillioides* infection in the embryo of germinating maize kernels (Casacuberta et al., 1991, 1992). Accumulation of PRms protein in the aleurone and scutellum of germinating maize kernels was observed during *F. verticillioides* infection (Murillo et al., 1999). This protein is thought to act as a defense regulator which possibly modulates sucrose and jasmonic acid (JA)/ethylene (ET) dependent systemic resistance (Gómez-Ariza et al., 2007; Huffaker et al., 2011). However, the role of this gene in the defense response to *A. flavus* infection has not been reported.

Changes in sugar metabolism are also associated with pathogen attack in plants, such as *Arabidopsis thaliana* (Botanga et al., 2012; Göhre et al., 2012), maize (Doehlemann et al., 2008), tomato (Berger et al., 2004), and grapevine (Santi et al., 2013). Maize *shrunken-1* (*Sh1*) (GRMZM2G089713) encodes sucrose synthase 1 (SS1), which is a sucrose-UDP glucosyltransferase (UGT). SS1 is involved in sucrose metabolism in maize kernels. The function of this enzyme is to catalyze the reversible conversion of sucrose and uridine diphosphate (UDP) into fructose and UDP-glucose (Xu et al., 1989). Fructose and UDP-glucose are important substrates for various metabolic pathways, including cell wall synthesis pathways and respiratory pathways (Delmer and Amor 1995; Huber and Huber 1996). Cobb and Hannah (1988) demonstrated that *Sh1* is not essential for sucrose synthesis in maize kernels. But overexpression of *Sh1* and other starch biosynthesis genes results in elevated levels of starch in maize (Jiang et al., 2013), indicating the important role of *Sh1* in starch biosynthesis. Results from previous studies suggest that expression of *Sh1* is highly

regulated in maize (Hauptmann et al., 1988; Maas et al., 1991; Vasil et al., 1989). McCarty et al. (1986) found that this gene was highly expressed only in response to specific developmental and environmental stimuli, such as anaerobic stress in the root. Moreover, genes encoding glucosyltransferases were found to be associated with disease resistance in *A. thaliana*, wheat, tobacco and tomato (Fraissinet-Tachet et al., 1998; Ma et al., 2010; O'Donnell et al., 1998; Poppenberger et al., 2003). Expression of an *A. thaliana UGT* was significantly increased during colonization by the Rhizobacterium *Pseudomonas fluorescens* in the root (van de Mortel et al., 2012). Furthermore, the UGTs were also involved in detoxification of deoxynivalenol (DON) in *A. thaliana* and wheat (Ma et al., 2010; Poppenberger et al., 2003). But the role of *Sh1* in the interactions between maize and its fungal pathogens remain unknown.

Robertson-Hoyt et al. (2007) argued that maize genes associated with ear rots and mycotoxin contamination caused by *A. flavus* and *F. verticillioides* were identical or genetically linked. The maize lipoxygenase (LOX) gene, *cssap 92*, was reported to be involved in defense against *Aspergillus* and *Fusarium* spp. (Wilson et al., 2001). Dolezal (2010) also identified a set of maize genes, including *PRms* and *Sh1*, which were up-regulated by *A. flavus*. But little is known about the infection processes by the two fungi, and whether their different trophic lifestyles affect tissue colonization and host response. How the host responds to these pathogens also remains unclear. In this study, we compared pathogenesis and host defense responses in maize kernels infected by *A. flavus* and *F. verticillioides*. Dynamic changes in the distribution of fungal tissue and transcripts of *PRms*

and *Sh1* were analyzed. We found that these maize genes were expressed in a tissue-specific fashion before visible fungal colonization.

MATERIALS AND METHODS

Plant and fungal materials

Maize inbred line B73 was grown at the Central Crops Research Station near Clayton, NC. Maize ears were hand-pollinated and covered with pollination bags. Fungal strains (*A. flavus* NRRL *3357*, *F. verticillioides n16*) were grown on potato dextrose agar (PDA) plates at 28^{o}C for 5 days. Conidial suspensions were harvested by adding sterile distilled water containing 0.5% (v/v) Triton X-100 (Fisher) and scraping the plates using a glass spreader. The concentration of conidia was determined using a hemocytometer (Hausser Scientific) and diluted to 1×10^{6} conidia/ml for use in plant inoculation.

Fungal inoculation and tissue collection

Maize ears were inoculated with either *A. flavus* or *F. verticillioides* in the field 21-22 days after pollination. Kernels were wounded with a needle bearing approximately 13 conidia. Kernels for the mock treatment were inoculated with sterile distilled water containing 0.5% (v/v) Triton X-100. Inoculated kernels were collected at 4, 12, 24, 48, 72, 96 and 120 hours post inoculation (hpi). Corresponding mock inoculated and non-wounded kernels were collected at 4, 12, 24, 48, 72, 96 and 120 hpi and used as negative controls. Three ears were harvested for each treatment as biological replicates. The greenhouse-grown ears were removed from the plants, inoculated with these two fungi, incubated in the greenhouse, and collected at 96 hpi. Three ears were harvested for each treatment as

biological replicates. Kernels for RNA extraction and qRT-PCR studies were harvested, frozen in liquid nitrogen immediately, and then stored at -80^{o}C.

Histology

Kernels were collected in tissue embedding capsules (Fisher). Samples were fixed, dehydrated, and embedded as described previously (chapter two; Livingston 2009, 2013). The paraffin blocks were sectioned with an RM2255 microtome (Leica) and mounted on glass slides. Ten micron sections were mounted on Microscope Slides (Gold Seal) for histology staining and imaging. Adjacent twenty micron sections were mounted on Probe Microscope Slides (Fisher) for RNA *in situ* hybridization. Two adjacent sections were mounted on the same slides as two technical controls. Slides were dried on a hot plate overnight and stored at room temperature. The staining was carried out as previously described (chapter two; Livingston et al., 2013).

RNA extraction and probe cloning

Eight kernels from individual ears were pooled and ground in liquid nitrogen with mortar and pestle. Ground tissue was added to 0.75 ml of saturated phenol, pH 6.6 (Fisher), and homogenized for 2 min. Samples were then dissolved in Tris EDTA buffer, pH 8.0 (ACROS Organics), extracted with 5:1 acid phenol: chloroform, pH 4.5 (Fisher), and precipitated with ice-cold 100% ethanol (ACROS Organics) overnight. Total RNA was further purified with an RNeasy Mini Kit (Qiagen) according to the manufacturer's instructions. The quantity and quality of RNA was analyzed using a ND-1000 spectrophotometer (NanoDrop Technologies, Wilmington, DE, USA). Following

manufacturer's instructions, RNA was treated with DNase (Promega), and cDNA synthesis was performed using the First Strand cDNA Synthesis Kit (Fermentas).

PRms and *Sh1* probe sequences were cloned using the PRms-1 and Sh1 primer sets, respectively (Table 1). RT-PCR was performed using Ex Taq (Chemicon). The PCR products were analyzed through a 0.8 % (w/v) agarose gel and cleaned using a QIAquick PCR purification kit (QIAGEN). The purified PCR products were inserted into the dual promoter vector PCR®II-TOPO® (Invitrogen) according to manufacturer's protocol, and sequenced. The vectors carrying *PRms* and *Sh1* sequences were linearized by the restriction enzymes Nco I and ApaL I, respectively. The antisense and sense probes were transcribed from the linearized vectors using the Riboprobe® System-SP6 and -T7 transcription kits (Promega) following the manufacturer's instructions.

RNA *in situ* hybridization

RNA *in situ* hybridization was carried out according to previously described protocols (Lincoln et al., 1994; Long and Barton, 1998; Franks et al., 2002). The hybridization temperature was 65^{o}C. The sense probes of each gene were included as negative controls. Mock inoculated kernels were hybridized with both antisense and sense probes as biological controls.

Microscopy

Images were collected on an Eclipse E600 light microscope (Nikon) with an Infinity 1-3C digital camera, and analyzed with the software Infinity Analyze software (Lumenera).

qRT-PCR expression analysis

RNA extraction and cDNA synthesis were performed as described above. Primers used for qRT-PCR are listed in Table 1. QRT-PCR was performed using a SYBR® Green kit (Applied Biosystems) according to the manufacturer's instructions. The expression levels of maize *ribosome* gene were used for normalization. Data were analyzed by the comparative CT method with the amount of target given by the calibrator $2^{-\Delta\Delta CT}$.

Table 1. Primers used in this study.

Gene (accession number)	Primer usage	Primers 5'-3'
PRms (X54325)	Probe	PRms-1F: TACAATGGAGGCATCCAACA
		PRms-1R: CATTGATCGCAGGCACAAT
	qRT-PCR	PRms-2F: TACAATGGAGGCATCCAACA
		PRms-2R: CTGTTTTGGGGAGTGAGGTA
Sh1 (NM_001279762)	Probe	Sh1-1F: TGGAGTAGCCTGCGTTCTACG
		Sh1-1R: TGCAGCCAATTCTCACCAT
	qRT-PCR	Sh1-2F: GGAGTAGCCTGCGTTCTACG
		Sh1-2R: GTCAATGTGCAGGCCAGATA
Actin1 (NM_001155179)	qRT-PCR	ACT1-F: GCCTACGTTGCCCTTGATTA
		ACT1-R: TTCTGACCCAATGGTGATGA
Ribosome (NM_001158589)	qRT-PCR	Rib-F: GGCTTGGCTTAAAGGAAGGT
		Rib-R: TCAGTCCAACTTCCAGAATGG

RESULTS

Colonization of maize kernels by *A. flavus* and *F. verticillioides*

Histological examination showed that *A. flavus* and *F. verticillioides* followed a similar pattern of colonization in maize kernels grown in the field (Fig. 1). Initial colonization by the fungi was observed in the aleurone and endosperm at the site of inoculation at 48 hpi (Fig. 2A). Mycelia and conidia of *A. flavus* were observed in the aleurone, endosperm and germ at 72 hpi (Fig. 2B). In contrast, *F. verticillioides* was detected only in the aleurone and endosperm at 72 hpi (Fig. 2B). Both fungi were observed in all kernel tissues by 96 hpi (Fig. 2C). We also analyzed colonization by these two fungi in kernels from greenhouse-grown plants. We found that both fungi were also capable of colonizing all tissues in these kernels.

Both *A. flavus* and *F. verticillioides* colonized and disrupted cells of the aleurone. Colonization of the aleurone was often restricted to cells adjacent to the site of inoculation at 48 hpi. Fungal mycelium was observed in the aleurone distant from the inoculation site at 72 hpi. In colonized tissue, extensive disruption of the cytoplasm and nuclei was observed in the aleurone colonized by *A. flavus* (Fig. 1F). In contrast, many aleurone cells colonized by *F. verticillioides* were either partially destroyed (Fig. 1G) or intact (Fig. 1H). Only in the later stages of infection by *F. verticillioides* was extensive degradation of the aleurone observed, and again the colonization appeared more localized (Fig. 1O and P). In contrast, both fungi extensively colonized and degraded tissues of the endosperm creating cavities that often contained sporulating mycelia of the infecting fungus (Fig. 1I and O). In some areas,

these fungi were observed ramifying through the endosperm without obvious degradation of the tissue (Fig. 1J and M).

In this study little colonization was observed in embryo tissue. Colonization of the scutellum tip was observed in only a few kernels that were extensively colonized and displayed severe tissue damage. Instead, *A. flavus* often formed a biofilm-like structure at the endosperm-scutellum interface (Fig. 1J-K and Fig. 2C). In many cases the mat covered an extensive area of the scutellum before colonization of the germ was observed (Fig. 1K). No similar fungal structure was observed in *F. verticillioides* infected kernels (Fig. 1N). *A. flavus* colonization of the basal endosperm transfer layer (BETL) was observed at 96 hpi (Fig. 1L). However, *F. verticillioides* colonization was observed only in the basal aleurone and endosperm near the BETL region at 96 and 120 hpi (Fig. 1O and P).

Figure 1. *A. flavus* and *F. verticillioides* colonization in maize kernels. A, Maize kernel showing site of inoculation and general location of maize tissues. B-D, The mock (B), *A. flavus* (C), and *F. verticillioides* (D) inoculated ears. E-P, Light microscope images taken from sections stained with safranin and fast green. E, The aleurone of a mock inoculated kernel. F, *A. flavus* colonization in the destroyed aleurone; G, *F. verticillioides* colonization in the partially intact aleurone. H, *F. verticillioides* colonization around the intact aleurone. I, *A. flavus* colonization at the inoculation site. J-K, *A. flavus* colonization at the endosperm-scutellum interface and the formation of a biofilm-like structure with (J) and without (K) invasion of the scutellum. L, *A. flavus* colonization in the BETL. M, *F. verticillioides* colonization at the inoculation site. N, *F. verticillioides* colonization in the endosperm near the scutellum. O, *F. verticillioides* colonization in the basal aleurone and endosperm and the formation of a cavity in the endosperm. P, *F. verticillioides* colonization in the basal aleurone. Pictures were taken at 96 hpi. Arrows denote fungal colonization; hpi: hours post inoculation. *Af*: *A. flavus*; *Fv*: *F. verticillioides*; Al: aleurone; BETL: basal endosperm transfer layer; En: endosperm; Sc: scutellum. Scale bars: 3 mm in B-D; 30 μm in E-H; 200 μm in I, M, O and P; 50 μm in J- L and N.

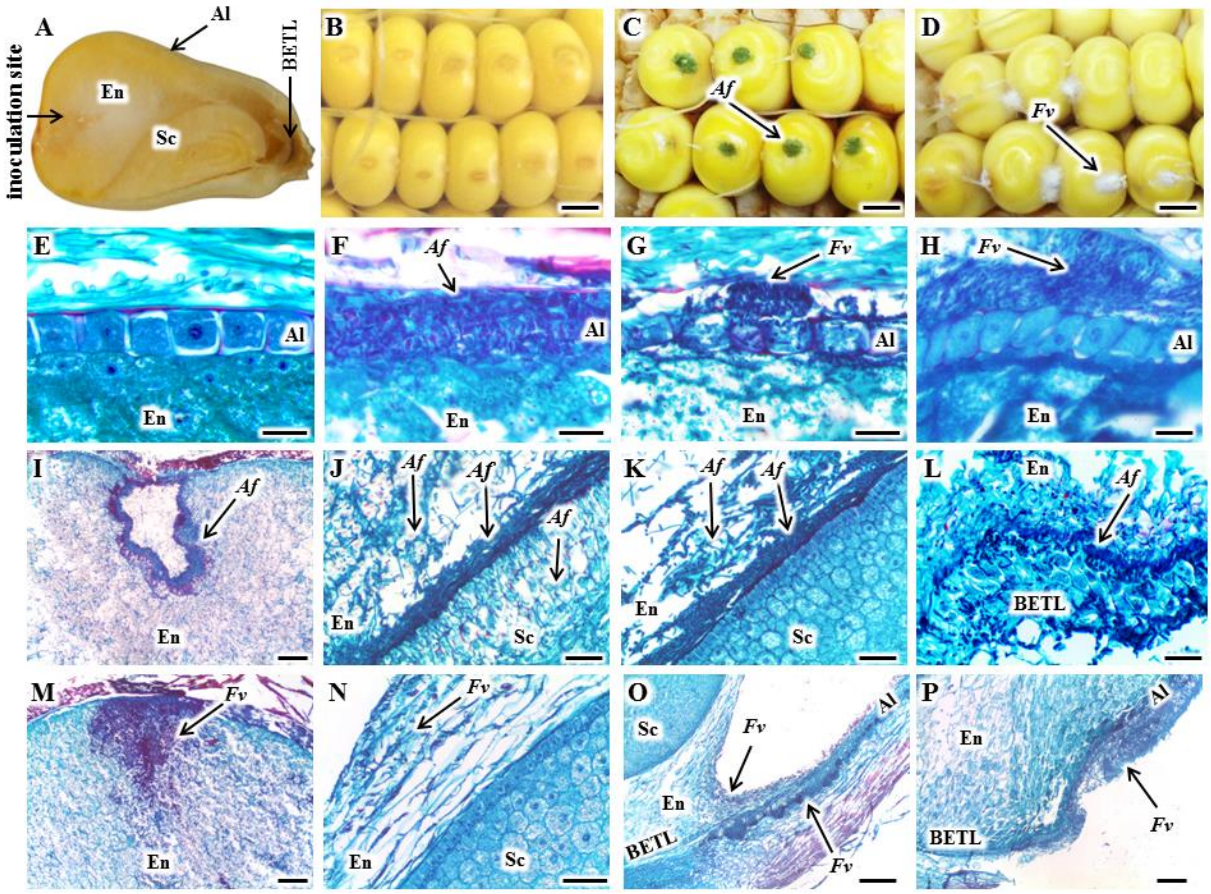
A
Al
BETL
inoculation site
En
Sc
B
C
Af
D
Fv
E
Al
En
F
Af
Al
En
G
Fv
Al
En
H
Fv
Al
En
I
Af
En
J
Af
Af
Af
En
Sc
K
Af
Af
En
Sc
L
En
Af
BETL
M
Fv
En
N
Fv
En
Sc
O
Sc
Fv
Al
En
BETL
Fv
P
Al
En
Fv
BETL

Tissue-specific gene expression of *PRms*

To assess the timing and localization of host gene expression in response to these two fungi we used RNA *in situ* hybridization in sections of infected maize kernels. We observed transcripts of *PRms* in aleurone cells during *A. flavus* infection by 48 hpi (Fig. 2A). *PRms* transcripts were detected also in the aleurone and scutellum during *F. verticillioides* infection at this time point. At 72 hpi, *PRms* was expressed in the aleurone and scutellum of kernels infected by either *A. flavus* or *F. verticillioides* (Fig. 2, 3 and 4). Transcripts of this gene were localized in some aleurone cells (Fig. 2A-D, F and I). In the scutellum, this gene was predominantly expressed at the tip and in the glandular layer (Fig. 2B-D, F, H and I). It was also expressed in the tissue inside the glandular layer (Fig. 2F and I). During *F. verticillioides* infection, *PRms* was often expressed in the basal scutellum near the BETL (Fig. 2K). No *PRms* transcripts were observed in the mock inoculated kernels (Fig. 2E; Fig. 4H) or kernels collected at 4, 12 and 24 hpi (data not shown). No *PRms* gene expression signal was observed in the sections hybridized with the control probe (Fig. 4C, F and I). For the greenhouse-grown kernels, *PRms* was also expressed in the aleurone and scutellum during infection by these two fungi at 96 hpi.

Figure 2. Colonization by *A. flavus* and *F. verticillioides*, and localization of *PRms* transcripts in maize kernels. Purple signal and arrows denote presence of *PRms* transcripts. A-C, Cartoon of vertical kernel sections showing colonization by *A. flavus* (green) and *F. verticillioides* (orange), as well as presence of *PRms* transcripts (purple) over time. A, At 48 hpi, *A. flavus* and *F. verticillioides* colonization at the inoculation site; presence of *PRms* transcripts in the aleurone. B, At 72 hpi, *A. flavus* colonization in the aleurone, endosperm, and scutellum; *F. verticillioides* colonization in the aleurone and endosperm; presence of *PRms* transcripts in the aleurone, scutellum tip, and glandular layer. C, At 96 hpi, *A. flavus* colonization in the aleurone, endosperm, scutellum, BETL, and at the endosperm-scutellum interface with the formation of a biofilm-like structure; *F. verticillioides* colonization in the aleurone, endosperm, and scutellum; presence of *PRms* transcripts in the aleurone, scutellum tip, and glandular layer. D-K, Light microscope images showing presence of *PRms* transcripts at 96 hpi. D, Presence of *PRms* transcripts in the aleurone, scutellum tip, and glandular layer during *A. flavus* infection. E, No *PRms* transcripts in the scutellum of mock inoculated kernels. F, Presence of *PRms* transcripts in the aleurone, scutellum tip, and glandular layer during *A. flavus* infection. G-H, Presence of *PRms* transcripts in the aleurone (G) and glandular layer (H) during *A. flavus* infection. I, Presence of *PRms* transcripts in the aleurone, scutellum tip, and glandular layer during *F. verticillioides* infection. J-K, presence of *PRms* transcripts in the aleurone (J) and scutellum near the BETL (K) during *F. verticillioides* infection. hpi: hours post inoculation; Al: aleurone; BETL: basal endosperm transfer layer; En: endosperm; Gl: glandular layer; Sc: scutellum. Scale bars: 1 mm in D; 30 μm in E, G, H, J and K; 200 μm in F and I.

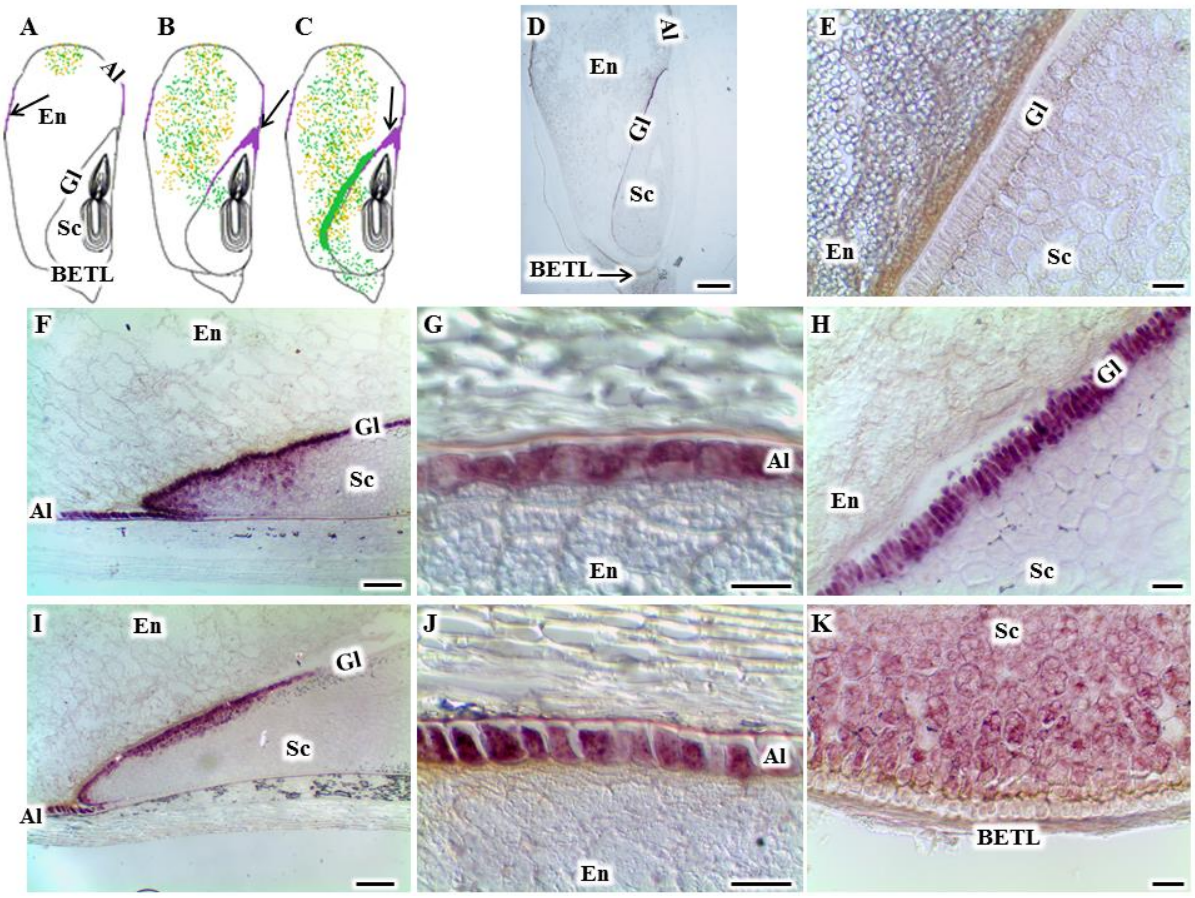
A
B
C
Al
En
Gl
Sc
BETL
D
Al
En
Gl
Sc
BETL
E
Gl
En
Sc
F
En
Gl
Sc
Al
G
Al
En
H
Gl
En
Sc
I
En
Gl
Sc
Al
J
Al
En
K
Sc
BETL

Tissue-specific gene expression of *Sh1*

Shrunken-1 (*Sh1*) encodes sucrose synthase 1 which is involved in sucrose metabolism in maize plants (Xu et al., 1989). Our RNA *in situ* hybridization showed that expression of *Sh1* was altered upon infection by *A. flavus* and *F. verticillioides*. *Sh1* was expressed in some aleurone cells in response to *A. flavus* infection at 48 hpi (data not shown), and at 72 and 96 hpi *Sh1* transcripts were detected in the aleurone and scutellum (Fig. 3A-C). However during *F. verticillioides* infection, *Sh1* was expressed in the aleurone at 24 hpi (data not shown), before the fungus was observed in the kernel. At 48, 72 and 96 hpi, this gene was expressed in the aleurone and scutellum (Fig. 3D-E). It was also expressed at the basal scutellum near the BETL region at 72 hpi (Fig. 3F). But transcripts of *Sh1* were not observed in the basal scutellum during *A. flavus* infection. Moreover, it appeared that *Sh1* was initially expressed at the scutellum tip and the glandular layer. Unlike *PRms*, *Sh1* was also expressed in the embryo regardless of fungal infection (Fig. 3E and I). We observed *Sh1* transcripts in the embryo of some mock inoculated (Fig. 3I) and non-wounded kernels. But transcripts of *Sh1* were not observed in the aleurone of either mock inoculated or non-wounded kernels (data not shown). *Sh1* transcripts were also detected in kernels inoculated with these two fungi and collected at 4 and 12 hpi (data not shown). However, *Sh1* was not expressed in the aleurone (Fig. 3G) and scutellum (Fig. 3H) of either mock inoculated or non-wounded kernels. *Sh1* transcripts were also absent for the aleurone and scutellum of fungal inoculated kernels collected at 4 and 12 hpi (data not shown). Thus in field-grown plants, *Sh1* was expressed in the embryo independent of fungal infection, but its expression in the aleurone

and scutellum was induced upon colonization by these two fungi. Additionally, no *Sh1* signal was observed in the sections hybridized with control probe (data not shown).

For kernels from greenhouse-grown plants, the expression pattern of *Sh1* was slightly different from the field-grown kernels. It was consistently expressed in the scutellum of *A. flavus* and *F. verticillioides* infected kernels at 96 hpi (data not shown). Transcripts of this gene were observed only in the aleurone of some kernels inoculated with *F. verticillioides* (data not shown). No *Sh1* transcripts were observed in the aleurone of the greenhouse-grown kernels infected with *A. flavus* (data not shown).

Figure 3. *Sh1* gene expression in the *A. flavus*, *F. verticillioides*, and mock inoculated maize kernels. A-C, *Sh1* gene expression in the aleurone (A), outermost layer of scutellum (B), and inner areas of scutellum (C) during infection by *A. flavus*. D-F, *Sh1* gene expression in the aleurone (D), scutellum and embryo (E), and scutellum near the BETL (F) during infection by *F. verticillioides*. G-H, No *Sh1* gene expression in the aleurone (G) and scutellum (H) of the mock inoculated kernel. I, *Sh1* gene expression in the embryo of the mock inoculated kernel. Sections were hybridized with *Sh1* probe. Kernels were collected at 72 hours post inoculation. Purple signal shows *Sh1* gene expression. Al: aleurone; BETL: basal endosperm transfer layer; Em: embryo; En: endosperm; Sc: scutellum. Scale bars: 30 μm in A, C, D, F and G I; 200 μm in B, E, H and I.

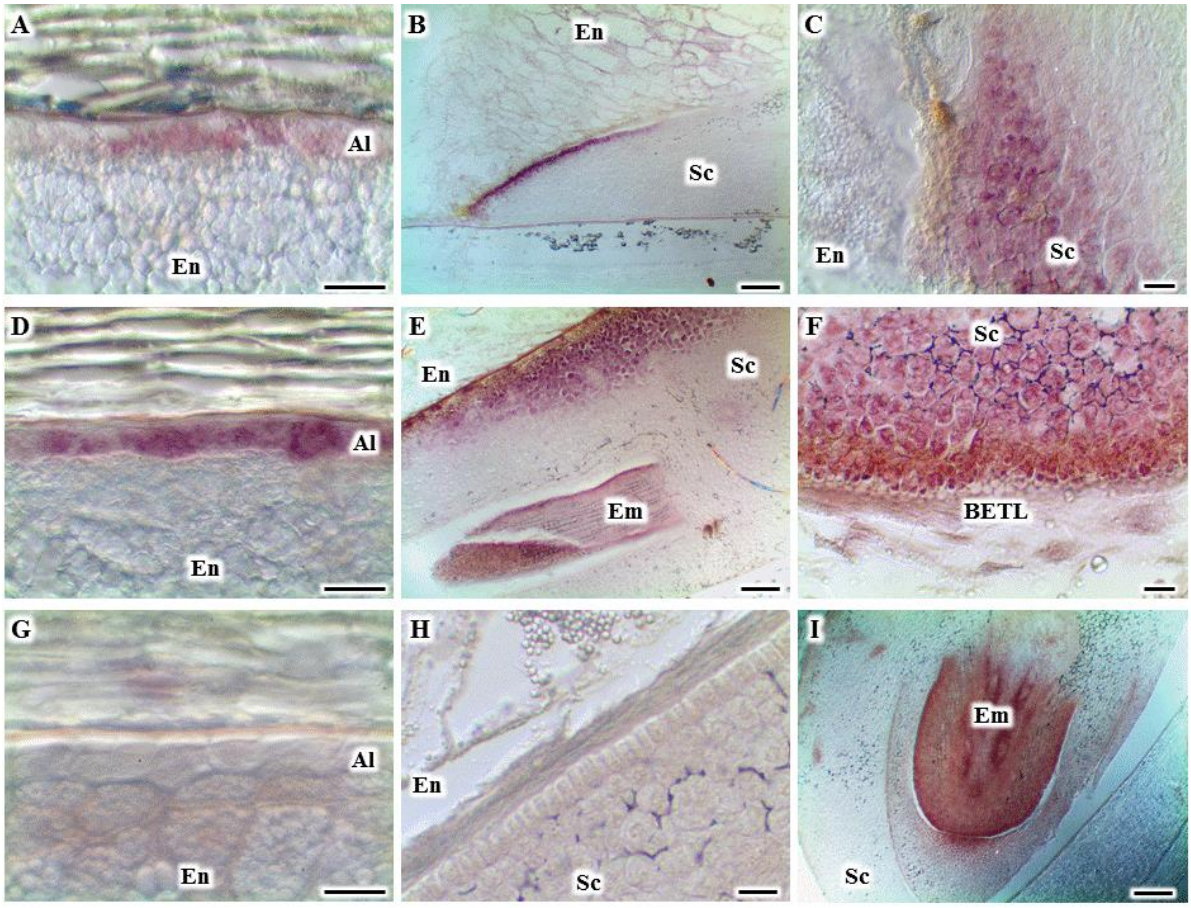
A
Al
En
B
En
Sc
C
En
Sc
D
Al
En
E
En
Sc
Em
F
Sc
BETL
G
Al
En
H
En
Sc
I
Em
Sc

Tissue-specific gene expression of *PRms* and *Sh1* before fungal colonization

By comparing histological and RNA *in situ* hybridization results from adjacent serial sections, we found that both *PRms* (Fig. 4) and *Sh1* (data not shown) were expressed in a tissue-specific fashion before visible fungal colonization. Transcripts of these two genes were detected in tissues where visible fungal colonization was not observed. The results indicate that the kernel responds to fungal invasion in advance of visible fungal colonization. Additionally, transcripts of both *PRms* and *Sh1* were observed in some scutellum cells colonized by these two fungi (data not shown), indicating these scutellum cells were still alive. However, no *PRms* or *Sh1* transcripts were detected in the aleurone cells that were colonized by these two fungi. It appeared that these aleurone cells were killed during infection by these two necrotrophic fungi.

Figure 4. Activation of *PRms* gene expression before visible fungal colonization. A-C, Adjacent serial sections of *A. flavus* inoculated kernel stained with safranin and fast green (A), hybridized with *PRms* probe (B), and hybridized with control probe (C). Purple signal shows *PRms* gene expression. A, *A. flavus* was not detected. B, *PRms* gene expression in the aleurone and scutellum tip during infection by *A. flavus*. C, No signal was observed in the section hybridized with control probe. D-F, Adjacent serial sections of *F. verticillioides* inoculated kernel stained with safranin and fast green (D), hybridized with *PRms* probe (E), and control probe (F). D, *F. verticillioides* was not detected. E, *PRms* gene expression in the aleurone and scutellum tip during infection by *F. verticillioides*. F, No signal was observed in the section hybridized with control probe. G-I, Adjacent serial sections of mock inoculated kernel stained with safranin and fast green (G), hybridized with *PRms* probe (H), and control probe (I). G, Fungal colonization was not detected. H, No *PRms* gene expression was detected. I, No signal was observed in the control section. Kernels were collected at 72 hours post inoculation; Al: aleurone; En: endosperm; Sc: scutellum. Scale bars: 50 μm.

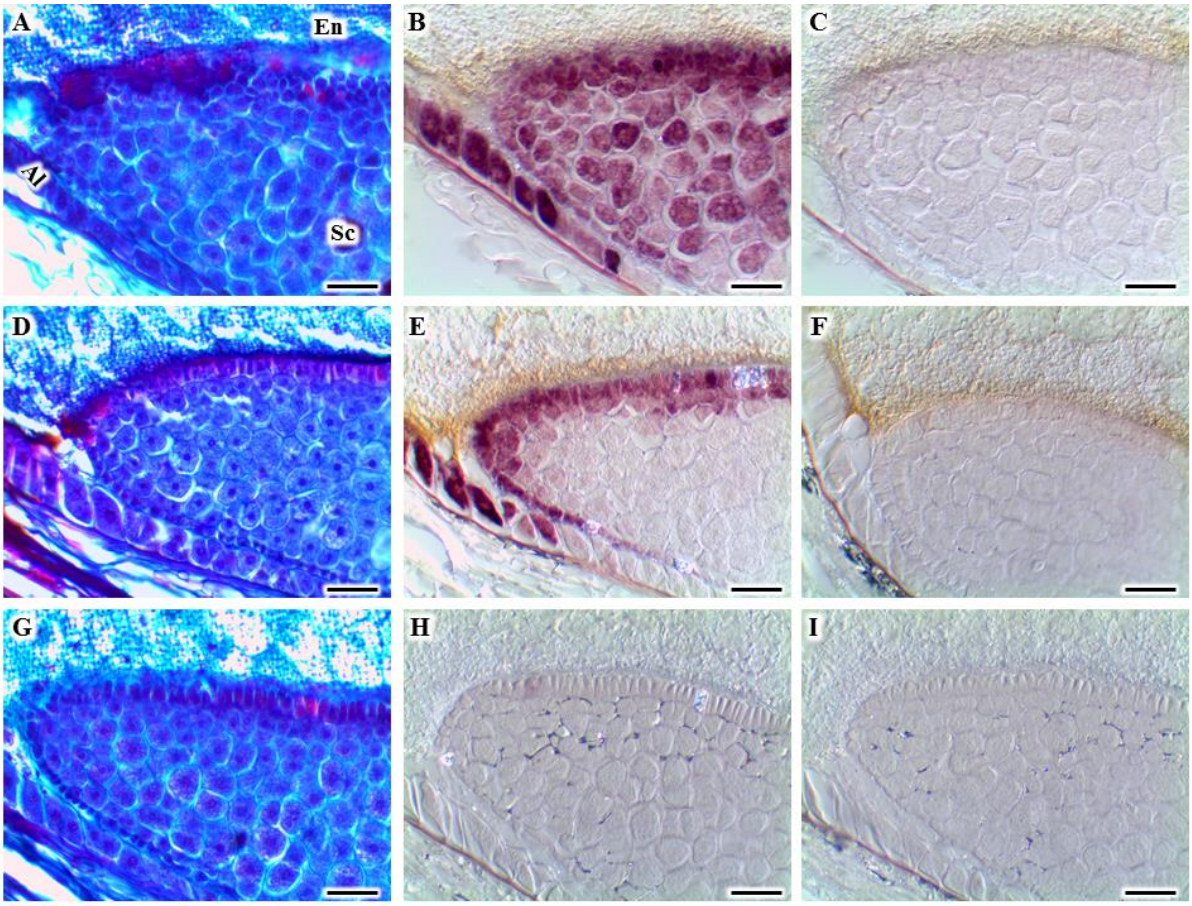
A
En
Al
Sc
B
C
D
E
F
G
H
I

Quantification of *PRms* and *Sh1* gene expression

Gene expression levels of *PRms* and *Sh1* were quantified by quantitative real-time RT-PCR (qRT-PCR) (Fig. 5). The results showed that *PRms* was not expressed in mock inoculated or non-wounded kernels nor inoculated kernels collected at 4 and 12 hpi (Fig. 5A). However, both fungi activated expression of this gene at 24, 48 and 72 hpi. Compared with the samples collected at 24 and 48 hpi, expression levels of *PRms* increased at 72 hpi upon infection by these two fungi. This finding is in agreement with the RNA *in situ* hybridization results.

However, *Sh1* was not differentially expressed during infection by these two fungi compared with non-wounded samples (Fig. 5B). It is likely that the total amount of *Sh1* transcripts in the kernel was not changed during fungal infection. *Sh1* was expressed in the embryo before fungal colonization which was confirmed by RNA *in situ* hybridization (Fig. 3I). During infection by *A. flavus* and *F. verticillioides*, expression of this gene was specifically activated in the aleurone and scutellum (Fig. 3A-F).

Figure 5. qRT-PCR analysis of *PRms* and *Sh1* gene expression in maize kernels during infection by *A. flavus* and *F. verticillioides*. A, *PRms* gene expression. B, *Sh1* gene expression. Expression levels were normalized by the maize *ribosome* gene, and were relative to the non-wounded kernels. hpi: hours post inoculation; *Af*: *A. flavus*; *Fv*: *F. verticillioides*.

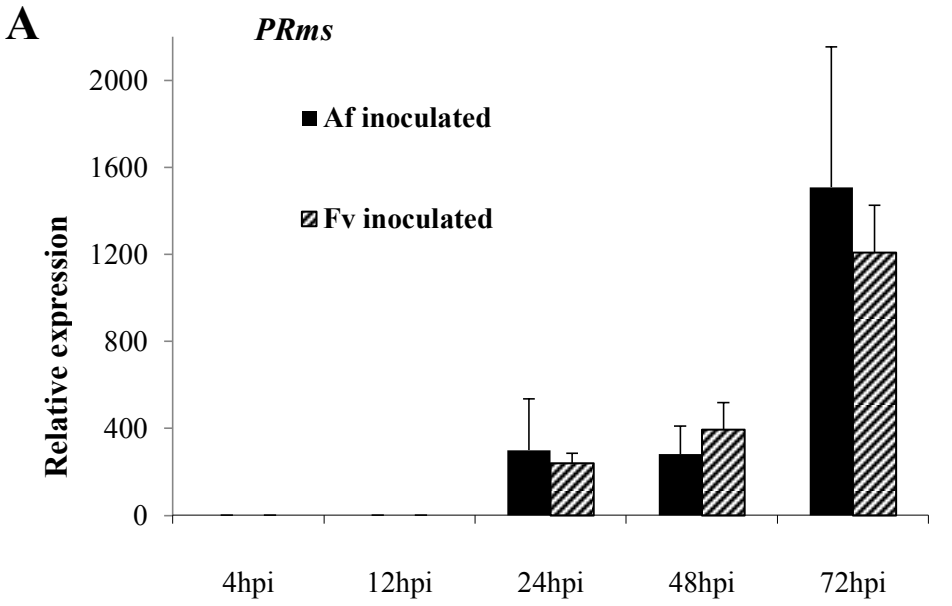
A
PRms
Af inoculated
Fv inoculated
Relative expression
2000
1600
1200
800
400
0
4hpi
12hpi
24hpi
48hpi
72hpi

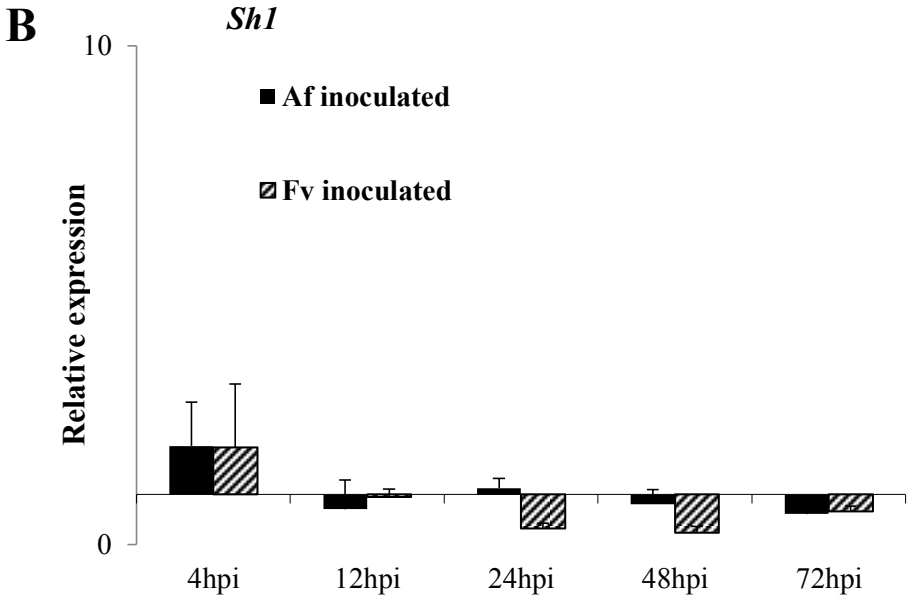
B
Sh1
Af inoculated
Fv inoculated
Relative expression
10
0
4hpi
12hpi
24hpi
48hpi
72hpi

DISCUSSION

Both *A. flavus* and *F. verticillioides* can cause maize ear rot and produce mycotoxins. We provide information of the colonization of kernels by these two fungi, and the time at which maize kernel tissue responds to infection. These two fungi were observed to follow a similar, but not identical pattern of seed colonization. We found that two maize genes, *PRms* and *Sh1,* were expressed in the aleurone and scutellum in advance of visible colonization by both fungi.

A. flavus and *F. verticillioides* followed a similar pattern of colonization

Both fungi were detected in the aleurone and endosperm at the inoculation site at 48 hpi, and reached all tissues at 72 hpi (Fig. 1). Perhaps structural or chemical characteristics of kernels favor a common path of colonization, or the two fungi share common pathogenicity factors necessary for colonizing maize kernels. Previous PCR studies showed that *A. flavus* was detected in the endosperm as early as 24 hpi and in the germ at 72 hpi (Dolezal et al., 2013). But in our study neither microscopic nor macroscopic symptoms were observed in inoculated kernels until 48 hpi. As was found by Dolezal et al. (2013) we observed both fungi in the aleurone, endosperm and germ 72 h after *A. flavus* inoculation.

At the onset of these studies we predicted that these two fungi might differ in their colonization of maize kernels because of described differences in their trophic behavior. Whereas *A. flavus* has been described as either a necrotroph or saprobe, *F. verticillioides* is considered an endophyte that can become a pathogen under certain environmental conditions (Munkvold et al., 1997; Payne, 1992).Consistent with the proposed lifestyles of these two

fungi, we observed that most of the aleurone cells were destroyed early during colonization by *A. flavus.* In contrast, aleurone cells colonized by *F. verticillioides* often remained intact even when visible fungal mycelium was observed around the host cells (Fig. 1G and H). It was not possible in our experiments to determine if the cells remained viable during the early stages of colonization. These differences in colonization of the aleurone tissue were observed even though we wounded the kernels during inoculation.

Previous studies suggested that endophytic growth of *F. verticillioides* in the aleurone was present only in nonsymptomatic maize kernels (Bacon et al., 2008; Duncan and Howard, 2010). A symptom associated with diseased kernels is starbursting. We did not observe starbusting in our studies as a consequence of infection by *F. verticillioides* perhaps due to our experimental design. Our observations do suggest that extensive colonization of kernels by *F. verticillioides* can occur without visible macroscopic symptoms of rot.

Infection of maize kernels by *A. flavus* was often associated with the formation of a biofilm-like structure at the endosperm-scutellum interface (Fig. 1J and K). This specialized structure of *A. flavus* also resembles the *A. fumigates* biofilm formed in human lung (Lousert et al., 2010). From our studies it was not possible to show that this structure was absolutely required for infection. It is likely that the *A. flavus* biofilm-like structure was formed in response to the seed environment in this region, perhaps because of the secretion of toxic compounds by the scutellum. Brown et al. (2009) showed that the oxygenase signaling network in *A. flavus* regulated a quorum-sensing mechanism governing density-dependent development, secondary metabolism, and host seed colonization of maize and peanut. It is

possible that oxygenase coordination is also associated with the formation of this biofilm-like structure at the endosperm-scutellum interface.

A. flavus and *F. verticillioides* induced tissue-specific gene expression

Maize aleurone and scutellum tissues are enriched in metabolites that are important substrates for hydrolytic enzymes secreted during seed germination. Antifungal compounds are known to accumulate in these tissues during pathogen infection (Balandin et al., 2005; Casacuberta et al., 1992; Chen et al., 2007; Guo et al., 1999; Royo et al., 2006). *PRms* is a well-studied defense-related gene in maize (Casacuberta et al., 1991; Casacuberta et al., 1992). *Sh1* is involved in sucrose degradation in maize kernels (Xu et al., 1989). *Sh1* was also observed to be differentially expressed upon *A. flavus* infection (Dolezal, 2010). Our RNA *in situ* hybridization data showed that the aleurone and scutellum expressed *PRms* and *Sh1* upon infection by *A. flavus* and *F. verticillioides*. These observations suggest that these two tissues are important for pathogen recognition and/or important sources of defense related compounds in the kernel. The induction of *PRms* often occurred first and its transcript levels were the highest at the tip of the scutellum. Colonization by these two fungi in the scutellum tip was rarely observed, perhaps because of an accumulation of defense-related compounds in this region. This suggests that increasing the expression levels or changing the timing of expression of defense related genes in this tissue may lead to enhanced resistance in the seed.

Our RNA *in situ* hybridization data support previous studies showing that *PRms* was expressed upon *F. verticillioides* infection in germinating maize kernels (Casacuberta et al.,

1991, 1992). In our study, we found that expression of this gene was associated with both *A. flavus* and *F. verticillioides* infection in the aleurone and scutellum. Additionally, we showed that the maize sugar degradation gene, *Sh1*, was expressed in the aleurone and scutellum during infection by these two fungi. Expression of *PRms* and *Sh1* occurred in the scutellum at 48 hpi upon *F. verticillioides* infection. But both genes were activated in the same tissue at 72 hpi in response to *A. flavus* infection. Although *A. flavus* more aggressively colonized the kernel and reached the germ earlier, these two genes were activated in tissues by *F. verticillioides* more quickly. Our hypothesis is that the kernel recognized *F. verticillioides* early and employed very efficient defense pathways. Moreover, *Sh1* was expressed in the aleurone 24 hours earlier than *PRms* during *F. verticillioides* infection. Furthermore, *Sh1* was expressed in the embryo regardless of fungal infection, and it was induced in the aleurone and scutellum by these two fungi. However, Wittich and Vreugdenhil (1998) argued that Sh1 protein was localized in the aleurone, endosperm and embryo. The difference may be due to the use of the maize hybrid line A188 in their studies, whereas we used the inbred line B73. Moreover, they did a histochemical enzyme assay to localize the Sh1 enzyme, and we did RNA *in situ* hybridization to localize the mRNA of *Sh1* in kernel tissues.

Possible resistance mechanisms involved in these host-parasite interactions

The plant signaling network plays a major role in balancing plant growth and defense responses to biotic and abiotic stresses (Denancé et al., 2013). *PRms* is postulated to function downstream of the sucrose and JA/ET signaling pathways (Gómez-Ariza et al., 2007; Huffaker et al., 2011). *Sh1* is involved in conversion of sucrose and UDP into fructose and

UDP-glucose (Xu et al., 1989). Upregulation of *Sh1* was also observed in maize leaves upon *U. maydis* infection, whereas sucrose contents were slightly increased in this interaction (Doehlemann et al., 2008). This gene was also reported to be associated with plant-microbe interactions in other plant species (Fraissinet-Tachet et al., 1998; Ma et al., 2010; O'Donnell et al., 1998; Poppenberger et al., 2003; van de Mortel et al., 2012). It is plausible that both *PRms* and *Sh1* are involved in the maize signaling network. Maize kernels have developed complex regulatory networks to reallocate the carbon source from growth and development to defense response (Doehlemann et al., 2008). Changes of carbon metabolism genes were observed in maize root during drought stress (Spollen et al., 2008). Induction of *Sh1* might enhance the sucrose degradation pathway and provide substrates for the synthesis of defense compounds (Cobb and Hannah, 1988; Delmer and Amor, 1995; Huber and Huber, 1996). Moreover, the fungal pathogens could employ some strategies to reprogram the maize sugar metabolism pathways and acquire nutrients from the host. The molecular mechanisms that govern these plant-parasite interactions need to be explored.

Summary

Safranin and fast green staining allowed sensitive detection of fungal mycelium and conidia within the maize seeds and thus it was possible to determine the location of the fungi within tissue types during colonization. Similarly, because of its ability to detect for both rare and abundant transcripts, RNA *in situ* hybridization allowed us to determine the temporal and spatial expression of genes in response to infection. By using these two powerful technologies in adjacent serial sections, we were able to follow fungal colonization and

tissue-specific gene expression in adjacent tissues. Maize *PRms* and *Sh1* were expressed in tissues before visible fungal colonization, indicating that the tissue responded to infection before it was colonized by the fungus. The long-distance signals involved in recognition of these fungi might be either plant endogenous signaling molecules or unknown fungal secretory factors.

In this study, we found that both *A. flavus* and *F. verticillioides* colonized all tissue types of immature maize kernels, and triggered tissue-specific expression of *PRms* and *Sh1*. These genes could be used as markers for breeding or genetic engineering.

LITERATURE CITED

Anderson, H. W., Nehring, E. W., and Wichser, W. R. 1975. Aflatoxin contamination of corn in the field. Food Chemistry 23: 775-782.

Bacon, C. W., Glenn, A. E., and Yates, I. E. 2008. *Fusarium verticillioides*: managing the endophytic association with maize for reduced fumonisins accumulation. Toxin Reviews 27: 411-446.

Balandin, M., Royo, J., Gomez, E., Muniz, L. M., Molina, A., and Hueros, G. 2005. A protective role for the embryo surrounding region of the maize endosperm, as evidenced by the characterisation of ZmESR-6, a defensin gene specifically expressed in this region. Plant Molecular Biology 58: 269-282.

Berger, S., Papadopoulos, M., Schreiber, U., Kaiser, W., and Roitsch, T. 2004. Complex regulation of gene expression, photosynthesis and sugar levels by pathogen infection in tomato. Physiologia Plantarum 122: 419-428.

Botanga, C. J., Bethke, G., Chen, Z., Gallie, D. R., Fiehn, O., and Glazebrook, J. 2012. Metabolite Profiling of Arabidopsis Inoculated with *Alternaria brassicicola* Reveals That Ascorbate Reduces Disease Severity. Molecular Plant-Microbe Interactions 25: 1628-1638.

Brown, S. H., Scott, J. B., Bhaheetharan, J., Sharpee, W. C., Milde, L., Wilson, R. A., and Keller, N. P. 2009. Oxygenase coordination is required for morphological transition and the host-fungus interaction of *Aspergillus flavus*. Molecular Plant-Microbe Interactions 22: 882-894.

Bush, B. J., Carson, M. L., Cubeta, M. A., Hagler, W. M., and Payne, G. A. 2004. Infection and Fumonisin Production by *Fusarium verticillioides* in Developing Maize Kernels. Phytopathology 94: 88-93.

Cao, A., Santiago, R., Ramos, A. J., MarÃn, S., Reid, L. M., and Butrón, A. 2013. Environmental factors related to fungal infection and fumonisin accumulation during the development and drying of white maize kernels. International Journal of Food Microbiology 164: 15-22.

Casacuberta, J. M., Puigdomenech, P., and San Segundo, B. 1991. A gene coding for a basic pathogenesis-related (PR-like) protein from *Zea mays*. Molecular cloning and

induction by a fungus (*Fusarium moniliforme*) in germinating maize seeds. Plant Molecular Biology 16: 527-536.

Casacuberta, J. M., Raventos, D., Puigdomenech, P., and San Segundo, B. 1992. Expression of the gene encoding the PR-like protein PRms in germinating maize embryos. Molecular Genetics and Genomics 234: 97-104.

CAST. 2003. Mycotoxins: Risks in plant, animal, and human systems. In: Potential Economic Costs of Mycotoxins in the United States Cast Task Force Report No. 139. January: p.136-142.

Chen, Z. Y., Brown, R. L., Damann, K. E., and Cleveland, T. E. 2007. Identification of Maize Kernel Endosperm Proteins Associated with Resistance to Aflatoxin Contamination by *Aspergillus flavus*. Phytopathology 97: 1094-1103.

Cobb, B. G., and Hannah, L. C. 1988. Shrunken-1 encoded sucrose synthase is not required for sucrose synthesis in the maize endosperm. Plant Physiology 88: 1219-1221.

Delmer, D. P., and Amor, Y. 1995. Cellulose biosynthesis. Plant Cell 7: 987-1000.

Denancé, N., Sánchez-Vallet, A., Goffner, D., and Molina, A. 2013. Disease resistance or growth: the role of plant hormones in balancing immune responses and fitness costs. Frontiers in Plant Science 4: 155.

Doehlemann, G., Wahl, R., Horst, R. J., Voll, L. M., Usadel, B., Poree, F., Stitt, M., Pons-Kuhnemann, J., Sonnewald, U., Kahmann, R., and Kamper, J. 2008. Reprogramming a maize plant: transcriptional and metabolic changes induced by the fungal biotroph *Ustilago maydis*. The Plant Journal 56: 181-195.

Dolezal, A. L. 2010. Interactions Between *Aspergillus flavus* and the Developing Maize Kernel. Doctoral dissertation Retrieved from ProQuest Dissertations and Theses: OCLC Number: 704568905.

Dolezal, A. L., Obrian, G. R., Nielsen, D. M., Woloshuk, C. P., Boston, R. S., and Payne, G. A. 2013. Localization, morphology and transcriptional profile of *Aspergillus flavus* during seed colonization. Molecular Plant Pathology 14: 898-909.

Duncan, K. E., and Howard, R. J. 2010. Biology of maize kernel infection by *Fusarium verticillioides*. Molecular Plant-Microbe Interactions 23: 6-16.

Fakhoury, A. M., and Woloshuk, C. P. 2001. Inhibition of growth of *Aspergillus flavus* and fungal alpha-amylases by a lectin-like protein from Lablab purpureus. Molecular Plant-Microbe Interactions 14: 955-961.

Fennell, D., Bothast, R., Lillehoj, E., and Peterson, R. 1973. Bright Greenish-Yellow Fluorescence and Associated Fungi in White Corn Naturally Contaminated with Aflatoxin. Cereal Chemistry 50: 404-413.

Fraissinet-Tachet, L., Baltz, R., Chong, J., Kauffmann, S., Fritig, B., and Saindrenan, P. 1998. Two tobacco genes induced by infection, elicitor and salicylic acid encode glucosyltransferases acting on phenylpropanoids and benzoic acid derivatives, including salicylic acid. FEBS Letters 437: 319-323.

Franks, R. G., Wang, C., Levin, J. Z., and Liu, Z. 2002. SEUSS, a member of a novel family of plant regulatory proteins, represses floral homeotic gene expression with LEUNIG. Development 129: 253-263.

Göhre, V., Jones, A. M. E., Sklenář, J., Robatzek, S., and Weber, A. P. M. 2012. Molecular Crosstalk Between PAMP-Triggered Immunity and Photosynthesis. Molecular Plant-Microbe Interactions 25: 1083-1092.

Gómez-Ariza, J., Campo, S., Rufat, M., Estopà, M., Messeguer, J., San Segundo, B., and Coca, M. 2007. Sucrose-mediated priming of plant defense responses and broad-spectrum disease resistance by overexpression of the maize pathogenesis-related PRms protein in rice plants. Molecular Plant-Microbe Interactions 20: 832-842.

Guo, B. Z., Chen, Z. Y., Brown, R. L., Lax, A. R., Cleveland, T. E., Russin, J. S., Mehta, A. D., Selitrennikoff, C. P., and Widstrom, N. W. 1997. Germination induces accumulation of specific proteins and antifungal activities in corn kernels. Phytopathology 87: 1174-1178.

Guo, B. Z., Cleveland, T. E., Brown, R. L., Widstrom, N. W., Lynch, R. E., and Russin, J. S. 1999. Distribution of antifungal proteins in maize kernel tissues using immunochemistry. Journal of Food Protection 62: 295-299.

Hauptmann, R. M., Ashraf, M., Vasil, V., Hannah, L. C., Vasil, I. K., and Ferl, R. 1988. Promoter strength comparisons of maize shrunken 1 and alcohol dehydrogenase 1 and 2 promoters in mono- and dicotyledonous species. Plant Physiology 88: 1063-1066.

Hesseltine, C. W., Shotwell, O. L., Kwolek, W. F., Lillehoj, E. B., Jackson, W. K., and Bothast, R. J. 1976. Aflatoxin Occurrence in 1973 Corn at Harvest. Mycologia 68: 341-353.

Horn, B. W., Moore, G. G., and Carbone, I. 2009. Sexual reproduction in *Aspergillus flavus*. Mycologia 101: 423-429.

Huber, S. C., and Huber, J. L. 1996. Role and regulation of sucrose-phosphate synthase in higher plants. Annual Review of Plant Physiology and Plant Molecular Biology 47: 431-444.

Huffaker, A., Dafoe, N. J., and Schmelz, E. A. 2011. ZmPep1, an ortholog of Arabidopsis elicitor peptide 1, regulates maize innate immunity and enhances disease resistance. Plant Physiology 155: 1325-1338.

Jiang, L., Yu, X., Qi, X., Yu, Q., Deng, S., Bai, B., Li, N., Zhang, A., Zhu, C., Liu, B., and Pang, J. 2013. Multigene engineering of starch biosynthesis in maize endosperm increases the total starch content and the proportion of amylose. Transgenic Research 22: 1-10.

Johann, H. 1935. Histology of the caryopsis of yellow dent corn, with reference to resistance and susceptibility to kernel rot. Journal of Agricultural Research 51: 855-883.

Johansson, A. S., Whitaker, T. B., Hagler, W. M., Jr., Bowman, D. T., Slate, A. B., and Payne, G. 2006. Predicting aflatoxin and fumonisin in shelled corn lots using poor-quality grade components. Journal of AOAC International 89: 433-440.

Jones, R. K., Duncan, H. E., Payne, G. A., and Leonard, K. J. 1980. Factors influencing infection by *Aspergillus flavus* in silk-inoculated corn. Plant Diseases 64: 859-863.

Keller, N. P., Butchko, R., Sarr, B., and Phillips, T. D. 1994. A Visual Pattern of Mycotoxin Production in Maize Kernels by *Aspergillus* spp. Phytopathology 84: 483-488.

Kelley, R. Y., Williams, W. P., Mylroie, J. E., Boykin, D. L., Harper, J. W., Windham, G. L., Ankala, A., and Shan, X. 2012. Identification of maize genes associated with host plant resistance or susceptibility to *Aspergillus flavus* infection and aflatoxin accumulation. PLoS One 7: e36892.

Koehler, B. 1942. Natural mode of entrance of fungi into Corn ears and some symptoms that indicate infection. Journal of Agricultural Research 64: 421-442.

Lee, L. S., Lillehoj, E. B., and Kwolek, W. F. 1980. Aflatoxin Distribution in Individual Corn Kernels from Intact Ears. Cereal Chemistry 57: 340-343.

Lillehoj, E. B., Kwolek, W. F., Fennell, D. I., and Milburn, M. S. 1975. Aflatoxin Incidence and Association with Bright Greenish-Yellow Fluorescence and Insect Damage in a Limited Survey of Freshly Harvested High-Moisture Corn. Cereal Chemistry 52: 403-411.

Lincoln, C., Long, J., Yamaguchi, J., Serikawa, K., and Hake, S. 1994. A knotted1-like homeobox gene in Arabidopsis is expressed in the vegetative meristem and dramatically alters leaf morphology when overexpressed in transgenic plants. Plant Cell 6: 1859-1876.

Livingston, D. P., Tuong, T. D., Haigler, C. H., Avci, U., Tallury, S. P. 2009. Rapid Microwave Processing of Winter Cereals for Histology Allows Identification of Separate Zones of Freezing Injury in the Crown. Crop Science 49: 1837-1842.

Livingston, D. P., Henson, C. A., Tuong, T. D., Wise, M. L., Tallury, S. P., and Duke, S. H. 2013. Histological Analysis and 3D Reconstruction of Winter Cereal Crowns Recovering from Freezing: A Unique Response in Oat (*Avena sativa* L.). PLoS One 8: e53468.

Long, J. A., and Barton, M. K. 1998. The development of apical embryonic pattern in Arabidopsis. Development 125: 3027-3035.

Loussert, C., Schmitt, C., Prevost, M. C., Balloy, V., Fadel, E., Philippe, B., Kauffmann-Lacroix, C., Latgé, J. P., and Beauvais, A. 2010. *In vivo* biofilm composition of *Aspergillus fumigatus*. Cellular Microbiology 12: 405-410.

Ma, L., Shang, Y., Cao, A., Qi, Z., Xing, L., Chen, P., Liu, D., and Wang, X. 2010. Molecular cloning and characterization of an up-regulated UDP-glucosyltransferase gene induced by DON from *Triticum aestivum* L. cv. Wangshuibai. Molecular Biology Reports 37: 785-795.

Maas, C., Laufs, J., Grant, S., Korfhage, C., and Werr, W. 1991. The combination of a novel stimulatory element in the first exon of the maize Shrunken-1 gene with the following intron 1 enhances reporter gene expression up to 1000-fold. Plant Molecular Biology 16: 199-207.

Maiorano, A., Reyneri, A., Sacco, D., Magni, A., and Ramponi, C. 2009. A dynamic risk assessment model (FUMAgrain) of fumonisin synthesis by *Fusarium verticillioides* in maize grain in Italy. Crop Protection 28:243-256.

Manns, T. F., and Adams, J. F. 1923. Parasitic fungi interval of seed corn. Journal of Agricultural Research 23: 495-524.

Marsh, S., and Payne, G. 1984. Preharvest Infection of Corn Silks and Kernels by *Aspergillus flavus*. Phytopathology 74: 1284-1289.

McCarty, D. R., Shaw, J. R., and Hannah, L. C. 1986. The cloning, genetic mapping, and expression of the constitutive sucrose synthase locus of maize. Proceedings of the National Academy of Sciences 83: 9099-9103.

Mideros, S. X., Warburton, M. L., Jamann, T. M., Windham, G. L., Williams, W. P., and Nelson, R. J. 2014. Quantitative Trait Loci Influencing Mycotoxin Contamination of Maize: Analysis by Linkage Mapping, Characterization of Near-Isogenic Lines, and Meta-Analysis. Crop Science 54: 127-142.

Moore, K. G., Price, M. S., Boston, R. S., Weissinger, A. K., and Payne, G. A. 2004. A Chitinase from Tex6 Maize Kernels Inhibits Growth of *Aspergillus flavus*. Phytopathology 94: 82-87.

Munkvold, G. P., McGee, D. C., and Carlton, W. M. 1997. Importance of Different Pathways for Maize Kernel Infection by *Fusarium moniliforme*. Phytopathology 87: 209-217.

Munkvold, G. P. 2003. Cultural and genetic approaches managing mycotoxins in maize. Annual Review of Phytopathology 41: 99-116.

Murillo, I., Cavallarin, L., and Segundo, B. S. 1999. Cytology of Infection of Maize Seedlings by *Fusarium moniliforme* and Immunolocalization of the Pathogenesis-Related PRms Protein. Phytopathology 89: 737-747.

Nielsen, K., Payne, G. A., and Boston, R. S. 2001. Maize ribosome-inactivating protein inhibits normal development of *Aspergillus nidulans* and *Aspergillus flavus*. Molecular Plant-Microbe Interactions 14: 164-172.

O'Donnell, P. J., Truesdale, M. R., Calvert, C. M., Dorans, A., Roberts, M. R., and Bowles, D. J. 1998. A novel tomato gene that rapidly responds to wound- and pathogen-related signals. The Plant Journal 14: 137-142.

Payne, G. A. 1983. Nature of Field Infection of Corn by *Aspergillus flavus*, pp. 16-19. Aflatoxin and *Aspergillus Flavus* in Corn Southern Cooperative Series Bulletin, 279. Diener UL, Asquith RL, Dickens JW eds. Auburn, Auburn University.

Payne, G., Thompson, D., Lillehoj, E., Zuber, M., and Adkins, C. 1988. Effect of temperature on the preharvest infection of maize kernels by *Aspergillus flavus*. Phytopathology 78: 1376-1380.

Payne, G. A. 1992. Aflatoxin in maize. Critical Reviews in Plant Sciences 10: 423-440.

Poppenberger, B., Berthiller, F., Lucyshyn, D., Sieberer, T., Schuhmacher, R., Krska, R., Kuchler, K., Glossl, J., Luschnig, C., and Adam, G. 2003. Detoxification of the *Fusarium* mycotoxin deoxynivalenol by a UDP-glucosyltransferase from *Arabidopsis thaliana*. The Journal of Biological Chemistry 278: 47905-47914.

Robertson-Hoyt, L. A., Betran, J., Payne, G. A., White, D. G., Isakeit, T., Maragos, C. M., Molnar, T. L., and Holland, J. B. 2007. Relationships Among Resistances to *Fusarium* and *Aspergillus* Ear Rots and Contamination by Fumonisin and Aflatoxin in Maize. Phytopathology 97: 311-317.

Royo, J., Gomez, E., Balandin, M., Muniz, L. M., and Hueros, G. 2006. ZmLrk-1, a receptor-like kinase induced by fungal infection in germinating seeds. Planta 223: 1303-1314.

Santi, S., De Marco, F., Polizzotto, R., Grisan, S., and Musetti, R. 2013. Recovery from stolbur disease in grapevine involves changes in sugar transport and metabolism. Frontiers in Plant Science 4: 171.

Smart, M. G., Wicklow, D. T., and Caldwell, R. W. 1990. Pathogenesis in *Aspergillus* Ear Rot of Maize: Light Microscopy of Fungal Spread from Wounds. Phytopathology 80: 1287-1294.

Sobek, E. A., and Munkvold, G. P. 1999. European corn borer (Lepidoptera: Pyralidae) larvae as vectors of *Fusarium moniliforme*, causing kernel rot and symptomless infection of maize kernels. Journal of Economic Entomology 92: 503-509.

Spollen, W. G., Tao, W., Valliyodan, B., Chen, K., Hejlek, L. G., Kim, J. J., Lenoble, M. E., Zhu, J., Bohnert, H. J., Henderson, D., Schachtman, D. P., Davis, G. E., Springer, G. K., Sharp, R. E., and Nguyen, H. T. 2008. Spatial distribution of transcript changes in the maize primary root elongation zone at low water potential. BMC Plant Biology 8: 32.

van de Mortel, J. E., de Vos, R. C., Dekkers, E., Pineda, A., Guillod, L., Bouwmeester, K., van Loon, J. J., Dicke, M., and Raaijmakers, J. M. 2012. Metabolic and transcriptomic changes induced in Arabidopsis by the rhizobacterium *Pseudomonas fluorescens* SS101. Plant Physiology 160: 2173-2188.

Vasil, V., Clancy, M., Ferl, R. J., Vasil, I. K., and Hannah, L. C. 1989. Increased gene expression by the first intron of maize *shrunken-1* locus in grass species. Plant Physiology 91: 1575-1579.

Warfield, C. Y., and Davis, R. M. 1996. Importance of the husk covering on the susceptibility of corn hybrids to *Fusarium* ear rot. Plant Disease 80: 208-210.

Widstrom, N. W., Butron, A., Guo, B. Z., Wilson, D. M., Snook, M. E., Cleveland, T. E., and Lynch, R. E. 2003. Control of preharvest aflatoxin contamination in maize by pyramiding QTL involved in resistance to ear-feeding insects and invasion by *Aspergillus* spp. European Journal of Agronomy 19: 563-572.

Wilson, R. A., Gardner, H. W., and Keller, N. P. 2001. Cultivar-dependent expression of a maize lipoxygenase responsive to seed infesting fungi. Molecular Plant-Microbe Interactions 14: 980-987.

Wittich, P. E., and Vreugdenhil, D. 1998. Localization of sucrose synthase activity in developing maize kernels by in situ enzyme histochemistry. Journal of Experimental Botany 49: 1163-1171.

Xu, D. P., Sung, S. J., Loboda, T., Kormanik, P. P., and Black, C. C. 1989. Characterization of Sucrolysis via the Uridine Diphosphate and Pyrophosphate-Dependent Sucrose Synthase Pathway. Plant Physiology 90: 635-642.

APPENDIX

Appendix A

Molecular Characterization and Functional Analysis of a Gene Family Encoding Necrosis- and Ethylene-Inducing Proteins in *Aspergillus flavus*

Authors: Xiaomei Shu[1], Andrea L. Dolezal[1], Gregory R. OBrian[1], David P. Livingston[2], Rebecca S. Boston[3], Charles P. Woloshuk[4], and Gary A. Payne[1*]

Charles P. Woloshuk[4], and Gary A. Payne[1*]

[1] Department of Plant Pathology, North Carolina State University, Raleigh, NC 27695-7567

[2] Department of Crop Science, North Carolina State University, Raleigh, NC 27695

[3] Department of Plant & Microbial Biology, North Carolina State University, Raleigh, NC 27695

[4] Department of Botany and Plant Pathology, Purdue University, West Lafayette, IN 47907

ABSTRACT

Necrosis- and ethylene-inducing protein (Nep)-like proteins (NLPs) are a novel family of microbial elicitors from fungi, oomycetes and bacteria. Many members of NLPs are able to cause necrosis and activate a host defense response in dicotyledonous plants. In this study, we analyzed the *NLP* family members of *Aspergillus flavus*: *nepA*, *nepB* and *nepC*. The three predicted *A. flavus* NLPs contain transmembrane signal peptides and conserved amino acid residues that are critical for necrosis-inducing activity. Expression analysis revealed that these *A. flavus NLPs* were not expressed when grown on potato dextrose broth (PDB). However, all the three *NLPs* were expressed during early pathogenesis on immature maize kernels. One of the *NLPs*, *nepA*, is more highly expressed during colonization of living kernels compared with autoclaved kernels. Targeted deletion of *nepA* resulted in impaired vegetative growth and reduced conidiation on potato dextrose agar (PDA) plates. But vegetative growth and conidiation of *A. flavus* on corn extract medium (CEM) and on minimal medium (MLS) were not affected by deletion of *nepA*. Moreover, the Δ*nepA* strain showed reduced pathogenicity in immature maize kernels. Overexpression (OE) of *nepA* in *A. flavus* resulted in increased growth in the aleurone of some maize kernels. But vegetative growth and conidiation on media were not affected by overexpression of *nepA*. Infiltration of *A. flavus* liquid culture into tobacco leaves revealed that the *nepA* OE strains were capable of causing necrosis. However, the *nepA* OE strains failed to cause necrosis in either *Arabidopsis thaliana* or maize seedlings. In summary, we found that the three *A. flavus NLPs* we expressed during pathogenesis, and *nepA* appears to be required for full virulence on maize kernels.

INTRODUCTION

Infectious plant pathogens employ wide-ranging virulence strategies to overcome the multifaceted host immune system and successfully invade their host plants. To disarm the pathogenic arsenal or attenuate its effect, plants have evolved effector-triggered immunity (ETI) and pathogen-associated molecular pattern (PAMP)-triggered immunity (PTI) pathways. ETI is typically activated by host-specific pathogen effectors, and characterized by programmed cell death (PCD), a reaction known as the hypersensitive response (HR) (Jones and Dangl, 2006). PTI is often associated with non-host resistance (Jones and Dangl, 2006). However, necrotrophic pathogens promote host cell death and acquire nutrients from dead tissue for growth and reproduction (Mengiste, 2012). Nonspecific toxins produced by broad host-range necrotrophs function most likely through triggering host cell death that mimics the plant immune response, and thus promotes infection. An example of such toxins are the necrosis- and ethylene-inducing protein 1 (Nep1)-like proteins (NLPs) produced by fungi, oomycetes and bacteria species (Gijzen and Nurnberger, 2006; Pemberton et al., 2004). NLPs are non-host specific elicitors capable of causing necrosis and activating host defense responses in dicotyledonous plants (Keates et al., 2003; Staats et al., 2007). NLPs associated defense responses include signaling transduction, accumulation of pathogenesis related (PR) proteins, phytoalexins, ethylene and reactive oxygen species (ROS) (Wang et al., 2004; Qutob et al., 2006; Zhang et al., 2012). Previous studies indicate that monocotyledonous plants are insensitive to NLPs (Bailey, 1995; Schouten et al., 2008).

The NLP NEP1, was isolated and purified from *Fusarium oxysporum* culture filtrates (Bailey, 1995). NEP1 was able to induce necrosis, ethylene accumulation, and expression of stress responsive genes in *Erythroxylum coca* (Bailey et al., 2002, 2005). NEP1 was demonstrated to be a potential bioherbicide (Jennings et al., 2000; Meir et al., 2009). Other NLPs were identified from species of *Phytophthora*, *Erwinia, Verticillium*, *Pythium*, *Streptomyces*, *Mycosphaerella*, *Botrytis*, *Fusarium*, *Aspergillus* and other taxonomically unrelated micro-organisms (Cuesta Arenas et al., 2010; Dong et al., 2012; Garcia et al., 2007; Keates et al., 2003; Luberacki et al., 2008; Mattinen et al., 2004). Multiple copies of *NLP* orthologs were identified from *Phytophthora* species, including *P. infestans*, *P. sojae P. citrophthora*, *P. capsici*, *P. palmivora*, and *P. megakarya* (Bae et al., 2006; Dong et al., 2012; Fellbrich et al., 2002; Kanneganti et al., 2006; Lee and Rose, 2010). Although eight NLPs were identified from *Verticillium dahliae*, only two of these NLPs were able to induce necrosis and defense responses in host plants (Santhanam et al., 2013; Zhou et al., 2012). Many fungal genomes only contain up to three *NLP* genes (Dallal Bashi et al., 2010; Garcia et al., 2007; Motteram et al., 2009; Schouten et al., 2008; Staats et al., 2007). However, five members of NLP were identified from the hemibiotrophic basidiomycete fungal pathogen *Moniliophthora perniciosa*, which causes Witches' Broom disease in cacao (Zaparoli et al., 2011).

NLPs generally share a conserved necrosis-inducing *Phytophthora* protein 1 (NPP1) domain containing a heptapeptide ‘GHRHDWE’ motif, cysteine residues, and other conserved amino acid residues (Cechin et al., 2008a, 2008b; Zhou et al., 2012). The

conserved heptapeptide and cysteine residues of the NPP1 domain are indispensable for the necrosis-inducing activity of the NLPs in *V. dahlia* (Zhou et al., 2012). Many NLPs are cytolytic toxins capable of inducing a host defense response by forming transmembrane pores on plant cells (Küfner et al., 2009; Ottmann et al., 2009; Qutob et al., 2006). Two fluorescently labelled *Botrytis cinerea* NLPs were observed to localize to the plasma membrane during infection of several dicotyledonous plant species (Schouten et al., 2008). The NLP from *F. oxysporum* was also associated with the plasma membrane of *Arabidopsis thaliana* (Bae et al., 2006). It is likely that NLPs from the same pathogen contribute to virulence in a host-dependent manner (Mattinen et al., 2004; Pemberton et al., 2005). Targeted deletion of *V. dahliae* genes encoding the cytotoxic NLP did not affect virulence on cotton, but showed reduced virulence on tomato and *A. thaliana* (Santhanam et al., 2013; Zhou et al., 2012). Deletion of *V. dahliae NLP1* showed compromised virulence on tobacco, whereas deletion of *NLP2* had no effect on tobacco (Santhanam et al., 2013). In addition, noncytotoxic NLPs were identified from the obligate biotrophic oomycete pathogen *Hyaloperonospora arabidopsidis* (Cabral et al., 2012).

Aspergillus flavus is a necrotrophic fungal pathogen capable of infecting plants, insects, animals, and immunocompromised patients (Payne and Brown, 1998; St Leger et al., 2000). *A. flavus* is notorious for its ability to cause maize ear rot and produce aflatoxins, which are carcinogenic secondary metabolites. The genome sequence of *A. flavus* is available, which greatly facilitates analysis of putative effector encoding genes (Payne et al., 2006). Several putative virulence factors have been reported. The *A. flavus*

endopolygalacturonase, P2c, is associated with virulence during infection of both maize and cotton bolls (Mellon et al., 2007; Shieh et al., 1997). In addition, an amylase and phytase from *A. flavus* have been shown to be associated with pathogenicity during colonization of maize kernels (Mellon et al., 2007; Reese et al., 2011). In this study, we analyzed three *A. flavus NLPs* that were expressed during early colonization of immature maize kernels. Mutagenesis studies revealed that one of the *A. flavus NLPs*, *nepA*, was involved in virulence of this fungus on immature maize kernels. In addition, it appears that the nepA protein is capable of inducing necrosis on tobacco leaves.

MATERIALS AND METHODS

Sequence analysis of *A. flavus NLPs* family members

The DNA sequence of the three *A. flavus NLPs* were obtained from the *A. flavus* genome database (Payne et al., 2006). The degree of homology was analyzed by aligning the sequences using EMBL-EBI ClustalW2 (Larkin et al., 2007). Then the predicted *A. flavus* NLP protein sequences were obtained from the NCBI database. Homologous NLP proteins from other micro-organisms were identified by a BLAST search of the amino acid sequence of *nepA* against the NCBI database. Several other NLPs that have been studied were selected for amino acid sequence alignment and phylogenetic analysis using the EMBL-EBI ClustalW2 (Larkin et al., 2007). Signal peptides were predicted using the SignalP-4.1 server (Emanuelsson et al., 2007).

Gene expression analysis using RNA-seq

Then maize inbred line B73 was grown at the Central Crops Research Station near Clayton, NC. Maize ears were hand-pollinated and covered with pollination bags. *A. flavus* WT strain *3357* was grown on PDA plates at 28^{o}C for 5 days. Conidial suspensions were harvested by adding sterile distilled water containing 0.5% (v/v) Triton X-100 (Fisher) and scraping the plates using a glass spreader. The concentration of conidia was determined using a hemocytometer (Hausser Scientific) and conidia were diluted to 1×10^{6} conidia/ml before being used for inoculation. Kernels were inoculated with *A. flavus* in the field 21-22 days after pollination by wounding the kernel with a 3 mm needle bearing approximately 13 conidia. Kernels for the mock treatment were inoculated with sterile distilled water containing 0.5% (v/v) Triton X-100. Kernels were collected at 12, 24, 48 and 72 hpi. Three ears were harvested for each treatment as three biological replicates. Kernels were frozen in liquid nitrogen immediately and stored at -80^{o}C. Eight frozen kernels from individual ears were pooled and ground in liquid nitrogen with mortar and pestle. About one hundred milligrams of ground tissue was added to 0.75 ml of saturated phenol, pH 6.6 (Fisher), and homognized for 2 min. homogenized tissue was dissolved in Tris EDTA buffer, pH 8.0 (ACROS Organics), extracted with 5:1 acid phenol: chloroform, pH 4.5 (Fisher), and precipitated with ice-cold 100% ethanol (ACROS Organics) overnight. Total RNA was further purified with an RNeasy Mini Kit (Qiagen) according to the manufacturer's instructions. The quality and concentration of RNA was analyzed using an RNA Pico chip on an Agilent Bioanalyzer.

RNA from the kernels collected at different time points was sequenced using the Illumina HiSeq by the Genomic Sciences Laboratory, North Carolina State University. Multiple samples with different barcodes were loaded in three lanes and sequenced to obtain 100 bp single-end reads. Illumina reads were sorted by barcodes, and adapter sequences were trimmed. The raw sequencing reads were then analyzed using the iPlant Collaborative Discovery Environment (Matasci and McKay, 2013). Reads of the same individual from multiple lanes were then concatenated using the app named 'Concatenate Multiple Files'. Quality of the reads was checked using FastQC 0.10.1. The reads were aligned to the *A. flavus* genome (JCV1-afl1-v2.0.14) by using TopHat2-SE (Trapnell et al., 2012). Then transcripts were assembled from the BAM files by using Cufflinks2 (Trapnell et al., 2012). The fragments per kilobase of exon per million fragments mapped (FPKM) values were used for gene expression analysis.

Generation of *A. flavus* Δ*nepA* and *nepA* OE strains

To generate the *nepA* deletion construct, non-coding flanking genomic sequences of the *nepA* coding region were amplified from genomic DNA of *A. flavus 3357* using the *nepA* seq primer set (Dolezal, 2010). The nepA deletion construct was made by overlapping PCR using six primers, *nepA*_1, *nepA*_2, *nepA*_3, *nepA*_4, *nepA*_5, and *nepA*_6 (Dolezal, 2010). The *nepA* coding sequence was replaced by the *Neurospora crassa pyr4* gene cassette through homologous recombination. The *pyr-4* gene of *N. crassa* encodes orotidine-5'-phosphate decarboxylase, which is involved in the pyrimidine biosynthesis (Newbury et al., 1986). The auxotrophic mutant strain *afc-1* was used to generate *A. flavus* Δ*nepA* strains. It is

a uracil and arginine deficient mutant originally developed from the *A. flavus* WT strain *3357*. Protoplasts of *afc-1* were generated and transformed with the Δ*nepA* construct (Woloshuk et al., 1989). Transformants were selected on MLS medium plus arginine. The Δ*nepA* constructs were verified by PCR. The Δ*nepA* strains were then transformed again with the *A. flavus argD* gene. Transformants were selected on MLS medium. The Δ*nepA* constructs were verified by PCR.

The *nepA* OE construct was generated by inserting the *nepA* gene into the plasmid pNOM102 driven by the *gpdA* constitutive promoter (Dolezal, 2010). The *gpdA* constitutive promoter was originally amplified from *A. nidulans* (Redkar et al., 1998). To generate *nepA* OE strains, *afc-1* was co-transformed with the *nepA* overexpression construct and *pyr4*. Transformants were selected on MLS medium plus arginine. The *nepA* OE construct was verified by PCR. The *nepA* OE strains were then transformed again with the *A. flavus argD* gene. Transformants were selected on MLS medium. The *nepA* OE construct was verified by PCR.

Additionally, the fully complemented *afc-1*$^{++}$ strain was generated by co-transformation of *afc-1* with the *pyr4* and *argD* genes. The *A. flavus* strains that were used in this study are listed in Table 1. Primers used to generate Δ*nepA* and *nepA* OE strains are listed in Table 2.

Table 1. *A. flavus* strains used in this study.

A. flavus strain	Genotype
3357	wide-type
afc-1	a uracil and arginine deficient mutant strain
afc-1^{++}	*afc-1* full complemented with *pyr4* and *argD*
Δ*nepA*-1	*nepA* deletion strain
Δ*nepA*-2	*nepA* deletion strain
Δ*nepA*-3	*nepA* deletion strain
nepA OE-1	*nepA* overexpression strain
nepA OE-2	*nepA* overexpression strain
nepA OE-3	*nepA* overexpression strain

Table 2. Primers used in this study.

Primer use	Primers 5'-3'
nepA cloning	*nepA* Seq 5': CAAGAACCTTTTGGCCATTC
	nepA Seq 3': TCCCTGGAAAGTTGAATCCTT
generating Δ*nepA* construct	*nepA*_1: TGTGGTGCACATTGTGATTG
	*nepA*_2: CGGTAAAGCCTCTCAATCTATGGACCACACGAGTCAA
	*nepA*_3: TTGACTCGTGTGGTCCATAGATTGAGAGGCTTTACCG
	*nepA*_4: GGCGGAGGATATTTCGTTTTCAGACGCTGTATGGGTGTATC
	*nepA*_5: GATACACCCATACAGCGTCTGAAAACGAAATATCCTCCGCC
	*nepA*_6: CCGAAGGCTCTCGAGTAATG
screening for Δ*nepA*	A_{nepA} : ATTGTGGTTGTGCGTTGGT
	B_{nepA} : CGATATCGGAACCGGAAGTA
	C_{nepA} : GGAGCGGGATATGTCTTTGA
	D_{nepA} : TCTAGGGGAGTGTCCAAACG
generating and screening *nepA*	*nepA* OE 5': CCATGGTTTCCAAGACCTTTTG
OE construct	*nepA* OE 3': CCTAGGCTAAAGAGCAGCCTTCTCAAGATTTC
	pNOM102 5': TCCCACTTCATCGCAGCTTG

Pathogenicity assay on maize kernels

A. flavus 3357, *afc-1*$^{++}$ and *nepA* mutant strains were grown on PDA plates and conidia were harvested. Maize ears were removed from the plants 21-22 days after pollination and inoculated with *A. flavus* strains in the lab. Kernels were wound-inoculated. Control ears were mock inoculated with sterile distilled water containing 0.5% (v/v) Triton X-100. Inoculated kernels were incubated in a greenhouse and collected at 96 hpi. Three ears were harvested for each treatment as three biological replicates. Three mock inoculated ears were harvested as controls. Kernels were either fixed for histology studies or frozen in liquid nitrogen immediately and stored at -80^{o}C.

For expression analysis, RNA was isolated as described above, and treated with DNase (Promega) according to the manufacturer's instructions. cDNA synthesis was performed using the First Strand cDNA Synthesis Kit (Fermentas) following the manufacturer's instructions. RT-PCR was performed using Ex Taq (Chemicon) according to the manufacturer's instructions. The PCR products were analyzed through a 0.8 % (w/v) agarose gel.

Kernels for histology studies were collected in tissue embedding capsules (Fisher). Samples were fixed, dehydrated, and embedded as described in chapter two. The paraffin blocks were sectioned with an RM2255 microtome (Leica) and mounted on glass slides. Slides were dried on a hot plate overnight and stored at room temperature. The staining was carried out as previously described (chapter two; Livingston et al., 2009, 2013). Images were collected on an Eclipse E600 light microscope (Nikon) with an Infinity1-3C digital camera.

Growth and conidiogenesis assays

Growth and conidiogenesis assays were performed by placing 10 µl of 1×10^4 conidia/ml conidia suspension in the center of a 100 mm × 15 mm (diameter × height) plate and incubating it at 28°C. Ten plates were included for each fungal strain. Three different types of media were used, PDA, MLS and CEM. CEM contains 30 grams of fresh maize kernels per liter. Colony diameters were measured 1, 2, 3, 4, 5, 6, and 7 days post inoculation (dpi). A no.2 cork borer (with an area of about 22.5 mm^2) was used to collect conidia located at about 0.5cm away from the center of the plate. Conidia were then diluted in 1ml 0.5% (v/v) Triton X-100. The number of conidia was counted using a hemocytometer.

Cytotoxic activity determination on tobacco, *A. thaliana*, and maize leaves

A. flavus 3357, *afc-1*$^{++}$ and *nepA* mutant strains were grown on PDA plates at 28°C for 5 days. Conidial suspensions were harvested, and grown on PDB at 28°C for 2 days with agitation (200 rpm). Mycelia and conidia were harvested by filtrating through a filter paper. RNA extraction and RT-PCR were performed as described above. Tobacco and *A. thaliana* plants were kindly provided by Dr. Ralph Dewey and Dr. Heike Sederoff, respectively. Maize seeds were allowed to germinate and grow in the lab for about four weeks before infiltration. *A. flavus* was infiltrated into leaves of tobacco, *A. thaliana*, and maize seedling using a syringe.

RESULTS

Identification and sequence analysis of *NLPs* from *A. flavus*

Three *A. flavus* genes contain the NPP1 domain, named *nepA* (AFLA_096450), *nepB* (AFLA_054320), and *nepC* (AFLA_013750). The degree of DNA sequence homology between the three *NLP* members is low with maximum identity of 62.81%. These *NLPs* are located in different chromosomes. *NepA* was mapped to the telomeric end of chromosome five. It is located between the aflatrem biosynthesis gene cluster and another secondary metabolite biosynthesis gene cluster. The other two *A. flavus NLPs*, *nepB* and *nepC*, were mapped to chromosome one and four, respectively.

We analyzed the predicted amino acid sequences of the three *A. flavus* NLPs. The three *A. flavus* NLPs were aligned with NLPs from other micro-organisms, including *Aspergillus fumigatus* (Nierman et al., 2005), *Fusarium verticillioides* (Ma et al., 2010), *F. oxysporum* (Meir et al., 2009), *Pythium aphanidermatum* (Veit et al., 2001), *P. sojae* (Qutob et al., 2002), *Botrytis elliptica* (Staats et al., 2007), and *V. dahliae* (Santhanam et al., 2013). *A. fumigatus* is a human pathogen which is taxonomically closely-related to *A. flavus*. The other six are plant pathogens which are taxonomically unrelated to *A. flavus*. It appears that nepA belongs to type I NLPs that contain two conserved cysteine (Cys) residues, Cys-62 and Cys-83, whereas nepB and nepC belong to type II NLPs that have five cysteines (Fig. 1A). The conserved Cys-62 and Cys-83 are likely involved in the formation of the disulfide bond of the NLP proteins (Ottmann et al., 2009). Only nepB and nepC have the intact heptapeptide motif. In nepA, the first amino acid of this motif is alanine, not glycine (Fig. 1A). In addition,

all three *A. flavus* NLPs were predicted to be secretory proteins containing signal peptides (Fig. 1A). Phylogenetic analysis indicated that nepA is more close-related to the NLP from *B. elliptica*, whereas nepB and nepC are more close-related to the *A. fumigatus* NLP (Fig. 1B).

Figure 1. Sequence analysis of NLPs from *A. flavus* and other micro-organisms. A, Alignment of amino acid sequence of the NLPs. Predicted signal peptides are framed; conserved Cys are highlighted in gray; conserved heptapeptide 'GHRHDWE' motifs are underlined. B, Phylogenetic relationship of the NLPs. *A. flavus* NLPs are framed. Accession numbers of NLPs: XP_002381464 (nepA$_{A. flavus}$), XP_002383557 (nepB$_{A. flavus}$), XP_002375395 (nepC$_{A. flavus}$), XP_748279 (NLP$_{A. fumigatus}$), FVEG_04647 (NLP$_{F. verticillioides}$), AAY88967 (NLP$_{F. oxysporum}$), AAD53944 (NLP$_{P. aphanidermatum}$), AAM48171 (NLP$_{P. sojae}$), ABB43265 (NLP$_{B. elliptica}$), and EGY15829 (NLP$_{V. dahliae}$).

A

Predicted signal peptides

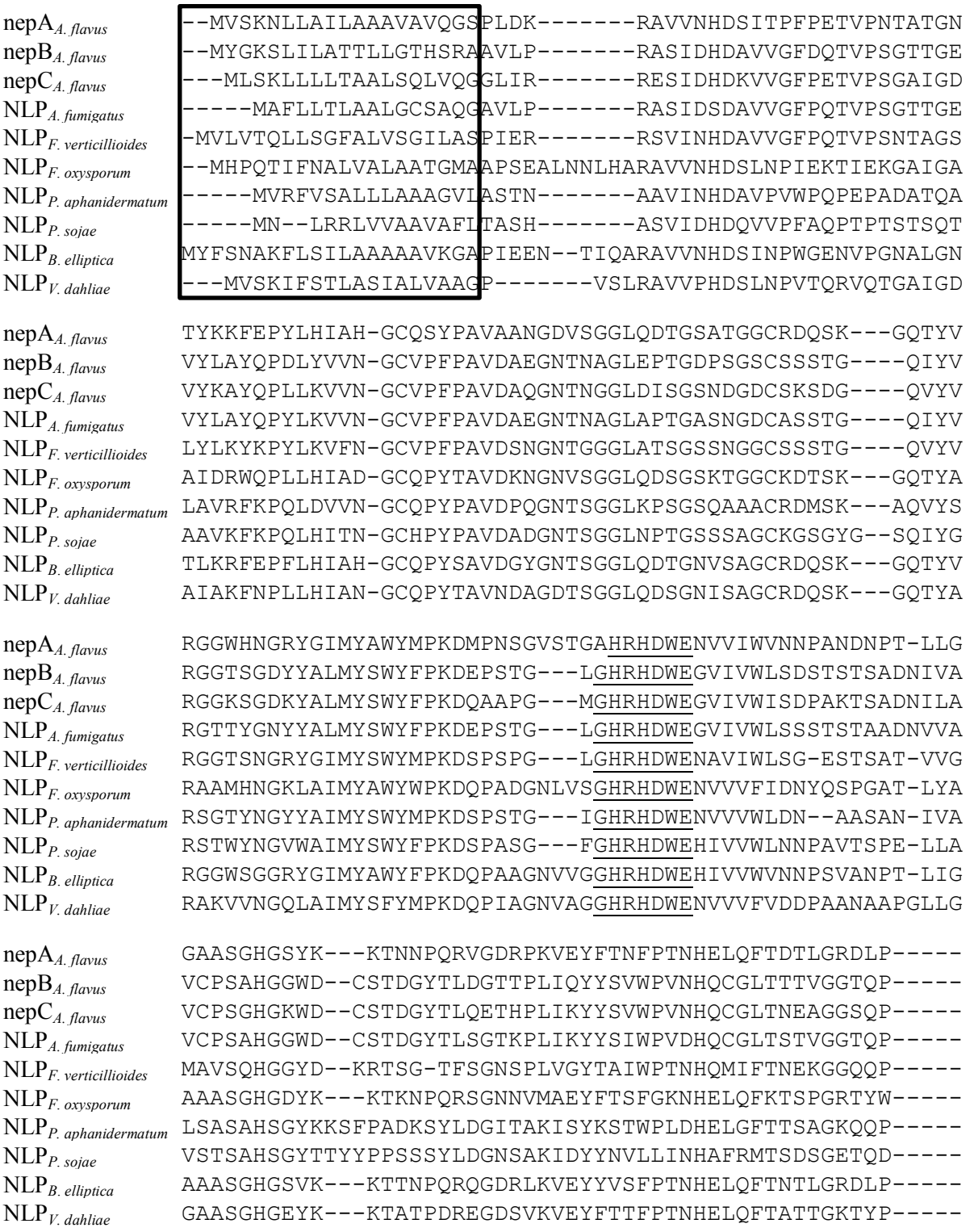

nepA *A. flavus*	------LIAWESLPEAARRGLES-------AEFGKATVPFKDSTFQGNLEKAAL-
nepB *A. flavus*	------LIAWESLPTAASTALED-------TDFGDANVPFKDANFSSNLEKATF-
nepC *A. flavus*	------LIAYESLPEPAKNALET-------VDFVKANVPFKEENWAENLGKATF-
NLP *A. fumigatus*	------LIAWESLPTVAQTALED-------TDFGDANVPFKNANFASNLAKATF-
NLP *F. verticillioides*	------LVAWESLTAAARTALTN-------TDFGSANVPFKDGSFESNLDKAAV-
NLP *F. oxysporum*	------IYDWAAMTPAAQKGLITGPSGDPNKPWGSANVPFIDANFGNNLNKAWS-
NLP *P. aphanidermatum*	------LIQWEQMTQAARDALES-------TDFGNANVPFK-SNFQDKLVKAFFQ
NLP *P. sojae*	------LIMWDQLTDAARTALEN-------TDFGDANVPFKDANFETKLANAWYK
NLP *B. elliptica*	------MVWYDFLPAVSKTALQN-------TSFGKANCPFNDHNFANNLAKAAI-
NLP *V. dahliae*	------ISDWDAMPQAARDALET-------TDFGSANVPFKDANFDSNLAKAAL-

B

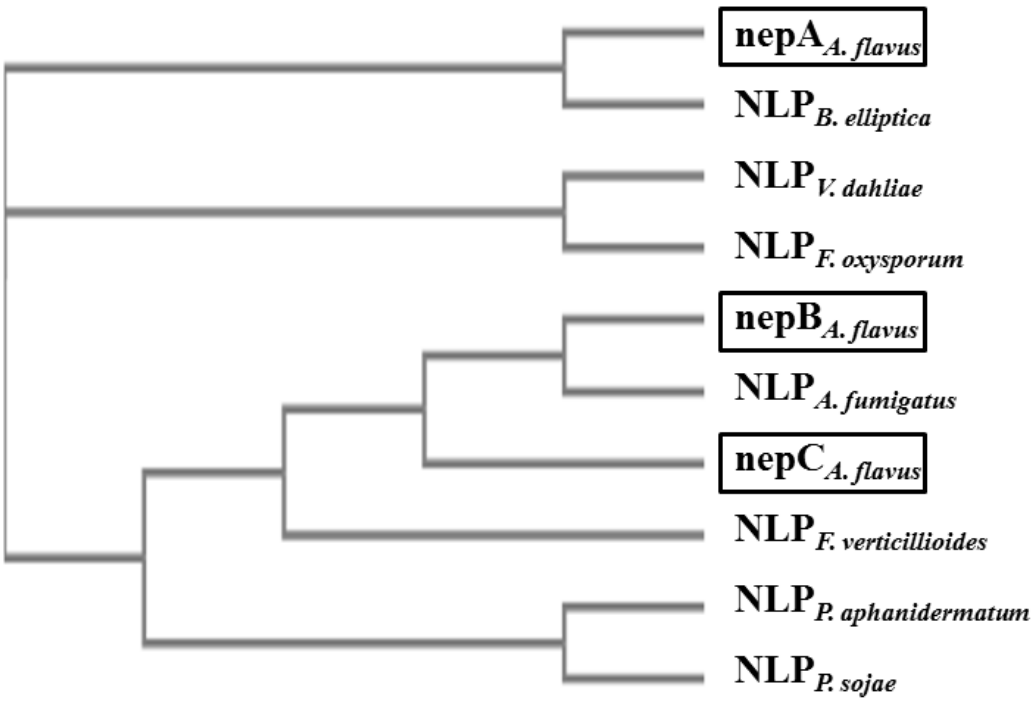

NepA is involved in virulence of _A. flavus_ on maize kernels

Our previous microarray studies showed that *nepA* was expressed 12.1 fold higher in living kernels compared with autoclaved kernels (Dolezal et al., 2013). In this study, we conducted RNA sequencing (RNA-seq) analysis to analyze the expression levels of these three *A. flavus NLPs*. We found that a large number of putative *A. flavus* secretory protein encoding genes were detected during early pathogenesis on maize kernels (Table S3). Of these putative *A. flavus* secretory protein encoding genes, the three *NLPs* were detectable at 24, 48 and 72 hpi (Fig. 2; Table S3). As expected, *nepA* was expressed at higher levels compared with both *nepB* and *nepC* at all three time points. But no transcripts of these three *A. flavus NLPs* was detected at 12 hpi (Fig. 2). RT-PCR analysis also revealed that *nepA* was expressed during colonization of maize kernels at 96 hpi (Fig. 3A), but was not expressed in PDB (Fig. 5A).

Targeted deletion and overexpression (OE) of *nepA* in *A. flavus* was pursued using the auxotrophic mutant *afc-1* strain. The Δ*nepA* strains were generated by replacing the *nepA* coding sequence with *pyrimidine-4* (*pyr-4*) through homologous recombination. The *nepA* OE strains were obtained by co-transforming *pyr4* and *nepA* gene driven by the *glyceraldehyde-3-phosphate dehydrogenase*, *Aspergillus nidulans* (*gpdA*) promoter into the auxotrophic mutant *afc-1* strain. Several independent Δ*nepA* and *nepA* OE strains were transformed again with the *A. flavus argD* gene to complement the arginine deficiency. We demonstrated that aflatoxins were produced by all fungal strains that we generated (data not shown).

Δ*nepA-1* and *nepA OE-3* strains were used for maize kernel assays. The maize kernel assay was performed in a four-year study from 2009 to 2012. The Δ*nepA-1* strain showed significantly compromised virulence on maize kernels. Kernels inoculated with the Δ*nepA-1* strain still developed ear rot symptoms, but had less colonization on the surface of the kernel compared with the ones that were inoculated with *nepA OE-3* or *3357* (Fig. 3B). Moreover, Δ*nepA-1* remained at the inoculation site in most kernels (Fig. 3E). In the aleurone near the inoculation site, a thin layer of Δ*nepA-1* mycelia accumulated between the pericarp and the intact aleurone cells (Fig. 3A). However, the *nepA OE-3* strain showed as much colonization as *3357*. Both *nepA OE-3* and *3357* were capable of colonizing all tissues of the kernel and forming a biofilm-like structure at the endosperm-scutellum interface [Fig. 3C(f and g)]. Most of the aleurone cells colonized by both *nepA OE-3* and *3357* were destroyed [Fig. 3C(b and c)]. A distinct feature of *nepA OE-3* was the formation of extensive hyphal tips in a few kernels [Fig. 3C(c)].

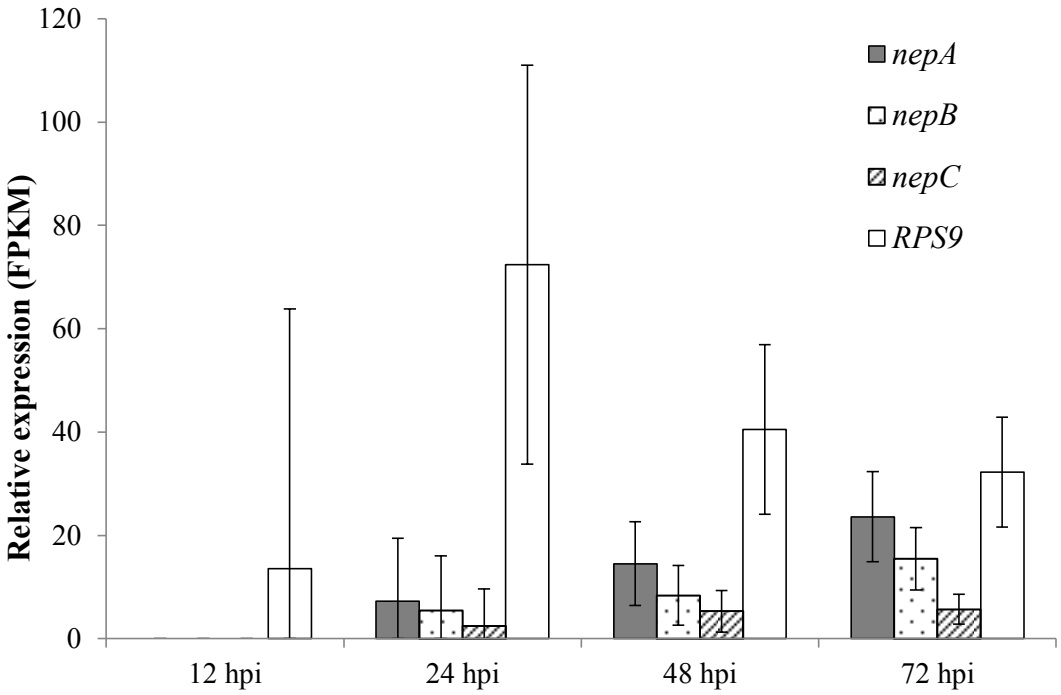

Figure 2. Expression analysis of *NLPs* during early infection by *A. flavus* on maize kernels. Kernels were wound-inoculated with wild-type *A. flavus* strain *3357*, and harvested at 12, 24, 48 and 72 hpi. After RNA isolation and cDNA library preparation, RNA-sequencing (RNA-seq) was performed using Illumina HiSeq. The relative expression levels of nepA, nepB and nepC were analyzed by comparing the fragments per kilobase of exon per million fragments mapped (FPKM). *RPS9*: *40S ribosomal protein S9*; hpi: hours post inoculation.

Figure 3. *NepA* is involved in virulence of *A. flavus* during colonization in maize kernels. A, RT-PCR analysis of *nepA* gene expression in the Δ*nepA*-1, *nepA* overexpression (OE)-3, and wild-type (WT) *3357* strains. *NepA* is not expressed in Δ*nepA*-1, but is strongly expressed in *nepA* OE-3 and expressed at a low level in *3357*. B, Δ*nepA*-1 shows reduced pathogenicity on the kernel compared with *nepA* OE-3 and *3357*. C, Light microscope images taken from sections stained with safranin and fast green: (a-d), The aleurone of Δ*nepA*-1(a), *nepA* OE-3 (b), *3357* (c) and mock (d) inoculated kernels. Δ*nepA*-1 growth was restricted between the pericarp and aleurone with very limited fungal growth. Both *nepA* OE-3 and *3357* extensively colonized and destroyed the aleurone. *NepA* OE-3 formed more straight hyphal tips in some kernels (c). (e), Δ*nepA*-1 was restricted at the inoculation site in most kernels. (f-h), The endosperm-scutellum interface of *nepA* OE-3 (f), *3357* (g) and mock (h) inoculated kernels. Both *nepA* OE-3 and *3357* colonized all kernel regions and formed a biofilm-like structure at the endosperm-scutellum interface. Mock inoculated kernels were used as controls. Kernels were harvested at 96 hours post inoculation. Arrows denote fungal colonization. *ZmCAT1*: *catalase 1*, *Zea mays*; *AfHis*: *histone*, *A. flavus*; *Af*: *A. flavus*; Al: aleurone; En: endosperm; Sc: scutellum. Scale bars: 5 mm in B; 50 μm in C (a, f-h); 30 μm in C (b-d); 200 μm in C(e).

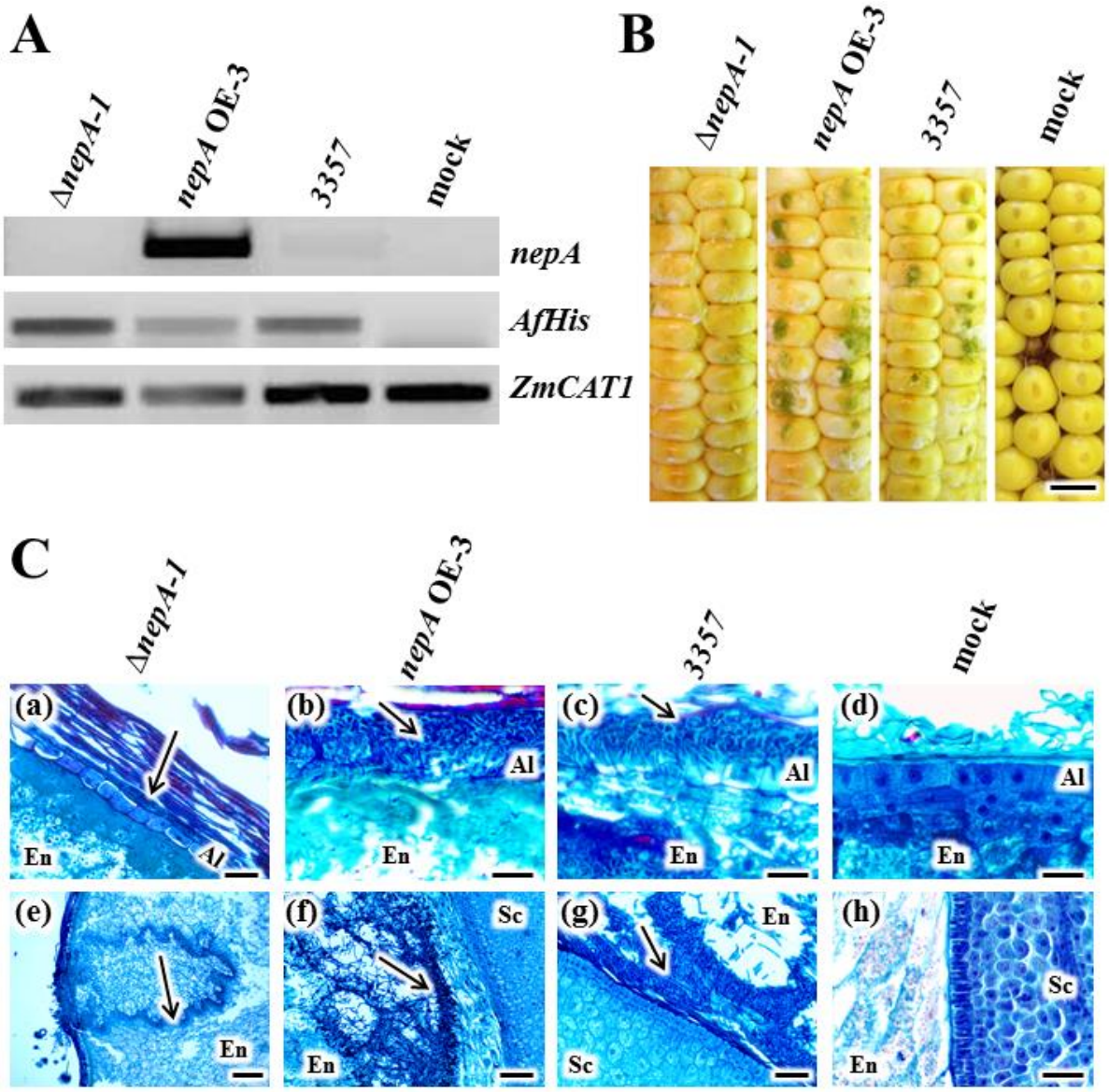
A
ΔnepA-1
nepA OE-3
3357
mock
nepA
AfHis
ZmCAT1
B
ΔnepA-1
nepA OE-3
3357
mock
C
ΔnepA-1
nepA OE-3
3357
mock
(a)
(b)
(c)
(d)
(e)
(f)
(g)
(h)
En
Al
Sc

NepA affects vegetative growth and conidiation of *A. flavus* on PDA

We analyzed radial growth and conidiation of three Δ*nepA* strains (Δ*nepA*-1, Δ*nepA*-2 and Δ*nepA*-3), three *nepA* OE strains (*nepA* OE-1, *nepA* OE-2 and *nepA* OE-3), and two control strains (*afc-1*$^{++}$ and *3357*). We found that radial growth and conidiation of all the Δ*nepA* and *nepA* OE strains were similar to those of the control strains on corn extract medium (CEM) and on minimal medium (MLS) plates. However, when grown on PDA plates, all three tested Δ*nepA* strains showed significantly reduced growth rates and produced less conidia than the *nepA* OE strains and the control strains (Table 1). Our previous studies also indicated that the Δ*nepA* strains were impaired in growth in PDB compared to WT and the *nepA* OE strains (Dolezal, 2010). Nevertheless, the morphology of both the Δ*nepA* and *nepA* OE strains is similar to that of the control strains (Fig. 4). Collectively, these data suggest that deletion of *nepA* affects fungal vegetative growth and asexual reproduction when grown on potato dextrose-based media. But overexpression of *nepA* has no effect on vegetative growth and asexual reproduction when grown on PDA, CEM or MLS.

Table 3. Growth and conidiation of *A. flavus* strains on PDA. Mean estimated growth rates (μ_{max}), time to visible growth (λ), and number of spores produced per 22.5 mm^2 after 7 days of incubation were shown. In each column, different letters next to the means show significant ($p<0.05$) according to Tukey HSD test. Three *A. flavus* Δ*nepA* strains, Δ*nepA*-1, Δ*nepA*-2 and Δ*nepA*-3, three *nepA* OE strains, *nepA* OE-1, *nepA* OE-2 and *nepA* OE-3, and two control strains, *3357* and *afc-1*$^{++}$, were used.

A. flavus	μ_{max} (mm/day) ± SD	λ (day) ± SD	No. of spores per ml ± SD
Δ*nepA-3*	11.9 ± 0.57^{a}	3 ± 0^{a}	(5.2e+06) ±(7.3e+05)^{a}
Δ*nepA-2*	12 ± 0.47^{ab}	3 ± 0^{a}	(5.2e+06) ± (7.3e+05)^{a}
Δ*nepA-1*	12 ± 0.71^{ab}	3 ± 0^{a}	(2.6e+06) ± (1.1e+05)^{a}
afc-1^{++}	13 ± 1.66^{b}	2 ± 0^{b}	(2.6e+07) ± (7.1e+06)^{e}
nepA OE-1	14.2 ± 1.1^{c}	2 ± 0^{b}	(1.2e+07) ± (2.5e+06)^{bc}
nepA OE-3	14.5 ± -.85^{c}	2 ± 0^{b}	(1.2e+07) ± (1.7e+06)^{cd}
3357	15.6 ± 0.84^{d}	2 ± 0^{b}	(1.6e+07) ± (3.6e+06)^{d}
nepA OE-2	17.3 ± 0.67^{e}	2 ± 0^{b}	(1.4e+07) ± (3.8e+06)^{cd}

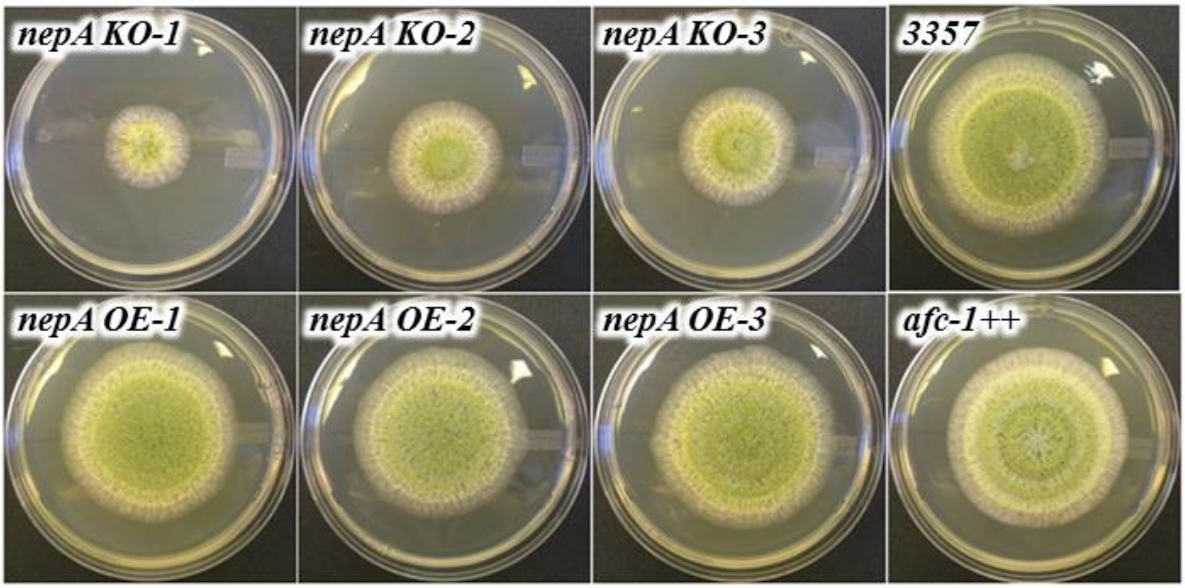

Figure 4. Radial growth and colony morphology of *A. flavus* strains on PDA. Pictures were taken 6 days after incubation at 28^{o}C. The 100 mm × 15 mm (diameter × height) plates were used. Three *A. flavus* Δ*nepA* strains, Δ*nepA*-1, Δ*nepA*-2 and Δ*nepA*-3, three *nepA* OE strains, *nepA* OE-1, *nepA* OE-2 and *nepA* OE-3, and two control strains, *3357* and *afc-1*$^{++}$, were used.

NepA overexpression mutant induces necrosis on tobacco leaves

It has been shown that NLPs from *P. sojae* and *V. dahliae* trigger necrosis after infiltration into leaves of dicotyledonous plants (Dong et al., 2012; Santhanam et al., 2013; Zhou et al., 2012). To test the necrosis-inducing activity of nepA, PDB cultures of three Δ*nepA* strains (Δ*nepA*-1, Δ*nepA*-2 and Δ*nepA*-3), three *nepA* OE strains (*nepA* OE-1, *nepA* OE-2 and *nepA* OE-3), and two control strains (*afc-1*$^{++}$ and *3357*) were infiltrated into the same tobacco leaf. Leaf tissue started to collapse at 16 hours post infiltration of all the *nepA* OE strains (data not shown). In contrast, no obvious tissue necrosis was observed upon infiltration of any of the Δ*nepA* strains or any of the control strains. Figure 5A shows the expression levels of *nepA* in the *A. flavus* strains grown in PDB that have been used for infiltration. Figure 5B shows necrosis induced by *nepA* OE-3, but not other strains. To investigate whether nepA is able to induce necrosis in other plant species, we infiltrated the Δ*nepA*, *nepA* OE, and control strains into leaves of *A. thaliana* and maize seedling. But no necrosis was observed in either *A. thaliana* or maize leaves (data not shown).

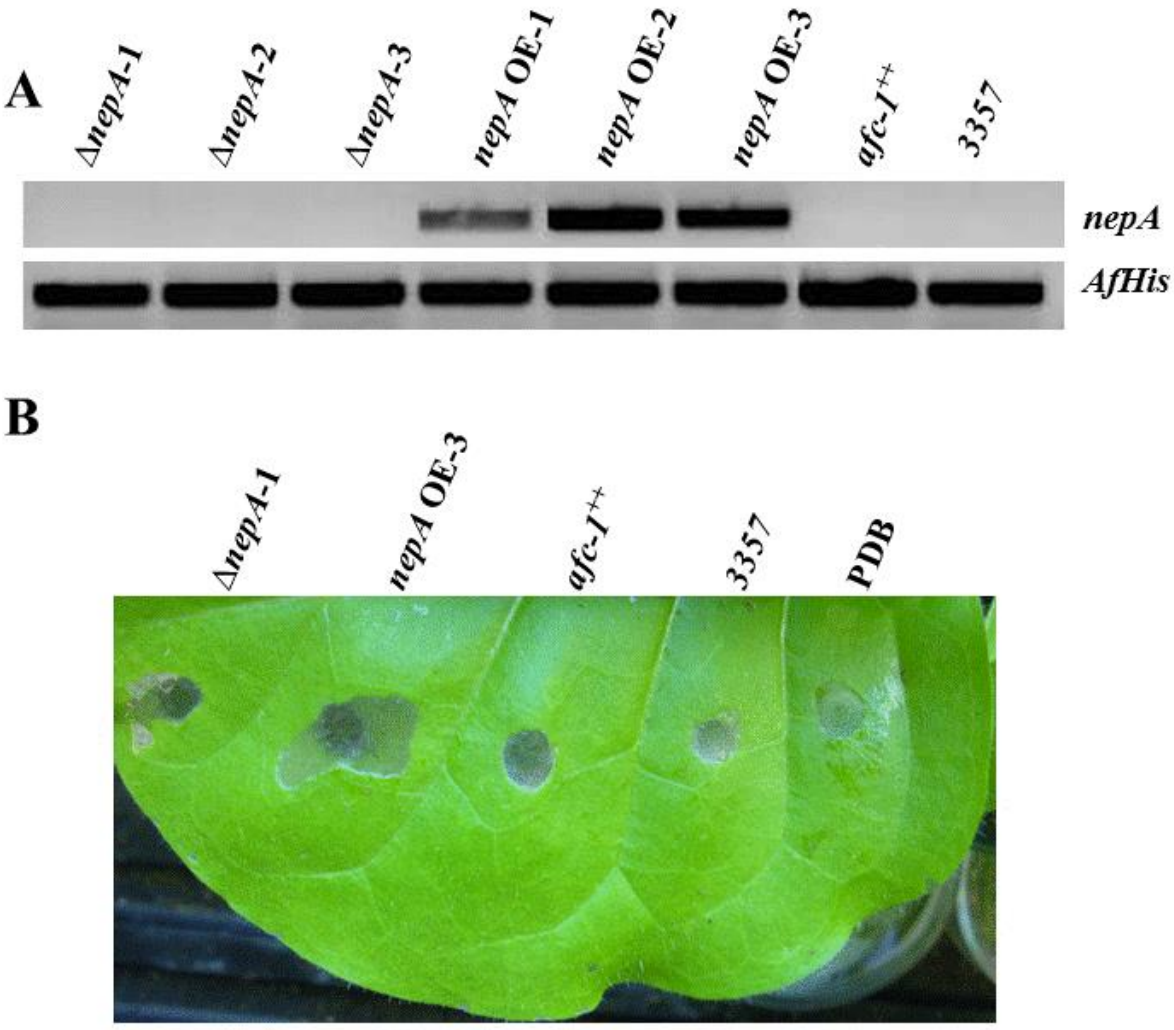

Figure 5. The necrosis-inducing activity of *A. flavus* nepA on tobacco leaves. A, RT-PCR analysis of *nepA* gene expression in the Δ*nepA* (Δ*nepA*-1, Δ*nepA*-2 and Δ*nepA*-3), *nepA* overexpression (OE) (*nepA* OE-1, *nepA* OE-2 and *nepA* OE-3), and control strains (*afc-1*$^{++}$ and *3357*) grown on PDB medium. *NepA* is not expressed in either the Δ*nepA* or the control strains, but is strongly expressed in *nep*A OE strains. B, *NepA* OE-3 induced necrosis near the injection site at 24 h after infiltration. Necrosis was not observed in areas infiltrated with either the Δ*nepA*-1 or control strains. *AfHis*: *histone*, *A. flavus*.

DISCUSSION

The NLPs are non-specific toxins capable of inducing host tissue necrosis and defense responses. Distinct features of NLP members, including signal peptides, conserved cysteine residues, and heptapeptide motifs, were found in the predicted amino acid sequences of three *A. flavus* NLPs (Fig. 1A). These conserved characteristics of NLPs appear to be important in formation of the three dimensional structures of these NLP proteins. Previous studies indicated that a NLP from *P. aphanidermatum* has structural homology to actinoporins which are toxins produced by sea anemones (Ottmann et al., 2009). Both NLPs and actinoporins are small polypeptides with a central β-sandwich architecture surrounded by helices, and signal peptides that target cellular surfaces (Birck et al., 2004; Ottmann et al., 2009). It appears that these NLP specific structures are important in forming transmembrane pores and causing a higher rate of metabolic leakage of plant cells (Qutob et al., 2006).

Several reports suggest that NLPs are associated with pathogenicity and host defense response only on dicotyledonous plants (Bailey, 1995; Schouten et al., 2008). In this study, we demonstrated that the three *NLPs* from *A. flavus* were expressed during pathogenesis on maize kernels. One of these *A. flavus NLPs*, *nepA*, was selected for further study because it was more highly expressed on living kernels than autoclaved kernels. We provide evidence showing that *nepA* is involved in virulence of *A. flavus* on maize kernels. The *A. flavus nepA* deletion mutant can still colonize at the inoculation site of the kernel, which could be attributed to the complementary roles of other effectors such as nepB and nepC. In our kernel assay, Δ*nepA* was localized at the inoculation site of kernels collected in the first three years.

However, colonization in the endosperm and germ was observed in two kernels collected in the fourth year. This difference could be potentially due to natural infection, cross contamination, or changes of the environmental conditions. The other possibility is that the *nepA* gene was reintroduced to Δ*nepA*-1 through vertical gene transfer or dynamic changes of the multinucleated fungal cells when growing in culture or on plants.

Our expression analysis indicated that *nepA* was not expressed when *A. flavus* was grown in PDB, but was expressed during early stages of infection in maize kernels. A NLP from the wheat leaf pathogen *Mycosphaerella graminicola* also was only expressed in plant tissue (Motteram et al., 2009). These findings are consistent with the hypothesis that NLPs are important in pathogenicity but are not essential for fungal growth. However, we did find that growth and reproduction of the Δ*nepA* mutants were reduced when grown on potato dextrose-based media (a medium commonly used to culture this fungus), but not when grown on corn extract medium (CEM) or minimal medium (MLS). These findings lead to the question of how nepA affects growth and conidiation of *A. flavus* under certain conditions, and how *A. flavus* balances pathogenicity and nutrient usage under pathogenic conditions. These data support the idea that reduced pathogenicity of the Δ*nepA* strain on maize kernels is not due to decreased growth rate.

In the large majority of our observations, overexpression of *nepA* resulted in increased colonization by *A. flavus* near the aleurone layer of the kernel. Similar to the WT, the *nepA* OE mutant was able to form a biofilm-like structure around the scutellum. However, the distinction between the overexpression mutant and wild type NRRL *3357* was

not clear in all sections from all kernels. We know that colonization patterns of *A. flavus* within the kernel can vary. This could be due to the location of the section in relation to the infection site, position of the kernel on the ear, or other environmental conditions. Observations of infected germ tissue after tetrazolium chloride staining showed that cell death is associated with infection by *A. flavus*, but it is unclear if NepA was involved in this necrosis. Further functional analysis of these *A. flavus* NLPs will be helpful in addressing these questions.

LITERATURE CITED

Bae, H., Kim, M. S., Sicher, R. C., Bae, H. J., and Bailey, B. A. 2006. Necrosis- and Ethylene-Inducing Peptide from *Fusarium oxysporum* Induces a Complex Cascade of Transcripts Associated with Signal Transduction and Cell Death in Arabidopsis. Plant Physiology 141: 1056-1067.

Bailey, B. A. 1995. Purification of a Protein from Culture Filtrates of *Fusarium oxysporum* that Induces Ethylene and Necrosis in Leaves of *Erythroxylum coca*. Phytopathology 85: 1250-1255.

Bailey, B. A., Apel-Birkhold, P. C., and Luster, D. G. 2002. Expression of NEP1 by *Fusarium oxysporum* f. sp. *erythroxyli* After Gene Replacement and Overexpression Using Polyethylene Glycol-Mediated Transformation. Phytopathology 92: 833-841.

Bailey, B. A., Bae, H., Strem, M. D., Antunez de Mayolo, G., Guiltinan, M. J., Verica, J. A., Maximova, S. N., and Bowers, J. H. 2005. Developmental expression of stress response genes in *Theobroma cacao* leaves and their response to Nep1 treatment and a compatible infection by *Phytophthora megakarya*. Plant Physiology and Biochemistry 43: 611-622.

Birck, C., Damian, L., Marty-Detraves, C., Lougarre, A., Schulze-Briese, C., Koehl, P., Fournier, D., Paquereau, L., and Samama, J. P. 2004. A New Lectin Family with Structure Similarity to Actinoporins Revealed by the Crystal Structure of *Xerocomus chrysenteron* Lectin XCL. Journal of Molecular Biology 344: 1409-1420.

Cabral, A., Oome, S., Sander, N., Kufner, I., Nurnberger, T., and Van den Ackerveken, G. 2012. Nontoxic Nep1-Like Proteins of the Downy Mildew Pathogen Hyaloperonospora arabidopsidis: Repression of Necrosis-Inducing Activity by a Surface-Exposed Region. Molecular Plant-Microbe Interactions 25: 697-708.

Cechin, A., Sinigaglia, M., Lemke, N., Echeverrigaray, S., Cabrera, O., Pereira, G., and Mombach, J. 2008a. Cupin: A candidate molecular structure for the Nep1-like protein family. BMC Plant Biology 8: 50.

Cechin, A. L., Sinigaglia, M., Mombach, J. C., Echeverrigaray, S., Lemke, N., Cabrera, O. G., Pereira, G. A., and Javier Medrano, F. 2008b. Can Nep1-like proteins form oligomers? Plant Signaling & Behavior 3: 906-907.

Choi, J., Park, J., Kim, D., Jung, K., Kang, S., and Lee, Y. H. 2010. Fungal secretome database: integrated platform for annotation of fungal secretomes. BMC Genomics 11: 105.

Cuesta Arenas, Y., Kalkman, E., Schouten, A., Dieho, M., Vredenbregt, P., Uwumukiza, B., Miriam Osés Ruiz, M., and van Kan, J. A. 2010. Functional analysis and mode of action of phytotoxic Nep1-like proteins of Botrytis cinerea. Physiological and Molecular Plant Pathology 74: 376-386.

Dallal Bashi, Z., Hegedus, D. D., Buchwaldt, L., Rimmer, S. R., and Borhan, M. H. 2010. Expression and regulation of *Sclerotinia sclerotiorum* necrosis and ethylene-inducing peptides (NEPs). Molecular Plant Pathology 11: 43-53.

Dolezal, A. L. 2010. Interactions Between *Aspergillus flavus* and the Developing Maize Kernel. Doctoral dissertation Retrieved from ProQuest Dissertations and Theses: OCLC Number: 704568905.

Dolezal, A. L., Obrian, G. R., Nielsen, D. M., Woloshuk, C. P., Boston, R. S., and Payne, G. A. 2013. Localization, morphology and transcriptional profile of *Aspergillus flavus* during seed colonization. Molecular Plant Pathology 14: 898-909.

Dong, S., Kong, G., Qutob, D., Yu, X., Tang, J., Kang, J., Dai, T., Wang, H., Gijzen, M., and Wang, Y. 2012. The NLP toxin family in Phytophthora sojae includes rapidly evolving groups that lack necrosis-inducing activity. Molecular Plant-Microbe Interactions 25: 896-909.

Emanuelsson, O., Brunak, S., von Heijne, G., and Nielsen, H. 2007. Locating proteins in the cell using TargetP, SignalP and related tools. Nature Protocols 2: 953-971.

Fellbrich, G., Romanski, A., Varet, A., Blume, B., Brunner, F., Engelhardt, S., Felix, G., Kemmerling, B., Krzymowska, M., and Nurnberger, T. 2002. NPP1, a *Phytophthora*-associated trigger of plant defense in parsley and *Arabidopsis*. The Plant Journal 32: 375-390.

Garcia, O., Macedo, J. A. N., Tibúrcio, R., Zaparoli, G., Rincones, J., Bittencourt, L. M. C., Ceita, G. O., Micheli, F., Gesteira, A., Mariano, A. C., Schiavinato, M. A., Medrano, F. J., Meinhardt, L. W., Pereira, G. A. G., and Cascardo, J. C. M. 2007. Characterization of necrosis and ethylene-inducing proteins (NEP) in the basidiomycete *Moniliophthora perniciosa*, the causal agent of witches' broom in *Theobroma cacao*. Mycological Research 111: 443-455.

Gijzen, M., and Nürnberger, T. 2006. Nep1-like proteins from plant pathogens: Recruitment and diversification of the NPP1 domain across taxa. Phytochemistry 67: 1800-1807.

Jennings, J. C., Apel-Birkhold, P. C., Bailey, B. A., and Anderson, J. D. 2000. Induction of Ethylene Biosynthesis and Necrosis in Weed Leaves by a *Fusarium oxysporum* Protein. Weed Science 48: 7-14.

Jones, J. D. G., and Dangl, J. L. 2006. The plant immune system. Nature 444: 323-329.

Kanneganti, T. D., Huitema, E., Cakir, C., and Kamoun, S. 2006. Synergistic Interactions of the Plant Cell Death Pathways Induced by *Phytophthora infestans* Nep1-Like Protein PiNPP1.1 and INF1 Elicitin. Molecular Plant-Microbe Interactions 19: 854-863.

Keates, S. E., Kostman, T. A., Anderson, J. D., and Bailey, B. A. 2003. Altered Gene Expression in Three Plant Species in Response to Treatment with Nep1, a Fungal Protein That Causes Necrosis. Plant Physiology 132: 1610-1622.

Küfner, I., Ottmann, C., Oecking, C., and Nürnberger, T. 2009. Cytolytic toxins as triggers of plant immune response. Plant Signaling & Behavior 4: 977-979.

Larkin, M. A., Blackshields, G., Brown, N. P., Chenna, R., McGettigan, P. A., McWilliam, H., Valentin, F., Wallace, I. M., Wilm, A., Lopez, R., Thompson, J. D., Gibson, T. J., and Higgins, D. G. 2007. Clustal W and Clustal X version 2.0. Bioinformatics 23: 2947-2948.

Lee, S. J., and Rose, J. K. 2010. Mediation of the transition from biotrophy to necrotrophy in hemibiotrophic plant pathogens by secreted effector proteins. Plant Signaling & Behavior 5: 769-772.

Livingston, D. P., Tuong, T. D., Haigler, C. H., Avci, U., Tallury, S. P. 2009. Rapid Microwave Processing of Winter Cereals for Histology Allows Identification of Separate Zones of Freezing Injury in the Crown. Crop Science 49: 1837-1842.

Livingston, D. P., Henson, C. A., Tuong, T. D., Wise, M. L., Tallury, S. P., and Duke, S. H. 2013. Histological Analysis and 3D Reconstruction of Winter Cereal Crowns Recovering from Freezing: A Unique Response in Oat (*Avena sativa* L.). PLoS One 8: e53468.

Luberacki, B., Weyand, M., Seitz, U., Koch, W., Oecking, C., and Ottmann, C. 2008. Purification, crystallization and preliminary X-ray diffraction analysis of an

oomycete-derived Nep1-like protein. Acta crystallographica. Section F, Structural biology and crystallization communications 64: 1178-1180.

Ma, L. J., van der Does, H. C., Borkovich, K. A., Coleman, J. J., Daboussi, M. J., Di Pietro, A., Dufresne, M., Freitag, M., Grabherr, M., Henrissat, B., Houterman, P. M., Kang, S., Shim, W. B., Woloshuk, C., Xie, X., Xu, J. R., Antoniw, J., Baker, S. E., Bluhm, B. H., Breakspear, A., Brown, D. W., Butchko, R. A., Chapman, S., Coulson, R., Coutinho, P. M., Danchin, E. G., Diener, A., Gale, L. R., Gardiner, D. M., Goff, S., Hammond-Kosack, K. E., Hilburn, K., Hua-Van, A., Jonkers, W., Kazan, K., Kodira, C. D., Koehrsen, M., Kumar, L., Lee, Y. H., Li, L., Manners, J. M., Miranda-Saavedra, D., Mukherjee, M., Park, G., Park, J., Park, S. Y., Proctor, R. H., Regev, A., Ruiz-Roldan, M. C., Sain, D., Sakthikumar, S., Sykes, S., Schwartz, D. C., Turgeon, B. G., Wapinski, I., Yoder, O., Young, S., Zeng, Q., Zhou, S., Galagan, J., Cuomo, C. A., Kistler, H. C., and Rep, M. 2010. Comparative genomics reveals mobile pathogenicity chromosomes in Fusarium. Nature 464: 367-373.

Matasci, N., and McKay, S. 2013. Phylogenetic Analysis with the iPlant Discovery Environment. Page Unit6 in: Current Protocols in Bioinformatics, John Wiley & Sons, Inc.

Mattinen, L., Tshuikina, M., Mäe, A., and Pirhonen, M. 2004. Identification and Characterization of Nip, Necrosis-Inducing Virulence Protein of *Erwinia carotovora* subsp. *carotovora*. Molecular Plant-Microbe Interactions 17: 1366-1375.

Meir, S., Amsellem, Z., Al-Ahmad, H., Safran, E., and Gressel, J. 2009. Transforming a NEP1 toxin gene into two Fusarium spp. to enhance mycoherbicide activity on Orobanche--failure and success. Pest Management Science 65: 588-595.

Mellon, J., Cotty, P. J., and Dowd, M. 2007. *Aspergillus flavus* hydrolases: Their roles in pathogenesis and substrate utilization. Applied Microbiology and Biotechnology 77: 497-504.

Mengiste, T. 2012. Plant Immunity to Necrotrophs. Annual Review of Phytopathology 50: 267-294.

Motteram, J., Kufner, I., Deller, S., Brunner, F., Hammond-Kosack, K. E., Nurnberger, T., and Rudd, J. J. 2009. Molecular characterization and functional analysis of MgNLP, the sole NPP1 domain-containing protein, from the fungal wheat leaf pathogen *Mycosphaerella graminicola*. Molecular Plant-Microbe Interactions 22: 790-799.

Newbury, S. F., Glazebrook, J. A., and Radford, A. 1986. Sequence analysis of the pyr-4 (orotidine 5'-P decarboxylase) gene of *Neurospora crassa*. Gene 43: 51-58.

Nierman, W. C., Pain, A., Anderson, M. J., Wortman, J. R., Kim, H. S., Arroyo, J., Berriman, M., Abe, K., Archer, D. B., Bermejo, C., Bennett, J., Bowyer, P., Chen, D., Collins, M., Coulsen, R., Davies, R., Dyer, P. S., Farman, M., Fedorova, N., Fedorova, N., Feldblyum, T. V., Fischer, R., Fosker, N., Fraser, A., Garcia, J. L., Garcia, M. J., Goble, A., Goldman, G. H., Gomi, K., Griffith-Jones, S., Gwilliam, R., Haas, B., Haas, H., Harris, D., Horiuchi, H., Huang, J., Humphray, S., Jimenez, J., Keller, N., Khouri, H., Kitamoto, K., Kobayashi, T., Konzack, S., Kulkarni, R., Kumagai, T., Lafon, A., Latge, J. P., Li, W., Lord, A., Lu, C., Majoros, W. H., May, G. S., Miller, B. L., Mohamoud, Y., Molina, M., Monod, M., Mouyna, I., Mulligan, S., Murphy, L., O'Neil, S., Paulsen, I., Penalva, M. A., Pertea, M., Price, C., Pritchard, B. L., Quail, M. A., Rabbinowitsch, E., Rawlins, N., Rajandream, M. A., Reichard, U., Renauld, H., Robson, G. D., Rodriguez de Cordoba, S., Rodriguez-Pena, J. M., Ronning, C. M., Rutter, S., Salzberg, S. L., Sanchez, M., Sanchez-Ferrero, J. C., Saunders, D., Seeger, K., Squares, R., Squares, S., Takeuchi, M., Tekaia, F., Turner, G., Vazquez de Aldana, C. R., Weidman, J., White, O., Woodward, J., Yu, J. H., Fraser, C., Galagan, J. E., Asai, K., Machida, M., Hall, N., Barrell, B., and Denning, D. W. 2005. Genomic sequence of the pathogenic and allergenic filamentous fungus *Aspergillus fumigatus*. Nature 438: 1151-1156.

Ottmann, C., Luberacki, B., Kufner, I., Koch, W., Brunner, F., Weyand, M., Mattinen, L., Pirhonen, M., Anderluh, G., Seitz, H. U., Nurnberger, T., and Oecking, C. 2009. A common toxin fold mediates microbial attack and plant defense. Proceedings of the National Academy of Sciences of the United States of America 106: 10359-10364.

Payne, G. A., and Brown, M. P. 1998. Genetics and physiology of aflatoxin biosynthesis. Annual Review of Phytopathology 36: 329-362.

Payne, G. A., Nierman, W. C., Wortman, J. R., Pritchard, B. L., Brown, D., Dean, R. A., Bhatnagar, D., Cleveland, T. E., Machida, M., and Yu, J. 2006. Whole genome comparison of *Aspergillus flavus* and *A. oryzae*. Medical Mycology 44: 9-11.

Pemberton, C. L., and Salmond, G. P. 2004. The Nep1-like proteins-a growing family of microbial elicitors of plant necrosis. Molecular Plant Pathology 5: 353-359.

Pemberton, C. L., Whitehead, N. A., Sebaihia, M., Bell, K. S., Hyman, L. J., Harris, S. J., Matlin, A. J., Robson, N. D., Birch, P. R. J., Carr, J. P., Toth, I. K., and Salmond, G.

P. C. 2005. Novel Quorum-Sensing-Controlled Genes in *Erwinia carotovora* subsp. *carotovora*: Identification of a Fungal Elicitor Homologue in a Soft-Rotting Bacterium. Molecular Plant-Microbe Interactions 18: 343-353.

Qutob, D., Kamoun, S., and Gijzen, M. 2002. Expression of a *Phytophthora sojae* necrosis-inducing protein occurs during transition from biotrophy to necrotrophy. The Plant Journal 32: 361-373.

Qutob, D., Kemmerling, B., Brunner, F., Kufner, I., Engelhardt, S., Gust, A. A., Luberacki, B., Seitz, H. U., Stahl, D., Rauhut, T., Glawischnig, E., Schween, G., Lacombe, B., Watanabe, N., Lam, E., Schlichting, R., Scheel, D., Nau, K., Dodt, G., Hubert, D., Gijzen, M., and Nurnberger, T. 2006. Phytotoxicity and Innate Immune Responses Induced by Nep1-Like Proteins. Plant Cell 18: 3721-3744.

Redkar, R. J., Herzog, R. W., and Singh, N. K. 1998. Transcriptional Activation of the *Aspergillus nidulans* gpdA Promoter by Osmotic Signals. Applied and Environmental Microbiology 64: 2229-2231.

Reese, B. N., Payne, G. A., Nielsen, D. M., and Woloshuk, C. P. 2011. Gene expression profile and response to maize kernels by *Aspergillus flavus*. Phytopathology 101: 797-804.

Santhanam, P., van Esse, H. P., Albert, I., Faino, L., Nürnberger, T., and Thomma, B. P. 2013. Evidence for Functional Diversification Within a Fungal NEP1-Like Protein Family. Molecular Plant-Microbe Interactions 26: 278-286.

Schouten, A., van Baarlen, P., and van Kan, J. A. 2008. Phytotoxic Nep1-like proteins from the necrotrophic fungus *Botrytis cinerea* associate with membranes and the nucleus of plant cells. New Phytologist 177: 493-505.

Shieh, M. T., Brown, R. L., Whitehead, M. P., Cary, J. W., Cotty, P. J., Cleveland, T. E., and Dean, R. A. 1997. Molecular genetic evidence for the involvement of a specific polygalacturonase, P2c, in the invasion and spread of *Aspergillus flavus* in cotton bolls. Applied and Environmental Microbiology 63: 3548-3552.

St Leger, R. J., Screen, S. E., and Shams-Pirzadeh, B. 2000. Lack of host specialization in *Aspergillus flavus*. Applied and Environmental Microbiology 66: 320-324.

Staats, M., V. A. N. Baarlen, P., Schouten, A., and V. A. N. Kan, J. A. 2007. Functional analysis of NLP genes from *Botrytis elliptica*. Molecular Plant Pathology 8: 209-214.

Trapnell, C., Roberts, A., Goff, L., Pertea, G., Kim, D., Kelley, D. R., Pimentel, H., Salzberg, S. L., Rinn, J. L., and Pachter, L. 2012. Differential gene and transcript expression analysis of RNA-seq experiments with TopHat and Cufflinks. Nature Protocols 7: 562-578.

Veit, S., Wörle, J. M., Nürnberger, T., Koch, W., and Seitz, H. U. 2001. A novel protein elicitor (PaNie) from *Pythium aphanidermatum* induces multiple defense responses in carrot, Arabidopsis, and tobacco. Plant Physiology 127: 832-841.

Wang, J. Y., Cai, Y., Gou, J. Y., Mao, Y. B., Xu, Y. H., Jiang, W. H., and Chen, X. Y. 2004. VdNEP, an Elicitor from *Verticillium dahliae*, Induces Cotton Plant Wilting. Applied and Environmental Microbiology 70: 4989-4995.

Woloshuk, C. P., Seip, E. R., Payne, G. A., and Adkins, C. R. 1989. Genetic transformation system for the aflatoxin-producing fungus *Aspergillus flavus*. Applied and Environmental Microbiology 55: 86-90.

Zaparoli, G., Barsottini, M. R., de Oliveira, J. F., Dyszy, F., Teixeira, P. J., Barau, J. G., Garcia, O., Costa-Filho, A. J., Ambrosio, A. L., Pereira, G. A., and Dias, S. M. 2011. The crystal structure of necrosis- and ethylene-inducing protein 2 from the causal agent of cacao's Witches' Broom disease reveals key elements for its activity. Biochemistry 50: 9901-9910.

Zhang, H., Li, D., Wang, M., Liu, J., Teng, W., Cheng, B., Huang, Q., Wang, M., Song, W., Dong, S., Zheng, X., and Zhang, Z. 2012. The *Nicotiana benthamiana* Mitogen-Activated Protein Kinase Cascade and WRKY Transcription Factor Participate in Nep1Mo-Triggered Plant Responses. Molecular Plant-Microbe Interactions 25: 1639-1653.

Zhou, B. J., Jia, P. S., Gao, F., and Guo, H. S. 2012. Molecular characterization and functional analysis of a necrosis- and ethylene-inducing protein encoding gene family from *Verticillium dahliae*. Molecular Plant-Microbe Interactions 25: 964-975.

Supplemental Material from Chapter Two

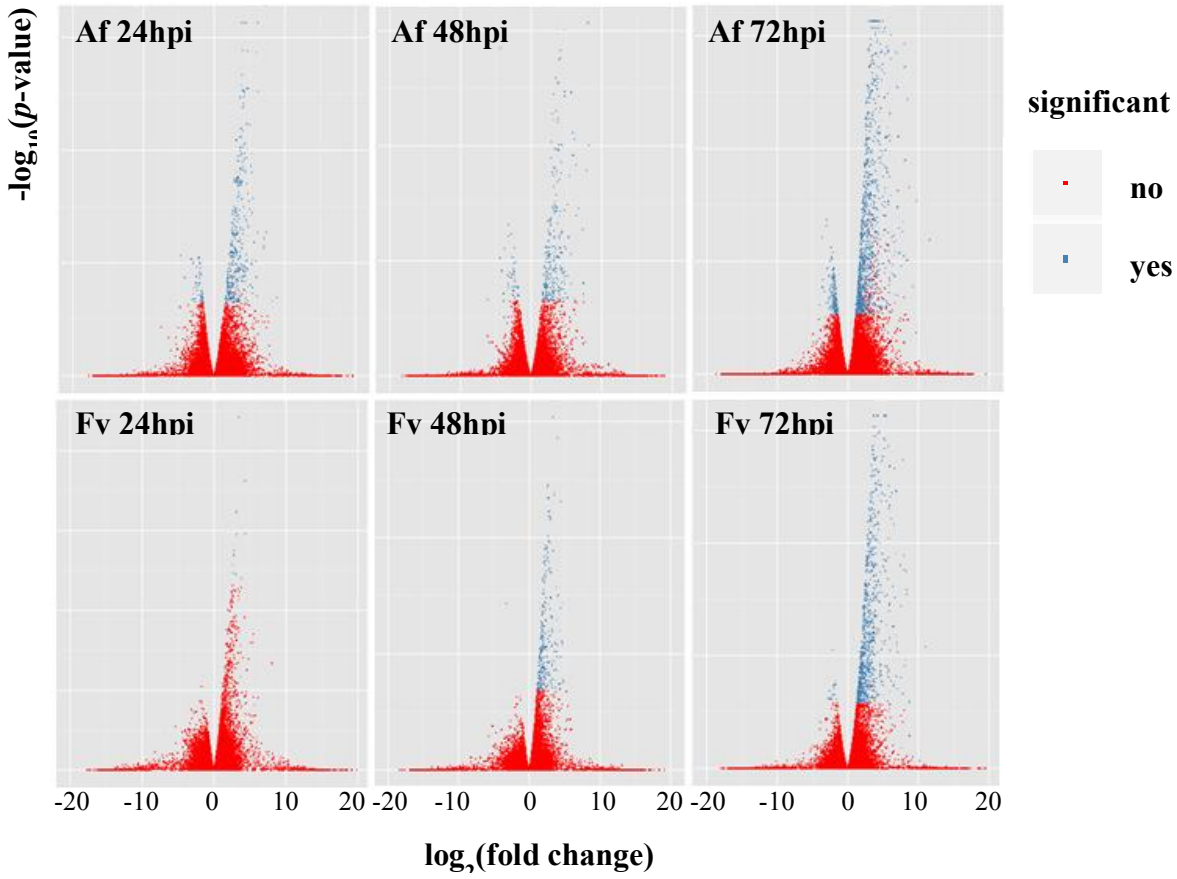

Figure S1. CummeRbund volcano plots revealing gene expression changes in maize kernels during *A. flavus* and *F. verticillioides* infection. Note that large fold changes in expression are not always significantly different, because the number of reads for those genes may be fewer due to low expression levels. Af: *A. flavus* inoculated kernels; Fv: *F. verticillioides* inoculated kernels; hpi: hours post inoculation.

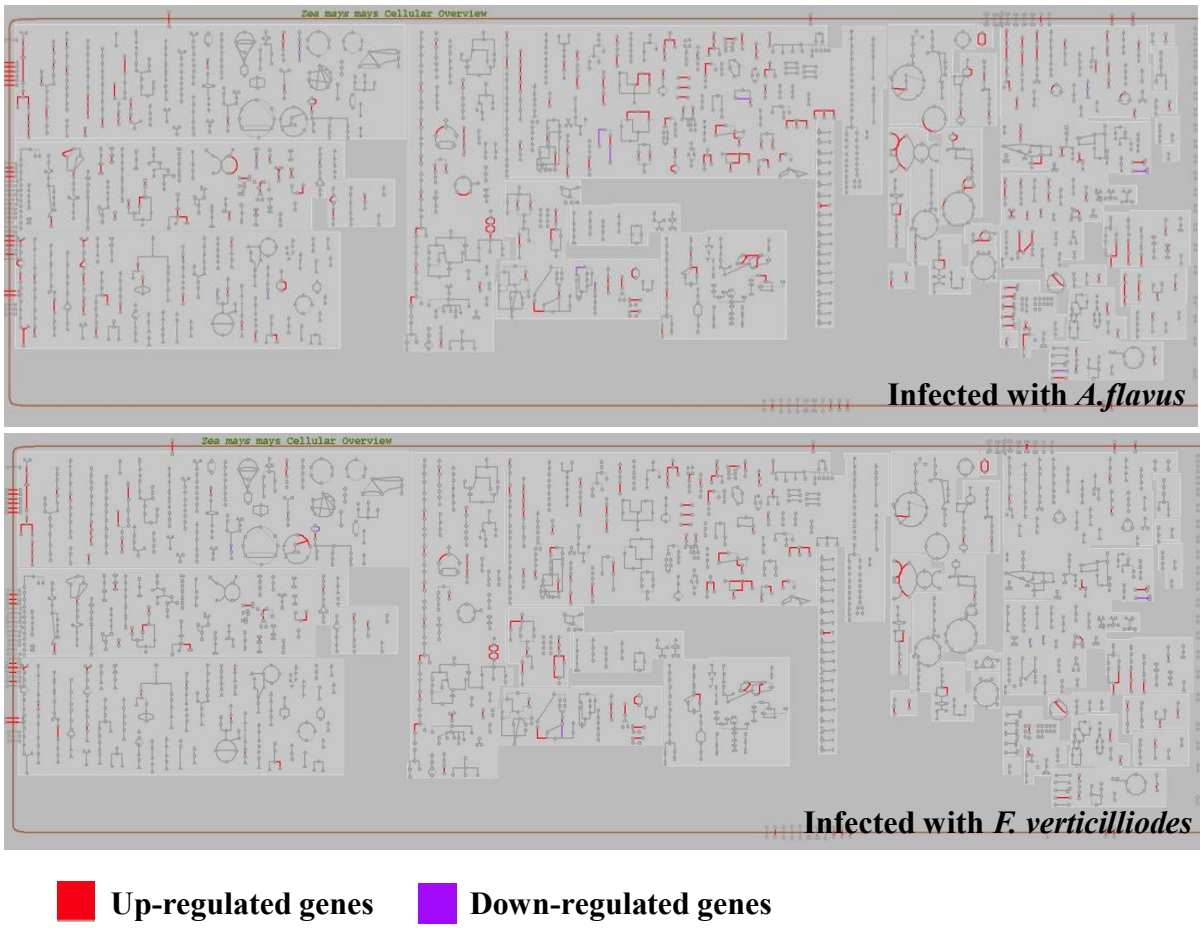

Figure S2. Overview of metabolic pathway changes in maize kernels during *A. flavus* and *F. verticillioides* infection. RNA-seq analysis was conducted for the kernels collected at 72 hpi. The bioinformatics software Biocyc was used. Red lines denote genes that were up-regulated. Purple lines denote genes that were down-regulated.

Table S1. Sequencing statistics for individual reads from the pooled RNA-Seq libraries. Samples were sequenced in three lanes of the Illumina HiSeq. Data were collected from TopHat2_SE output. Af, *A. flavus* infected maize kernels; Fv, *F. verticillioides* infected maize kernels; mock, mock inoculated maize kernels; hpi, hours post inoculation; rep, biological replicates.

sample name	raw reads	filtered reads	Zm aligned 1 time	Zm aligned >1 time	Af aligned 1 time	Af aligned >1 time	Fv aligned 1 time	Fv aligned >1 time
Af 24hpi rep1	8211619	8209860	1915768 (23.33%)	3561164 (43.38%)	275817 (3.36%)	91250 (1.11%)	785 (0.01%)	54317 (0.66%)
Af 24hpi rep2	9650455	9648270	2512189 (26.04%)	5636564 (58.42%)	79800 (0.83%)	44716 (0.46%)	236 (0.00%)	33531 (0.35%)
Af 24hpi rep3	1E+07	10153555	2704971 (26.64%)	6263965 (61.69%)	80884 (0.80%)	68132 (0.67%)	264 (0.00%)	54618 (0.54%)
Af 48hpi rep1	1.2E+07	12138102	2826897 (23.29%)	6337058 (52.21%)	1017499 (8.38%)	67109 (0.55%)	1703 (0.01%)	45455 (0.37%)
Af 48hpi rep2	1.3E+07	13236640	2962051 (22.38%)	6284100 (47.48%)	1904865 (14.39%)	76533 (0.58%)	3161 (0.02%)	47091 (0.36%)
Af 48hpi rep3	8725318	8723247	2268016 (26.00%)	5244160 (60.12%)	315524 (3.62%)	35964 (0.41%)	749 (0.01%)	23069 (0.26%)
Af 72hpi rep1	1.1E+07	10807719	2195336 (20.31%)	4496919 (41.61%)	2225101 (20.59%)	151538 (1.40%)	3810 (0.04%)	76234 (0.71%)
Af 72hpi rep2	6171913	6170385	795275 (12.89%)	1610319 (26.10%)	2281934 (36.98%)	150892 (2.45%)	3238 (0.05%)	64230 (1.04%)
Af 72hpi rep3	9546884	9544716	1192019 (12.49%)	2284284 (23.93%)	3775197 (39.55%)	233676 (2.45%)	5543 (0.06%)	93074 (0.98%)
Fv 24hpi rep1	3.4E+07	33515074	10013189 (29.88%)	17529753 (52.30%)	161 (0.00%)	142269 (0.42%)	10052 (0.03%)	124429 (0.37%)
Fv 24hpi rep2	3.7E+07	37262165	10706610 (28.73%)	21039870 (56.46%)	67 (0.00%)	76799 (0.21%)	3223 (0.01%)	64367 (0.17%)
Fv 24hpi rep3	1.8E+07	18025843	5516769 (30.60%)	8905667 (49.40%)	89 (0.00%)	91284 (0.51%)	43268 (0.24%)	79758 (0.44%)
Fv 48hpi rep1	2.6E+07	25542561	7473907 (29.26%)	12510490 (48.98%)	408 (0.00%)	85783 (0.34%)	1103477 (4.32%)	155354 (0.61%)
Fv 48hpi rep2	3.6E+07	35641066	9784132 (27.45%)	18224938 (51.13%)	457 (0.00%)	65019 (0.18%)	2103675 (5.90%)	156558 (0.44%)
Fv 48hpi rep3	2.9E+07	28734612	8603081 (29.94%)	15324007 (53.33%)	138 (0.00%)	67167 (0.23%)	358421 (1.25%)	67823 (0.24%)
Fv 72hpi rep1	3E+07	30309760	8320996 (27.45%)	12451610 (41.08%)	1055 (0.00%)	45614 (0.15%)	4631867 (15.28%)	175525 (0.58%)
Fv 72hpi rep2	3.4E+07	33776535	8016750 (23.73%)	13871450 (41.07%)	199942 (0.59%)	296387 (0.88%)	3204135 (9.49%)	730673 (2.16%)
Fv 72hpi rep3	3.5E+07	35460716	10115726 (28.53%)	17445490 (49.20%)	540 (0.00%)	73771 (0.21%)	2067253 (5.83%)	184092 (0.52%)
mock 24hpi rep1	3.9E+07	38963116	11746275 (30.15%)	21494974 (55.17%)	183 (0.00%)	69410 (0.18%)	2530 (0.01%)	60270 (0.15%)
mock 24hpi rep2	3.3E+07	33474139	9707341 (29.00%)	18248372 (54.51%)	181 (0.00%)	115372 (0.34%)	1667 (0.00%)	99961 (0.30%)
mock 24hpi rep3	4.2E+07	42306413	11878792 (28.08%)	22949097 (54.24%)	150 (0.00%)	166534 (0.39%)	2370 (0.01%)	147631 (0.35%)
mock 48hpi rep1	2.8E+07	27847499	8063312 (28.96%)	14995525 (53.85%)	90 (0.00%)	82509 (0.30%)	1413 (0.01%)	67909 (0.24%)
mock 48hpi rep2	2.5E+07	24714093	7001696 (28.33%)	13446730 (54.41%)	89 (0.00%)	93930 (0.38%)	1193 (0.00%)	78514 (0.32%)
mock 48hpi rep3	2.5E+07	25189608	7377053 (29.29%)	13695801 (54.37%)	224 (0.00%)	69528 (0.28%)	1258 (0.00%)	56443 (0.22%)
mock 72hpi rep1	3.4E+07	34313793	10352174 (30.17%)	19114836 (55.71%)	64 (0.00%)	29933 (0.09%)	5305 (0.02%)	24394 (0.07%)
mock 72hpi rep2	4E+07	40167261	12216804 (30.41%)	22261056 (55.42%)	284 (0.00%)	38898 (0.10%)	2139 (0.01%)	32634 (0.08%)
mock 72hpi rep3	3.4E+07	33614893	9252626 (27.53%)	17579380 (52.30%)	144 (0.00%)	162145 (0.48%)	2763 (0.01%)	137111 (0.41%)

Table S2. Differentially expressed maize genes during infection by *A. flavus* and *F. verticillioides*. Fold change of genes that were not differentially expressed in some comparisons were left blank. Positive and negative fold changes denote up- and down-regulation, respectively. Af, *A. flavus* infected maize kernels; Fv, *F. verticillioides* infected maize kernels; hpi, hours post inoculation.

gene name	annotation	Af24hpi	Af48hpi	Af72hpi	Fv24hpi	Fv48hpi	Fv72hpi
GRMZM2G032602	Disease resistance gene analog PIC17 Fragment	5.15		7.97			8.42
GRMZM2G402631	pathogenesis related protein-5	12.13	4.44	8.93		3.63	
GRMZM2G075283	pathogenesis related protein 10 (LOC100280981), mRNA	6.9		8.33		2.62	7.44
GRMZM2G129189	endochitinase PR4	3.58		4.61		3.18	11.6
GRMZM2G465226	pathogenesis related protein4	20.83	8.72	35.41		5.49	12.89
GRMZM2G178199	PR protein			-3.88			
GRMZM2G051943	Endochitinase A Precursor (EC 3.2.1.14)(Seed chitinase A)	7.96				4.68	
GRMZM2G453805	chitinase chem5	9.46		11.37			
GRMZM2G145461	chitinase2 (chn2)	6.69	3.72	15.73			21.49
GRMZM2G162505	chitinase 2	27.96	6.59	14.32		7.72	28.11
GRMZM2G151257	endoglucanase 1			3.81			
GRMZM2G065585	Glucan endo-1,3-beta-glucosidase, acidic isoform Precursor (EC 3.2.1.39)((1->3)-beta-glucan endohydrolase)((1->3)-beta-glucanase)(Beta-1,3-endoglucanase)	139.76	18.27	511.8			66.58
GRMZM2G006853	thaumatin-like protein			38.15			
GRMZM2G136372	thaumatin-like protein	17.48	13.38	88.8			39.74
GRMZM2G008271	basal layer antifungal peptide		-6.44				
GRMZM2G102912	AIG2-like protein (LOC100284125), mRNA	-3.1					
GRMZM5G837822	hevamine-A	4.59					
GRMZM2G380656	low-molecular-weight cysteine-rich protein LCR70 (LOC100286345), mRNA		-3.37				
GRMZM2G129266	10-deacetylbaccatin III 10-O-acetyltransferase			-4.27			
GRMZM2G011553	harpin-induced protein			-3.66			
GRMZM2G093418	harpin-induced protein			7.74			6.02
GRMZM2G078771	harpin-induced protein (LOC100280903), mRNA						6.38
GRMZM2G328171	xylanase inhibitor protein 1			3.05			
GRMZM2G447795	xylanase inhibitor protein 1					3.28	
GRMZM2G082199	elicitor-responsive protein 1						3.37
GRMZM2G101741	TMV response-related protein			9.49			
GRMZM2G354190	TMV response-related protein						10.9
GRMZM2G073548	TMV response-related protein		28.63	40.27			7.76
GRMZM2G050607	late embryogenesis abundant protein Lea14-A	4.09		4.15		2.88	4.96
GRMZM2G061403	Cellulase	10.68		5.2		5.74	10.97
GRMZM2G039639	protein P21	15.52	4.29	14.19	5.87	4.78	8.1
GRMZM2G063733	glyoxal oxidase			-3.27			
GRMZM2G109262	lactoylglutathione lyase			8.47			
GRMZM2G082959	Biodegradation of Xenobiotics			3.11			3.11
GRMZM2G445261	Biodegradation of Xenobiotics			4.8			4.98
GRMZM2G065471	Biodegradation of Xenobiotics	9.96		9.85		3.39	9.19
GRMZM2G067915	Biodegradation of Xenobiotics			-2.75			
GRMZM2G124229	Biodegradation of Xenobiotics	17.8	10.2	22.12		6.91	14.68
GRMZM2G062576	stress.biotic		10.55				
GRMZM2G081458	stress.biotic			14.31			
GRMZM2G394027	stress.biotic			3.11			
GRMZM2G117971	stress.biotic			8.18			
GRMZM2G466835	stress.biotic			4.1			
GRMZM2G093951	stress.biotic					2.46	
GRMZM2G092474	stress.biotic	10.01		6.89		4.65	
GRMZM2G117942	stress.biotic	6.3	3.19	6.83		3.58	
GRMZM2G128693	stress.biotic			11.7			10.46
GRMZM2G147908	stress.biotic			53.29			28.94
GRMZM2G151553	stress.biotic			5.09			3.9
GRMZM2G304442	stress.biotic			14.65			4.89
GRMZM2G133781	stress.biotic			4.61			5.11
GRMZM2G061527	stress.biotic	14.76		18.14			11.62

Table S2 Continued

gene name	annotation	Af24hpi	Af48hpi	Af72hpi	Fv24hpi	Fv48hpi	Fv72hpi
GRMZM2G178875	stress.biotic	5.78		26.92			15.25
GRMZM2G456997	stress.biotic			8.99		4.59	9.39
GRMZM2G459110	stress.biotic			3.27		2.65	2.99
GRMZM2G062974	stress.biotic		4.01	6.13		4.5	7
GRMZM2G010048	stress.biotic	13.67	4.06	9.67		6.07	14.79
GRMZM2G078667	stress.biotic	6.1	3.98	9.35		3.5	8.43
GRMZM2G051921	stress.biotic	20.51	4.9	10.73	8.54	5.04	12.63
GRMZM2G098460	drought-induced protein 1			4.37			4.58
GRMZM2G075290	stress.abiotic.drought/salt			-2.66			
GRMZM2G127911	Phosphopantothenoylcysteine decarboxylase			3.32			
GRMZM2G179462	stress.abiotic.drought/salt	6.23		6.43			7.71
GRMZM2G118453	HSF26			2.83			
GRMZM2G105348	HSF18			2.86			3.4
GRMZM2G149647	heat shock protein26			3.78			
GRMZM2G428391	heat shock cognate 70 kDa protein 2			4.46			
GRMZM5G833699	Heat shock protein 82			2.61			
GRMZM5G849535	16.9 kDa class I heat shock protein 1 (LOC100284416), mRNA						5.77
GRMZM2G399136	chaperone protein dnaJ 11			5.94			
GRMZM2G029385	mitochondrial import inner membrane translocase subunit TIM14			3.57			
GRMZM2G058358	subtilisin-chymotrypsin inhibitor CI-1C			-3.3			
GRMZM2G159691	hypoxia induced protein conserved region containing protein			2.26			
GRMZM2G087111	germin-like protein subfamily 1 member 11			134.43			278.07
GRMZM5G885126	systemin receptor SR160 (LOC100285871), mRNA	26.15		25.28		4.59	19.62
GRMZM2G306679	stress.abiotic.heat			6.22			
GRMZM2G324956	stress.abiotic.heat			10.53			
GRMZM2G135960	stress.abiotic.heat		9.79	3.89			
GRMZM2G059502	stress.abiotic.heat			7.87		8.17	8.56
GRMZM2G040517	stress.abiotic			-3			
GRMZM2G093076	stress.abiotic						321.08
GRMZM2G093606	stress.abiotic						136.03
GRMZM2G093622	stress.abiotic			93.66		20.82	259.82
GRMZM2G157298	stress.abiotic			219.87		30.42	360.6
GRMZM2G170829	stress.abiotic			132.93		12.9	266.29
GRMZM2G387127	stress.abiotic			60.34		28.49	96.34
GRMZM2G090245	stress.abiotic	23.04		46.43		4.41	24.43
GRMZM2G030772	stress.abiotic		19.5	74.04		22.54	154.89
GRMZM2G178817	stress.abiotic		21.77	130.4		17.02	120.64
GRMZM2G071390	stress.abiotic		23.5	270.67		25.87	227.76
GRMZM2G049930	stress.abiotic	41.55	63.6	146.18		26.87	90.2
GRMZM2G149714	stress.abiotic	27.89	10.2	37.52		17.35	84.29
GRMZM2G122018	stress.abiotic	7.02	11.77	111.26		7.11	25.64
GRMZM2G151249	stress.abiotic	3.84	6.43	13.32		4.82	13.66
GRMZM2G136960	2-Sep	-2.94					
GRMZM2G420743	dirigent-like protein pDIR3			-3.97			
GRMZM2G410766	Stress responsive protein					5.27	
GRMZM2G348125	stress responsive protein (LOC100283176), mRNA					3.64	
GRMZM2G156877	glutathione S-transferase 8			35.92			
GRMZM2G019090	glutathione S-transferase GST 18			11.22			
GRMZM2G428168	glutathione S-transferase GST 21			8.91			
GRMZM2G146913	glutathione S-transferase GSTU6			5.08			
GRMZM2G043291	glutathione S transferase			2.84			
GRMZM2G025190	Glutathione S-transferase GSTU6		17.81	10.45			
GRMZM2G056388	Glutathione S-transferase GSTU6		28.11	59.85			
GRMZM2G302373	glutathione S transferase			49.33			14.36
GRMZM2G156877	glutathione S-transferase 8			352.9			181.43
GRMZM2G150474	glutathione S-transferase GST 15			4.48			3.11
GRMZM2G052571	glutathione S-transferase	10.36		135.22			36.71
GRMZM2G480439	glutathione S transferases		6.92	10.91			4.98
GRMZM2G161891	glutathione transferase35			4.94			
GRMZM5G809218	glutathione transferase5 (gst5), mRNA		7.42	5.32		2.88	
GRMZM2G475059	glutathione transferase31		11.49	25.21			7.8
GRMZM2G032856	glutathione transferase24	13.72	31.03	63.24		4.64	18.79
GRMZM2G028556	glutathione transferase7	60.61	175.28	343.18		9.4	81.82

Table S2 Continued

gene name	annotation	Af24hpi	Af48hpi	Af72hpi	Fv24hpi	Fv48hpi	Fv72hpi
GRMZM2G042639	Protein IN2-1			32.08			
GRMZM2G042639	Protein IN2-1		24.85	29.09			
GRMZM2G042639	Protein IN2-1		27.91	24.26			9.71
GRMZM2G162486	IN2-1 protein		8.31	15.86			5.42
GRMZM2G089895	Peroxidase			-3.47			
GRMZM2G177792	peroxidase 1			-3.74			
GRMZM2G107228	Peroxidase	46.97				4.33	
GRMZM2G103342	Peroxidase	12.37	6.65	12.69		4.44	
GRMZM2G097934	Peroxidase						21.43
GRMZM2G326222	Peroxidase						34.84
GRMZM2G176085	peroxidase 51						3.18
GRMZM2G126261	Peroxidase 42 Precursor (EC 1.11.1.7)(Plasma membrane-bound peroxidase 3-1)(pmPOX3-1)	3.26					3.01
GRMZM2G022740	Peroxidase			300.28			431.63
GRMZM2G116823	Peroxidase			7.07			17.36
GRMZM2G108219	anionic peroxidase			94.3			32.64
GRMZM2G173195	Peroxidase			3.85			2.83
AC205413.4_FG001	Peroxidase			43.09			26.18
GRMZM2G171078	Peroxidase			424.88			332.92
GRMZM2G080183	Peroxidase			4.43			6.14
AC197758.3_FG004	peroxidase 52			36.11			13.47
GRMZM2G089982	peroxidase 72			15.11			8.1
GRMZM2G427815	Peroxidase	156.86		14.78	21.06		10.3
GRMZM2G076562	peroxidase					7.92	58.73
GRMZM2G117706	Peroxidase	74.23		70.64		7.91	161.33
GRMZM2G450233	Peroxidase	9.93		3.37		3.33	3.38
GRMZM2G135108	Peroxidase Fragment	14.79		5.64		5.67	9.01
GRMZM2G108207	Peroxidase	180.99	10.7	42	20.14	23.27	59.95
GRMZM2G108103	polyphenol oxidase	34.9					
GRMZM2G359298	primary amine oxidase			-3.56			
GRMZM2G019872	NADP-dependent oxidoreductase P2						-5.63
GRMZM2G013781	oxidase			15.32			17.75
GRMZM5G841893	oxidase	15.53	17.2	36.06		15.64	36.44
GRMZM2G438386	oxidase			-3.01			
GRMZM5G891656	oxidase		248.35	328.56			
GRMZM2G303044	Grx_A2 - glutaredoxin subgroup III	-3.76					
GRMZM2G311898	Grx_I1 - glutaredoxin subgroup III			4.72			
GRMZM2G178886	redox.glutaredoxins			3.62			
GRMZM2G169329	redox.heme		8.44	6.04			
GRMZM2G064106	redox.ascorbate and glutathione.ascorbate						3.74
GRMZM2G170016	redox.ascorbate and glutathione			10.07			7.45
GRMZM2G148387	Grx_C2.1 - glutaredoxin subgroup I		5.52	5.94			3.8
GRMZM2G067402	Non-symbiotic hemoglobin (Hbt)(ZEAmp GLB1)	6.49	20.19	22.93		4.21	5.96
GRMZM2G126772	benzoate carboxyl methyltransferase			32.94			
GRMZM2G107402	Shikimate dehydrogenase			2.92			
GRMZM5G877500	3-phosphoshikimate 1-carboxyvinyltransferase Fragment (EC 2.5.1.19)			3.44			
GRMZM2G158083	Shikimate O-hydroxycinnamoyltransferase			2.33			
GRMZM2G087192	12-oxo-phytodienoic acid reductase5 (opr5)			7.24			
GRMZM2G000236	12-oxo-phytodienoic acid reductase2 (opr2)		19.43	48.14			
GRMZM2G156712	12-oxo-phytodienoic acid reductase (OPR3)		21.32	90.89			11.85
GRMZM2G106303	12-oxo-phytodienoic acid reductase1 (opr1)		72.82	211.05			52.19
GRMZM5G822593	Lipoxygenase			8.23			6.61
GRMZM2G109056	lipoxygenase (LOX4)			3.84		2.36	3.97
GRMZM2G072529	acc oxidase	10.79		17.17			10.58
GRMZM2G164405	Acc synthase		5.1	13.03			6.98
GRMZM5G894619	1-aminocyclopropane-1-carboxylate synthase7 (acs7)	4.5	4.77	5.54		4.63	6.35
GRMZM2G013448	1-aminocyclopropane-1-carboxylate oxidase 1					5.21	5.98
GRMZM2G166616	1-aminocyclopropane-1-carboxylic acid oxidase Fragment			69.45			13.94
GRMZM2G166639	Aminocyclopropanecarboxylate oxidase			34.1			13.15
GRMZM2G332423	Aminocyclopropanecarboxylate oxidase			76.19			39.72
GRMZM2G166639	Aminocyclopropanecarboxylate oxidase			12.2			9.98
GRMZM2G382569	ethylene metabolism gene			6.44			8.36
GRMZM2G086573	EREB24			3.03			
GRMZM2G080516	EREB2					2.53	

Table S2 Continued

gene name	annotation	Af24hpi	Af48hpi	Af72hpi	Fv24hpi	Fv48hpi	Fv72hpi
GRMZM2G076896	EREB111			9.95			11.04
GRMZM2G457562	EREB113			4.71			4.65
GRMZM2G381441	EREB58			13.59			13.1
GRMZM2G016434	EREB129	26.85		15.49			16.04
GRMZM2G087059	EREB131	11.37		7.23			7.64
GRMZM2G100727	EREB133	6.46		10.28			8.61
GRMZM2G466044	EREB195	8.34		8.33		4.76	7.17
GRMZM2G055180	EREB198	3.53		5.9		3.09	5.75
GRMZM2G474326	EREB134		6.93	11.82		3.93	8.04
GRMZM2G123119	EREB177	9.69	11.68	26.41		7.4	14.11
GRMZM2G033656	EREB150	-3.38	-5.45	-3.39			
GRMZM2G175525	AP2-EREBP family			4.03			
GRMZM2G175856	dehydration-responsive element-binding protein 1B			8.54			
GRMZM2G141535	aldehyde oxidase		3.52	6.72			
GRMZM2G019799	Xanthine dehydrogenase			29.78			
GRMZM2G417954	viviparous-14			6.63			5.62
GRMZM2G180596	abscisic acid metabolism gene			2.94			2.98
GRMZM2G178509	abscisic acid metabolism gene			5.85			3.94
GRMZM2G179147	(+)-abscisic acid 8'-hydroxylase			3.52			5.66
GRMZM2G126505	(+)-abscisic acid 8'-hydroxylase	6.66		13.13			5.64
GRMZM2G024131	Indole-3-acetate beta-glucosyltransferase (EC 2.4.1.121)(IAA-Glu synthase)((Uridine 5'-diphosphate-glucose:indol-3-ylacetyl)-beta-D-glucosyl transferase)			-3.1			
GRMZM5G875732	Indoleacetaldoxime dehydratase			7.25			
GRMZM2G170047	Indoleacetaldoxime dehydratase			13.14			6.33
GRMZM2G124175	Xanthine dehydrogenase		12.06	32.56			4.95
GRMZM5G899851	Xanthine dehydrogenase		17.89	47.59			5.66
GRMZM2G091540	auxin metabolism gene			9.63			7.14
GRMZM2G432060	SAUR11 – auxin-responsive SAUR family member	-4.51					
GRMZM2G332390	SAUR16 – auxin-responsive SAUR family member			4.76			3.34
GRMZM2G151656	SAUR52 – auxin-responsive SAUR family member			8.64			
GRMZM2G089273	auxin metabolism gene			27.88			
GRMZM2G407969	auxin metabolism gene			99.58			
GRMZM2G089854	auxin metabolism gene			2.36			
GRMZM2G033359	auxin metabolism gene	5.22		3.18		3.15	
GRMZM2G365188	auxin metabolism gene						4.06
GRMZM5G859099	auxin metabolism gene						12.31
GRMZM2G066029	auxin-inducible protein			3.65			3.68
GRMZM2G066202	auxin metabolism gene			33.9			28.38
GRMZM2G003506	auxin metabolism gene			4.04			4.89
GRMZM2G020631	auxin metabolism gene		15.42	42.96			7.9
GRMZM2G329077	auxin-inducible protein (LOC100283113), mRNA	22.42		15.39			14.26
GRMZM2G030465	IAA9 – auxin-responsive Aux/IAA family member	6.72	5.72	4.98		4.03	5.9
GRMZM2G031724	Gibberellin 2-beta-dioxygenase						3.47
GRMZM2G022679	Gibberellin 2-beta-dioxygenase						6.42
GRMZM2G044481	Ent-copalyl diphosphate synthase			19.08			
GRMZM2G016922	Ent-kaurene synthase			63.26			62.54
GRMZM2G161472	Ent-kaurene oxidase	9.24	4.02	11.65		3.73	8.71
GRMZM2G099467	gibberellin 20 oxidase 2 (LOC100284800), mRNA	7.96	12.4	44.65		4.88	15.99
GRMZM2G028438	chitin-inducible gibberellin-responsive protein 2			3.25			
GRMZM2G049675	gibberellin receptor GID1L2			-3.48			
GRMZM2G104938	gibberellin receptor GID1L2			3.03			
GRMZM2G062527	203ibberellin responsive gene			-3.84			
GRMZM2G150688	203ibberellin responsive gene			-3.49			
GRMZM2G007195	UDP-glucuronate decarboxylase			3.62			
GRMZM5G881887	Helminthosporium carbonum susceptibility1			2.86			
GRMZM2G131205	cinnamoyl CoA reductase1					2.45	
GRMZM2G138907	3-beta-hydroxy-Delta(5)-steroid dehydrogenase			3.54			2.95
GRMZM2G013726	Dihydrokaempferol 4-reductase			4.16		2.76	6.6
GRMZM2G068917	3-beta-hydroxy-Delta(5)-steroid dehydrogenase	4.79		9.07		3.84	11.1
GRMZM2G073929	DET2		19.9	3091.72		23.45	2101.56
GRMZM2G349665	BRASSINOSTEROID INSENSITIVE 1-associated receptor kinase 1			4.85			
GRMZM2G145440	BRASSINOSTEROID INSENSITIVE 1-associated receptor kinase 1			16.15			20.87

Table S2 Continued

gene name	annotation	Af24hpi	Af48hpi	Af72hpi	Fv24hpi	Fv48hpi	Fv72hpi
GRMZM2G319965	Trans-zeatin O-beta-D-glucosyltransferase		9.41				
GRMZM2G083935	Trans-zeatin O-beta-D-glucosyltransferase			12.54			
GRMZM2G004858	Trans-zeatin O-beta-D-glucosyltransferase			5.01			
GRMZM2G095280	Trans-zeatin O-beta-D-glucosyltransferase			22.08			16.85
GRMZM2G173315	Trans-zeatin O-beta-D-glucosyltransferase			10.94			6.32
GRMZM2G132706	Trans-zeatin O-beta-D-glucosyltransferase	10.65		3.73			4.94
GRMZM2G334336	Trans-zeatin O-beta-D-glucosyltransferase		12.4	27.97			15.69
GRMZM5G888620	Trans-zeatin O-beta-D-glucosyltransferase		20.28	30.96			10.66
GRMZM2G098892	Trans-zeatin O-beta-D-glucosyltransferase		12.75	22.64			9.08
GRMZM2G304712	Trans-zeatin O-beta-D-glucosyltransferase		3.73	9.32			6.84
GRMZM2G178209	Trans-zeatin O-beta-D-glucosyltransferase	7.21	15.87	38.52			13.39
GRMZM2G457929	Trans-zeatin O-beta-D-glucosyltransferase	9.47	12.04	121.73			32.93
GRMZM2G051683	Trans-zeatin O-beta-D-glucosyltransferase			6.09		2.77	5.52
GRMZM2G301148	Trans-zeatin O-beta-D-glucosyltransferase	27.15		16.96		5.5	18.05
GRMZM2G056335	Trans-zeatin O-beta-D-glucosyltransferase	15.57	10.44	13.33		9.67	14.48
GRMZM2G168474	Cis-zeatin O-glucosyltransferase 1 (cisZOG1)(EC 2.4.1.215)						12.06
GRMZM2G168474	Cis-zeatin O-glucosyltransferase 1 (cisZOG1)(EC 2.4.1.215)	6.95	7.23	39.72			22.84
GRMZM2G120016	Cis-zeatin O-glucosyltransferase	9.78	14.63	19.85		6.32	9.48
GRMZM2G010987	anthocyanidin 5,3-O-glucosyltransferase			3.69			
GRMZM2G061321	anthocyanidin 3-O-glucosyltransferase			18.25			10.83
GRMZM2G135722	anthocyanidin 3-O-glucosyltransferase		112.24	108.25			40.72
GRMZM5G854655	cytokinin-O-glucosyltransferase 3			-3.44			
GRMZM2G479038	cytokinin-O-glucosyltransferase 3	6.06		12.59			8.51
GRMZM5G834303	cytokinin-O-glucosyltransferase 2	18.46	8.52	47.68			20.45
GRMZM2G078465	indole-3-acetate beta-glucosyltransferase			4.79			
GRMZM2G325612	Cytokinin dehydrogenase			12.59			
GRMZM2G084462	Isopentenyl transferase IPT2	-3.38	-5.1	-4.29			
GRMZM2G165060	LRR receptor-like kinase			3.25			
GRMZM2G149051	LRR receptor-like kinase			-2.8			
GRMZM2G429714	LRR receptor-like kinase			5.06			
GRMZM2G001812	LRR receptor-like kinase						4.24
GRMZM2G474777	LRR receptor-like kinase						4.65
GRMZM2G080851	LRR receptor-like kinase			3.78			4.13
GRMZM2G176206	LRR receptor-like kinase	8.45		3.96			3.68
GRMZM2G356076	LRR receptor-like kinase	5.19		8.59			4.64
GRMZM2G132212	LRR receptor-like kinase	6.83		9.36		3.25	7.22
GRMZM2G177883	LRR receptor-like kinase	10.11	4.81	14.31		4.03	10.95
GRMZM2G115420	somatic embryogenesis receptor-like kinase2 (serk2)			2.63			
GRMZM2G303965	Lectin domain receptor protein kinase-- LRK			3.25			
GRMZM2G443843	Lectin domain receptor protein kinase-- LRK						53.35
GRMZM2G465165	Lectin domain receptor protein kinase-- LRK						23.6
GRMZM2G474153	Lectin domain receptor protein kinase-- LRK			3.13			3.34
GRMZM2G054023	Lectin domain receptor protein kinase-- LRK	12.24		3.9			4.35
GRMZM2G443829	Lectin domain receptor protein kinase-- LRK	29.74	8	17.86		9.86	17.73
GRMZM2G438871	Lectin domain receptor protein kinase-- LRK	9.95		21		3.98	15.09
GRMZM2G028568	kinase; LRK10L-1			6.28			4.49
GRMZM2G079219	LRK10L-2. Receptor-like protein kinase	7.5		7.65			5.05
GRMZM2G475948	lectin-like receptor kinase 7	6.15		3.29			3.95
GRMZM5G832149	WAK2 - OsWAK receptor-like cytoplasmic kinase (OsWAK-RLCK)			3.67			3.49
GRMZM2G077655	WAK80 - OsWAK receptor-like protein kinase			10.88			9.4
GRMZM2G359986	Wall Associated Kinase-Like. RLCKIII. WAK kinase	8.58		11.17		4.11	11.45
GRMZM2G328785	Putative receptor protein kinase ZmPK1 Precursor (EC 2.7.11.1)	11.2		7.45			5.63
GRMZM2G304897	receptor-like protein kinase	4.48		6.59		4.25	4.94
GRMZM2G065021	receptor-like protein kinase			-2.75			
GRMZM2G101245	Receptor-like cytoplasminc kinase			4.81			5.53
GRMZM2G175164	Receptor-like cytoplasminc kinase			3.64			
GRMZM5G852177	serine/threonine-protein kinase receptor			2.85			
GRMZM2G026406	serine/threonine kinase-like protein			5.87			9.26
GRMZM2G068151	serine/threonine-protein kinase NAK			3.71			2.79
GRMZM2G177050	CBL-interacting serine/threonine-protein kinase 11			3.18			
GRMZM2G334165	DUF26 receptor-like kinase			3.03			
GRMZM2G076943	DUF26 receptor-like kinase			3.11			

Table S2 Continued

gene name	annotation	Af24hpi	Af48hpi	Af72hpi	Fv24hpi	Fv48hpi	Fv72hpi
GRMZM2G465999	DUF26 receptor-like kinase			9.94			
GRMZM2G403719	DUF26 receptor-like kinase	4.61		7.73			
GRMZM2G075247	DUF26 receptor-like kinase						5.29
GRMZM2G309380	DUF26 receptor-like kinase						10.28
GRMZM2G465987	DUF26 receptor-like kinase						11.36
GRMZM2G333875	DUF26 receptor-like kinase			5.53			3.71
GRMZM2G374309	DUF26 receptor-like kinase			2.82			2.75
GRMZM2G406601	S-locus receptor-like protein kinase						3.94
GRMZM2G009166	S-locus receptor-like protein kinase			4.92			3.47
GRMZM2G076212	S-locus receptor-like protein kinase			5.48			3.76
GRMZM2G113158	S-locus receptor-like protein kinase			2.96			2.79
GRMZM2G059740	S-locus receptor-like protein kinase			8.23			5.89
GRMZM2G344388	MAPK			4.02			
GRMZM2G163709	MAPK			4.04			
GRMZM2G344388	MAPKK			3.84			3.63
GRMZM2G400470	MAPKK			3.02			
GRMZM2G314396	calcium dependent protein kinase (CDPK1)			2.69			
GRMZM2G115518	calcium dependent protein kinase1 (cdpk1)			2.36			
GRMZM2G173928	CDPK-related protein kinase			2.87			
GRMZM2G134332	Ribosomal Protein S6 Kinase			-4.99			
GRMZM2G019567	Ribosomal Protein S6 Kinase			4.13			
GRMZM2G120839	Crinkly 4_Like kinase			3.65			
GRMZM2G084609	Inositol-tetrakisphosphate 1-kinase			3.97			
GRMZM2G179473	Inositol-tetrakisphosphate 1-kinase			2.53			
GRMZM2G017334	Uridine kinase			2.61			
GRMZM2G020429	Uridine kinase			2.76			
GRMZM2G080375	6-phosphofructokinase			12.75			
GRMZM2G059078	6-phosphofructokinase 2	20.01		12.35		4.34	8.74
GRMZM2G025459	SNF1-related protein kinase regulatory subunit beta-1	6.65		8.84			5.75
GRMZM2G086869	Riboflavin kinase			18.43			
GRMZM2G086869	Riboflavin kinase			9.23			9.98
GRMZM2G117378	homoserine kinase		10.85	19.31		11.83	27.97
GRMZM5G859195	Homoserine kinase			4.18			3.63
GRMZM2G168976	glutamate 5-kinase	25.81		34.36			18.82
GRMZM2G084463	guanylate kinase			3.09			
GRMZM2G173965	kinase			9.36			
GRMZM2G071478	kinase			11.3			16.44
GRMZM2G024024	protein kinase			2.96			2.89
GRMZM2G026151	protein kinase			4.26			4.91
GRMZM2G334181	protein kinase	18.04	4.58	32.62		7.11	38.47
GRMZM5G868679	acid phosphatase	3.43					
GRMZM2G073860	Acid phosphatase	6.23		3.79		2.85	3.69
GRMZM2G159660	alkaline phosphatase D			2.45			
GRMZM5G836174	phosphatase			3.52			
GRMZM2G045976	phosphatase			8.41			4.47
GRMZM2G141277	stem 28 kDa glycoprotein						-4.44
GRMZM2G023921	DNA-binding WRKY			-3.46			
GRMZM2G169966	WRKY57			15.23			
GRMZM2G063216	WRKY16			2.51			
GRMZM2G052671	WRKY71			2.62			
GRMZM2G139815	WRKY37			4.04			
GRMZM2G054125	WRKY36			17.98			13.28
GRMZM2G106560	WRKY108			17.19			12
GRMZM2G111711	WRKY124			40.64			54.38
GRMZM2G304573	WRKY84			36.44			17.47
GRMZM2G453571	WRKY117			5.1			6.06
GRMZM5G871347	WRKY93			10.26			6.22
GRMZM2G120320	WRKY48			4.42			4.79
GRMZM2G163054	WRKY125			7.26			4.87
GRMZM2G012724	WRKY83			4.87			4.09
GRMZM2G449681	WRKY92			5.21			4.94
GRMZM2G030272	WRKY32			5.08			3.21
GRMZM2G057116	WRKY34			9.59			8.82
GRMZM2G176489	WRKY56	13.7		8.47			8.83
GRMZM2G475984	WRKY27	20.33		13.88			12.45
GRMZM2G148087	WRKY43	7.33		6.98			5.79

Table S2 Continued

gene name	annotation	Af24hpi	Af48hpi	Af72hpi	Fv24hpi	Fv48hpi	Fv72hpi
GRMZM2G063880	WRKY106	11.74		14.26		5.17	11.31
GRMZM5G863420	WRKY82	5.56		6.64		4.03	6.26
GRMZM2G083350	WRKY26	42.43	5.4	22.13		8.52	33.9
GRMZM2G048295	MYB72			3.43			4.77
GRMZM2G160840	MYB118			4.6			5.33
GRMZM5G803355	MYB51		-5.82				
GRMZM2G111306	MYBR1	-3.26		-3.2			
GRMZM2G121111	MYBR81		-5.2	-4.49			
GRMZM2G160838	MYB32			3.11			
GRMZM2G147346	MYB121			4.69			
GRMZM2G139284	MYB70			4.62			
GRMZM2G106558	MYB146						6.18
GRMZM2G070849	MYB75						3.84
GRMZM2G100709	GLK31						16.48
GRMZM2G131442	MYB4			8.64			8.76
GRMZM2G176327	MYB family			13.85			9.47
GRMZM2G069325	MYB130			3.77			3.68
GRMZM2G419239	MYB42	29.6		9.7			10.83
GRMZM2G081557	MYB9		13.91	39.4			20.55
GRMZM2G048826	NAC92		37.07				
GRMZM2G180328	NAC20			2.97			
GRMZM2G068973	NAC23			14.66			
GRMZM2G347043	NAC49			4.33			
GRMZM2G163251	NAC7	4.65					2.97
GRMZM2G109627	NAC118			12.37			8.8
GRMZM2G112548	NAC74			4.2			4.83
GRMZM2G100583	NAC75			5.07			3.91
GRMZM2G074358	NAC42	21.98		6.2			12.57
GRMZM2G068973	NAC23	5.44	6.92	15.53		4.3	10.27
GRMZM2G092137	bZIP9			4.07			
GRMZM2G042278	NLP15			6.31			
GRMZM2G365754	bZIP67						4.36
GRMZM2G377613	tumor-related protein-like						3.95
GRMZM2G400281	C2H2 zinc finger family						3.7
GRMZM2G048154	C2H2 zinc finger family			45.59			61.92
GRMZM5G804618	C2H2 zinc finger family	7.46	5.93	6.86		3.55	6.59
GRMZM2G376061	C2H2 zinc finger family			11.02			5.27
GRMZM2G400714	C2H2 family			2.89			
GRMZM2G069176	C2H2 family			15.09			14.68
GRMZM2G112799	C2H2 family			7.5			4.05
GRMZM2G106026	C2H2 family		24.86	378.49			188.97
GRMZM2G113860	C2H2 family	22.98		28.71		9.87	28.97
GRMZM2G117007	C3H7			4.16			
GRMZM2G002805	ZFP16-2			3.86			
GRMZM2G173425	zinc finger protein LSD2			3.09			
GRMZM2G140694	DOF29	7.16					3.03
GRMZM2G125775	AN17			8.96			5.09
GRMZM2G378490	DOF7			4.82			4.21
GRMZM2G413113	Orphan38	-3.72					
GRMZM2G023346	Orphan92			4.73			
GRMZM2G016145	Orphan123		-8.5				
GRMZM2G090264	Orphan213	-7.76	-6.24				
GRMZM2G180430	Orphan65			2.4			
GRMZM2G134671	Orphan43			3.25			
GRMZM2G097135	Orphan301			3.2			
GRMZM2G000603	Orphan8						7.6
GRMZM2G342197	Orphan127						28.61
GRMZM2G073823	GRAS68			68.18			
GRMZM2G163427	GRAS34			4.28			
GRMZM2G163427	GRAS34			5.85			
GRMZM2G073805	GRAS72			3.38			
GRMZM2G420280	GRAS family		7.49	16.09			4.65
GRMZM2G018254	GRAS48		8.21	15.18			8.35
GRMZM5G839518	bHLH152			-2.82			
GRMZM2G082586	bHLH105			-4.33			
GRMZM2G159937	bHLH57			2.94			

Table S2 Continued

gene name	annotation	Af24hpi	Af48hpi	Af72hpi	Fv24hpi	Fv48hpi	Fv72hpi
GRMZM2G094892	bHLH family			14.99			14.55
GRMZM5G849600	bHLH94			2.97		3.09	3.4
GRMZM2G036351	ZIM4			2.89			
GRMZM2G343157	ZIM26			3.22			
GRMZM2G445634	ZIM16			3.35			
GRMZM2G173596	ZIM10			18.87			12.7
GRMZM2G116614	ZIM28	16.05		36.61			29.76
GRMZM2G166041	HB24	5.3					
GRMZM2G062244	HB107			6.94			
GRMZM2G396527	HB70						5.07
GRMZM2G333775	GNAT family						4.8
GRMZM2G031062	GNAT family			12.81			13
GRMZM2G089736	pnFL-2			3.13			
GRMZM5G838098	pnFL-2			4.46			3.69
GRMZM2G145568	LOB family			11.8			14.28
GRMZM2G092483	LOB family			8.47			11.29
GRMZM2G167576	CADR12			-5.94			
GRMZM2G038303	CA2P15			-4.49			
GRMZM2G020187	Protein SUPPRESSOR OF GENE SILENCING 3 homolog (ZmSGS3)(Protein LEAFBLADELESS 1)			-3.57			
GRMZM2G086403	PLATZ family			3.7			
GRMZM2G175761	pollen-specific protein SF3			4.26			
GRMZM2G127776	Homeobox transcription factor family			5.68			7.53
GRMZM5G865508	MYND finger family protein			11.79			9
GRMZM2G040481	EIL8	6.88		15.18			13.49
GRMZM2G090603	TF	7.12					
GRMZM2G140994	TF			2.36			
GRMZM2G163717	TF			3.56			
GRMZM5G862467	TF			2.69			
GRMZM2G168431	TF			35.45			20.29
GRMZM2G126079	TF			7.77			4.73
GRMZM2G036365	TF			8.1		9.93	20.31
GRMZM2G175927	TF	24.46	9.6	18.04		7.19	15.7
GRMZM2G089506	TF	42.76	9.72	72.56		9.25	31.79
GRMZM2G046061	TF			11.24			7.67
AC197705.4_FG004	Ubiquitin System Ringfinger protein			-3.7			
GRMZM2G053707	Ubiquitin System Ringfinger protein	-3.34		-2.75			
GRMZM2G042538	Ubiquitin System Ringfinger protein			6.98			
GRMZM2G047167	Ubiquitin System Ringfinger protein			3.25			
GRMZM2G320399	Ubiquitin System Ringfinger protein			3.44			
GRMZM2G075019	Ubiquitin System Ringfinger protein			3.64			
GRMZM2G077809	Ubiquitin System Ringfinger protein			2.72			
GRMZM2G027120	Ubiquitin System Ringfinger protein			5.66			
GRMZM2G004519	Ubiquitin System Ringfinger protein						4.14
GRMZM2G061663	Ubiquitin System Ringfinger protein			5.17			4.96
GRMZM2G067865	Ubiquitin System Ringfinger protein			2.87			2.71
GRMZM2G318220	Ubiquitin System Ringfinger protein			9.82			6.87
GRMZM2G329195	Ubiquitin System Ringfinger protein			4.39			4.24
GRMZM2G355846	Ubiquitin System Ringfinger protein			5.78			3.34
GRMZM2G397684	Ubiquitin System Ringfinger protein			3.29			2.69
GRMZM2G134023	Ubiquitin System Ringfinger protein			5.03			5.54
GRMZM2G035704	Ubiquitin System Ringfinger protein			13.21			6.93
GRMZM2G095873	Ubiquitin System Ringfinger protein			3.73			3.65
GRMZM2G044537	Ubiquitin System Ringfinger protein			4.65			5.06
GRMZM2G082653	Ubiquitin System Ringfinger protein	16.23		24.31			21.19
GRMZM2G460958	Ubiquitin System Ringfinger protein		42.66	66.28			17.56
GRMZM2G044773	Ubiquitin System Ringfinger protein		15.92	146.9		8.82	79.34
GRMZM2G015753	Ubiquitin System Ringfinger protein	9.51	4.86	22.48		3.56	11.86
GRMZM2G303964	Ubiquitin System Ubox protein			3.07			
GRMZM2G092128	Ubiquitin System Ubox protein						15.73
GRMZM2G302499	Ubiquitin System Ubox protein						18.23
GRMZM2G098128	Ubiquitin System Ubox protein						81.11
GRMZM2G169690	Ubiquitin System Ubox protein						8.36
GRMZM2G071484	Ubiquitin System Ubox protein			3.18			4.16
GRMZM2G361100	Ubiquitin System Ubox protein			40.87			22.34
GRMZM2G031624	Ubiquitin System Ubox protein	13.36		9.03			9.54

Table S2 Continued

gene name	annotation	Af24hpi	Af48hpi	Af72hpi	Fv24hpi	Fv48hpi	Fv72hpi
GRMZM2G447480	Ubiquitin System Ubox protein			6.85			8.2
GRMZM2G041959	Ubiquitin System Ubox protein			32.42			13.64
GRMZM2G142357	Ubiquitin System Ubox protein			8.51			7.64
GRMZM2G014022	Ubiquitin System Ubox protein	3.58		9.41		2.66	8.93
AC214635.3_FG002	Ubiquitin System Ubox protein			10.58			
GRMZM2G440543	F-box protein GID2			2.66			2.98
GRMZM2G059042	photoperiod responsive protein			2.47			
GRMZM2G123212	ubiquitin-protein ligase CIP8			5.4			
GRMZM2G124417	proteasome subunit beta type 1		8.45	11.53			
GRMZM2G055052	immediate-early fungal elicitor protein CMPG1	5.51		7.28		5.01	14.58
GRMZM2G151204	immediate-early fungal elicitor protein CMPG1	12.9		18.87		4.82	15.03
GRMZM2G165633	gluco-, galacto- and mannosidases.glycosyl hydrolase family 5			-3.03			
GRMZM2G151992	catalytic/ hydrolase			3.11			
GRMZM2G025154	serine carboxypeptidase F13S12.6	5.33		3.85			
GRMZM2G475265	aspartic proteinase nepenthesin-1						26.6
GRMZM2G012140	beta 1,3 glucan hydrolase			11.75			5.2
GRMZM2G019619	beta 1,3 glucan hydrolase			3.96			2.74
GRMZM2G179768	metalloendoproteinase 1 (LOC100285384), mRNA			5.94			5.15
GRMZM2G125032	Cellulase	12.08		6.45		3.57	5.87
GRMZM2G168115	aspartic-type endopeptidase/ pepsin A (LOC100281436), mRNA	6.51		6.03		3.3	7.23
GRMZM2G468657	aspartic proteinase nepenthesin-1	13.42	12.71	35.12		7.13	29.45
GRMZM2G067485	Bowman-Birk type trypsin inhibitor			-5.99			
GRMZM2G075315	putative Bowman-Birk serine protease inhibitor					2.8	
GRMZM2G156632	Bowman-Birk type wound-induced proteinase inhibitor WIP1 Precursor	14.68		6.58	6.92	2.65	
GRMZM2G401374	cystatin8 (psei8)			-4.46			
GRMZM2G015869	cystinosin (LOC100283468), mRNA			3.48			
GRMZM2G404688	trypsin/factor XIIA inhibitor			-2.67			
GRMZM2G081464	Probable non-specific lipid-transfer protein 2 (LTP 2)		-3.83				
GRMZM2G387360	nonspecific lipid-transfer protein		-3.17	-3.33			
GRMZM2G089400	lipid binding protein			2.71			
GRMZM2G040689	LTP family protein	4.45		3.44			
GRMZM2G006047	LTP family protein			32.36			8.11
GRMZM2G136364	LTP family protein			-4.2			
GRMZM2G320373	nonspecific lipid-transfer protein AKCS9	17.47			10.97	3.27	3.75
GRMZM2G179800	dnaJ domain containing protein			2.64			
GRMZM2G011098	cell death.plants			3.28			
GRMZM2G339563	Lethal leaf-spot 1 Fragment			2.54			
GRMZM2G341658	cell death.plants			4.41			2.94
GRMZM2G170734	Chlorophyllase		89.39	296.23			113.86
GRMZM2G467184	calmodulin-like protein 1			2.31			
GRMZM2G015912	EF hand family protein			13.35			
GRMZM2G459663	EF hand family protein			9.93			6.63
GRMZM2G459663	EF hand family protein			6.78			6.61
GRMZM2G053833	EF hand family protein			6.41		3.86	5.63
GRMZM2G033846	caltractin		7.17	10.71			3.94
GRMZM2G031876	calmodulin binding protein	6.72	10.15	18.72			6
GRMZM2G056467	calmodulin binding protein			11.66		3.28	10.92
GRMZM2G424509	signalling related protein						3.41
GRMZM2G077744	signal recognition particle 19 kDa protein	-3.99					
GRMZM2G005652	G-protein			3.11			
GRMZM2G429113	G-protein			2.62			
GRMZM2G055469	G-protein			3.18			2.9
GRMZM2G016290	G-protein			4.31			4.33
GRMZM2G062121	G-protein		64.49	69.38			16.91
GRMZM2G157727	phytochromeA1 (phyA1)			3.46			
GRMZM2G099097	wax metabolism gene			3.42			
GRMZM2G083526	Octadecanal decarbonylase			2.71			
GRMZM2G077375	Long-chain-alcohol O-fatty-acyltransferase			6.65		5.13	5.91
GRMZM2G143494	strictosidine synthase 3 (LOC100284402), mRNA						4.24
GRMZM2G093125	Tyrosine/DOPA decarboxylase 2	74.08	36.15	118.94			54.71
GRMZM2G021277	alkaloid-like metabolism gene	69.49	175.14	131.08			46.3
GRMZM2G056469	alkaloid-like metabolism gene	138.08	11.59	46.1		9.34	48.69
GRMZM2G021388	alkaloid-like metabolism gene	10.13	19.38	55.33		9.18	37.24

Table S2 Continued

gene name	annotation	Af24hpi	Af48hpi	Af72hpi	Fv24hpi	Fv48hpi	Fv72hpi
GRMZM2G043295	Trans-zeatin O-beta-D-glucosyltransferase			-3.89			
GRMZM2G051474	Trans-zeatin O-beta-D-glucosyltransferase			2.78			
GRMZM2G426242	Trans-zeatin O-beta-D-glucosyltransferase			7.2			6.88
AC206788.3_FG015	Trans-zeatin O-beta-D-glucosyltransferase		6.89	17.41			8.22
GRMZM2G035755	Trans-zeatin O-beta-D-glucosyltransferase		15.29	37.94			7.97
GRMZM2G130119	Trans-zeatin O-beta-D-glucosyltransferase	11.6	4.82	14.27			9.19
GRMZM2G372068	Trans-zeatin O-beta-D-glucosyltransferase	4.32	4.22	8.8		4.36	7.65
GRMZM2G179063	Trans-zeatin O-beta-D-glucosyltransferase	9.49	75.2	56.6		15.05	29.37
GRMZM2G067424	flavonol-3-O-glycoside-7-O-glucosyltransferase 1		8.05				
GRMZM2G175812	chalcones metabolism gene			5.36			
GRMZM2G007795	hydroquinone glucosyltransferase						8.14
GRMZM2G146234	dihydroflavonol metabolism gene			2.91			2.77
GRMZM2G152175	dihydroflavonol-4-reductase			4.13			3.88
AC212219.3_FG005	Flavanone 3-dioxygenase			147.35			117.35
GRMZM2G062396	Flavanone 3-dioxygenase	13.36		8.12			5.38
GRMZM2G050234	Flavanone 3-dioxygenase		15.28	40.34		9.43	34.81
GRMZM2G162158	leucoanthocyanidin dioxygenase			19.21			6.35
GRMZM2G098569	Dimethylallyltranstransferase	3.19		5.96			3.63
GRMZM2G175076	chalcone--flavonone isomerase	7.22		8.54		3.63	8.61
GRMZM2G382785	anthocyanin 5-aromatic acyltransferase'	9.96	9.82	27.66		4.25	13.66
GRMZM2G174192	anthocyanidin 3-O-glucosyltransferase	8.46	8.06	10.17		3.43	9.75
GRMZM2G422750	Chalcone synthase C2 (EC 2.3.1.74)(Naringenin-chalcone synthase C2)	5.8	5.79	6.2		10.74	9.62
GRMZM2G105644	geranylgeranyl hydrogenase			-3.53			
GRMZM2G127087	terpene synthase 6			20.92			
GRMZM2G127087	terpene synthase 6	12.89		9.45			
GRMZM5G856881	2-C-methyl-D-erythritol 4-phosphate cytidylyltransferase			9			
GRMZM2G172032	2-C-methyl-D-erythritol 4-phosphate cytidylyltransferase			7.7			5.11
GRMZM2G056975	dxr protein			4.97			3.7
GRMZM2G102550	Putative geranylgeranyl pyrophosphate synthase 2	3.7		11.15			7.72
GRMZM2G137409	hydroxymethylbutenyl 4-diphosphate synthase	5.31		6.97			5.25
GRMZM2G027059	4-hydroxy-3-methylbut-2-enyl diphosphate reductase	4.99		6.71			5.24
GRMZM2G132169	L-ascorbate oxidase			5.02			
GRMZM2G320786	simple phenol metabolism gene	42.73	53.47	620.11		9.84	240.87
GRMZM2G169033	putative laccase	6.14	10.66	44.48		6.85	34.92
GRMZM2G016890	Beta-glucosidase, chloroplastic Precursor (EC 3.2.1.21)(Gentiobiase)(Cellobiase)(Beta-D-glucoside glucohydrolase)			622.86			
GRMZM2G016890	Beta-glucosidase, chloroplastic Precursor (EC 3.2.1.21)(Gentiobiase)(Cellobiase)(Beta-D-glucoside glucohydrolase)	29.42		49.79			10.08
GRMZM2G048522	Trans-feruloyl-CoA synthase	21.66					
GRMZM2G090980	CAD			41.94			
GRMZM2G090980	CAD			12.14			8.71
GRMZM2G139874	C4H			4.56			
GRMZM2G147245	C4H	3.91		5.15			3.65
GRMZM2G100158	F5H	11.08		7.89		5.23	10.78
GRMZM2G334660	PAL	17.67	4.86	11.19		6.37	14.11
GRMZM2G160541	Phenylalanine ammonia-lyase			5.42			
GRMZM2G160541	Phenylalanine ammonia-lyase			4.77			9.73
GRMZM2G170692	Phenylalanine ammonia-lyase	27.85	11.12	24.38	9.45	9.37	22.35
GRMZM2G118345	phenylalanine ammonia-lyase	13.28	5.14	6.14		3.47	5.7
GRMZM2G443445	mannitol dehydrogenase		12.29	26.8			
GRMZM2G075333	Trans-feruloyl-CoA synthase			2.85		2.42	
GRMZM2G048522	Trans-feruloyl-CoA synthase						13.66
GRMZM2G099420	Cinnamoyl-CoA reductase					2.96	4.01
GRMZM2G423331	Quercetin 3-O-methyltransferase	38.91	6.67	15.4	14.98	6.67	12.42
GRMZM2G362298	phenylpropanoid metabolism gene			11.88			
GRMZM2G061806	phenylpropanoid metabolism gene			2.95			3.42
GRMZM2G093092	phenylpropanoid metabolism gene			9.45			8.65
GRMZM2G099297	phenylpropanoid metabolism gene			3.42			3.32
GRMZM2G141026	phenylpropanoid metabolism gene			48			23.89
GRMZM2G127418	phenylpropanoid metabolism gene	15.05		13.35			6.65
GRMZM2G115422	phenylpropanoid metabolism gene			2.7		2.53	3.2

Table S2 Continued

gene name	annotation	Af24hpi	Af48hpi	Af72hpi	Fv24hpi	Fv48hpi	Fv72hpi
GRMZM2G057483	phenylpropanoid metabolism gene	10.42		2.95		3.58	5.23
GRMZM2G125448	phenylpropanoid metabolism gene	13.92		5.78		5.36	13.81
GRMZM2G064969	phenylpropanoid metabolism gene	16.17		9.51		5.24	10.89
GRMZM2G124815	phenylpropanoid metabolism gene	3.94	5.12	18.52		3.23	12.73
GRMZM2G336824	phenylpropanoid metabolism gene	53.16	9.19	116.13		7.51	76.36
GRMZM2G114918	phenylpropanoid metabolism gene	20.38	13.59	16.54		12.55	18.57
GRMZM2G015793	phenylpropanoid metabolism gene	6.67	5.83	7.57		5.54	7.61
GRMZM2G311036	phenylpropanoid metabolism gene	18.35	5.63	18.41		3.4	16.63
GRMZM2G082034	beta-amylase			6.53			
GRMZM2G035749	Beta-amylase			3.5			
GRMZM2G070172	Alpha-amylase	19.09		38.47			57.38
GRMZM2G138468	alpha-amylase	175.34	26.51	79.76			129.2
GRMZM2G026889	transferase, transferring glycosyl groups	5.76		6.28		2.64	7.03
GRMZM2G119689	miniature seed1		-5.42	-4.09			
GRMZM2G089836	invertase2 (ivr2)			2.98			
GRMZM2G139300	cell wall invertase1 (incw1)			5.6			
GRMZM2G394450	invertase1 (ivr1)	8.76		15.39			8.28
GRMZM2G097641	Sucrose-phosphatase 2 (ZmSPP2)(EC 3.1.3.24)			51.13			24.45
GRMZM2G032619	inorganic diphosphatase			3.35			
GRMZM2G120079	Inorganic diphosphatase			198.64			124.59
GRMZM2G150906	stachyose synthase			-3.75			
GRMZM2G146463	Galactinol--raffinose galactosyltransferase			-3.07			
GRMZM2G415579	NAD(P)H-dependent oxidoreductase			2.52			
GRMZM2G127147	alkaline alpha galactosidase 2			9.08			
GRMZM2G118462	Alpha,alpha-trehalose-phosphate synthase (UDP-forming)			2.92			
GRMZM2G178546	trehalose-phosphate phosphatase			3.32			
GRMZM2G132875	minor CHO metabolism gene			16.31			
GRMZM2G479423	minor CHO metabolism gene			3.45			
GRMZM2G066413	carbon concentrating related gene			5.17			
GRMZM2G085019	NADP-dependent malic enzyme, chloroplastic Precursor (NADP-ME)(EC 1.1.1.40)			20.27			
GRMZM5G810727	gluco-, galacto- and mannosidase			-3.72			
GRMZM2G426467	gluco-, galacto- and mannosidase						41.72
GRMZM2G120962	gluco-, galacto- and mannosidase			185.1			74.38
GRMZM2G029243	gluco-, galacto- and mannosidase	24.1		62.66			44.18
GRMZM2G057930	UDP glucosyl and glucoronyl transferase			-3.96			
GRMZM2G111428	UDP glucosyl and glucoronyl transferase			6.17			
GRMZM2G086925	UDP glucosyl and glucoronyl transferase			9.05			
GRMZM2G344993	UDP glucosyl and glucoronyl transferase			3.31			
GRMZM2G099740	UDP glucosyl and glucoronyl transferase			4.86			3.6
GRMZM2G066067	UDP glucosyl and glucoronyl transferase	6.52		5.3		3.07	6.4
GRMZM2G173192	Glycerol-3-phosphate dehydrogenase (NAD(+))			16.8		18.97	12.32
GRMZM5G801949	sugar carrier protein C	10.91					
GRMZM2G418343	sugar transporter		-3.5	-7.27			
GRMZM2G160430	sugar transporter			3.58			
GRMZM2G066801	major facilitator superfamily protein			2.93			
GRMZM2G160614	sugar transport protein 14	9.09		18.56			
GRMZM2G064437	sugar transporter					2.93	
GRMZM2G087901	sucrose transporter		-6.2	-4.24			
GRMZM2G004694	sugar transporter			7.62			
GRMZM2G066820	arabinose-proton symporter			3.17			
GRMZM2G060183	sugar transporter			2.46			
GRMZM2G135739	monosaccharide transporter1	10.53		3.81			
GRMZM2G019974	carbohydrate transporter/ sugar porter	10.66		18.13			10.72
GRMZM2G404965	hexose carrier protein HEX6	5.51		7.93		7.08	5.6
GRMZM2G035599	ribose-5-phosphate isomerase			5			3.59
GRMZM2G358153	calvin cycle related gene	10.81	5.14	17.06		3.9	14.1
GRMZM2G057093	calvin cycle related gene			18.98			13.69
GRMZM2G015132	dihydrolipoamide S-acetyltransferase			2.64			
GRMZM2G010823	Fumarate hydratase			2.58			
GRMZM2G087259	carbonic anhydrase			7.8			
GRMZM2G113191	carbonic anhydrase	15.69		7.86		3.46	6.19
GRMZM2G134708	Monodehydroascorbate reductase (NADH)			6.9			
GRMZM2G113165	Monodehydroascorbate reductase (NADH)			107.03			127.85
GRMZM2G025366	Isocitrate dehydrogenase (NAD(+))			3.01			

Table S2 Continued

gene name	annotation	Af24hpi	Af48hpi	Af72hpi	Fv24hpi	Fv48hpi	Fv72hpi
GRMZM2G088689	2-oxoisovalerate dehydrogenase (acylating)			4.57			
GRMZM2G118800	Methylmalonate-semialdehyde dehydrogenase (acylating)	4.35		5.36			
GRMZM2G015844	H(+)-transporting two-sector ATPase		3.59	8.16			3.82
GRMZM2G122431	cellulose synthase (UDP-forming)			2.88			
GRMZM2G103972	Cellulose synthase (UDP-forming)	29.93		12.2		5.77	14.43
GRMZM2G014558	CSLE6 - cellulose synthase-like family E			9.42			4.96
GRMZM2G470010	hemicellulose biosynthesis gene			20.35			16.56
GRMZM2G103128	hemicellulose biosynthesis gene			3.89			3.66
GRMZM2G147756	Polygalacturonase			-2.91			
GRMZM2G098912	Polygalacturonase			-4.73			-2.96
GRMZM2G318299	Pectinesterase			5.5			
GRMZM2G380284	Pectinesterase			159.39			140.5
GRMZM2G025105	polygalacturonase inhibitor	23.77	18.32	41.15		12.55	35.02
GRMZM2G174708	polygalacturonase inhibitor 1	24.33	6.98	20.1		6	16.08
GRMZM2G055101	cell wall degradation related gene			3.08			
GRMZM5G800586	cell wall degradation related gene		3.53			3.44	
GRMZM2G333980	cell wall degradation related gene	7.72	5.2	14.17		3.7	4.68
GRMZM2G094523	cell wall modification related gene			-2.88			
GRMZM2G113761	xyloglucan endotransglucosylase/hydrolase protein 32		-4.78	-4.48			
GRMZM2G392125	xyloglucan endotransglucosylase/hydrolase protein 15			3.01			3.27
GRMZM2G342246	beta-expansin 7			6.27			
GRMZM2G173826	cell wall modification related gene			23.19			
GRMZM2G146540	cell wall modification related gene			103.1			
GRMZM2G021427	cell wall modification related gene						-4.17
GRMZM2G099491	LRR cell wall protein			3.62			2.82
GRMZM2G003917	AGP		6.78				
GRMZM2G074401	omega 3 desaturase			4.01			
GRMZM2G353444	Triacylglycerol lipase			-4.32			
GRMZM2G075456	Triacylglycerol lipase			97.57			
GRMZM2G080940	Triacylglycerol lipase			3.49			
GRMZM2G174860	Triacylglycerol lipase						7.04
GRMZM2G085176	Triacylglycerol lipase			3.92			3.06
GRMZM2G036217	acyl CoA reductase			5.27			
GRMZM2G172098	Acylglycerol lipase			4.52		2.92	4.42
GRMZM2G152179	Flavonol 3-sulfotransferase		3.38	3.04			
GRMZM2G124276	protein SUR2						24.34
GRMZM2G106177	erg28 like protein	5.3		6.09			5.75
GRMZM2G315726	lipid metabolism gene	8.32	6.21	11.62			7.88
GRMZM2G044337	lipid metabolism gene			2.7			
GRMZM2G058630	lipid metabolism gene			4.79			5.15
GRMZM2G174621	lipid metabolism gene			4.44			7.75
GRMZM2G105330	acyl coa ligase			2.61			
GRMZM2G143625	acyl-desaturase (LOC100284973), mRNA			6.54			
GRMZM2G157269	Acetate--CoA ligase			2.75			
GRMZM2G135027	1-acylglycerol-3-phosphate O-acyltransferase			2.46			
GRMZM2G070304	1-acylglycerol-3-phosphate O-acyltransferase	32.78	44.39	55.43		15.6	35.11
GRMZM2G063024	Beta-ketoacyl-acyl-carrier-protein synthase I			3.99			
GRMZM2G160417	Beta-ketoacyl-acyl-carrier-protein synthase I			2.95			
GRMZM2G104626	Beta-ketoacyl-acyl-carrier-protein synthase I			7.49			4.19
GRMZM2G059637	Glycerol-3-phosphate O-acyltransferase			5.72			
GRMZM2G065203	Glycerol-3-phosphate O-acyltransferase						-3.86
GRMZM2G166176	Glycerol-3-phosphate O-acyltransferase			7.18			5.42
GRMZM2G169240	Delta(12)-fatty-acid desaturase	14.63		10.16			
GRMZM2G169261	Delta(12)-fatty-acid desaturase	19.62		7.96			
GRMZM2G425249	Ethanolamine kinase	3.49		3.2			
GRMZM2G079109	abhydrolase domain-containing protein 5		3.41	5.86			
GRMZM5G812228	ACS-like protein			11.26			9.73
GRMZM2G077187	Phosphatidate phosphatase	6.59		8.12			5.84
GRMZM2G439268	lipid transfer proteins			-11.73			
GRMZM2G010868	phospholipid transfer protein					3.3	
GRMZM2G087462	GDSL-motif lipase		-9.03				
GRMZM2G700208	GDSL-motif lipase		14.05				
GRMZM2G158205	GDSL-motif lipase			-3.3			
GRMZM2G465046	GDSL-motif lipase			5.66			
GRMZM2G022279	GDSL-motif lipase			3.37			

Table S2 Continued

gene name	annotation	Af24hpi	Af48hpi	Af72hpi	Fv24hpi	Fv48hpi	Fv72hpi
GRMZM2G048200	GDSL-motif lipase						2.87
GRMZM2G335280	GDSL-motif lipase			7.95			10.49
GRMZM2G087827	esterase	8.73	8.85	29.72		9.73	28.31
GRMZM2G117030	alpha-L-fucosidase 2			-3.72			
GRMZM2G060866	anther-specific proline-rich protein APG			12.44			
GRMZM2G147701	2,3-dihydro-2,3-dihydroxybenzoate dehydrogenase			5.87			
GRMZM2G167431	2,3-dihydro-2,3-dihydroxybenzoate dehydrogenase						3.07
GRMZM2G052288	diaminopimelate decarboxylase			3.32			
GRMZM2G098875	Glutamate decarboxylase			2.73			
GRMZM2G153536	branched-chain-amino-acid aminotransferase			3.29			
GRMZM2G163925	phosphoribosylanthranilate transferase			2.96			
GRMZM2G005024	Tryptophan synthase beta chain 2, chloroplastic Precursor; Fragment (EC 4.2.1.20)(Orange pericarp 2)			2.76			
GRMZM2G454719	3-deoxy-7-phosphoheptulonate synthase	43.58		61.69			
GRMZM2G396212	3-deoxy-7-phosphoheptulonate synthase			7.2			4.1
GRMZM2G139813	Tyrosine transaminase		37.16	7.62			
GRMZM2G464137	S-methyl-5-thioribose kinase			3.65			3.38
GRMZM2G010468	Trans-cinnamate 4-monooxygenase			17			13.41
GRMZM2G028677	trans-cinnamate 4-monooxygenase	11.03	4.5	8.94		6.6	13.02
GRMZM2G181227	CHY1	5.41		9.47			4.99
GRMZM2G181135	Histidinol-phosphate transaminase	4.3		8.6			4.89
GRMZM2G125923	prephenate dehydratase	3.64		3.48			3.33
GRMZM2G437912	Prephenate dehydratase			3		2.26	3.35
GRMZM5G802221	serine acetyltransferase1 (sat1), mRNA	4.2	5.56	12.43		3.72	10.93
GRMZM2G117956	proline oxidase			-2.82			
GRMZM2G381051	Isovaleryl-CoA dehydrogenase			3.31			
GRMZM2G021406	lysine decarboxylase-like protein			4.06			
GRMZM2G076394	O-methyl transferases			3.65			
GRMZM2G047613	Carboxylesterase			6.11			
GRMZM2G043579	esterase PIR7B						4.05
GRMZM2G428987	esterase PIR7B			13.03			12.92
GRMZM2G080839	troponine reductase	20.1	3.97	9.94		5.29	21.63
GRMZM2G403076	troponine reductase	14.6		9.15	6.98	3.29	10.81
GRMZM2G151801	troponine reductase						4.21
GRMZM2G177812	ABC transporter C05D10.3 in chromosome III						3.8
GRMZM2G319138	ABC transporter	9.41					
GRMZM2G391815	ABC transporter		28				
GRMZM5G892675	ABC transporter			7.24			
GRMZM2G054332	ABC transporter			2.85			
GRMZM2G115658	ABC transporter			3.69			
GRMZM2G142870	ABC transporter		4.76	3.72			
GRMZM2G003411	ABC transporter						6.2
GRMZM2G035276	ABC transporter						6.71
GRMZM2G161310	ABC transporter			7.09			5.52
GRMZM2G336448	ABC transporter	4.05	12.07	13.87			6.51
GRMZM2G099619	ABC transporter	5.17		15.66		3.38	10.54
GRMZM2G134888	amino acid permease	11.14		33.01			24.02
GRMZM2G145989	amino acid permease 1	3.82					2.58
GRMZM2G175321	AATL2						6.69
GRMZM2G149216	LHT1 (LOC100285777), mRNA						8.91
GRMZM2G127328	LHT1	14.21		6.19			6.1
GRMZM2G136300	amino acid transporter			3.54			
GRMZM2G082434	amino acid transporter			8.47			
GRMZM2G136508	amino acid permease	5.64		3.62			
GRMZM5G805732	amino acid transporter	6.1					3.99
GRMZM2G332562	amino acid transporter			3.7			2.97
GRMZM2G036448	amino acid transporter			8.91			11.85
GRMZM2G082434	amino acid transporter			10.77			8.65
GRMZM2G175140	ammonium transporter			5.17			
GRMZM2G107481	ATPase						10.04
GRMZM2G407825	ATPase			5.41			2.95
GRMZM2G090528	cyclic nucleotide-gated ion channel 2			-4.55			
GRMZM2G129375	cyclic nucleotide or calcium regulated channel related transporter			3.57			2.85
GRMZM2G063975	plasma membrane associated protein		5.5				
GRMZM2G057283	plasma membrane associated protein			5.03			

Table S2 Continued

gene name	annotation	Af24hpi	Af48hpi	Af72hpi	Fv24hpi	Fv48hpi	Fv72hpi
GRMZM2G075828	transparent testa 12 protein			3.17			
GRMZM5G842695	transparent testa 12 protein (LOC100282798), mRNA			-3.73			-3.36
GRMZM2G011078	SC3 protein			3.33			
GRMZM2G133006	transporter		10.19				
GRMZM2G010765	transporter			7.82			
GRMZM2G010765	transporter			7.3			
GRMZM2G151903	transporter			5.46			
GRMZM2G115105	transporter			4.89			
GRMZM2G089952	transporter			3.41			
GRMZM2G031938	transporter	4.76		7.2			
GRMZM2G072034	transporter					2.94	
GRMZM2G166459	transporter						3.33
GRMZM2G704053	transporter			2.71			2.86
GRMZM2G027016	transporter	8.12		3.79			4.56
GRMZM2G470075	transporter	7.33	7.34	6.31			3.88
GRMZM2G135175	transporter					9.63	34.23
GRMZM2G080992	transporter	10.72	9.53	26.72		5.7	21.14
GRMZM2G093090	Aquaporin TIP4-4 (Tonoplast intrinsic protein 4-4)(ZmTIP4-4)(ZmTIP4;4)			-4.77			
GRMZM2G168439	Aquaporin TIP1-2 (Tonoplast intrinsic protein 1-2)(ZmTIP1-2)(ZmTIP1;2)			9.71			
GRMZM2G081843	Aquaporin PIP1-5 (Plasma membrane intrinsic protein 1-5)(ZmPIP1-5)(ZmPIP1;5)(ZmPIP1-5b)			20.77			7.1
GRMZM2G154628	Aquaporin PIP2-4 (Plasma membrane intrinsic protein 2-4)(ZmPIP2-4)(ZmPIP2;4)			3.95			3.55
GRMZM2G160710	ATFP4	7.29					
GRMZM2G169726	ATFP4			3.41			4.26
GRMZM2G119975	ATFP4	5.13		10.35		3.65	12.68
GRMZM2G118497	metal transporter			-3.05			
GRMZM2G014454	metal transporter			2.7			
GRMZM2G003179	metal transporter			3.27			2.73
GRMZM2G150450	Copper-exporting ATPase			-5.39			
GRMZM2G169788	Copper-exporting ATPase			3.12			
GRMZM2G092867	metal ion binding protein			3.83			
GRMZM2G080887	mitochondrial membrane associated transporter			22.6		13.66	13.41
GRMZM2G331393	mitochondrial membrane associated transporter			20.99		4.46	12.87
GRMZM2G009045	mitochondrial membrane associated transporter	19.43	5.8	32.6		5.04	20.94
GRMZM2G179294	high affinity nitrate transporter			4.59			
GRMZM2G455124	nitrate transporter	5.73		2.87			2.85
GRMZM2G113800	nucleotide transporter	4.68		3.35			
GRMZM2G044851	peptides and oligopeptides transporter	-5.38		-5.68			
GRMZM2G026459	peptides and oligopeptides transporter			8.43			
GRMZM2G150468	peptides and oligopeptides transporter						27.43
GRMZM2G112456	oligopeptide transporter 4			10.93			
GRMZM2G326707	phosphate transporter protein1	3.93					
GRMZM2G154090	phosphate transporter protein2	18.09					11.51
GRMZM2G112377	inorganic phosphate transporter 3			106.63			24.12
GRMZM2G142919	sialin	4.12		5.97			4.19
GRMZM2G020766	potassium transporter			3.36			
GRMZM2G142661	potassium transporter			3.36			
GRMZM2G097505	potassium transporter						9.5
GRMZM2G084779	potasium ion uptake permease 1	16.96	6.29	14.63		3.19	13.51
GRMZM2G154211	sulphate transporter			-3.46			
GRMZM2G158013	sulphate transporter			7.94			
GRMZM2G042171	sulphate transporter			5.32			
GRMZM2G342907	sulphate transporter	19.67		23.02			15.84
GRMZM2G140754	Alanine--tRNA ligase			5.44			4.4
GRMZM2G027851	Sodium/hydrogen exchanger Fragment			6.32			
GRMZM2G089631	unspecified cation transporter	39.76	9.51				
GRMZM2G121070	unspecified cation transporter			4.32			3.11
GRMZM2G176430	unspecified cation transporter		9.77	29.86			10.66
GRMZM2G126572	transposon protein			9.62			7.88
GRMZM5G828581	transporter			6.64			
GRMZM2G030831	cytochrome P450			-2.93			
GRMZM2G126055	cytochrome P450		-4.88	-4			
GRMZM2G175250	cytochrome P450		-4.63	-3.19			

Table S2 Continued

gene name	annotation	Af24hpi	Af48hpi	Af72hpi	Fv24hpi	Fv48hpi	Fv72hpi
GRMZM2G075244	Cytochrome P450 CYP709C14			59.12			
GRMZM2G021436	Cytochrome P450 monooxygenase CYP72A26			9.15			
GRMZM2G129860	cytochrome P450			13.19			
GRMZM2G181236	cytochrome P450			40.28			
GRMZM2G138074	5-O-(4-coumaroyl)-D-quinate 3'-monooxygenase			5.39			
GRMZM2G321033	Flavonoid 3'-monooxygenase			3.32			
GRMZM2G014395	cytochrome P450		7.49	6.83			
GRMZM2G021310	cytochrome P450		39.55	5.28			
GRMZM2G159353	cytochrome P450					2.52	
GRMZM2G040728	cytochrome P450					3.8	
GRMZM2G154828	cytochrome P450	7.68	4.44	11.29		4.15	
GRMZM2G123037	cytochrome P450						-3.72
GRMZM2G370745	cytochrome P450 10						3.47
GRMZM2G171118	Cytochrome P450 CYP71W7						9.8
GRMZM2G024331	cytochrome P450			7.96			6.93
GRMZM2G134597	cytochrome P450			15.02			12.32
GRMZM2G147774	cytochrome P450			134.74			105.6
GRMZM2G148441	cytochrome P450			3.63			4.29
GRMZM2G407650	cytochrome P450			22.84			13.9
GRMZM2G075461	cytochrome P450			274.83			126.41
GRMZM2G056247	cytochrome P450			3.73			3.09
GRMZM2G138008	cytochrome P450	5.43		3.96			3.67
GRMZM2G164074	cytochrome P450	5.97		6.53			3.95
GRMZM2G090432	Cytochrome P450 CYP81A9		12.68	9.2			4
GRMZM2G129860	cytochrome P450		5.19	10.07			8.58
GRMZM2G312069	cytochrome P450		13.18	27.79			8
GRMZM2G075244	Cytochrome P450 CYP709C14	7.66	13.61	29.25			19.72
GRMZM2G181236	cytochrome P450	10.52	35.62	59.67			14.81
GRMZM2G118809	cytochrome P450	12.92		6.59		3.17	5.93
GRMZM2G154870	cytochrome P450	8.64		5.4		4.39	4.47
GRMZM2G069722	cytochrome P450	17.18	72.3	81.49		17.22	17.59
GRMZM2G067591	cytochrome P450	74.13	15.43	40.09		3.63	6.97
GRMZM2G087875	cytochrome P450	7.52	18.94	26.38		4.32	11.99
GRMZM2G147752	cytochrome P450	12.36	10.05	37.41		5.71	21.42
GRMZM2G122654	cytochrome P450	19.9	6.25	20.84	7.28	3.77	13.82
GRMZM2G021378	vesicel associated transporter			2.44			
GRMZM2G029270	vesicel associated transporter			7.96			7.52
GRMZM2G414540	syntaxin 121			3.06			3.09
GRMZM2G397044	peptidylprolyl isomerase			2.91			
GRMZM2G462118	cell cycle related gene			6.27			
GRMZM2G311003	cell division related gene			17.91			
GRMZM2G073693	lectin-like protein			3.85			
GRMZM2G109842	Profilin-2 (ZmPRO2)						15.17
GRMZM2G016435	dynein light chain LC6, flagellar outer arm			9.69			7.7
GRMZM2G123977	protein binding protein			4.36			3.09
GRMZM2G375593	cell organization related gene	4.73					
GRMZM2G090728	cell organization related gene			-5.96			
GRMZM2G043857	cell organization related gene			3.96			
GRMZM2G053284	cell organization related gene			7.53			7.98
GRMZM2G018375	Thiazole biosynthetic enzyme 1-1, chloroplastic Precursor	-2.89					
GRMZM2G135816	molybdenum cofactor			3.88			
GRMZM2G105466	GTP cyclohydrolase II						2.75
GRMZM2G502035	meg2 protein	-8.29	-16.71				
GRMZM2G021614	phosphatidylethanolamine-binding protein9 (zcn9)			-3.73			
GRMZM2G114619	actin binding protein			4.58			
GRMZM2G103617	B12D protein			2.84			
GRMZM2G092968	meiosis 5			10.59			
GRMZM2G131087	senescence-associated protein DIN1			18.56			
GRMZM2G310947	cell Division Protein AAA ATPase family		3.31	4.56			
GRMZM2G063287	embryonic protein DC-8					2.36	
GRMZM2G118441	nodulin-like protein			-4.86			-3.12
GRMZM2G119755	cell number regulator 7						6.35
GRMZM2G148904	embryonic abundant protein-like			28.72			10.59
GRMZM2G148904	embryonic abundant protein-like			13.98			18.07
GRMZM2G175444	lachrymatory-factor synthase			7.1			9.45

Table S2 Continued

gene name	annotation	Af24hpi	Af48hpi	Af72hpi	Fv24hpi	Fv48hpi	Fv72hpi
GRMZM2G153358	seven-transmembrane-domain protein 1			7.86			9
GRMZM2G114048	YZ1			2.87			3.23
GRMZM2G045155	B12D protein (LOC100280945), mRNA					2.75	3.76
GRMZM2G467893	development related gene	5.86					
GRMZM2G141325	development related gene			-8.13			
GRMZM2G171752	development related gene			-3.42			
GRMZM2G129879	development related gene	-3.86		-3.91			
GRMZM2G324903	development related gene			3.2			
GRMZM2G113726	development related gene			3.34			
GRMZM2G088053	development related gene					3.15	
GRMZM2G009080	development related gene						6.96
GRMZM2G179349	development related gene			9.72			7.82
GRMZM2G075563	development related gene			5.68			4.79
GRMZM2G073114	development related gene	9.89		16.04			27.2
GRMZM2G043893	Prolyl aminopeptidase			9.94			
GRMZM2G043893	Prolyl aminopeptidase	6.7		8.38			6.99
AF546188.1_FG007	Zein-alpha 19C2 Precursor (19 kDa zein 19C2)			-3.11			
GRMZM2G349749	storage protein	20.52		23.5		8.17	41.47
GRMZM2G154523	storage protein	42.17		25.44		13.37	25.88
GRMZM2G447984	Histone H3.2			-2.82			
GRMZM2G448458	histone						3.79
GRMZM2G053779	Blue copper protein			-3.81			
GRMZM2G027198	blue copper protein	4.47	6.47	10.33		2.45	5.33
GRMZM2G010762	early nodulin-like protein 3		-4.37	-3.69			
GRMZM2G148884	uclacyanin-2						-4.76
GRMZM2G043300	chemocyanin						8.34
GRMZM2G023847	plastocyanin-like	5.69	5.16	11.2		3.11	7.98
GRMZM2G123407	plastocyanin-like			-3.63			
GRMZM2G086628	plastocyanin-like						12.44
GRMZM2G141607	2,3-dihydro-2,3-dihydroxybenzoate dehydrogenase			-3.72			
GRMZM2G009188	2,3-dihydro-2,3-dihydroxybenzoate dehydrogenase			7.26			
GRMZM2G143669	2,3-dihydro-2,3-dihydroxybenzoate dehydrogenase			273.44			47.03
GRMZM2G458659	2,3-dihydro-2,3-dihydroxybenzoate dehydrogenase		275.17	346.68			58.25
GRMZM2G148355	2,3-dihydro-2,3-dihydroxybenzoate dehydrogenase		305.13	416.82			63.25
GRMZM2G354909	2,3-dihydro-2,3-dihydroxybenzoate dehydrogenase	9.78	9.79	25.95		4.24	18.89
GRMZM2G170017	2,3-dihydro-2,3-dihydroxybenzoate dehydrogenase	22.85	16.29	56.12	8.96	6.25	30.28
GRMZM2G135277	alcohol dehydrogenase (NAD)			-5			
GRMZM2G308351	Alcohol dehydrogenase						12.66
GRMZM2G118183	alcohol dehydrogenase (NAD)		19.58	57.67			16.89
GRMZM2G087323	Beta-ketoacyl reductase GL8B			3.4			
GRMZM2G025885	Hydroxymethylbilane synthase						3.42
GRMZM2G455809	Sex determination protein tasselseed-2		9.4	19.01			9.95
GRMZM2G170625	myrosinases-lectin-jacalin			-2.94			
GRMZM2G104655	myrosinases-lectin-jacalin						6.68
GRMZM2G015136	myrosinases-lectin-jacalin	12.27		5.83			5.64
GRMZM2G466298	myrosinases-lectin-jacalin		5.19	11.6		4.06	9.78
GRMZM2G038243	transferase family protein			-3.86			
GRMZM2G342856	N-acetyltransferase						3.61
GRMZM2G313101	allyl alcohol dehydrogenase-like protein	-2.85		-2.95			
GRMZM2G155058	calcineurin-like phosphoesterase family protein			3.29			2.75
GRMZM2G052825	oxidoreductase		3.77	6.57			3.9
GRMZM2G384884	oxidoreductase	4.04	4.91	17.93		3.29	11.65
GRMZM2G449133	hypothetical protein LOC100383654			-3.93			
GRMZM2G032910	hypothetical protein LOC100192768			3.67			
GRMZM2G055883	hypothetical protein LOC100382468						4.13
GRMZM2G048616	hypothetical protein LOC100191301		5.43	12.74			5.51
GRMZM2G135387	hypothetical protein LOC100382386	3.87	4.41	14.13		3.06	9.47
GRMZM2G154881	LOC100282281		5.1	15.38			5.17
GRMZM2G003796				-3.44			
GRMZM2G399530				5.88			4.46
GRMZM2G434792	Pyruvate decarboxylase		164.47				
GRMZM2G097706	cytosolic aldehyde dehydrogenase RF2D			-3.81			
GRMZM2G397055	UDP-glucose 6-dehydrogenase			10.16			6.27
GRMZM2G122715	calcium sensing receptor			3.92			3.54
GRMZM2G070912	metallothionein-like protein type 2					3.67	
GRMZM2G036629	metallothionein-like protein 1			5.4			5.56

Table S2 Continued

gene name	annotation	Af24hpi	Af48hpi	Af72hpi	Fv24hpi	Fv48hpi	Fv72hpi
GRMZM2G086163	metal ion binding protein			2.89			
GRMZM2G096008	metal handling related gene			11.25			5.42
GRMZM2G075502	metal handling related gene	4.06		7.39			5.55
GRMZM2G010348	Cytochrome c			2.54			
GRMZM2G070199	cytochrome c			3.38			
GRMZM2G145972	NADH-DH			4.66			
GRMZM2G041418	NADH-DH		21.23	24.61			8.73
GRMZM2G074761	transposon protein (LOC100281353), mRNA			40.83			15.74
GRMZM2G074743	alternative oxidase AOX3 precursor	35.62	19.13	141.83		8.21	79.97
GRMZM2G125669	alternative oxidase1	9.38	49.94	28.73		4.14	7.11
GRMZM2G427097	Glutamate dehydrogenase			2.48			
GRMZM5G878558	Nitrate reductase (NADH)			14.32			
GRMZM2G102959	Ferredoxin--nitrite reductase			5.51			
GRMZM2G133213	nitrate metabolism gene			2.93			3.12
GRMZM2G135385	Cytochrome b5			4.75		3.97	6.35
GRMZM2G082924	putative cytidine deaminase			3.27			
GRMZM2G091891	purine degradation related gene			5.48			5.22
GRMZM2G138355	nudix hydrolase 13			9.51			8.44
GRMZM2G034152	Polyamine oxidase Precursor (EC 1.5.3.14)(EC 1.5.3.15)			7.73			
GRMZM2G056350	MKI67 FHA domain-interacting nucleolar phosphoprotein-like	-3.81					
GRMZM2G125529	RNA binding protein			4.13			
GRMZM2G051043	RNA binding protein			2.8			
GRMZM2G177340	ribonuclease	10.2		22.36			12.48
GRMZM2G051270	ATP sulfurylase			4.36			
GRMZM2G000739	Uroporphyrinogen-III C-methyltransferase			7.61			3.58
GRMZM2G180080	mitochondrial protein						7.71
GRMZM2G105604	siroheme uroporphyrinogen methyltransferase1 (sum1)		6.16	19.91			6.21
GRMZM2G335593	verprolin			7.88			
GRMZM2G034206	LGC1 (LOC100281001), mRNA		-5.39				
GRMZM2G107142	PHI-1			-2.72			
GRMZM2G317614	nucleotide binding protein			11.83			
GRMZM2G003738	long cell-linked locus protein						6.39
GRMZM5G819965	Long cell-linked locus protein						2.81
GRMZM2G050159	membrane protein			3.67			6
GRMZM2G094602	protein binding protein	11.19		19.5			15.36
GRMZM2G076343	legume lectins beta domain containing protein	10	4.57	9.59		4.59	10.25
GRMZM2G045779	plant-specific domain TIGR01615 family protein			4			
GRMZM2G023081	PGPS/D12			4.82		3.87	8.03
GRMZM2G325477	PGPS/D12			8.99		8.19	15.95
GRMZM2G101409	VQ motif family protein (LOC100283271), mRNA						6.04
GRMZM2G420715	VQ motif family protein	4.01		7.57			6.33
GRMZM2G333049	VQ motif family protein			4.12		3.46	3.8
GRMZM2G138370	VQ motif family protein	11.97		9.13		7.62	10.19
GRMZM2G118172	VQ motif family protein			5.51		2.73	4.93
GRMZM2G180262	VQ					2.94	3.31
GRMZM2G171616	LOC100279655 (IDP1984), mRNA			2.85			
GRMZM2G066326	LOC100283433 (IDP105)		3.55	2.49			
GRMZM2G043878	LOC542242 (wusl1032), mRNA			21.08			92.7
GRMZM2G104961	Putative uncharacterized protein	-7.43					
GRMZM2G174168	Putative uncharacterized protein	-2.89					
GRMZM5G826547	Putative uncharacterized protein		11.72				
GRMZM2G044771	Putative uncharacterized protein			-3.45			
GRMZM2G045082	Putative uncharacterized protein			-3.51			
GRMZM2G057630	Putative uncharacterized protein			-3.27			
GRMZM2G094360	Putative uncharacterized protein			-3.29			
GRMZM2G129405	Putative uncharacterized protein			-2.91			
GRMZM2G171108	Putative uncharacterized protein			-3.35			
GRMZM2G404599	Putative uncharacterized protein			-3.2			
GRMZM2G424577	Putative uncharacterized protein			-2.79			
GRMZM5G824221	Putative uncharacterized protein			-4.31			
GRMZM5G847270	Putative uncharacterized protein			-3.09			
GRMZM2G079547	Putative uncharacterized protein		-4.95	-5.29			
GRMZM2G107931	Putative uncharacterized protein	-3.67	-5.38	-4.65			

Table S2 Continued

gene name	annotation	Af24hpi	Af48hpi	Af72hpi	Fv24hpi	Fv48hpi	Fv72hpi
GRMZM2G027447	Putative uncharacterized protein			3.84			
GRMZM2G037130	Putative uncharacterized protein			2.96			
GRMZM2G081333	Putative uncharacterized protein			79.4			
GRMZM2G081536	Putative uncharacterized protein			2.61			
GRMZM2G160454	Putative uncharacterized protein			4.13			
GRMZM2G333337	Putative uncharacterized protein			5.24			
GRMZM2G445616	Putative uncharacterized protein			3.51			
GRMZM2G542272	Putative uncharacterized protein			4.32			
GRMZM5G808266	Putative uncharacterized protein			15.07			
GRMZM5G816571	Putative uncharacterized protein			6.21			
GRMZM5G856773	Putative uncharacterized protein			3.7			
GRMZM5G877090	Putative uncharacterized protein			155.42			
GRMZM5G885104	Putative uncharacterized protein			3.77			
GRMZM5G886974	Putative uncharacterized protein			7.68			
GRMZM5G892535	Putative uncharacterized protein			14.1			
GRMZM2G100675	Putative uncharacterized protein		16.9	4.5			
GRMZM5G853055	Putative uncharacterized protein	13.53	7.61	15.97			
GRMZM2G413717	Putative uncharacterized protein			-3.89		2.27	
GRMZM2G129019	Putative uncharacterized protein			3.23		3.07	
GRMZM5G817967	Putative uncharacterized protein	12.2		5.71		3.8	
GRMZM5G802646	Putative uncharacterized protein						-5.56
GRMZM2G339866	Putative uncharacterized protein			-12.31			-4.29
GRMZM2G022014	Putative uncharacterized protein						2.65
GRMZM2G097524	Putative uncharacterized protein						8.29
GRMZM2G387594	Putative uncharacterized protein						2.77
GRMZM2G420883	Putative uncharacterized protein						3.15
GRMZM2G436856	Putative uncharacterized protein						8.5
GRMZM2G526706	Putative uncharacterized protein						3.25
GRMZM5G834345	Putative uncharacterized protein						7.92
GRMZM5G862843	Putative uncharacterized protein						3.32
GRMZM2G157218	Putative uncharacterized protein	6.94					5.3
AC198725.4_FG007	Putative uncharacterized protein			6.76			3.65
GRMZM2G382568	Putative uncharacterized protein			8.33			8.89
GRMZM5G818346	Putative uncharacterized protein			37.54			18.91
GRMZM5G820360	Putative uncharacterized protein			19.92			11.4
GRMZM5G820360	Putative uncharacterized protein			25.97			11.62
GRMZM5G845904	Putative uncharacterized protein			4.87			5.72
GRMZM5G858128	Putative uncharacterized protein			5.31			3.33
GRMZM5G859801	Putative uncharacterized protein			5.47			6.37
GRMZM5G895899	Putative uncharacterized protein			7.33			6.16
GRMZM5G895980	Putative uncharacterized protein			2.99			5.24
GRMZM2G000665	Putative uncharacterized protein	5.69		5.25			3.29
GRMZM5G821304	Putative uncharacterized protein	4.12		4.06			4.17
GRMZM5G853702	Putative uncharacterized protein	4.72		4.96			3.98
GRMZM5G871801	Putative uncharacterized protein	61.62		30.46			29.6
GRMZM2G089776	Putative uncharacterized protein		32.18	24.22			60.23
GRMZM5G805124	Putative uncharacterized protein	8.25	6.48	13.48			8.57
GRMZM5G872861	Putative uncharacterized protein	3.84	14.51	39.15			15.96
GRMZM2G000453	Putative uncharacterized protein			2.66		3	3.01
GRMZM2G137821	Putative uncharacterized protein			3.19		2.79	3.57
GRMZM2G396951	Putative uncharacterized protein			21.73		16.2	20.68
GRMZM5G810434	Putative uncharacterized protein	11.04		4.05		3	4.44
GRMZM5G868816	Putative uncharacterized protein		4.69	14.57		3.24	11.02
GRMZM5G803072	Putative uncharacterized protein	26.51	20.98	40.6		4.73	17.21
GRMZM5G806169	Putative uncharacterized protein	8.65	6.17	10.46		10.95	26.58
GRMZM5G873446	Putative uncharacterized protein	6.55	18.72	32.85		3.47	13.45
GRMZM2G022645	hypothetical protein LOC100272952, mRNA	3.1					
GRMZM2G423202	hypothetical protein LOC100275793, mRNA	6.97					
GRMZM2G047124	hypothetical protein LOC100381914, mRNA	-4.18	-4.72	-3.21			
GRMZM5G887949	hypothetical protein LOC100279644, mRNA			2.64			
GRMZM5G803881	hypothetical protein LOC100381887, mRNA			44.03			
GRMZM2G001332	hypothetical protein LOC100276009, mRNA						9.8
GRMZM2G175874	hypothetical protein LOC100279706, mRNA						4.09
GRMZM2G122028	hypothetical protein LOC100276388, mRNA			4.57			3.27
GRMZM2G420108	hypothetical protein LOC100277204, mRNA			4.4			6.72
GRMZM2G329069	hypothetical protein LOC100279141, mRNA			3.56			3.05

Table S2 Continued

gene name	annotation	Af24hpi	Af48hpi	Af72hpi	Fv24hpi	Fv48hpi	Fv72hpi
GRMZM2G001200	hypothetical protein LOC100382872, mRNA			3.06			3.73
GRMZM2G001375	hypothetical protein LOC100278795, mRNA		6.81	10.58			6.34
GRMZM2G056068	hypothetical protein LOC100382730, mRNA	4.18		10.65		3.25	7.42
GRMZM2G181236	hypothetical protein LOC100279598			59.74			
GRMZM2G097404	hypothetical protein LOC100273950	-5.07					
GRMZM2G137375	hypothetical protein LOC100275111	-2.98					
GRMZM2G351484	hypothetical protein LOC100275136	-6.26					
GRMZM2G044174	hypothetical protein LOC100275455	-2.93					
GRMZM2G032350	hypothetical protein LOC100276200	-4.28					
GRMZM2G152703	hypothetical protein LOC100277102	-2.75					
GRMZM2G405017	hypothetical protein LOC100278922	-5.98					
GRMZM2G022694	hypothetical protein LOC100192630	3.46					
GRMZM2G035045	hypothetical protein LOC100272949	5.43					
GRMZM2G421126	hypothetical protein LOC100274299	5.6					
GRMZM2G162359	hypothetical protein LOC100274481	6.5					
GRMZM2G136771	hypothetical protein LOC100279046		-8.87				
GRMZM2G075595	hypothetical protein LOC100384061		53.36				
GRMZM2G426336	hypothetical protein LOC100191536			-3.38			
GRMZM2G148167	hypothetical protein LOC100193781			-2.94			
GRMZM2G071100	hypothetical protein LOC100216594			-3.33			
GRMZM2G043493	hypothetical protein LOC100216770			-3.23			
GRMZM2G124047	hypothetical protein LOC100217003			-3.52			
GRMZM2G150444	hypothetical protein LOC100272265			-5.99			
GRMZM2G457621	hypothetical protein LOC100272838			-3.58			
GRMZM5G834837	hypothetical protein LOC100273136			-3.63			
GRMZM2G107771	hypothetical protein LOC100273397			-3.46			
GRMZM2G031733	hypothetical protein LOC100273806			-4.66			
GRMZM5G832281	hypothetical protein LOC100274599			-3.25			
GRMZM2G136663	hypothetical protein LOC100275127			-3.18			
GRMZM2G034623	hypothetical protein LOC100275953			-4.26			
AC210193.4_FG002	hypothetical protein LOC100276953			-5.04			
GRMZM2G438243	hypothetical protein LOC100277095			-3.73			
GRMZM2G322917	hypothetical protein LOC100277625			-3.72			
GRMZM2G134064	hypothetical protein LOC100278163			-4.09			
GRMZM5G845644	hypothetical protein LOC100280037			-4.35			
GRMZM5G819835	hypothetical protein LOC100280137			-3.73			
GRMZM2G162127	hypothetical protein LOC100303844			-3.88			
GRMZM2G415470	hypothetical protein LOC100304274			-3.49			
GRMZM2G148404	hypothetical protein LOC100381686			-6.09			
GRMZM2G147942	hypothetical protein LOC100382040			-3.3			
GRMZM2G417107	hypothetical protein LOC100275319	-4.48		-3.94			
GRMZM2G056431	hypothetical protein LOC100276276	-4.3		-2.9			
GRMZM2G390150	hypothetical protein LOC100277984	-3.14		-3.61			
GRMZM2G132162	hypothetical protein LOC100303861		-5.06	-4.33			
GRMZM2G306643	hypothetical protein LOC100278004	-2.87	-3.5	-3.2			
GRMZM2G027472	hypothetical protein LOC100279126	-8.37	-8.98	-4.86			
GRMZM2G121137	hypothetical protein LOC100279160	-4.39	-6.77	-4.07			
GRMZM2G383408	hypothetical protein LOC100192085			2.73			
GRMZM2G068350	hypothetical protein LOC100192819			6.11			
GRMZM2G169931	hypothetical protein LOC100194368			3.09			
GRMZM5G828820	hypothetical protein LOC100216907			2.39			
GRMZM2G141665	hypothetical protein LOC100272718			2.48			
GRMZM5G876379	hypothetical protein LOC100274220			2.87			
GRMZM2G339562	hypothetical protein LOC100274353			2.68			
GRMZM2G094543	hypothetical protein LOC100274993			3.39			
GRMZM2G113480	hypothetical protein LOC100275199			6.55			
GRMZM2G157683	hypothetical protein LOC100275408			11.04			
GRMZM2G133430	hypothetical protein LOC100275437			2.58			
GRMZM2G136831	hypothetical protein LOC100276499			3.97			
GRMZM2G377647	hypothetical protein LOC100276586			3.28			
GRMZM2G302171	hypothetical protein LOC100277362			6.1			
GRMZM2G170742	hypothetical protein LOC100278075			15.9			
GRMZM2G164912	hypothetical protein LOC100278639			2.45			
GRMZM2G117993	hypothetical protein LOC100278684			3.52			
GRMZM2G093270	hypothetical protein LOC100278906			2.6			
GRMZM2G131055	hypothetical protein LOC100279381			3.15			

Table S2 Continued

gene name	annotation	Af24hpi	Af48hpi	Af72hpi	Fv24hpi	Fv48hpi	Fv72hpi
GRMZM2G177878	hypothetical protein LOC100279545			3.98			
GRMZM2G004880	hypothetical protein LOC100279565			2.41			
GRMZM2G061723	hypothetical protein LOC100279877			13.38			
GRMZM2G175396	hypothetical protein LOC100280069			3.58			
GRMZM2G128477	hypothetical protein LOC100280249			4.19			
GRMZM2G164475	hypothetical protein LOC100280402			3.2			
GRMZM2G134067	hypothetical protein LOC100303805			4.01			
GRMZM2G157327	hypothetical protein LOC100304412			4.19			
GRMZM2G076152	hypothetical protein LOC100381813			4.01			
GRMZM2G312661	hypothetical protein LOC100382070			2.82			
GRMZM2G130191	hypothetical protein LOC100382131			2.81			
GRMZM2G113583	hypothetical protein LOC100382196			8.62			
GRMZM2G178752	hypothetical protein LOC100383314			5.14			
GRMZM2G152189	hypothetical protein LOC100383538			7.17			
GRMZM2G004377	hypothetical protein LOC100383559			5.18			
GRMZM2G006977	hypothetical protein LOC100383926			3.18			
GRMZM2G008353	hypothetical protein LOC100383991			3.27			
GRMZM5G816086	hypothetical protein LOC100384717			6.58			
GRMZM2G468111	hypothetical protein LOC100277849		9.93	4.25			
GRMZM2G160611	hypothetical protein LOC100278801		28.69	12.01			
GRMZM2G100475	hypothetical protein LOC100304211		8.82	3.85			
GRMZM2G063765	hypothetical protein LOC100382742					2.59	
GRMZM5G822699	hypothetical protein LOC100382851						-3.59
GRMZM2G098102	hypothetical protein LOC100191602						14.82
GRMZM2G035557	hypothetical protein LOC100191804						2.67
GRMZM2G126975	hypothetical protein LOC100192940						8.64
GRMZM5G883250	hypothetical protein LOC100193298						2.58
GRMZM2G060714	hypothetical protein LOC100193379						5.51
GRMZM2G069694	hypothetical protein LOC100193809						4.01
GRMZM2G008528	hypothetical protein LOC100273559						7.27
GRMZM2G110220	hypothetical protein LOC100274259						5.9
GRMZM2G475956	hypothetical protein LOC100275132						3.16
GRMZM2G467072	hypothetical protein LOC100275382						15.62
GRMZM2G116640	hypothetical protein LOC100275790						3.16
GRMZM2G428216	hypothetical protein LOC100276732						3.38
GRMZM2G068826	hypothetical protein LOC100277874						5.21
GRMZM2G049654	hypothetical protein LOC100278542						11.13
GRMZM2G046353	hypothetical protein LOC100278926						5.56
GRMZM2G090328	hypothetical protein LOC100383500						6.53
GRMZM2G135013	hypothetical protein LOC100273022	16.17					12.01
GRMZM2G054807	hypothetical protein LOC100191889			4.66			4.63
GRMZM2G159477	hypothetical protein LOC100216915			4.14			3.33
GRMZM2G429617	hypothetical protein LOC100272958			45.35			26.13
GRMZM2G082943	hypothetical protein LOC100273016			2.57			2.77
GRMZM2G412986	hypothetical protein LOC100273057			3.53			3.33
GRMZM2G309327	hypothetical protein LOC100273276			4.13			4.94
GRMZM2G100650	hypothetical protein LOC100273327			5.6			2.96
GRMZM2G156310	hypothetical protein LOC100273481			6.09			4.39
GRMZM2G133613	hypothetical protein LOC100274035			8.32			4.83
GRMZM5G869299	hypothetical protein LOC100274346			3.75			2.69
GRMZM2G061702	hypothetical protein LOC100274378			12.94			6.72
GRMZM2G381071	hypothetical protein LOC100274538			6.34			5.53
GRMZM2G371167	hypothetical protein LOC100274648			6.46			3.89
GRMZM2G320960	hypothetical protein LOC100274847			9.23			5.46
GRMZM2G446201	hypothetical protein LOC100274970			4.12			4.28
GRMZM2G051151	hypothetical protein LOC100275200			5.36			4.48
AC194056.3_FG008	hypothetical protein LOC100275201			42.19			25.68
GRMZM2G039961	hypothetical protein LOC100275320			4.45			4.25
GRMZM2G165325	hypothetical protein LOC100275463			6.1			3.27
GRMZM5G856929	hypothetical protein LOC100275515			6.21			3.82
GRMZM2G022368	hypothetical protein LOC100276175			6.5			6.73
GRMZM2G133198	hypothetical protein LOC100276750			12.43			13.42
GRMZM2G430623	hypothetical protein LOC100277063			7.45			6.15
GRMZM2G140674	hypothetical protein LOC100277970			2.67			3.61
GRMZM2G408537	hypothetical protein LOC100278119			17.16			12.64
GRMZM2G033175	hypothetical protein LOC100278137			4.9			4.3

Table S2 Continued

gene name	annotation	Af24hpi	Af48hpi	Af72hpi	Fv24hpi	Fv48hpi	Fv72hpi
GRMZM2G444819	hypothetical protein LOC100278748			9.82			5.75
GRMZM2G444621	hypothetical protein LOC100280399			3.04			5.19
GRMZM2G046317	hypothetical protein LOC100303919			4.77			4.76
GRMZM5G882075	hypothetical protein LOC100304424			31.42			14.9
GRMZM2G316555	hypothetical protein LOC100382115			4.43			7.97
GRMZM2G021909	hypothetical protein LOC100382192			5.72			5.35
GRMZM5G863146	hypothetical protein LOC100382758			3.91			4.42
GRMZM2G037998	hypothetical protein LOC100383638			3.82			3.82
GRMZM2G346837	hypothetical protein LOC100384130			3.71			3.99
GRMZM2G105522	hypothetical protein LOC100384163			10.97			9.82
GRMZM2G119705	hypothetical protein LOC100192066	14.15		9.28			4.07
GRMZM2G155321	hypothetical protein LOC100216791	3.85		5.68			5.12
GRMZM2G164781	hypothetical protein LOC100276523	12.25		20.03			7.36
GRMZM2G094510	hypothetical protein LOC100278059	7.31		11.86			10.46
GRMZM2G170281	hypothetical protein LOC100279547	4.05		4.67			3.03
GRMZM5G812099	hypothetical protein LOC100384058	4.43		5.43			3.59
GRMZM2G166870	hypothetical protein LOC100273000		29.09	154.89			57.76
GRMZM2G138918	hypothetical protein LOC100192105	5.35	4.28	14.42			7.97
GRMZM2G176472	hypothetical protein LOC100382268	7.13	4.43	14.32			9.65
GRMZM2G449709	hypothetical protein LOC100382369	3.63	4.47	11.99			6.88
GRMZM2G100372	hypothetical protein LOC100191911					4.26	9.93
GRMZM2G032682	hypothetical protein LOC100278952	14.28				10.84	17.96
GRMZM2G091226	hypothetical protein LOC100193008			4.38		3.5	4.39
GRMZM2G092146	hypothetical protein LOC100275352			5.82		3.53	6.32
GRMZM2G334734	hypothetical protein LOC100278663			11.74		10.13	33.2
GRMZM2G061723	hypothetical protein LOC100279877			5.72		4.27	7.62
GRMZM2G041022	hypothetical protein LOC100273268	11.03		4.65		6.1	5.47
GRMZM2G131099	hypothetical protein LOC100275282	8.73		12.18		4.96	11.11
GRMZM2G325683	hypothetical protein LOC100276188	14.95		11.77		4.06	7.59
GRMZM2G151230	hypothetical protein LOC100277715	12.67		7.33		5.6	10.55
GRMZM2G039362	hypothetical protein LOC100277767	12.75		5.75		4.36	6.65
GRMZM2G037485	hypothetical protein LOC100382367	9.32		5.24		3.5	7.44
GRMZM2G323943	hypothetical protein LOC100383124	4.74		13.21		3.83	9.94
GRMZM2G152396	hypothetical protein LOC100304256		5.61	6.41		3.28	5.21
GRMZM2G364208	hypothetical protein LOC100275239	5.29	3.66	6.43		3.63	6.79
GRMZM2G161521	hypothetical protein LOC100275439	10.53	5.46	13.93		7.72	16.64
GRMZM2G041068	hypothetical protein LOC100275684	26.25	5.64	16.66		7.8	16.66
GRMZM2G325693	hypothetical protein LOC100277209	17.77	3.9	12.1		3.89	8.18
GRMZM2G010702	hypothetical protein LOC100382154	7	6.38	18.91		5.56	12.89
GRMZM2G449094	hypothetical protein LOC100384448	8.56	8.13	16.32		5.37	14.32
GRMZM2G322618	LOC100283550			-2.81			
GRMZM2G149935	LOC100280586			3.7			
GRMZM2G092817	LOC100280732			4.01			
GRMZM2G457309	LOC100281002			11.25			
GRMZM2G083538	LOC100281771			3.42			
GRMZM2G472248	LOC100283996			5.37			
GRMZM2G094428	LOC100284721			2.29			
GRMZM2G174719	LOC100285882			7.04			
GRMZM2G109959	LOC100280774					2.47	
GRMZM2G423129	LOC100281922			2.3		2.66	
GRMZM2G062283	LOC100282390			4.08			5.08
GRMZM2G133029	LOC100283967			3.77			2.89
GRMZM2G116629	LOC100283078	5.95		3.7			3.52
GRMZM2G108847	LOC100037813	14.34		11.62		3.41	7.07
GRMZM2G088819	LOC100284831	4.55	9.56	19.93		5.15	8.98
XLOC_038117	unknown	-3.28					
XLOC_103255	unknown	-3.81					
XLOC_112218	unknown	-5.7					
XLOC_037951	unknown	-3.43					
XLOC_084409	unknown	-7.05					
XLOC_103280	unknown	-9.79					
AC225346.3_FG001	unknown	-5.54					
GRMZM2G012901	unknown	-3.18					
GRMZM2G141864	unknown	-3.37					
GRMZM2G337581	unknown	-2.95					
GRMZM2G340307	unknown	-4.04					

Table S2 Continued

gene name	annotation	Af24hpi	Af48hpi	Af72hpi	Fv24hpi	Fv48hpi	Fv72hpi
GRMZM2G050768	unknown	64.37					
GRMZM2G058808	unknown	4.16					
GRMZM2G070978	unknown	135.07					
GRMZM2G087538	unknown	21.6					
GRMZM2G137231	unknown	3.85					
GRMZM2G455283	unknown	16.89					
GRMZM2G514005	unknown	4.06					
GRMZM5G825935	unknown	8.84					
XLOC_084321	unknown		-4.83				
GRMZM2G006985	unknown		-5.64				
GRMZM2G031131	unknown		-20.74				
GRMZM2G047699	unknown		-6.64				
GRMZM2G086727	unknown		-7.72				
GRMZM2G158407	unknown		-9.88				
GRMZM2G406557	unknown		-3.62				
GRMZM2G426161	unknown		-14.09				
GRMZM2G581751	unknown		-9.37				
XLOC_084215	unknown	-26.12	-20.02				
XLOC_074746	unknown	-17.28	-68.92				
GRMZM5G800473	unknown	-7.48	-8.7				
AC234163.1_FG003	unknown		178.3				
GRMZM2G004517	unknown		21.42				
GRMZM2G022874	unknown		9.09				
GRMZM2G051915	unknown		10.75				
GRMZM2G053182	unknown		12.37				
GRMZM2G064527	unknown		15.85				
GRMZM2G099554	unknown		31.32				
GRMZM2G100166	unknown		15.78				
GRMZM2G106310	unknown		11.76				
GRMZM2G114182	unknown		28.05				
GRMZM2G119737	unknown		14.81				
GRMZM2G144546	unknown		8.13				
GRMZM2G144978	unknown		8.72				
GRMZM2G158547	unknown		19.04				
GRMZM2G473356	unknown		18.71				
GRMZM5G832100	unknown		4.77				
XLOC_062711	unknown			-3.61			
XLOC_038162	unknown			-4.26			
AF546188.1_FG003	unknown			-4.19			
GRMZM2G043565	unknown			-3.75			
GRMZM2G045098	unknown			-5.96			
GRMZM2G048854	unknown			-6.17			
GRMZM2G111271	unknown			-3			
GRMZM2G119766	unknown			-2.65			
GRMZM2G125130	unknown			-3.62			
GRMZM2G143452	unknown			-4.01			
GRMZM2G152764	unknown			-3.38			
GRMZM2G318121	unknown			-4.09			
GRMZM2G362312	unknown			-2.93			
GRMZM2G471447	unknown			-2.98			
GRMZM2G514379	unknown			-7.98			
GRMZM2G553069	unknown			-2.88			
GRMZM2G561107	unknown			-9.69			
GRMZM5G883407	unknown			-15.67			
XLOC_103369	unknown	-3.55	-5.53	-3.31			
XLOC_074718	unknown	-5.99	-13.09	-6.28			
XLOC_074837	unknown			871.08			
XLOC_103328	unknown			3.2			
XLOC_062641	unknown			12.58			
XLOC_062606	unknown			78.13			
XLOC_093400	unknown			10.32			
AC193632.2_FG002	unknown			9.3			
AC205250.3_FG006	unknown			39.94			
AC213614.3_FG002	unknown			7.3			
AC233851.1_FG008	unknown			5.25			
GRMZM2G003274	unknown			5.06			

Table S2 Continued

gene name	annotation	Af24hpi	Af48hpi	Af72hpi	Fv24hpi	Fv48hpi	Fv72hpi
GRMZM2G005461	unknown			8.31			
GRMZM2G008839	unknown			4.09			
GRMZM2G014839	unknown			5			
GRMZM2G017682	unknown			3.25			
GRMZM2G027107	unknown			53.23			
GRMZM2G030869	unknown			10.64			
GRMZM2G040309	unknown			8.21			
GRMZM2G049109	unknown			4.67			
GRMZM2G055107	unknown			3.91			
GRMZM2G090226	unknown			6.82			
GRMZM2G099496	unknown			18.41			
GRMZM2G101128	unknown			7.92			
GRMZM2G103748	unknown			29.71			
GRMZM2G107373	unknown			4.34			
GRMZM2G110252	unknown			3.63			
GRMZM2G110395	unknown			4.04			
GRMZM2G113875	unknown			10.18			
GRMZM2G121514	unknown			2.57			
GRMZM2G123394	unknown			6.27			
GRMZM2G126370	unknown			28.98			
GRMZM2G131084	unknown			23.76			
GRMZM2G139811	unknown			3.2			
GRMZM2G140269	unknown			4.32			
GRMZM2G150919	unknown			4.79			
GRMZM2G151950	unknown			4.51			
GRMZM2G162216	unknown			5.64			
GRMZM2G166548	unknown			8.32			
GRMZM2G168931	unknown			3.05			
GRMZM2G170982	unknown			3.45			
GRMZM2G172695	unknown			4.58			
GRMZM2G176057	unknown			6.12			
GRMZM2G176124	unknown			3.85			
GRMZM2G176998	unknown			2.62			
GRMZM2G178955	unknown			2.98			
GRMZM2G300119	unknown			5.76			
GRMZM2G301939	unknown			2.89			
GRMZM2G314927	unknown			16.61			
GRMZM2G314927	unknown			36.57			
GRMZM2G315317	unknown			6.25			
GRMZM2G316033	unknown			38.89			
GRMZM2G352289	unknown			97.82			
GRMZM2G357620	unknown			2.95			
GRMZM2G358830	unknown			7.11			
GRMZM2G368123	unknown			5.61			
GRMZM2G369182	unknown			33.13			
GRMZM2G370040	unknown			65.47			
GRMZM2G374077	unknown			3.61			
GRMZM2G377624	unknown			13.31			
GRMZM2G404530	unknown			4.71			
GRMZM2G430224	unknown			2.98			
GRMZM2G438583	unknown			5.94			
GRMZM2G460765	unknown			7.75			
GRMZM2G461777	unknown			4.31			
GRMZM2G464393	unknown			3.48			
GRMZM2G468585	unknown			3.93			
GRMZM2G468821	unknown			35.74			
GRMZM2G474537	unknown			4.54			
GRMZM2G475185	unknown			14.33			
GRMZM2G475952	unknown			14.95			
GRMZM2G479717	unknown			6.28			
GRMZM2G497094	unknown			10.98			
GRMZM2G499084	unknown			4.43			
GRMZM2G500285	unknown			7.53			
GRMZM2G508692	unknown			51.33			
GRMZM2G524570	unknown			7.65			
GRMZM2G570945	unknown			52.61			

Table S2 Continued

gene name	annotation	Af24hpi	Af48hpi	Af72hpi	Fv24hpi	Fv48hpi	Fv72hpi
GRMZM2G586921	unknown			10.03			
GRMZM5G807406	unknown			3.52			
GRMZM5G807838	unknown			9.23			
GRMZM5G861127	unknown			3.83			
GRMZM5G868355	unknown			2.39			
GRMZM5G885169	unknown			6.46			
GRMZM5G891543	unknown			5.25			
GRMZM5G892921	unknown			15.29			
TCONS_00144565	unknown			7.21			
XLOC_034571	unknown			16.96			
XLOC_045627	unknown			8.76			
XLOC_095338	unknown			28.45			
GRMZM2G023073	unknown	9.27		4.68			
GRMZM2G108615	unknown	8.3		5.37			
GRMZM2G306714	unknown	6.01		6.86			
GRMZM2G330792	unknown	38.84		61.05			
GRMZM2G567649	unknown	11.08		5.29			
GRMZM2G025107	unknown		18.24	10.06			
GRMZM2G039757	unknown		3.15	3.87			
GRMZM2G108095	unknown		15.72	13.57			
GRMZM2G326911	unknown		53.19	31.97			
GRMZM2G327907	unknown		9.46	4.72			
GRMZM2G391215	unknown		15.14	8.27			
GRMZM5G884772	unknown		89.55	14.38			
XLOC_084296	unknown	16.44	9.35	29.84			
XLOC_112434	unknown	16.16	18.39	305.23			
GRMZM2G007944	unknown	16.99	14.73	33.51			
GRMZM2G031730	unknown	24.64	22.17	53.75			
GRMZM2G084421	unknown	6.58	6.17	6.12			
GRMZM2G174147	unknown	5.41	4.19	3.53			
GRMZM2G552982	unknown	7.85	6.92	6.89			
GRMZM2G042510	unknown	6.32				-13.25	
AC234165.1_FG003	unknown					3.2	
GRMZM2G164539	unknown					3.68	
GRMZM2G443439	unknown			-3.86		2.33	
GRMZM2G137550	unknown						-6.76
GRMZM2G177915	unknown			-10.98			-2.9
GRMZM2G088273	unknown	-3.3		-7.72			-3.13
XLOC_093338	unknown						19.23
XLOC_024506	unknown						4.04
AC203430.3_FG007	unknown						9.07
GRMZM2G003440	unknown						8.72
GRMZM2G004207	unknown						4.69
GRMZM2G017157	unknown						11.83
GRMZM2G023683	unknown						31.33
GRMZM2G039212	unknown						8.25
GRMZM2G046733	unknown						37.04
GRMZM2G046848	unknown						11.21
GRMZM2G058884	unknown						9.22
GRMZM2G067946	unknown						4.65
GRMZM2G069335	unknown						3.56
GRMZM2G070503	unknown						5.26
GRMZM2G084979	unknown						8.12
GRMZM2G089720	unknown						10.63
GRMZM2G104366	unknown						5.63
GRMZM2G111132	unknown						68.21
GRMZM2G135378	unknown						22.59
GRMZM2G141071	unknown						6.33
GRMZM2G141133	unknown						13.12
GRMZM2G145045	unknown						5.78
GRMZM2G160515	unknown						28.9
GRMZM2G304528	unknown						4.07
GRMZM2G305159	unknown						3.48
GRMZM2G322547	unknown						3.74
GRMZM2G340654	unknown						6.64
GRMZM2G341499	unknown						11.16

Table S2 Continued

gene name	annotation	Af24hpi	Af48hpi	Af72hpi	Fv24hpi	Fv48hpi	Fv72hpi
GRMZM2G378080	unknown						57.17
GRMZM2G382035	unknown						8.35
GRMZM2G382035	unknown						7.95
GRMZM2G413135	unknown						233.93
GRMZM2G422499	unknown						3.22
GRMZM2G440965	unknown						32.31
GRMZM2G440972	unknown						17.46
GRMZM2G444948	unknown						71.83
GRMZM2G450228	unknown						96
GRMZM2G460465	unknown						3.74
GRMZM5G815077	unknown						10.83
GRMZM5G815784	unknown						6.64
GRMZM5G815835	unknown						3.78
GRMZM5G831843	unknown						2.72
GRMZM5G891259	unknown						4.63
GRMZM2G359033	unknown	6.37					3.41
XLOC_074965	unknown			14.3			6.02
AC183315.4_FG006	unknown			4.17			3.55
AC190885.4_FG006	unknown			8.02			7.29
AC209050.3_FG001	unknown			14.82			13.23
GRMZM2G001355	unknown			18.69			5.96
GRMZM2G005825	unknown			21.04			50.53
GRMZM2G006197	unknown			9.56			6.22
GRMZM2G016004	unknown			3.08			4.5
GRMZM2G024175	unknown			5.74			7.48
GRMZM2G024793	unknown			9.26			13.81
GRMZM2G030688	unknown			12.47			6.45
GRMZM2G031581	unknown			6.74			4.67
GRMZM2G035890	unknown			54.16			11.54
GRMZM2G039630	unknown			23.19			27.46
GRMZM2G057672	unknown			2.57			2.97
GRMZM2G062618	unknown			7.71			5.82
GRMZM2G074236	unknown			10.91			7.49
GRMZM2G082504	unknown			20.49			11.38
GRMZM2G087740	unknown			58.84			28.13
GRMZM2G091857	unknown			3.84			2.93
GRMZM2G092718	unknown			5.9			5.97
GRMZM2G100495	unknown			322.47			316.77
GRMZM2G103785	unknown			3.91			2.97
GRMZM2G111975	unknown			5.36			4.14
GRMZM2G122123	unknown			31.22			67.25
GRMZM2G126413	unknown			5.17			3.99
GRMZM2G126749	unknown			7.87			5.49
GRMZM2G129140	unknown			3.03			2.92
GRMZM2G139708	unknown			250.6			93.45
GRMZM2G159768	unknown			4.37			4.13
GRMZM2G162396	unknown			4.14			3.17
GRMZM2G164542	unknown			3.56			4.35
GRMZM2G175606	unknown			54.62			87.14
GRMZM2G176630	unknown			7.64			4.61
GRMZM2G303972	unknown			51.18			12.45
GRMZM2G305783	unknown			3.5			3.14
GRMZM2G308422	unknown			24.77			49.28
GRMZM2G322729	unknown			9.87			6.62
GRMZM2G333274	unknown			12.42			9.02
GRMZM2G391696	unknown			22.99			14.49
GRMZM2G414503	unknown			8.6			5.68
GRMZM2G421160	unknown			16.18			25.79
GRMZM2G424599	unknown			4.91			3.84
GRMZM2G426046	unknown			3.87			3.11
GRMZM2G438121	unknown			18.39			14.35
GRMZM2G448656	unknown			7.82			4.94
GRMZM2G454514	unknown			12.11			12.92
GRMZM2G454514	unknown			6.12			7.57
GRMZM2G455122	unknown			3.41			2.78
GRMZM2G458052	unknown			12.21			11.71

Table S2 Continued

gene name	annotation	Af24hpi	Af48hpi	Af72hpi	Fv24hpi	Fv48hpi	Fv72hpi
GRMZM2G460138	unknown			3.56			5.03
GRMZM2G474905	unknown			3.13			3.11
GRMZM2G475971	unknown			4.52			7.15
GRMZM5G826899	unknown			13.1			6.73
GRMZM5G855994	unknown			12.57			9.38
GRMZM5G869635	unknown			8.73			6.33
GRMZM5G872578	unknown			11.91			8.96
GRMZM5G875504	unknown			9.43			9.81
GRMZM5G896564	unknown			2.81			3.22
XLOC_034075	unknown			4.65			5.06
GRMZM2G057506	unknown	7		6.21			6.6
GRMZM2G076938	unknown	5.14		4.25			3.37
GRMZM2G123452	unknown	38.64		21.28			40.99
GRMZM2G169535	unknown	12.97		47.1			64.17
GRMZM2G322728	unknown	7.39		8.57			5.48
GRMZM2G342033	unknown	18.08		12.97			10.53
GRMZM2G472655	unknown	8.45		7.59			6.71
GRMZM2G509665	unknown	502.28		20.32			101.33
GRMZM2G566151	unknown	322.73		38.71			63.86
GRMZM2G575389	unknown	17.55		22.12			16.82
GRMZM5G894980	unknown	10.04		8.25			3.79
GRMZM2G146866	unknown		9.63	10.34			6.64
GRMZM2G169953	unknown		10.58	16.44			12.22
GRMZM2G176182	unknown		4.88	9.03			4.18
GRMZM5G886315	unknown		14.19	10.98			5.88
GRMZM2G070207	unknown	24	9.47	37.5			61.4
GRMZM2G106392	unknown	14.32	76.59	198.2			37.96
GRMZM2G416008	unknown	5.9	28.96	56.11			16.4
GRMZM2G453575	unknown	9.61	9.9	52.97			40.28
XLOC_024561	unknown					-8.95	5.72
GRMZM2G026143	unknown					4.4	6.16
GRMZM2G057841	unknown					3.52	4.85
GRMZM2G163110	unknown					21.46	40.19
GRMZM2G152611	unknown	21.5				4.66	8.48
GRMZM2G010333	unknown			5.63		2.89	4.83
GRMZM2G303509	unknown			8.41		11.49	18.94
GRMZM2G380789	unknown			116.04		15.68	194.79
AC196576.3_FG002	unknown	12.93		15.44		6.39	12.17
GRMZM2G045031	unknown	28.9		17.4		9.88	55.95
GRMZM2G071436	unknown	45.49		19.05		20.29	80.47
GRMZM2G116520	unknown	6.34		5.54		3.05	7.44
GRMZM2G317426	unknown	5.06		9.74		3.64	10.06
GRMZM2G317428	unknown	6.45		17.86		8.95	20.33
GRMZM2G318652	unknown	10.83		9.06		6.38	12.67
GRMZM2G323757	unknown	9.94		4.84		3.2	5.51
GRMZM2G435986	unknown	5.24		23.22		7.18	27.9
GRMZM5G830509	unknown	7.56		10.68		4.6	15.78
GRMZM2G096454	unknown		8.38	12.2		6.58	9.23
GRMZM2G473266	unknown		16.88	21.51		28	46.34
GRMZM2G032062	unknown	11.7	4.55	13.9		3.13	7.75
GRMZM2G039040	unknown	32.21	6.49	19.29		7.01	17.15
GRMZM2G366910	unknown	6.26	7.21	18.53		5.25	11.96
GRMZM2G429634	unknown	12.81	13.85	37.15		5.16	20.95
GRMZM2G467520	unknown	25.6	10.49	30.48		8.38	28.22
GRMZM2G472367	unknown	9.01	5.46	17.23		11.66	13.53
GRMZM2G480364	unknown	6.5	14.16	18.98		6.68	13.45
GRMZM2G061527	unknown			23.52			

Supplemental Material from Appendix A

Table S3. *A. flavus* secretory protein encoding genes that were detected during infection of maize kernels. Kernels were collected at 12, 24, 48 and 72 hpi. The fungal secretome database was used to analyze *A. flavus* genes coding for predicted secretory proteins (Choi et al., 2010). '+' denotes presence of transcripts. Genes that were not detected were left blank. hpi, hours post inoculation.

Secretome ID	Secretome gene description	12hpi	24hpi	48hpi	72hpi
AFLA_116630	(S)-2-hydroxy-acid oxidase, putative	+	+	+	+
AFLA_068300	1,3-beta-glucanosyltransferase Bgt1	+	+	+	+
AFLA_108860	1,3-beta-glucanosyltransferase Gel2	+	+	+	+
AFLA_067550	1,4-beta-D-glucan-cellobiohydrolyase, putative		+	+	
AFLA_127510	3-beta hydroxysteroid dehydrogenase family protein		+	+	+
AFLA_052930	3-ketosteroid-delta-1-dehydrogenase, putative		+	+	+
AFLA_000710	6-hydroxy-D-nicotine oxidase, putative		+	+	+
AFLA_104930	6-hydroxy-D-nicotine oxidase, putative		+	+	+
AFLA_138230	6-hydroxy-D-nicotine oxidase, putative			+	+
AFLA_059780	A-agglutinin anchorage subunit, putative		+	+	+
AFLA_039020	Acetylcholinesterase, putative		+	+	+
AFLA_008930	Acid phosphatase AphA		+	+	+
AFLA_013740	Acid phosphatase, putative		+	+	+
AFLA_041320	Acid phosphatase, putative		+	+	+
AFLA_081670	Acid phosphatase, putative	+	+	+	+
AFLA_104760	Acid phosphatase, putative		+	+	+
AFLA_113270	Acid sphingomyelinase, putative	+	+	+	+
AFLA_038790	Adenosine deaminase family protein	+	+	+	+
AFLA_034000	Aegerolysin Aa-Pri1, putative				+
AFLA_139190	AflK/ vbs/ VERB synthase	+	+	+	+
AFLA_094280	Agmatinase, putative		+	+	+
AFLA_020590	Aldose 1-epimerase, putative	+	+	+	+
AFLA_097970	Alkaline D-peptidase, putative		+	+	+
AFLA_110330	Alkaline phosphatase			+	+
AFLA_075170	Alkaline phosphatase, putative			+	+
AFLA_027810	Alkaline serine protease Alp1	+	+	+	+
AFLA_106870	Alkaline serine protease AorO, putative		+	+	+
AFLA_087430	Allergen Asp F4	+	+	+	+
AFLA_053080	Allergen Asp F4-like, putative		+	+	+
AFLA_113260	Allergen Asp F7	+	+	+	+
AFLA_090070	Allergen, putative		+	+	+
AFLA_006310	Alpha glucosidase II, alpha subunit, putative	+	+	+	+
AFLA_090490	Alpha,alpha-trehalose glucohydrolase TreA/Ath1	+	+	+	+
AFLA_037130	Alpha/beta superfamily hydrolase, putative			+	+
AFLA_119700	Alpha-1,2-mannosidase family protein		+	+	+
AFLA_068830	Alpha-1,2-mannosidase family protein, putative		+	+	+
AFLA_073970	Alpha-1,2-mannosidase, putative			+	+
AFLA_090590	Alpha-1,2-mannosidase, putative subfamily		+	+	+
AFLA_087590	Alpha-1,3-glucanase/mutanase, putative		+	+	+
AFLA_091790	Alpha-1,3-glucanase/mutanase, putative	+	+	+	+

Table S3 Continued

Secretome ID	Secretome gene description	12hpi	24hpi	48hpi	72hpi
AFLA_026140	Alpha-amylase, putative	+	+	+	+
AFLA_062690	Alpha-1,6 mannosyltransferase subunit (Mnn9), putative		+	+	+
AFLA_091920	Alpha-1,6-mannosyltransferase subunit (Och1), putative		+	+	+
AFLA_105840	Alpha-galactosidase, putative		+	+	+
AFLA_026150	Alpha-glucosidase AgdA, putative	+	+	+	+
AFLA_060310	Alpha-glucosidase, putative		+	+	+
AFLA_083300	Alpha-glucosidase, putative	+	+	+	+
AFLA_063490	Alpha-L-arabinofuranosidase, putative		+	+	+
AFLA_053690	Alpha-L-fucosidase 2, putative	+	+	+	+
AFLA_076120	Alpha-L-fucosidase 2, putative		+	+	+
AFLA_025440	Alpha-L-rhamnosidase A, putative		+	+	+
AFLA_050140	Alpha-L-rhamnosidase B, putative		+	+	+
AFLA_089770	Alpha-N-arabinofuranosidase A, putative		+	+	+
AFLA_097160	Alpha-N-arabinofuranosidase A, putative			+	
AFLA_041900	Amidase family protein	+	+	+	+
AFLA_061030	Amidase family protein		+	+	+
AFLA_024300	Amidase, putative		+	+	+
AFLA_004880	Amine oxidase, flavin-containing superfamily				+
AFLA_077160	Amine oxidase, putative		+	+	+
AFLA_124420	Amine oxidase, putative		+	+	+
AFLA_066430	Aminoadipic semialdehyde synthase, putative		+	+	+
AFLA_034640	Aminopeptidase Y, putative	+	+	+	+
AFLA_114830	Aminopeptidase, putative		+	+	+
AFLA_123170	Amylase, putative	+	+	+	+
AFLA_103170	Anaphase-promoting complex subunit Apc5, putative			+	+
AFLA_046630	Ankyrin repeat domain, putative		+	+	+
AFLA_040040	Antigenic cell wall galactomannoprotein, putative		+	+	+
AFLA_073070	Arabinan-endo 1,5-alpha-L-arabinase, putative		+	+	+
AFLA_127930	Arabinogalactan endo-1,4-beta-galactosidase GalA		+	+	+
AFLA_016210	Arabinosidase, putative		+	+	+
AFLA_073080	Arabinosidase, putative		+	+	+
AFLA_096120	Arylsulfatase, putative		+	+	+
AFLA_122380	Arylsulfatase, putative		+	+	+
AFLA_094450	Aspartic endopeptidase Pep1/aspergillopepsin F	+	+	+	+
AFLA_031250	Aspartic endopeptidase Pep2	+	+	+	+
AFLA_054660	Aspartic-type endopeptidase (OpsB), putative	+	+	+	+
AFLA_038650	Aspartic-type endopeptidase, putative	+	+	+	+
AFLA_121260	Aspartic-type endopeptidase, putative	+	+	+	+
AFLA_019190	Aspartyl protease, putative		+	+	+
AFLA_090060	Aspergillopepsin, putative	+	+	+	+
AFLA_116740	Aspergillopepsin, putative		+	+	+
AFLA_099020	Autophagic serine protease Alp2	+	+	+	+
AFLA_043640	Autophagy related lipase Atg15, putative	+	+	+	+
AFLA_091500	Beta galactosidase, putative	+	+	+	+

Table S3 Continued

Secretome ID	Secretome gene description	12hpi	24hpi	48hpi	72hpi
AFLA_128480	Beta glucosidase, putative		+	+	+
AFLA_047270	Beta-1,6-glucan boisynthesis protein (Knh1), putative		+	+	+
AFLA_017100	Beta-galactosidase	+	+	+	+
AFLA_016530	Beta-galactosidase, putative	+	+	+	+
AFLA_037600	Beta-galactosidase, putative		+	+	+
AFLA_090730	Beta-glucosidase		+	+	+
AFLA_069670	Beta-glucosidase 1, putative		+	+	+
AFLA_126780	Beta-glucosidase 2, putative		+	+	+
AFLA_014190	Beta-glucosidase, putative		+	+	+
AFLA_023350	Beta-glucosidase, putative		+	+	+
AFLA_051140	Beta-glucosidase, putative	+	+	+	+
AFLA_039000	Beta-lactamase, putative			+	+
AFLA_128610	Beta-mannosidase	+	+	+	+
AFLA_078900	Beta-N-acetylhexosaminidase NagA, putative	+	+	+	+
AFLA_057680	Beta-N-hexosaminidase, putative		+	+	+
AFLA_119790	Beta-xylosidase		+	+	+
AFLA_011080	Beta-xylosidase, putative		+	+	+
AFLA_028000	BNR/Asp-box repeat domain protein	+	+	+	+
AFLA_025130	BYS1 domain protein, putative	+	+	+	+
AFLA_035740	Bys1 family protein				+
AFLA_095090	C6 transcription factor, putative		+	+	
AFLA_029170	C-8 sterol isomerase (Erg-1), putative	+	+	+	+
AFLA_059900	Calcium-binding protein, putative				+
AFLA_042310	cAMP-regulated D2 esterase, putative		+		+
AFLA_081630	Carboxyl ester lipase, zebrafish, putative		+	+	+
AFLA_045610	Carboxylesterase domain containing protein, putative		+	+	+
AFLA_126000	Carboxylesterase hlo, putative			+	+
AFLA_046500	Carboxylesterase, putative		+	+	+
AFLA_049530	Carboxylesterase, putative		+	+	+
AFLA_057790	Carboxylesterase, putative		+	+	+
AFLA_060140	Carboxylesterase, putative		+	+	+
AFLA_104460	Carboxylesterase, type B, putative		+	+	+
AFLA_008990	Carboxypeptidase CpyA/Prc1, putative	+	+	+	+
AFLA_012020	Carboxypeptidase S1, putative	+	+	+	+
AFLA_085960	Cell surface protein, putative	+	+	+	+
AFLA_126860	Cell wall cysteine-rich protein		+	+	+
AFLA_078320	Cell wall glucanase (Scw11), putative	+	+	+	+
AFLA_052780	Cell wall glucanase (Scw4), putative		+	+	+
AFLA_128120	Cell wall glucanase, putative	+	+	+	+
AFLA_064740	Cell wall glycosyl hydrolase YteR, putative		+	+	+
AFLA_023600	Cell wall protein PhiA	+	+	+	+
AFLA_061960	Cell wall protein, putative		+	+	+
AFLA_086990	Cell wall protein, putative	+	+	+	+
AFLA_039410	Cell wall serine-threonine-rich galactomannoprotein Mp1	+	+	+	+
AFLA_069820	Cellobiohydrolase, putative	+	+	+	+

Table S3 Continued

Secretome ID	Secretome gene description	12hpi	24hpi	48hpi	72hpi
AFLA_095340	Cellobiose dehydrogenase, putative			+	+
AFLA_013320	Cellulase family protein		+	+	+
AFLA_008480	CFEM domain protein	+	+	+	+
AFLA_037570	CFEM domain protein, putative	+	+	+	+
AFLA_040330	Chitin binding domain protein Peritrophin-A, putative	+	+	+	+
AFLA_041970	Chitin binding protein, putative	+	+	+	+
AFLA_010440	Chitinase, putative		+		+
AFLA_010110	Choline dehydrogenase, putative			+	+
AFLA_070810	Cholinesterase, putative	+	+	+	+
AFLA_077450	Cinnamoyl-CoA reductase, putative	+	+	+	+
AFLA_052760	Class I alpha-mannosidase 1A	+	+	+	+
AFLA_101800	Class III chitinase, putative			+	+
AFLA_054470	Class V chitinase Chi100		+	+	+
AFLA_104680	Class V chitinase ChiB1				+
AFLA_110170	Collagen EMF1-alpha, putative		+		+
AFLA_014260	Conidial hydrophobin RodB/HypB	+	+	+	+
AFLA_036560	Conserved threonine rich protein		+	+	+
AFLA_072700	Cutinase 1		+	+	+
AFLA_023390	Cutinase, putative	+	+	+	+
AFLA_039350	Cutinase, putative		+	+	+
AFLA_104920	Cutinase, putative	+	+	+	+
AFLA_029850	Cysteine-rich secreted protein	+	+	+	+
AFLA_041790	Cytochrome P450 alkane hydroxylase, putative		+	+	+
AFLA_089870	Cytochrome P450 alkane hydroxylase, putative		+	+	+
AFLA_116530	Cytochrome P450 alkane hydroxylase, putative		+		
AFLA_045270	Cytochrome P450 family protein, putative	+	+	+	+
AFLA_013520	Cytochrome P450, putative	+	+	+	+
AFLA_101720	Cytochrome P450, putative				+
AFLA_121500	Cytochrome P450, putative		+	+	+
AFLA_123860	Cytochrome P450, putative			+	+
AFLA_138460	Cytochrome P450, putative		+	+	+
AFLA_065050	Defensin domain protein				+
AFLA_029420	Dipeptidyl-peptidase II, putative	+	+	+	+
AFLA_103980	DnaJ and TPR domain protein		+	+	+
AFLA_002760	DUF1237 domain protein	+	+	+	+
AFLA_018910	Elastase, putative		+	+	+
AFLA_038530	Elastinolytic metalloproteinase Mep	+	+	+	+
AFLA_035800	Endo xylanase, putative		+	+	+
AFLA_116030	Endo xylanase, putative		+	+	+
AFLA_029950	Endo-1,3(4)-beta-glucanase, putative	+	+	+	+
AFLA_028950	Endo-1,3-beta-glucanase Engl1	+	+	+	+
AFLA_118170	Endo-1,4-beta-glucanase		+	+	+
AFLA_013760	Endo-1,4-beta-glucanase, putative		+	+	+
AFLA_010870	Endo-1,4-beta-xylanase		+	+	+
AFLA_138360	Endo-1,4-beta-xylanase	+	+	+	+
AFLA_066150	Endo-1,4-beta-xylanase A, putative	+	+	+	+

Table S3 Continued

Secretome ID	Secretome gene description	12hpi	24hpi	48hpi	72hpi
AFLA_009060	Endo-1,4-beta-xylanase, putative	+	+	+	+
AFLA_085590	Endo-arabinanase, putative		+	+	+
AFLA_131570	Endo-arabinase, putative		+	+	+
AFLA_045690	Endo-beta-1,6-glucanase, putative		+	+	+
AFLA_038420	Endo-chitosanase B			+	+
AFLA_011440	Endoglucanase, putative	+	+	+	+
AFLA_029160	Endoglucanase, putative	+	+	+	+
AFLA_066300	Endoglucanase, putative	+	+	+	+
AFLA_077840	Endoglucanase, putative	+	+	+	+
AFLA_087870	Endoglucanase, putative	+	+	+	+
AFLA_105910	Endoglucanase, putative	+	+	+	+
AFLA_111970	Endoglucanase, putative	+	+	+	+
AFLA_138380	Endoglucanase, putative		+	+	+
AFLA_039160	Endoglucanase-1, putative		+	+	+
AFLA_126410	Endoglucanase-1, putative	+	+	+	+
AFLA_123210	Endoglucanase-4, putative		+		+
AFLA_012960	Endoglycoceramidase, putative		+	+	+
AFLA_003810	Endonuclease/exonuclease/phosphatase family protein	+	+	+	+
AFLA_083730	Epoxide hydrolase, putative		+	+	+
AFLA_028270	Esterase family protein				+
AFLA_002200	Esterase, putative	+	+	+	+
AFLA_063680	Esterase, putative		+	+	+
AFLA_105900	Esterase, putative	+	+	+	+
AFLA_041950	Exo-beta-1,3-glucanase Exg0	+	+	+	+
AFLA_107800	Exo-beta-1,3-glucanase, putative	+	+	+	+
AFLA_096690	Exopolygalacturonase, putative		+	+	+
AFLA_138170	Exopolygalacturonase, putative	+	+	+	+
AFLA_002640	Exo-polygalacturonase, putative		+		+
AFLA_123690	Extracellular arabinanase, putative	+	+	+	+
AFLA_014920	Extracellular aspartic endopeptidase, putative		+	+	+
AFLA_105150	Extracellular carboxylesterase, putative			+	+
AFLA_061810	Extracellular cellulase CelA/allergen Asp F7-like, putative	+	+	+	+
AFLA_023500	Extracellular conserved serine-rich protein	+	+	+	+
AFLA_010120	Extracellular dioxygenase, putative		+	+	+
AFLA_020430	Extracellular dioxygenase, putative		+	+	+
AFLA_131820	Extracellular dioxygenase, putative		+	+	+
AFLA_110160	Extracellular dipeptidyl-peptidase Dpp4	+	+	+	+
AFLA_059500	Extracellular endo-1,5-alpha-L-arabinase, putative	+	+	+	+
AFLA_045290	Extracellular endoglucanase/cellulase, putative	+	+	+	+
AFLA_001420	Extracellular exo-polygalacturonase, putative		+	+	+
AFLA_050150	Extracellular exo-polygalacturonase, putative		+		+
AFLA_126750	Extracellular glycine-rich protein			+	
AFLA_039400	Extracellular guanyl-specific ribonuclease RntA	+	+	+	+
AFLA_020170	Extracellular lipase, putative		+	+	+

Table S3 Continued

Secretome ID	Secretome gene description	12hpi	24hpi	48hpi	72hpi
AFLA_025190	Extracellular lipase, putative		+	+	+
AFLA_065540	Extracellular lipase, putative	+	+	+	+
AFLA_122390	Extracellular lipase, putative		+	+	+
AFLA_078590	Extracellular matrix protein, putative			+	+
AFLA_019800	Extracellular phytase, putative	+	+	+	+
AFLA_089400	Extracellular phytase, putative		+	+	+
AFLA_085500	Extracellular proline-glycine rich protein	+	+	+	+
AFLA_123700	Extracellular proline-rich protein		+	+	+
AFLA_064810	Extracellular proline-serine rich protein	+	+	+	+
AFLA_109400	Extracellular protein, putative		+	+	+
AFLA_070940	Extracellular rhamnogalacturonase, putative	+	+	+	
AFLA_002090	Extracellular serine carboxypeptidase, putative	+	+	+	+
AFLA_137110	Extracellular serine-rich protein, putative			+	
AFLA_085140	Extracellular thaumatin domain protein, putative	+	+	+	+
AFLA_137880	Extracellular triacylglycerol lipase, putative				+
AFLA_007560	F5/8 type C domain protein			+	+
AFLA_075370	FAD binding domain protein		+	+	+
AFLA_004220	FAD dependent oxidoreductase, putative		+	+	+
AFLA_096380	FAD dependent oxidoreductase, putative		+		+
AFLA_135400	FAD dependent oxidoreductase, putative		+	+	+
AFLA_139470	FAD dependent oxidoreductase, putative	+	+	+	+
AFLA_049190	FAD/FMN-containing isoamyl alcohol oxidase MreA	+	+	+	+
AFLA_136670	FAD/FMN-containing isoamyl alcohol oxidase MreA-like, putative		+	+	+
AFLA_124950	FAD/FMN-containing protein		+	+	+
AFLA_078060	FAD-binding oxidoreductase, putative				+
AFLA_110890	FAD-dependent oxygenase, putative	+	+	+	+
AFLA_042090	Fasciclin domain family protein	+	+	+	+
AFLA_081980	Ferulic acid esterase (FaeA), putative		+	+	+
AFLA_000910	Feruloyl esterase B, putative			+	+
AFLA_001440	Feruloyl esterase B, putative		+	+	+
AFLA_128870	Feruloyl esterase, putative		+	+	+
AFLA_028830	FG-GAP repeat protein, putative	+	+	+	+
AFLA_118340	Flavin containing polyamine oxidase, putative	+	+	+	+
AFLA_138050	Flavonoid 3-hydroxylase, putative	+	+	+	+
AFLA_064300	Fructosyl amino acid oxidase, putative		+	+	+
AFLA_104300	Fungal alpha-L-arabinofuranosidase, putative		+	+	+
AFLA_071790	Galactose oxidase, putative			+	+
AFLA_042800	Gamma-gliadin, putative			+	
AFLA_057690	GDSL lipase/acylhydrolase family protein		+	+	+
AFLA_039660	GDSL-like lipase/acylhydrolase domain protein		+	+	+
AFLA_001230	Gloeobacteria sulfatase, putative				+
AFLA_021600	Glucan 1,3-beta-glucosidase, putative	+	+	+	
AFLA_107790	Glucan 1,3-beta-glucosidase, putative	+	+	+	+
AFLA_122400	Glucan 1,4-alpha-glucosidase, putative	+	+	+	+
AFLA_034920	Glucan endo-1,3-alpha-glucosidase agn1, putative		+	+	+

Table S3 Continued

Secretome ID	Secretome gene description	12hpi	24hpi	48hpi	72hpi
AFLA_034950	Glucoamylase, putative	+	+	+	+
AFLA_076820	Glucose oxidase, putative	+	+	+	+
AFLA_018040	Glucose-methanol-choline (Gmc) oxidoreductase, putative	+	+	+	+
AFLA_035080	Glucose-methanol-choline (Gmc) oxidoreductase, putative		+	+	+
AFLA_040600	Glucose-methanol-choline (Gmc) oxidoreductase, putative		+	+	+
AFLA_092920	Glucose-methanol-choline (Gmc) oxidoreductase, putative		+	+	+
AFLA_107410	Glucose-methanol-choline (Gmc) oxidoreductase, putative			+	+
AFLA_014380	Glutamate carboxypeptidase, putative		+	+	+
AFLA_072960	Glutamate carboxypeptidase, putative				+
AFLA_109490	Glutamate carboxypeptidase, putative		+	+	+
AFLA_101230	Glutaminase GtaA	+	+	+	+
AFLA_031760	Glutaminase, putative	+	+	+	+
AFLA_111400	Glutaminyl cyclase, putative	+	+	+	+
AFLA_063250	Glutaminyl-peptide cyclotransferase, putative		+	+	+
AFLA_041450	Glutamyl-tRNA(Gln) amidotransferase, subunit A		+	+	+
AFLA_120940	Glycan biosynthesis protein (PigL), putative		+	+	+
AFLA_095790	Glycoside hydrolase, putative		+	+	+
AFLA_120410	Glycosyl hydrolase family 43 protein		+	+	+
AFLA_062930	Glycosyl hydrolase, family 43, putative		+	+	+
AFLA_001640	Glycosyl hydrolase, putative			+	+
AFLA_092470	Glycosyl hydrolase, putative	+	+	+	+
AFLA_104880	Glycosyl hydrolase, putative		+	+	+
AFLA_097890	Glycosyl hydrolases family 32 superfamily	+	+	+	+
AFLA_060420	Glycosyl transferase family 8 family, putative		+	+	+
AFLA_137460	Glycosyl transferase, putative			+	+
AFLA_016860	GMC oxidoreductase, putative		+	+	+
AFLA_082250	GMC oxidoreductase, putative		+	+	+
AFLA_087060	GMC oxidoreductase, putative		+	+	+
AFLA_110510	GPI anchored cell wall protein, putative		+	+	+
AFLA_113240	GPI anchored cell wall protein, putative	+	+	+	+
AFLA_115840	GPI anchored cell wall protein, putative		+	+	+
AFLA_123410	GPI anchored cell wall protein, putative		+	+	+
AFLA_106450	GPI anchored CFEM domain protein		+		+
AFLA_077810	GPI anchored dioxygenase, putative		+	+	+
AFLA_004200	GPI anchored glycoprotein, putative	+	+	+	+
AFLA_002270	GPI anchored protein, putative			+	+
AFLA_011700	GPI anchored protein, putative	+	+	+	+
AFLA_021260	GPI anchored protein, putative		+	+	+
AFLA_025060	GPI anchored protein, putative		+	+	+
AFLA_040110	GPI anchored protein, putative	+	+	+	+
AFLA_047090	GPI anchored protein, putative	+	+	+	+

Table S3 Continued

Secretome ID	Secretome gene description	12hpi	24hpi	48hpi	72hpi
AFLA_058410	GPI anchored protein, putative	+	+	+	+
AFLA_068360	GPI anchored protein, putative	+	+	+	+
AFLA_069090	GPI anchored protein, putative		+	+	+
AFLA_091650	GPI anchored protein, putative	+	+	+	+
AFLA_051250	GPI anchored serine-rich protein	+	+	+	+
AFLA_021660	GPI anchored serine-threonine rich protein		+	+	+
AFLA_028340	GPI anchored serine-threonine rich protein	+	+	+	+
AFLA_103140	GPI anchored serine-threonine rich protein		+	+	+
AFLA_113120	GPI-anchored cell wall organization protein Ecm33	+	+	+	+
AFLA_087490	Heme/steroid binding protein, putative		+	+	+
AFLA_015090	HET-C domain protein		+	+	+
AFLA_039870	Histidine acid phosphatase, putative		+	+	+
AFLA_108950	Histidine acid phosphatase, putative	+	+	+	+
AFLA_059610	Homeobox-containing protein wariai, putative		+		+
AFLA_104890	Hydrolase, putative		+	+	+
AFLA_131460	Hydrophobin family protein		+	+	+
AFLA_081480	IgE-binding protein	+	+	+	+
AFLA_135590	Inosine-uridine preferring nucleoside hydrolase, putative		+	+	+
AFLA_007630	Integral membrane protein, Mpv17/PMP22 family, putative		+	+	+
AFLA_102480	Isoamyl alcohol oxidase		+	+	+
AFLA_017080	Isoamyl alcohol oxidase, putative			+	+
AFLA_063120	Isoamyl alcohol oxidase, putative	+	+	+	+
AFLA_065010	Isochorismatase family hydrolase, putative		+	+	+
AFLA_000890	Laccase TilA		+	+	+
AFLA_123160	Laccase, putative		+	+	+
AFLA_088610	Lactonohydrolase, putative		+	+	+
AFLA_138110	Lactonohydrolase, putative				+
AFLA_121230	L-amino acid oxidase LaoA				+
AFLA_084170	L-ascorbate oxidase, putative		+	+	+
AFLA_080660	L-asparaginase		+	+	+
AFLA_013880	Lipase 2, putative	+	+	+	+
AFLA_121020	Lipase 8, putative		+	+	+
AFLA_016150	Lipase, putative		+	+	+
AFLA_102380	Lipase, putative		+	+	+
AFLA_126740	Lipase, putative		+		
AFLA_029690	Lipase/esterase, putative		+	+	+
AFLA_110960	Lysophospholipase Plb1	+	+	+	+
AFLA_059410	Lysophospholipase Plb3	+	+	+	+
AFLA_070170	Lysosomal alpha-glucosidase, putative	+	+	+	+
AFLA_107990	Lysosomal protective protein, putative		+	+	+
AFLA_132770	Lysosomal protective protein, putative		+	+	+
AFLA_138180	Lysozyme, putative				+
AFLA_081910	Major allergen Asp F2		+	+	+
AFLA_038730	Mannan endo-1,4-beta-mannosidase A, putative		+	+	+

Table S3 Continued

Secretome ID	Secretome gene description	12hpi	24hpi	48hpi	72hpi
AFLA_033400	Mannosidase MsdS	+	+	+	+
AFLA_095980	Mannosylphosphate transferase (Mnn4), putative		+	+	+
AFLA_037920	Mating alpha-pheromone PpgA		+	+	+
AFLA_040370	Membrane copper amine oxidase, putative		+	+	+
AFLA_134170	ML domain protein, putative	+	+	+	+
AFLA_061110	Mono-and diacylglycerol lipase, putative		+	+	+
AFLA_096240	Monooxygenase, putative		+	+	+
AFLA_119350	Monooxygenase, putative		+	+	+
AFLA_122300	Monooxygenase, putative				+
AFLA_113300	Monoxygenase, putative	+		+	+
AFLA_006190	Multicopper oxidase, putative			+	+
AFLA_053930	Multicopper oxidase, putative		+		+
AFLA_045660	Multicopper oxidase/laccase, putative		+	+	+
AFLA_091580	Multiple inositol polyphosphate phosphatase, putative	+	+	+	+
AFLA_028300	Muramidase, putative		+		
AFLA_052730	Muramidase, putative		+	+	+
AFLA_119040	Muramidase, putative	+	+	+	+
AFLA_090690	Mycelial catalase Cat1	+	+	+	+
AFLA_013540	Neuroligin, putative		+	+	+
AFLA_095530	Neuroligin, putative				+
AFLA_057670	Neutral protease 2, putative	+	+	+	+
AFLA_127540	Neutral/alkaline nonlysosomal ceramidase, putative		+	+	+
AFLA_107610	NmrA-like family protein			+	+
AFLA_083420	Non-hemolytic phospholipase C, putative		+	+	+
AFLA_096450	NPP1 domain protein		+	+	+
AFLA_013750	NPP1 domain protein, putative		+	+	+
AFLA_054320	NPP1 domain protein, putative		+	+	+
AFLA_004810	Nuclear pore glycoprotein p62, putative	+	+	+	+
AFLA_064860	Nuclease S1, putative	+	+	+	+
AFLA_067380	Nucleoside diphosphatase Gda1	+	+	+	+
AFLA_121160	Oxalate decarboxylase oxdC, putative			+	
AFLA_073210	Oxalate decarboxylase, putative	+	+	+	+
AFLA_121990	Oxidoreductase, putative		+	+	+
AFLA_016360	PAF acetylhydrolase family protein	+	+	+	+
AFLA_019760	Palmitoyl-protein thioesterase	+	+	+	+
AFLA_111130	Pantetheine-phosphate adenylyltransferase family protein	+	+	+	+
AFLA_057770	Pectate lyase A	+	+	+	+
AFLA_044970	Pectate lyase, putative		+	+	+
AFLA_077040	Pectate lyase, putative		+	+	+
AFLA_116650	Pectate lyase, putative		+	+	+
AFLA_121970	Pectate lyase, putative	+	+	+	+
AFLA_007720	Pectin lyase	+	+	+	+
AFLA_017180	Pectin lyase A, putative		+	+	+
AFLA_116040	Pectin lyase B		+	+	+
AFLA_025400	Pectin lyase D, putative		+	+	+

Table S3 Continued

Secretome ID	Secretome gene description	12hpi	24hpi	48hpi	72hpi
AFLA_119860	Pectin lyase, putative	+	+	+	+
AFLA_124660	Pectin lyase, putative	+	+	+	+
AFLA_100100	Pectin methylesterase, putative		+	+	+
AFLA_001410	Pectinesterase		+	+	+
AFLA_020000	Pectinesterase		+	+	+
AFLA_039450	Penicillin-binding protein, putative		+	+	+
AFLA_065450	Penicillolysin/deuterolysin metalloprotease, putative	+	+	+	+
AFLA_037450	Peptidase, putative	+	+	+	+
AFLA_120180	Pheromone processing carboxypeptidase (Sxa2), putative	+	+	+	+
AFLA_013680	Phosphatidylglycerol specific phospholipase C, putative	+	+	+	+
AFLA_007870	Phosphatidylserine decarboxylase, putative		+	+	+
AFLA_038690	Phosphoglycerate mutase family protein, putative		+	+	+
AFLA_004420	Phospholipase D, putative		+	+	+
AFLA_029800	Phospholipase D, putative		+	+	+
AFLA_117760	Phytase, putative	+	+	+	+
AFLA_132650	Polysaccharide deacetylase (NodB), putative	+	+	+	+
AFLA_102060	Polysaccharide deacetylase, putative			+	+
AFLA_085430	Prenylcysteine lyase, putative		+	+	+
AFLA_021870	Probable 1,4-beta-D-glucan cellobiohydrolase A	+	+	+	+
AFLA_045570	Probable acetylxylan esterase A		+	+	+
AFLA_074520	Probable alpha-galactosidase A	+	+	+	+
AFLA_025300	Probable alpha-galactosidase B		+	+	+
AFLA_138090	Probable alpha-glucuronidase A	+	+	+	+
AFLA_090240	Probable endo-1,4-beta-xylanase A	+	+	+	+
AFLA_065190	Probable endo-1,4-beta-xylanase B	+	+	+	+
AFLA_063510	Probable endo-1,4-beta-xylanase F1		+	+	+
AFLA_008110	Probable endo-1,4-beta-xylanase F3		+	+	+
AFLA_105920	Probable endopolygalacturonase B	+	+	+	+
AFLA_074250	Probable endopolygalacturonase D	+	+	+	+
AFLA_108160	Probable endopolygalacturonase I	+	+	+	+
AFLA_082390	Probable exo-1,4-beta-xylosidase xlnD		+	+	+
AFLA_122480	Probable exopolygalacturonase B		+	+	+
AFLA_086360	Probable exopolygalacturonase C		+	+	+
AFLA_131770	Probable exopolygalacturonase X		+	+	+
AFLA_066140	Probable feruloyl esterase A		+	+	+
AFLA_028260	Probable glucan 1,3-beta-glucosidase A		+	+	+
AFLA_116950	Probable mannan endo-1,4-beta-mannosidase A		+	+	+
AFLA_069870	Probable mannan endo-1,4-beta-mannosidase F	+	+	+	+
AFLA_138570	Protease S8 tripeptidyl peptidase I, putative	+	+	+	+
AFLA_057990	Purine nucleoside permease, putative		+	+	+
AFLA_058940	Pyruvate dehydrogenase, putative		+	+	+
AFLA_090700	Quercetin 2,3-dioxygenase, putative		+	+	+
AFLA_086080	Restculine oxidase, putative		+	+	+
AFLA_060280	Rhamnogalacturonan acetylesterase RgaE		+	+	+

Table S3 Continued

Secretome ID	Secretome gene description	12hpi	24hpi	48hpi	72hpi
AFLA_025660	Rhamnogalacturonan acetylesterase, putative		+	+	+
AFLA_041820	Rhamnogalacturonase B, putative	+	+	+	+
AFLA_124310	Rhamnogalacturonase, putative		+	+	+
AFLA_072650	Salicylate hydroxylase, putative	+	+	+	
AFLA_074380	Salicylate hydroxylase, putative		+	+	+
AFLA_096290	Salicylate hydroxylase, putative		+	+	+
AFLA_137280	Sarcosine oxidase, putative		+	+	+
AFLA_067000	SCP-like extracellular protein, putative	+	+	+	+
AFLA_045980	Secreted dipeptidyl peptidase DppV	+	+	+	+
AFLA_024050	Secretory lipase, putative		+	+	+
AFLA_077710	Secretory lipase, putative	+	+	+	+
AFLA_132930	Secretory pathway protein Ssp120, putative		+	+	+
AFLA_100650	Serine carboxypeptidase (CpdS), putative	+	+	+	+
AFLA_112580	Serine carboxypeptidase, putative				+
AFLA_041800	Serine peptidase, family S28, putative			+	+
AFLA_104670	Serine peptidase, putative	+	+	+	+
AFLA_110210	Serine protease, putative		+	+	+
AFLA_024600	Short chain oxidoreductase (CsgA), putative			+	+
AFLA_102400	Siderophore biosynthesis enzyme, putative	+	+	+	+
AFLA_002020	Spherulin 4-like cell surface protein, putative			+	+
AFLA_094440	Spherulin 4-like cell surface protein, putative		+	+	+
AFLA_104470	Spherulin-1B, putative				+
AFLA_093550	Stress response protein Rds1, putative		+	+	+
AFLA_067180	Sulfatase-1, sulf-1, putative			+	+
AFLA_076430	SUN domain protein (Uth1), putative	+	+	+	+
AFLA_068080	Superoxide dismutase [Cu-Zn]	+	+	+	+
AFLA_011550	Tannase, putative		+	+	+
AFLA_104840	Tannase, putative			+	+
AFLA_006350	Thioredoxin reductase, putative	+	+	+	+
AFLA_101550	Thioredoxin reductase, putative			+	+
AFLA_132020	Toxin biosynthesis peroxidase, putative		+	+	+
AFLA_041880	Triacylglycerol lipase (LipA), putative				+
AFLA_011910	Triacylglycerol lipase, putative		+	+	+
AFLA_000860	Tripeptidyl peptidase A	+	+	+	+
AFLA_086160	Tripeptidyl peptidase SED3		+	+	+
AFLA_040430	Tripeptidyl-peptidase (TppA), putative	+	+	+	+
AFLA_018450	Tyrosinase, putative	+	+	+	+
AFLA_067860	Tyrosinase, putative		+	+	+
AFLA_120380	Tyrosinase, putative		+	+	+
AFLA_126850	Vacuolar protease A, putative	+		+	+
AFLA_015670	Vacuolar segregation protein (Pep7), putative	+	+	+	+
AFLA_126680	WD repeat-containing protein, putative	+		+	+
AFLA_101270	WSC domain protein, putative	+	+	+	+
AFLA_136480	Xylosidase : arabinofuranosidase		+	+	+
AFLA_004380	Xylosidase : arabinofuranosidase, putative			+	+
AFLA_053070	Yapsin, putative	+	+	+	+

Table S3 Continued

Secretome ID	Secretome gene description	12hpi	24hpi	48hpi	72hpi
AFLA_046240	Zinc carboxypeptidase, putative		+	+	+
AFLA_116140	Putative secreted protein			+	+
AFLA_000830	Putative uncharacterized protein		+	+	+
AFLA_000850	Putative uncharacterized protein		+	+	+
AFLA_001490	Putative uncharacterized protein		+	+	+
AFLA_001840	Putative uncharacterized protein		+	+	+
AFLA_002010	Putative uncharacterized protein		+	+	+
AFLA_004080	Putative uncharacterized protein		+	+	+
AFLA_004140	Putative uncharacterized protein		+	+	+
AFLA_004190	Putative uncharacterized protein	+	+	+	+
AFLA_004410	Putative uncharacterized protein	+	+	+	+
AFLA_004490	Putative uncharacterized protein		+	+	+
AFLA_005390	Putative uncharacterized protein		+		+
AFLA_005720	Putative uncharacterized protein	+	+	+	+
AFLA_006010	Putative uncharacterized protein			+	
AFLA_006040	Putative uncharacterized protein	+	+	+	+
AFLA_006080	Putative uncharacterized protein			+	+
AFLA_006340	Putative uncharacterized protein	+	+	+	+
AFLA_006820	Putative uncharacterized protein		+	+	+
AFLA_007360	Putative uncharacterized protein			+	+
AFLA_007430	Putative uncharacterized protein	+	+	+	+
AFLA_007480	Putative uncharacterized protein	+	+	+	+
AFLA_007610	Putative uncharacterized protein		+	+	+
AFLA_007690	Putative uncharacterized protein			+	+
AFLA_007730	Putative uncharacterized protein			+	+
AFLA_007880	Putative uncharacterized protein				+
AFLA_007930	Putative uncharacterized protein	+	+	+	
AFLA_008750	Putative uncharacterized protein		+	+	+
AFLA_009320	Putative uncharacterized protein			+	+
AFLA_009870	Putative uncharacterized protein			+	+
AFLA_011000	Putative uncharacterized protein				+
AFLA_011060	Putative uncharacterized protein			+	+
AFLA_011140	Putative uncharacterized protein				+
AFLA_011240	Putative uncharacterized protein	+	+	+	+
AFLA_011360	Putative uncharacterized protein	+	+	+	+
AFLA_011370	Putative uncharacterized protein	+	+	+	+
AFLA_011530	Putative uncharacterized protein	+	+	+	+
AFLA_012950	Putative uncharacterized protein		+	+	+
AFLA_013210	Putative uncharacterized protein				+
AFLA_013260	Putative uncharacterized protein		+	+	+
AFLA_013310	Putative uncharacterized protein		+	+	+
AFLA_013630	Putative uncharacterized protein		+	+	+
AFLA_013770	Putative uncharacterized protein	+	+	+	+
AFLA_013780	Putative uncharacterized protein	+	+	+	+
AFLA_014250	Putative uncharacterized protein	+	+	+	+
AFLA_014290	Putative uncharacterized protein		+	+	+

Table S3 Continued

Secretome ID	Secretome gene description	12hpi	24hpi	48hpi	72hpi
AFLA_014620	Putative uncharacterized protein	+	+	+	+
AFLA_014890	Putative uncharacterized protein		+	+	+
AFLA_015560	Putative uncharacterized protein	+			
AFLA_015960	Putative uncharacterized protein				+
AFLA_016240	Putative uncharacterized protein			+	+
AFLA_016980	Putative uncharacterized protein		+	+	+
AFLA_017230	Putative uncharacterized protein			+	+
AFLA_017350	Putative uncharacterized protein		+	+	+
AFLA_017460	Putative uncharacterized protein		+	+	+
AFLA_017740	Putative uncharacterized protein			+	+
AFLA_017750	Putative uncharacterized protein	+	+	+	+
AFLA_018920	Putative uncharacterized protein		+	+	+
AFLA_019160	Putative uncharacterized protein	+	+	+	+
AFLA_019170	Putative uncharacterized protein		+	+	+
AFLA_019510	Putative uncharacterized protein	+	+	+	+
AFLA_019620	Putative uncharacterized protein	+	+	+	+
AFLA_020010	Putative uncharacterized protein		+	+	+
AFLA_020420	Putative uncharacterized protein		+	+	+
AFLA_021010	Putative uncharacterized protein		+	+	+
AFLA_021530	Putative uncharacterized protein	+	+	+	+
AFLA_023130	Putative uncharacterized protein				+
AFLA_023150	Putative uncharacterized protein				+
AFLA_023250	Putative uncharacterized protein	+	+	+	+
AFLA_023610	Putative uncharacterized protein	+		+	+
AFLA_023830	Putative uncharacterized protein		+	+	+
AFLA_023850	Putative uncharacterized protein		+	+	+
AFLA_023990	Putative uncharacterized protein		+	+	+
AFLA_024190	Putative uncharacterized protein	+		+	+
AFLA_024550	Putative uncharacterized protein		+	+	+
AFLA_025010	Putative uncharacterized protein		+	+	+
AFLA_025230	Putative uncharacterized protein		+	+	+
AFLA_025260	Putative uncharacterized protein		+	+	+
AFLA_025880	Putative uncharacterized protein	+	+	+	+
AFLA_027210	Putative uncharacterized protein	+	+	+	+
AFLA_028880	Putative uncharacterized protein				+
AFLA_029470	Putative uncharacterized protein		+	+	+
AFLA_029550	Putative uncharacterized protein		+	+	+
AFLA_029970	Putative uncharacterized protein		+	+	+
AFLA_030270	Putative uncharacterized protein		+	+	+
AFLA_030550	Putative uncharacterized protein	+	+	+	+
AFLA_031040	Putative uncharacterized protein		+	+	+
AFLA_031050	Putative uncharacterized protein		+	+	+
AFLA_031440	Putative uncharacterized protein			+	+
AFLA_032330	Putative uncharacterized protein		+	+	+
AFLA_032670	Putative uncharacterized protein	+	+	+	+
AFLA_032930	Putative uncharacterized protein		+	+	+

Table S3 Continued

Secretome ID	Secretome gene description	12hpi	24hpi	48hpi	72hpi
AFLA_034090	Putative uncharacterized protein		+	+	+
AFLA_034710	Putative uncharacterized protein	+	+	+	+
AFLA_034760	Putative uncharacterized protein				+
AFLA_035730	Putative uncharacterized protein		+	+	+
AFLA_036400	Putative uncharacterized protein	+	+	+	+
AFLA_036540	Putative uncharacterized protein			+	+
AFLA_038270	Putative uncharacterized protein	+	+	+	+
AFLA_038350	Putative uncharacterized protein		+	+	+
AFLA_038360	Putative uncharacterized protein	+	+	+	+
AFLA_038450	Putative uncharacterized protein			+	+
AFLA_038520	Putative uncharacterized protein	+	+	+	+
AFLA_038710	Putative uncharacterized protein		+	+	+
AFLA_038920	Putative uncharacterized protein		+		
AFLA_038970	Putative uncharacterized protein			+	
AFLA_039340	Putative uncharacterized protein		+	+	+
AFLA_039520	Putative uncharacterized protein		+	+	+
AFLA_039540	Putative uncharacterized protein		+	+	+
AFLA_039580	Putative uncharacterized protein			+	+
AFLA_039730	Putative uncharacterized protein		+	+	+
AFLA_040050	Putative uncharacterized protein		+	+	+
AFLA_040100	Putative uncharacterized protein				+
AFLA_040440	Putative uncharacterized protein	+	+	+	
AFLA_040750	Putative uncharacterized protein				+
AFLA_041180	Putative uncharacterized protein		+	+	+
AFLA_041460	Putative uncharacterized protein			+	+
AFLA_041490	Putative uncharacterized protein		+	+	+
AFLA_041760	Putative uncharacterized protein		+	+	+
AFLA_042600	Putative uncharacterized protein		+	+	+
AFLA_042790	Putative uncharacterized protein				+
AFLA_042890	Putative uncharacterized protein		+	+	+
AFLA_042900	Putative uncharacterized protein	+	+	+	+
AFLA_043770	Putative uncharacterized protein		+	+	+
AFLA_043860	Putative uncharacterized protein	+	+	+	+
AFLA_045430	Putative uncharacterized protein		+		+
AFLA_046290	Putative uncharacterized protein		+	+	+
AFLA_049400	Putative uncharacterized protein				+
AFLA_049430	Putative uncharacterized protein	+	+	+	+
AFLA_049540	Putative uncharacterized protein			+	+
AFLA_049930	Putative uncharacterized protein	+	+	+	+
AFLA_050200	Putative uncharacterized protein		+	+	+
AFLA_051020	Putative uncharacterized protein	+	+	+	+
AFLA_053100	Putative uncharacterized protein		+	+	+
AFLA_053110	Putative uncharacterized protein		+	+	+
AFLA_053240	Putative uncharacterized protein				+
AFLA_053440	Putative uncharacterized protein			+	+
AFLA_053570	Putative uncharacterized protein			+	+

Table S3 Continued

Secretome ID	Secretome gene description	12hpi	24hpi	48hpi	72hpi
AFLA_053730	Putative uncharacterized protein			+	+
AFLA_053920	Putative uncharacterized protein		+		+
AFLA_054020	Putative uncharacterized protein		+	+	+
AFLA_054220	Putative uncharacterized protein				+
AFLA_054240	Putative uncharacterized protein		+	+	+
AFLA_054330	Putative uncharacterized protein		+	+	+
AFLA_054460	Putative uncharacterized protein			+	
AFLA_056240	Putative uncharacterized protein		+	+	+
AFLA_056470	Putative uncharacterized protein		+	+	+
AFLA_056760	Putative uncharacterized protein		+		
AFLA_056870	Putative uncharacterized protein			+	+
AFLA_057050	Putative uncharacterized protein		+	+	+
AFLA_057180	Putative uncharacterized protein				+
AFLA_057500	Putative uncharacterized protein		+	+	+
AFLA_057520	Putative uncharacterized protein			+	+
AFLA_059820	Putative uncharacterized protein		+	+	+
AFLA_059840	Putative uncharacterized protein		+	+	+
AFLA_060110	Putative uncharacterized protein		+	+	+
AFLA_060350	Putative uncharacterized protein		+		+
AFLA_061050	Putative uncharacterized protein		+	+	+
AFLA_061460	Putative uncharacterized protein		+	+	+
AFLA_061650	Putative uncharacterized protein				+
AFLA_061720	Putative uncharacterized protein		+	+	+
AFLA_062430	Putative uncharacterized protein		+	+	+
AFLA_062640	Putative uncharacterized protein	+	+	+	+
AFLA_062890	Putative uncharacterized protein		+	+	+
AFLA_063040	Putative uncharacterized protein		+	+	+
AFLA_063070	Putative uncharacterized protein		+	+	+
AFLA_063080	Putative uncharacterized protein				+
AFLA_063110	Putative uncharacterized protein				+
AFLA_063260	Putative uncharacterized protein	+	+	+	+
AFLA_063480	Putative uncharacterized protein		+	+	+
AFLA_064620	Putative uncharacterized protein		+	+	+
AFLA_064680	Putative uncharacterized protein		+		+
AFLA_064820	Putative uncharacterized protein				+
AFLA_064840	Putative uncharacterized protein	+	+	+	+
AFLA_064900	Putative uncharacterized protein	+	+	+	+
AFLA_065270	Putative uncharacterized protein				+
AFLA_065430	Putative uncharacterized protein			+	+
AFLA_066120	Putative uncharacterized protein			+	+
AFLA_066670	Putative uncharacterized protein				+
AFLA_066760	Putative uncharacterized protein		+	+	+
AFLA_067140	Putative uncharacterized protein		+	+	+
AFLA_068220	Putative uncharacterized protein		+	+	+
AFLA_068610	Putative uncharacterized protein	+	+	+	+
AFLA_069600	Putative uncharacterized protein		+		

Table S3 Continued

Secretome ID	Secretome gene description	12hpi	24hpi	48hpi	72hpi
AFLA_069610	Putative uncharacterized protein		+	+	+
AFLA_069620	Putative uncharacterized protein		+	+	+
AFLA_069880	Putative uncharacterized protein		+	+	+
AFLA_070230	Putative uncharacterized protein			+	+
AFLA_070350	Putative uncharacterized protein		+		
AFLA_070470	Putative uncharacterized protein	+	+	+	+
AFLA_070490	Putative uncharacterized protein		+	+	+
AFLA_070600	Putative uncharacterized protein	+	+	+	+
AFLA_070660	Putative uncharacterized protein		+	+	+
AFLA_071440	Putative uncharacterized protein	+	+	+	+
AFLA_072350	Putative uncharacterized protein				+
AFLA_072460	Putative uncharacterized protein		+	+	+
AFLA_072810	Putative uncharacterized protein		+	+	+
AFLA_073020	Putative uncharacterized protein		+	+	+
AFLA_073230	Putative uncharacterized protein				+
AFLA_073360	Putative uncharacterized protein		+		+
AFLA_073610	Putative uncharacterized protein		+	+	+
AFLA_074240	Putative uncharacterized protein			+	+
AFLA_074290	Putative uncharacterized protein		+	+	+
AFLA_074650	Putative uncharacterized protein		+		+
AFLA_074740	Putative uncharacterized protein			+	+
AFLA_074920	Putative uncharacterized protein		+	+	+
AFLA_074960	Putative uncharacterized protein				+
AFLA_075190	Putative uncharacterized protein	+	+	+	+
AFLA_075480	Putative uncharacterized protein		+	+	+
AFLA_075580	Putative uncharacterized protein		+	+	+
AFLA_075800	Putative uncharacterized protein		+	+	+
AFLA_075900	Putative uncharacterized protein		+	+	+
AFLA_075960	Putative uncharacterized protein				+
AFLA_077190	Putative uncharacterized protein		+	+	+
AFLA_077200	Putative uncharacterized protein			+	+
AFLA_077650	Putative uncharacterized protein	+	+	+	+
AFLA_078310	Putative uncharacterized protein		+	+	+
AFLA_078360	Putative uncharacterized protein			+	+
AFLA_079420	Putative uncharacterized protein	+	+	+	+
AFLA_080430	Putative uncharacterized protein		+	+	+
AFLA_080530	Putative uncharacterized protein	+	+	+	+
AFLA_081900	Putative uncharacterized protein	+	+	+	+
AFLA_082000	Putative uncharacterized protein		+	+	+
AFLA_085460	Putative uncharacterized protein		+	+	+
AFLA_085550	Putative uncharacterized protein			+	+
AFLA_085820	Putative uncharacterized protein			+	+
AFLA_085850	Putative uncharacterized protein		+	+	+
AFLA_085870	Putative uncharacterized protein		+	+	+
AFLA_086510	Putative uncharacterized protein		+	+	+
AFLA_087960	Putative uncharacterized protein		+	+	

Table S3 Continued

Secretome ID	Secretome gene description	12hpi	24hpi	48hpi	72hpi
AFLA_089300	Putative uncharacterized protein		+	+	+
AFLA_089460	Putative uncharacterized protein				+
AFLA_090090	Putative uncharacterized protein		+	+	+
AFLA_090410	Putative uncharacterized protein		+	+	+
AFLA_090560	Putative uncharacterized protein		+	+	+
AFLA_090710	Putative uncharacterized protein		+	+	+
AFLA_092020	Putative uncharacterized protein		+	+	+
AFLA_092170	Putative uncharacterized protein		+	+	+
AFLA_094140	Putative uncharacterized protein		+	+	+
AFLA_094270	Putative uncharacterized protein		+		+
AFLA_094600	Putative uncharacterized protein	+	+	+	+
AFLA_094770	Putative uncharacterized protein			+	+
AFLA_094980	Putative uncharacterized protein	+	+	+	+
AFLA_095000	Putative uncharacterized protein			+	+
AFLA_095200	Putative uncharacterized protein		+	+	+
AFLA_095400	Putative uncharacterized protein	+	+	+	+
AFLA_095950	Putative uncharacterized protein	+	+	+	+
AFLA_096130	Putative uncharacterized protein	+	+	+	+
AFLA_096230	Putative uncharacterized protein			+	+
AFLA_096470	Putative uncharacterized protein				+
AFLA_096650	Putative uncharacterized protein			+	+
AFLA_096660	Putative uncharacterized protein			+	+
AFLA_096780	Putative uncharacterized protein			+	+
AFLA_097130	Putative uncharacterized protein		+	+	+
AFLA_097190	Putative uncharacterized protein		+	+	+
AFLA_097270	Putative uncharacterized protein			+	+
AFLA_097310	Putative uncharacterized protein			+	+
AFLA_097340	Putative uncharacterized protein	+	+	+	+
AFLA_097670	Putative uncharacterized protein	+	+	+	+
AFLA_097770	Putative uncharacterized protein			+	+
AFLA_098660	Putative uncharacterized protein			+	+
AFLA_099050	Putative uncharacterized protein	+	+	+	+
AFLA_099110	Putative uncharacterized protein	+	+	+	+
AFLA_099390	Putative uncharacterized protein		+		
AFLA_100560	Putative uncharacterized protein				+
AFLA_101330	Putative uncharacterized protein	+	+	+	+
AFLA_101350	Putative uncharacterized protein				+
AFLA_101540	Putative uncharacterized protein	+	+	+	+
AFLA_101960	Putative uncharacterized protein		+	+	+
AFLA_102080	Putative uncharacterized protein	+	+	+	+
AFLA_102190	Putative uncharacterized protein		+	+	+
AFLA_102360	Putative uncharacterized protein		+	+	+
AFLA_102440	Putative uncharacterized protein			+	+
AFLA_103460	Putative uncharacterized protein			+	+
AFLA_104690	Putative uncharacterized protein		+	+	+
AFLA_105020	Putative uncharacterized protein		+	+	+

Table S3 Continued

Secretome ID	Secretome gene description	12hpi	24hpi	48hpi	72hpi
AFLA_105140	Putative uncharacterized protein			+	+
AFLA_105270	Putative uncharacterized protein		+	+	+
AFLA_105280	Putative uncharacterized protein	+	+	+	+
AFLA_105420	Putative uncharacterized protein		+	+	+
AFLA_105460	Putative uncharacterized protein		+		+
AFLA_105500	Putative uncharacterized protein				+
AFLA_106530	Putative uncharacterized protein		+	+	+
AFLA_107430	Putative uncharacterized protein	+	+	+	+
AFLA_107860	Putative uncharacterized protein	+	+	+	+
AFLA_108290	Putative uncharacterized protein				+
AFLA_108500	Putative uncharacterized protein				+
AFLA_109960	Putative uncharacterized protein		+	+	+
AFLA_110270	Putative uncharacterized protein		+	+	+
AFLA_111540	Putative uncharacterized protein		+	+	+
AFLA_112540	Putative uncharacterized protein	+	+	+	+
AFLA_113380	Putative uncharacterized protein			+	+
AFLA_113590	Putative uncharacterized protein		+	+	+
AFLA_115080	Putative uncharacterized protein		+	+	+
AFLA_115370	Putative uncharacterized protein	+	+	+	+
AFLA_116020	Putative uncharacterized protein	+	+	+	
AFLA_116340	Putative uncharacterized protein		+	+	+
AFLA_116540	Putative uncharacterized protein				+
AFLA_116550	Putative uncharacterized protein		+	+	+
AFLA_116900	Putative uncharacterized protein		+	+	+
AFLA_116940	Putative uncharacterized protein		+	+	+
AFLA_116970	Putative uncharacterized protein		+		
AFLA_117030	Putative uncharacterized protein			+	+
AFLA_117090	Putative uncharacterized protein		+	+	+
AFLA_117130	Putative uncharacterized protein				+
AFLA_117170	Putative uncharacterized protein		+	+	+
AFLA_118130	Putative uncharacterized protein			+	+
AFLA_118420	Putative uncharacterized protein	+	+	+	+
AFLA_118490	Putative uncharacterized protein	+	+	+	+
AFLA_118510	Putative uncharacterized protein	+	+	+	+
AFLA_118600	Putative uncharacterized protein		+	+	+
AFLA_118690	Putative uncharacterized protein		+	+	+
AFLA_118790	Putative uncharacterized protein		+	+	+
AFLA_119150	Putative uncharacterized protein			+	+
AFLA_119240	Putative uncharacterized protein		+	+	+
AFLA_119680	Putative uncharacterized protein		+	+	+
AFLA_119690	Putative uncharacterized protein		+	+	+
AFLA_119770	Putative uncharacterized protein		+	+	+
AFLA_121570	Putative uncharacterized protein		+	+	+
AFLA_121660	Putative uncharacterized protein		+	+	+
AFLA_121670	Putative uncharacterized protein			+	+
AFLA_121740	Putative uncharacterized protein		+		+

Table S3 Continued

Secretome ID	Secretome gene description	12hpi	24hpi	48hpi	72hpi
AFLA_121940	Putative uncharacterized protein				+
AFLA_121950	Putative uncharacterized protein				+
AFLA_122180	Putative uncharacterized protein		+	+	+
AFLA_122240	Putative uncharacterized protein		+	+	+
AFLA_122970	Putative uncharacterized protein				+
AFLA_123340	Putative uncharacterized protein		+	+	+
AFLA_123580	Putative uncharacterized protein		+	+	+
AFLA_123660	Putative uncharacterized protein	+	+	+	
AFLA_123800	Putative uncharacterized protein			+	+
AFLA_124070	Putative uncharacterized protein		+	+	+
AFLA_124890	Putative uncharacterized protein			+	+
AFLA_125360	Putative uncharacterized protein		+		
AFLA_125390	Putative uncharacterized protein				+
AFLA_125580	Putative uncharacterized protein		+	+	
AFLA_125650	Putative uncharacterized protein		+	+	+
AFLA_125950	Putative uncharacterized protein		+	+	+
AFLA_126240	Putative uncharacterized protein		+	+	+
AFLA_126430	Putative uncharacterized protein		+	+	+
AFLA_126570	Putative uncharacterized protein		+	+	+
AFLA_126870	Putative uncharacterized protein		+	+	+
AFLA_127130	Putative uncharacterized protein	+	+	+	+
AFLA_127190	Putative uncharacterized protein		+	+	+
AFLA_127950	Putative uncharacterized protein	+	+	+	+
AFLA_128410	Putative uncharacterized protein		+	+	+
AFLA_129080	Putative uncharacterized protein			+	+
AFLA_129230	Putative uncharacterized protein	+	+	+	+
AFLA_131400	Putative uncharacterized protein	+	+	+	+
AFLA_131910	Putative uncharacterized protein		+	+	+
AFLA_132110	Putative uncharacterized protein		+	+	+
AFLA_133630	Putative uncharacterized protein		+	+	+
AFLA_133640	Putative uncharacterized protein		+	+	+
AFLA_133810	Putative uncharacterized protein	+	+	+	+
AFLA_134850	Putative uncharacterized protein		+	+	+
AFLA_135210	Putative uncharacterized protein	+	+	+	+
AFLA_135310	Putative uncharacterized protein			+	+
AFLA_136270	Putative uncharacterized protein		+	+	+
AFLA_136610	Putative uncharacterized protein		+	+	+
AFLA_137180	Putative uncharacterized protein		+	+	+
AFLA_138140	Putative uncharacterized protein		+	+	+
AFLA_138150	Putative uncharacterized protein	+	+	+	+
AFLA_138310	Putative uncharacterized protein			+	+
AFLA_138690	Putative uncharacterized protein				+
AFLA_138790	Putative uncharacterized protein		+	+	+
AFLA_138840	Putative uncharacterized protein			+	+
AFLA_139000	Putative uncharacterized protein		+	+	+
AFLA_139050	Putative uncharacterized protein				+

Table S3 Continued

Secretome ID	Secretome gene description	12hpi	24hpi	48hpi	72hpi
AFLA_139640	Putative uncharacterized protein		+	+	+